THESIS

MODELING THE STREAM TEMPERATURE REGIME OF THE EAST FORK OF THE VIRGIN RIVER IN ZION NATIONAL PARK

Submitted by

Karen L. Peterson

Department of Civil Engineering

In partial fulfillment of the requirements

for the Degree of Master of Science

Colorado State University

Fort Collins, Colorado

Summer 1991

COLORADO STATE UNIVERSITY

May 16, 1991

WE HEREBY RECOMMEND THAT THE THESIS PREPARED UNDER OUR SUPERVISION BY KAREN PETERSON ENTITLED MODELING THE STREAM TEMPERATURE REGIME OF THE EAST FORK OF THE VIRGIN RIVER IN ZION NATIONAL PARK BE ACCEPTED AS FULFILLING IN PART REQUIREMENTS FOR THE DEGREE OF MASTER OF SCIENCE.

Committee on Graduate Work

David W Hendricks

Stanley L. Pierce

Robert C. Ward

Advisor

Department Head

ABSTRACT OF THESIS

MODELING THE STREAM TEMPERATURE REGIME

OF THE EAST FORK OF THE VIRGIN RIVER IN ZION NATIONAL PARK

The following stream temperature study was conducted as part of a general study by the Water Rights Branch, Water Resources Division, National Park Service, to evaluate the physical habitat of the aquatic organisms within Zion National Park (ZION). Stream temperature is an aquatic habitat characteristic that is known to be a controlling variable in the successful existence of the Virgin spinedace (Espinosa, 1978). The Virgin River spinedace, a non-game fish which is endemic to the East Fork of the Virgin River, was delineated as the target organism as it has been recommended for classification as threatened (50 F.R. 37959).

The first objective of the study was to measure and describe existing stream temperatures of the East Fork of the Virgin River at Virgin River Mile (VRM) 157.3. Diurnal fluctuations in the stream temperature of 10°C were common. The average maximum, mean, and minimum stream temperatures for the study period were 26.7°C, 21.8°C, and 17.0°C, respectively during which the average flow was 1076 l/s.

A second objective of the study was to predict the response of the daily fluctuations and mean daily stream temperature at VRM 157.3 to perturbations in stream temperature and discharge at the upstream (eastern) Zion National Park

boundary. Stream, shading, and site characteristic data were collected along a 9.3 km reach on the East Fork and input into TEMP-84, a stream temperature model, for simulation of existing and perturbed flows of 283 l/s (10 cfs), 566 l/s (20 cfs), 2,124 l/s (75 cfs), 2,832 l/s (100 cfs), 14,160 l/s (500 cfs), and 28,320 l/s (1000 cfs). Perturbed inflow temperature conditions were delineated as equal to the average ambient temperature and groundwater temperature. Modeled results were evaluated in terms of the relative change in maximum, mean, and minimum stream temperature from that modeled for existing conditions. The relative change was then applied to measured stream temperatures to estimate stream temperatures for the selected hypothetical condition.

Results from the modeling exercise demonstrated sharply dampened diurnal fluctuations at VRM 157.3 from an average of 10.1°C under existing conditions to 4.7°C as the flow increased to 2,832 l/s. As the flow was increased beyond 2,832 l/s, the diurnal fluctuation at VRM 157.3 decreases further and approached that of VRM 163.1 at the upstream end of the study reach. Mean stream temperatures at VRM 157.3 decreased by an average of 2.4°C as the flow increased to 14,160 l/s. Flows less than baseflow simulated dramatically increased diurnal fluctuations; diurnal fluctuations of 17.3°C were simulated for flows of 283 l/s. Mean stream temperatures increased by an average of 1.5°C when inflow was decreased to 283 l/s. Hypothetical inflow temperature simulations depicted a clear shift in the diurnal fluctuation at VRM 157.3 in the direction of the change in inflow stream temperature at VRM 163.1. Mean stream temperatures increased by an average of 4.6°C when inflow was equal to the average ambient temperature and decreased by an average of 2.0°C when inflow was equal to groundwater temperature.

Karen L. Peterson
Civil Engineering Department
Colorado State University
Fort Collins, CO 80523
Spring 1991

TABLE OF CONTENTS

LIST OF TABLES

LIST OF FIGURES

Figure Page

Introduction

The Virgin spinedace is a non-game fish that is endemic to the East Fork of the Virgin River within Zion National Park (ZION). This organism is considered an important water related resource attribute of ZION as it has been recommended to be classified as endangered (50 F.R. 37959). In order to ensure the unimpaired existence of this native organism, the Water Rights Branch (WRB) of the Water Resources Division (WRD) of the National Park Service (NPS) has undertaken the study of the physical aquatic habitat of the spinedace and its relationship to differing flow conditions.

This document presents the stream temperature study which was conducted as part of the general study by the NPS to evaluate the physical habitat of the Virgin spinedace. Stream temperature is a critical component of the aquatic habitat. In particular, growth rate, timing of the onset of spawning, and breeding are a few of the reproductive components of the Virgin spinedace that are related to stream temperature (Rinne, 1971). The stream temperature regime also affects the concentration of dissolved oxygen and the rate of oxidation of organic matter among other physical characteristics of the stream.

The need for maximum, mean, and minimum stream temperatures or an estimate of diurnal fluctuation was expressed at a meeting concerning the development of an aquatic habitat study (Johns, 1987). This information was deemed important as the Virgin spinedace have a preferred stream temperature tolerance range beyond which they will not exist. This temperature range fluctuates depending on the temperature at which the spinedace are acclimated. Acclimated at a temperature within the range of 8.5 to 20°C, the spinedace can survive maximum temperatures ranging from 29.3°C to 31.4°C with a 50 percent probability of survival.

The purpose of this study is to measure the existing stream temperature regime of the East Fork at the WRB selected aquatic habitat site and to predict the response of stream temperature at this site to changes in stream temperature and discharge at the upstream end of the selected study reach. This study is conducted for that time period during which maximum stream temperatures occur which is usually July (Deacon, 1988). Results from this study are intended to be utilized by fisheries biologists to further analyze the effect of flow and inflow temperature on the spinedace at the aquatic habitat site.

The objectives are to:

A. Describe the existing stream temperature regime at the aquatic habitat site in terms of daily fluctuations and mean daily temperatures during the period during which maximum stream temperatures occur.

B. Predict the response of daily fluctuations in stream temperature at the aquatic habitat site to perturbations in stream temperature and discharge at the upstream (eastern) Zion National Park boundary for the same time period as noted in A.

C. Predict the response of mean daily stream temperature at the aquatic habitat site to perturbations in stream temperature and discharge at the upstream (eastern) Zion National Park boundary for the same time period as noted in A.

The objectives of this study were accomplished through field data collection during June, July, and August of 1988 and stream temperature modeling of four days selected from the study period which was defined as June 29 through July 23. Data collection encompassed describing stream, shading, and site characteristic data along the East Fork of the Virgin River during the summer of 1988. Measured stream temperatures at the aquatic habitat site were used to describe the existing stream temperature regime. Stream temperatures for hypothetical flow and inflow temperature conditions were simulated utilizing the stream temperature model TEMP-84 (Beschta, 1984). The results from hypothetical simulations were analyzed relative to TEMP-84 simulations of existing conditions. These results were then applied to measured stream temperature data to predict the expected stream temperatures under the given selected hypothetical conditions.

This report initially presents the literature review of stream temperature modeling and the selection and overview of the model TEMP-84. An overview of the study site topography, vegetation, climate, and flow characteristics is given in Chapter 3. A description of the field data collection methods is then presented followed by a complete description of data analysis techniques used to prepare data for model input. TEMP-84 simulations of existing conditions are presented in Chapter 6 along with sensitivity analysis results illustrating the relative sensitivity of each variable to the modeled output. Finally, Chapter 7 presents the results from modeling hypothetical flow and inflow temperature conditions and estimates of the stream temperatures one might expect given the stated hypothetical conditions. The results are then followed by a discussion of the project, conclusions, and recommendations for future research.

Chapter 1. Literature Review

1.1 Virgin River Spinedace and Stream Temperature

The unimpaired existence of the Virgin spinedace (Lepidomeda mollispinis mollispinis) is dependent, in part, on the temperature of the stream in which it lives. Studies carried out by Espinosa (1978) show that upper lethal temperature (i.e., temperature at which a maximum of 50 percent of the fish can be presumed to exist) for the spinedace when acclimated at a temperature within the range of 8.5°C to 20°C for a given time period ranged from 29.3°C to 31.4°C. Deacon (1987) documented Critical Thermal Maximum (CTM), (i.e., the temperature at which the organism loses equilibrium) at 30.25°C and 37.02°C when acclimated at 10°C and 25°C respectively. It has also been shown that the Virgin River spinedace can survive relatively rapid elevations in temperature, 14.5°C in one hour for yearlings, less for juveniles (Espinosa, 1978). Another important temperature characteristic is thermal preference which is the temperature the organism selects when exposed to a range of temperatures after being acclimated at a given temperature. Studies have shown that the thermal preference temperature increases as the acclimation temperature increases (Deacon, 1988). Fry (1947) defines the final thermal preference as that temperature at which the preferred temperature is equal to the temperature at which the organism was acclimated. This is 23.1 +/- 0.5°C for the Virgin River spinedace (Deacon, 1987).

Time periods during which the temperature regime is critical for maintaining normal population sizes are believed to be the spawning period which is mid-May through June (Espinosa, 1978) and the period during which maximum stream temperatures occur (Deacon, 1988). Research is still needed to precisely define which time periods are most critical.

Stream temperature affects the Virgin spinedace as it serves to maintain various aspects of aquatic habitat. Changes in stream temperature affect the solubility of dissolved gases of which oxygen is the primary concern; microbial and algal metabolism is altered which affects all higher organisms within the food chain; growth rate, incubation duration, and species interaction is perturbed; bacteriological activity is altered which can result in increased susceptibility to disease; and warm or cold sections of stream may prevent the continued migration of an organism (Ward, 1979; Currier, 1980).

1.2 Stream Temperature and its Relationship with the Environment

The stream temperature of a volume of water is regulated by the heat transfer processes occurring across its boundaries. These heat transfer processes are in turn regulated by meteorological conditions, surrounding topography, surrounding riparian vegetation, and hydrologic conditions (Ward, 1979).

The net heat transfer occurring across water volume boundaries drives the mean stream temperature toward the equilibrium temperature (Sullivan, 1988; Edinger, 1968). Equilibrium temperature is the stream temperature at which the heat gain into the stream is equal to the heat loss (Edinger, 1968). At this point thermal stability is reached and the effect on downstream reaches is an increase in the constancy of the temperature regime (Currier 1980).

The extent to which the various environmental factors effect the stream temperature is a function of the stream size. Brown (1969), Beschta (1984), and Theurer (1984), among others, address the effect of stream size by applying the calculated net heat transfer to the ratio of stream surface area to discharge. Sullivan (1988), conducted a dimensional analysis on this ratio and illustrated that stream temperature is inversely proportional to stream depth. Several sources have documented that small, shallow streams respond rapidly to the microclimate and reach a point of equilibrium within short distances from their sources (Macan, 1959; Swift, 1971; Sullivan, 1988). In contrast, the larger, deeper streams, which have greater thermal inertia, required days to equilibrate (Sullivan, 1988). The magnitude of diurnal fluctuation is also affected by stream size; Sullivan (1988) documented that water temperature fluctuations around the mean decreased rapidly with increased depth.

Several studies have documented the effect of riparian vegetation on stream temperature. Levno (1967) documented an increase in the maximum stream temperature for a small (less than one cubic foot per second) stream after its surroundings had been logged and then scoured by a flood. Similar studies by Swift (1971), Brown and Krygier (1970), Macan (1959), Brown (1971), and Moore (1967), further support an increase in the magnitude of the diurnal stream temperature fluctuation with increased exposure to solar radiation. The majority of the above listed studies attribute the response primarily to the increase in solar radiation. Sullivan

(1988) notes that removal of riparian vegetation has effects in addition to increasing the solar radiation component. Moreover, removal of riparian vegetation increases surrounding air temperatures, decreases evapotranspiration rates, and increases the water volume within the soil; all of which have an effect on the stream temperature. Fowler (1987) notes increased wind passage and wind speeds as a result of canopy removal.

Moore (1967) noted mean stream temperatures on east-west oriented streams to be slightly higher than mean air temperature while on the north-south oriented streams, the mean stream temperatures were slightly cooler than the mean air temperatures. Therefore, solar radiation was considered the dominant variable regulating stream temperature. Moore further supported this theory by the fact that the two streams approached the same mean temperature after three consecutive days of complete cloud cover. Solar radiation as the dominant variable in regulating stream temperature is supported by Brown and Krygier (1970), Brown (1969), and Pluhowski (1970).

Several studies have noted an excellent relationship between mean air temperatures and mean water temperatures (Macan, 1959; Sullivan, 1988; Moore, 1967; Kothandaraman, 1972). Sullivan and Adams (1988) documented, for a variety of stream sizes and degree of vegetation, that mean water temperature adjusts to mean daily air temperature with the exact relationship determined by the relative influence of various environmental factors such as groundwater flow and riparian canopy density. In addition, diurnal water temperature fluctuation was found to be proportional to diurnal air temperature with the ratio varying with stream depth.

Kothandaraman (1972) presented a mathematical model which, given a representative relationship between air and water temperature, would predict annual cyclic trends in stream temperature based on air temperature record.

Heat transfer between the stream and bedrock was delineated by Brown (1969). He predicted stream temperature along a 610 m (2000 ft) reach of a small stream within approximately 0.5°C (1°F) when the bedrock heat transfer component was accounted for, in contrast to approximately 8.5°C (15°F) when it was neglected (Brown, 1971). This was supported by Hauser (1987); stream temperature regime studies which accounted for bedrock heat transfer simulated measured temperatures significantly closer than those which neglected this heat transfer component. Beschta (1984), documenting Brown's work, stated that 15 to 20 percent of the net solar radiation reaching the stream bed could be absorbed by the bedrock at depths less than 20 cm. The heat stored was then available for release back to the stream during the evening.

The influence of tributary and groundwater influx on stream temperature is a function of the percentage of total flow contributed by the groundwater entering the stream and the temperature difference between the main stem and groundwater (Currier, 1980). Several studies quantify the effects of groundwater and tributaries through mass balance analyses (Brown, 1971; Beschta, 1984; Theurer, 1984; Raphael, 1962; Sullivan, 1988). Swift (1971) noted a warming response of the stream as a result of influx of warm tributary flow. This effect was witnessed by Macan (1959) as high stream temperatures occurred after rainfall due to the warm runoff heated by the warm ground surface.

1.3 Reservoir Effects on Stream Temperature

Construction of a reservoir on a stream has been shown to have considerable effect on the stream temperature regime of the downstream system (Ward, 1974; Moore, 1967). Four major factors of reservoir operation govern the effect on downstream temperature regime: (1) volume of water impounded by the reservoir, (2) depth of the impoundment, (3) depth at which water is withdrawn, and (4), the rate of withdrawal as compared with the rate of natural flow (Moore, 1967). Deep reservoirs, for which the water is withdrawn from the bottom, generally lower the maximum stream temperature during the summer and raise the maximum temperature during the winter (Moore, 1967; Ward, 1974). On the other hand, downstream temperatures from shallow reservoir releases are generally warmer during late spring to early fall and unchanged during other times of the year (Moore, 1967). Overall, the effect of a reservoir is to dampen the diurnal fluctuation, increase the seasonal constancy, elevate winter temperatures, elevate or depress summer temperatures depending on depth of release, alter thermal patterns, alter the natural flow pattern, and alter the water temperature gradient between sites (USFWS, 1978; Moore, 1967). The stream recovers with distance from the release as it responds to the surrounding environmental factors (Ward, 1974). Depending on the size of the impoundment and the rate of recovery of the stream, a reservoir can affect the stream temperature regime for many miles downstream. Comparisons between January mean monthly stream temperatures before construction of the Brownlee Reservoir on the Snake River in Oregon and January mean monthly stream temperatures after construction showed that the stream temperature regime was affected up to 145 miles downstream (Moore, 1967).

1.4 Modeling Stream Temperature

The accepted approach to simulating stream temperature, used by virtually all of the models to be discussed, is application of an energy budget to quantify the net heat flux between the stream and its surroundings. Theoretical basis for this approach was established by Anderson (1954) through his detailed analysis of an energy budget for the purpose of quantifying evaporation on Lake Hefner. Brown's work (1969) was a cornerstone for stream temperature modeling because he established that small dynamic streams which have little thermal inertia and respond quickly to changes in heat transfer can be successfully simulated with the use of an accurate energy budget analysis.

Raphael (1962) and Delay and Seaders (1966) used stream surface area, water volume, tributary inflow and an energy budget encompassing short and long-wave radiation, evaporation, and convection in a simple differential equation to calculate the change in stream temperature for a given time interval. Raphael utilized his model on a long reach (75 miles) and qualitatively showed that the predicted temperatures approached actual temperatures. Delay and Seaders (1966) implemented their model on a large stream (45,000 liter/sec) and simulated the stream temperature within 0.8°C (1.5°F).

Edinger, Duttweiler and Geyer (1968) developed an expression for heat flux across the air/water interface as a function of a thermal exchange coefficient and the temperature gradient between the equilibrium stream temperature and the actual stream temperature. It was theorized that the equilibrium stream temperature changes with variations in meteorological conditions and the actual stream temperature responds by moving toward this equilibrium value. Studies depicted that a lag time exists between exposure of the stream to a change in meteorological conditions and the complete response of its temperature. Furthermore, as the depth of the stream increases the length of this lag time increases while the amplitude of the diurnal variations decrease.

Brown's (1969) stream temperature model based, again, on an energy budget analysis, encompassed net thermal radiation, evaporative flux, conductive flux, convective flux, and advective flux. The first to include heat transfer across the substrate, he found that conduction to the substrate can have a considerable effect for bedrock-bottomed streams, whereas conduction to the substrate for gravel-bottomed streams is insignificant. Brown used his stream temperature model to illustrate that the net thermal radiation received at the stream surface is the controlling heat transfer variable for small streams during daylight hours. This model, which was developed for small streams, simulated actual stream temperatures within 2° to 3°C for a single reach 610 m (2000 ft) long with uniform shading and channel geometry.

Morse (1972) developed a mathematical model for solution to stream temperature modeling. Considering heat transport by thermal advection, thermal dispersion, and interphase energy transfer across system boundaries, he theorized a multigradient energy balance equation representing the accumulation of heat within a fixed volume, moving, parcel of water. Assuming (1) dispersion terms can be ignored, (2) constant longitudinal velocity, and (3), dominance of the longitudinal component of stream temperature, the theoretical energy conservation model was simplified to an energy conservation one dimensional partial differential equation. Morse (1970) documented the nearly parabolic relationship between water temperature and net heat flux with water temperature as the independent variable. The coefficients which were solved for, given a determined net heat flux, were then employed in a manipulated form of the simplified energy conservation equation to solve for water temperature.

In addition to the deterministic model, Morse (1978) has expanded the energy conservation partial differential equation into a non-deterministic model which encompasses the stochastic nature of stream temperature. The non-deterministic model was only partially tested on one set of historical data. Statistical tests at 0.05 level showed that hypotheses of normality, stochastic independence and equality between means and standard deviations could not be rejected. Advantages of the non-deterministic model include reduced data requirements and less computation as no simulation is involved.

Crittenden (1977) developed a theoretical energy balance stream temperature model for use on a stationary column of water in small clear streams with little shading or heat transfer due to groundwater. Predicted temperatures represent those that would be reached after several days within the defined environment. He calculated direct and diffuse solar radiation through regression equations in terms of the angle of solar elevation. He also addressed, in detail, conduction of heat to the substrate and the thermal profile through the water column. A sensitivity analysis showed that wind speed had the greatest relative sensitivity with diffusivity of the substrate being second. Following, in descending order of relative sensitivity, are the other variables examined in the analysis: solar declination (i.e., season), stream depth, shading angle, initial water temperature, ambient vapor pressure, mean air temperature, and stream bed albedo. He concluded that conduction and evaporation were the most important forms of heat loss for the water column under study.

Sullivan and Adams (1988) initially developed Tempest for the purpose of studying the physics of stream heating and the relative importance of the regulating environmental factors. While still based on an energy budget this model approaches the problem from a more thermodynamic oriented theory base. It differs from previous models as it calculates the diurnal fluctuation around the mean separately from calculation of the mean value. This model also boasts a simplified set of data input requirements. It emphasizes the controlling variables of stream depth and surrounding air temperature and takes an abbreviated view of streamside vegetation and topographic shading.

Through the last decade, several coded stream temperature models have been developed and are available for use for individual studies. Each predicts downstream temperature responses to user defined environmental factors, hydrologic regimes, and site descriptions. Use of the energy balance continues to remain the primary mode for quantification of the heat transfer within the study reach. Models differ primarily in the treatment of environmental factors, computation of the individual energy budget components, organizational approach to analyzing the system, input data required, and the form of the stream temperature regime predicted. The following models for natural systems with steady flow conditions were obtained through various federal agencies and reviewed for use in this study.

1.4.1 QUAL2E

QUAL2E, the Enhanced Stream Water Quality Model (Brown 1987), developed through cooperative agreement between Tufts University, Department of Civil Engineering and the EPA Center for Water Quality Modeling, is a widely used, comprehensive stream water quality model. This model, which has been evolving since inception in 1971 by the Texas Water Development Board, can simulate dynamic and steady state stream temperatures for steady flow branched stream systems. In addition to stream temperature QUAL2E can simulate any one or combination of the following constituents: dissolved oxygen, biochemical oxygen demand, algae as chlorophyll a, organic Nitrogen as N, Ammonia as N, Nitrite as N, Nitrate as N, organic Phosphorus as P, dissolved Phosphorus as P, coliforms, an arbitrary non-conservative constituent, and three conservative constituents.

1.4.2 Simplified Steady-State Temperature and Dissolved Oxygen Model

The Simplified Steady-State Temperature and Dissolved Oxygen Model (Martin, 1986) developed through the Waterways Experiment Station of the Army Corps of Engineers simulates steady state stream temperature conditions for simple river systems, branches, and tributaries. Advantages of this model include ease of application and minimal data requirements. Its use is appropriate where long term, time averaged, stream temperature predictions are suitable for study objectives.

1.4.3 Instream Flow Stream Temperature Model

The Instream Flow Stream Temperature Model (Theurer, Voos, and Miller, 1984) was developed by the Instream Flow and Aquatic Systems Group in cooperation with the Soil Conservation Service and the U. S. Fish and Wildlife Service. It is a component of the Instream Flow Incremental Methodology (IFIM). This model simulates daily mean stream temperatures and diurnal fluctuations for any size steady state flow network. Site specific regression equations are utilized and diurnal fluctuations are developed through assumed symmetrical stream temperature versus time profiles.

1.4.4 Lagrangian Transport Model

The Lagrangian Transport Model (LTM) (Schoellhamer, 1986) developed by the U. S. Geological Survey is a one dimensional transport model which simulates up to ten water quality constituents in a stream system. The main program carries out transport calculations for steady as well as unsteady branched stream systems. A variety of subroutines, in addition to the user written subroutine option, are available to carry out the decay and constituent reaction calculations for the water quality constituents. The LTM model allows the user to define the flow field in a fixed nodal reference frame while taking advantage of the Lagrangian (moving) reference frame for water quality constituent calculations. Output consists of stream temperatures defined at user specified grid points for user specified increments of time.

1.4.5 JDYN-RQUAL

JDYN-RQUAL (Hauser, 1987) is a one dimensional, steady or unsteady flow, water quality modeling system which was developed by Tennessee Valley Authority (TVA). It is comprised of two independent models JDYN and RQUAL, which are linked together through user control codes. JDYN has been developing since 1978 into a comprehensive, detailed, unsteady flow regime modeling tool. RQUAL which began development in 1982, utilizes JDYN output and has the capacity to simulate daily mean and diurnal fluctuations in stream temperature for a branched unsteady or steady state flow network. It also can simulate nitrogenous oxygen demand (NOD), biochemical oxygen demand (BOD) and dissolved oxygen concentration (DO). JDYN-RQUAL was developed for in-house use by TVA. The model is not marketed and external use is only supported when the user have interacted with TVA sufficiently enough to ensure proper use of the modeling tool.

1.4.6 TEMP-84

Temp-84 (Beschta, 1984) is a comprehensive, one dimensional stream temperature model developed through the Watershed Systems Development Group of the USDA Forest Service. It was composed to serve as a management tool by simulating maximum temperature of streams in response to timber harvesting and streamside vegetation management. This model simulates diurnal fluctuations in stream temperature at user defined time increments for steady state flow, branching, stream systems. Data inputs encompass site characteristics, stream characteristics, and characteristics of streamside vegetation.

Chapter 2. TEMP-84, A Stream Temperature Model

Six stream temperature models were reviewed for the components incorporated in the respective solution algorithm and the approach utilized in characterizing the flow regime and meteorological conditions. Table 2.1 summarizes the results from this review; a star in the table indicates that the model incorporates the respective component.

2.1 Model Selection

TEMP-84 was selected among the six models because it allowed the most detailed, site specific description of meteorological, topographic, vegetative, and stream characteristics. Considering the quick response of small streams' temperature to changes in surrounding conditions (Sullivan, 1988), detail in describing the study reach conditions was considered necessary.

TEMP-84 is a physical process computer model developed to simulate temperature responses in small mountain streams. It incorporates site, stream, and stream-adjacent vegetation characteristics in its solution algorithm. It was developed primarily to assist the land manager in evaluating management strategies for streamside vegetation in forest harvesting operations.

TEMP-84 encompasses variables important at the study site. Because the stream flows through a canyon bordered by steep, nearly vertical (approximately 305

Table 2.1. A summary of the components incorporated in stream temperature models considered for use in the East Fork of the Virgin River stream temperature study.

COMPONENTS	MODELS					
	QUAL2E	J DYN-RQUAL	LTM	SIMPLE STEADY STATE	IFIM	TEMP-84
TOPOGRAPHIC SHADING		*			*	*
VEGETATION SHADING		*			*	*
GROUNDWATER FLOW	*	*	*		*	*
GROUNDWATER TEMPERATURE	*	*	*		*	*
SUBSTRATE HEAT TRANSFER		*			*	*
SPATIALLY VARIABLE METEOROLOGICAL DATA	* (1)					*
DIURNALLY DYNAMIC METEOROLOGICAL DATA	*	*	*		* (2)	*
DYNAMIC FLOW REGIME		*	*			
ROUTED FLOW REGIME		*				
CALCULATES SOLAR RADIATION	*				*	*
OUTPUTS MAXIMUM AND MINIMUM TEMPERATURES	*	*	*		*	*

(1) Climatological data is allowed to vary spatially when simulating the steady state temperature.

(2) Diurnal variations in air temperature are developed from sinusoidal approximations and regression equations which incorporate average daily air temperatures, solar radiation, relative humidity, and

m) sandstone walls, incorporating the effects of topographic shading was considered a priority. Localized descriptions of ambient temperature were also important considering the driving force of ambient air temperature in the heat transfer components and the probable variations from cool conditions in the narrow canyon upstream to the dry, hot, desert conditions as the canyon widens downstream. Incorporating groundwater influx was also a priority as groundwater influx to the stream was evident from observations by park employees who had investigated the East Fork upstream of the selected study reach.

TEMP-84 does not attempt to model the flow regime. Rather, the discharge, velocity, and width are described for each individual section in the data input set. While this is not the most accurate method of simulating flow, it is the most reasonable considering the long (approximately 9.5 km) length of the study reach and the dynamics and frequency of the pool, rapids, run, and riffle sequences. Moreover, modeling the flow through routing techniques would demand intense data collection beyond the scope of this project.

2.2 TEMP-84 Solution Approach

TEMP-84 is a stream temperature simulation model which, at relatively short time intervals (fifteen minutes or less), calculates flow, stream surface area, and instantaneous net energy flux. The net energy flux is evaluated for each water parcel as it travels from sub-section to sub-section throughout the system. The length of a sub-section corresponds to the distance traveled by a water parcel during the time interval between computations. Time intervals are kept short to assume constant energy transfer rates. Calculated output temperature for each water parcel (input temperature

+ net energy gain) from a sub-section is the inflow water temperature for the adjacent downstream sub-section.

TEMP-84 assesses the energy flux occurring during a time interval through an energy budget accounting procedure. Incorporated into the budget are the following components:

(1) net clear-sky solar radiation

(2) net longwave heat flux

(3) evaporative heat flux at the water surface

(4) convective heat flux at the air-water interface

(5) conductive heat flux between bedrock and water

(6) advective heat flux from groundwater seepage

The solution equation for the change in stream temperature for each section is as follows:

$$\Delta T = \Delta H * SA/Q/D/W * K \qquad \text{Eq. 2.1}$$

where:

ΔT is the temperature change (°C)

ΔH is the net energy flux (Ly/s)

SA is the section's surface area ($m^{\wedge 2}$)

Q is the streamflow (L/s)

D is water density (1 g/$cm^{\wedge 3}$)

W is the heat capacity of water (1 cal/g/°C)

K is a conversion factor (1 m/100 cm) (1000 L/$m^{\wedge 3}$)

The net energy flux is the sum of the energy budget components which are considered constant for each time interval.

Net solar radiation encompasses both direct and diffuse components. Direct radiation is calculated by routing the radiation through the atmosphere, accounting for transmissivity and optical air mass, to a plane surface above the canopy. Cloud effects are not incorporated into the algorithm. The diffuse component is calculated from the ratio of direct to diffuse radiation incident on a horizontal surface as a function of the zenith angle ((Brooks, 1959) in Reifsnyder and Lull, 1965). Both diffuse and direct beam radiation are then routed through the forest canopy. The amount to which the radiation is attenuated is determined by the canopy cover coefficient and the path length of the radiation through the vegetation. In addition to the forest canopy, radiation is also attenuated by overhanging vegetation which provides direct shading. At the stream surface the direct and diffuse radiation components are evaluated for that portion which is reflected, absorbed, or transmitted by the stream.

Heat transfer between bedrock and the stream is evaluated for the percentage of stream which is less than twenty centimeters in depth and comprised of bed material greater than twenty-five centimeters in axis. The model assumes all solar radiation entering the stream is absorbed within the top twenty centimeters of the water surface and the heat storage capacity of particles smaller than twenty-five centimeters is negligible. Modeling this energy transfer is carried out by storing heat in those portions of the stream which are less than twenty centimeters in depth and comprised of bed material greater than twenty-five centimeters in axis until the net solar radiation level decreases to less than or equal to one-half of the daily maximum. The stored energy is then released at a uniform rate over an eight-hour period. Justification for this energy transfer process lies in observations by Brown (1969) that fifteen to twenty percent of the net solar radiation reaching the stream bed could be absorbed by bedrock during the day and released back to the stream during the late afternoon and evening hours.

Net longwave radiation is calculated as the difference between incoming longwave radiation absorbed by the water surface and outgoing longwave radiation emitted from the water surface. The Stefan Boltzman radiation law which calculates longwave radiation as a function of media emissivity, the Stefan Boltzman constant, and the fourth power of the media temperature is implemented in determining both incoming and outgoing longwave flux. Incoming longwave flux is the sum of that emitted from the atmosphere and surrounding forest canopy. Atmospheric longwave radiation, like solar radiation, is routed through the canopy. The longwave radiation entering the water is assumed to be absorbed and is not routed through the water column. Tennessee Valley Authority (1972) found that water absorbs longwave radiation within fractions of a millimeter below the water surface. Longwave radiation emitted from the water surface is calculated from the water temperature and an assumed water emissivity.

Evaporative heat transfer is calculated from the latent heat of vaporization multiplied by an evaporation rate. The evaporation rate is calculated by an empirical formula which incorporates the vapor pressure gradient and a wind function ((Duttweiler (1963) in Ellis, 1981). This formula replaces the evaporation formula originally coded in TEMP-84. The original empirical evaporative formula was cited from Ryan and Harleman (1973) and Brocard and Harleman (1976). It was developed for cooling pond type conditions where free convection resulting from the virtual temperature difference between the stream and atmosphere as well as forced (wind driven) convection is important. Ryan and Harleman (1973) document that "above a heated water surface both forced (wind driven) and free (buoyancy driven) convection may be important" whereas "above a natural water surface (i.e. no waste heat input) forced convection dominates." In addition, Brocard and Harleman (1976) state that the evaporative rate formula, which was originally implemented in TEMP-84, "compared well with both laboratory and cooling pond field data." It was evident that the originally coded evaporative flux equation was not appropriate for natural stream conditions. Accordingly, the literature was reviewed for evaporative rate equations applicable to natural conditions. Seven equations were selected and implemented on the field data. The calculated evaporation rates from each formula for the modeled days were compared to the evaporation rates from the Saint George, Utah, NOAA weather station (#7516). A least squares analysis was conducted and the evaporation formula which produced the smallest sum of the squared differences between calculated and measured evaporation was selected for use in TEMP-84. Table 2.2 documents the comparison of calculated evaporation rates to NOAA published evaporation rates from Saint George, Utah.

The convective heat component includes those energy transfers due to conduction and convection across the air-water interface. Convection occurs from the dispersive action of molecular and macro air mass turbulence and conduction occurs as a result of the sensible heat gradient between the air and water. According to

Table 2.2. A comparison of evaporation rates calculated from selected evaporation models using ZION weather conditions to NOAA published evaporation rates for Saint George, UT.

DATE	SAINT GEORGE cm/day	DUTT-WEILER cm/day	MARCINO-HARBECK cm/day	QUALIIE cm/day	ZAYKOV cm/day	DELAY-SEADERS cm/day	BROWN cm/day	IFIM cm/day
6-30-88	0.94	0.53	0.23	0.51	0.46	0.15	0.46	0.41
7-08-88	0.79	0.66	0.43	0.69	0.61	0.28	0.86	0.41
7-15-88	0.71	0.84	0.61	0.86	0.76	0.38	1.22	0.46
7-21-88	0.53	0.94	0.84	1.09	0.94	0.53	1.73	0.41
SUM OF SQUARED DIFFERENCES:		0.056	0.114	0.083	0.067	0.153	0.564	0.079

SAINT GEORGE: PUBLISHED EVAPORATION * (PAN COEFFICIENT = .69)

DUTTWEILER: E(cm/s) = 2.4 * 10^-7(cm/s/mb) + 1.1 * 10^-7(cm/m/mb) * U(m/s) * (SWVP(mb) - AVP(mb)),

MARCINO-HARBECK: E(cm/s) = 1.36 * 10^-2 * U(m/s) * (SWVP(mb) - AVP(mb)) referenced in Macagno and Kennedy (1974).

QUALIIE: E(ft/hr) = 6.8 * 10^-4 (ft/hr/in. Hg.) + 2.7 * 10^-4 (ft/hr/in. Hg./mph) * U(mph) * (SWVP(in. Hg) - AVP (in. Hg)), referenced in EPA/600/3-87/007.

ZAYKOV: E(cm/s) = 1.5 * 10^-2 + 1.08 * 10^-2 * U(m/s) * (SWVP(mb) - AVP(mb)) referenced in Macagno and Kennedy (1974).

DELAY-SEADERS: Q(BTU/ft^2/hr) = .34 * U(mph) * (SWVP(mb) - AVP(mb)) referenced in Delay and Seaders (1966).

BROWN: Q(BTU/ft^2/min) = .6140 * U(m/s) * (SWVP(in. Hg.) - AVP(in. Hg.)) referenced in Brown (1969).

IFIM: Q(J/m^2/s) = (40.0 + 15.0 * U(m/s)) * (RH * (1.064)^Ta(C) - (1.0640)^Tw(C)) referenced in FWS/OBS-84/15.

where:
- Q = evaporative heat flux
- E = evaporation rate
- U = wind speed
- SWVP= saturated water vapor pressure
- AVP= air vapor pressure
- Ta = air temperature
- Tw = water temperature
- RH = relative humidity

Bowen (1926), the ratio of heat losses by conduction and convection to evaporative heat transfer is equal to a proportion which is a function of the Bowen constant, temperature gradient, and vapor pressure gradient between the air and water. TEMP-84 utilizes the Bowen ratio and the calculated evaporative heat transfer to calculate the conduction/convection heat transfer component across the air/water interface.

Advective heat transfer results from inflow volume and temperature of groundwater which is assumed to be constant throughout the entire section for which it is defined. It is evaluated in TEMP-84 through a mass balance mixing equation. The resulting temperature change due to groundwater influx is added onto the temperature change calculated from the energy budget analysis. In calculating the energy budget for each sub-section, half the groundwater component entering within the sub-section is added to the sub-section inflow discharge. Thus the increase in flow as a result of groundwater is incorporated throughout the study reach.

Chapter 3. Study Site Description

The East Fork of the Virgin River is a tributary to the Virgin River in southwest Utah. Following is a description of the East Fork watershed, climate conditions, and the selected study reach.

3.1 The Watershed

The East Fork of the Virgin River flows in an east-west direction through Zion National Park (ZION) in southwest Utah. It headwaters 56.8 km northeast of ZION (Pacific Southwest River Mile Index, 1974) and confluences with the North Fork of the Virgin River approximately 4.0 km downstream from where the stream leaves ZION. The drainage basin is approximately 64 km in length and approximately 16 km wide with a total area of approximately 105,000 Ha (405 sq. miles) (Turner, 1949). Upon confluence of the North and East Forks, the Virgin River continues to flow in a southwest direction until it eventually enters Lake Mead.

The East Fork of the Virgin River enters ZION along the east boundary of the park at a latitude of 37.2 degrees and longitude of 112.9 degrees. The general direction of the stream is west for approximately 3.2 km and then shifts to an aspect of approximately 20 degrees south of west. It flows at this aspect for approximately 8.0 km after which it exits ZION. The average elevation of the stream within ZION was calculated at 1241 m, and ranges from 1317 m to 1219 m. Elevations within the drainage basin ranges from 2438 m to 1219 m (Turner, 1949).

The East Fork headwaters in the Wasatch Formation of the Tertiary located in the Markagunt Plateau northeast of ZION. It then flows through the Tropic Formation and possibly Dakota sandstone of the Cretaceous (Gregory, 1950). This area is mountainous terrain with deeply entrenched drainage systems (Turner, 1949). Within this region, the stream flows at a gentle slope through meadowlands, sparse forests, and open rural districts, paralleling the Sevier River basin. It then briefly passes through Entrada sandstone and Carmel Formation of the Jurassic, and enters the Navajo sandstone formation. This area is characterized by sand flood plains sparsely vegetated with grasses, cacti, sagebrush, and occasional trees. As the stream passes through approximately 37 km of Navajo sandstone, it gradually narrows until the stream bed at 6 m to 24 m wide abruptly meets vertical or undercut walls (Gregory, 1950). As the stream narrows, the sinuosity of the stream increases until sharp meandering occurs throughout the narrowest sections.

The East Fork enters ZION in this narrow, meandering state and the Kayenta Formation is exposed at the stream level. Approximately 4.8 km downstream of the east boundary the Moenave Formation bounds either side of the alluvial flood plain. As the stream flows through ZION the canyon gradually widens from approximately 0.4 km to over 1.6 km at the canyon rim. Near the east park boundary Navajo sandstone cliffs tower at heights of 300 m over the mainstem, talus slopes reach the stream edge, and an alluvial flood plain is essentially non-existent. By the west park boundary, while the Navajo sandstone cliffs still dominate, the alluvial flood plain widens and extends 0.4 to 0.8 km on either side of the stream.

Narrow bands of cottonwood, willow, ash, and boxelder are common near the stream side. Alluvial benches and terraces are dominated by various sparse grasses, scrub brush, pinon, juniper, and cactus. Small drainage areas from spring sources harbor oases of dense, green, virulent vegetation.

3.2 Climate Conditions

The ZION region embodies deep canyons, wide valleys, broad slopes, and plateau tops (Gregory, 1950). Typically, the winters are cool and moist with snow existing in the high elevations and freezing temperatures occurring occasionally on the canyon floor. Between November and February, 1988, monthly average temperatures at Zion National Park (NOAA station #9717) ranged from 5.3°C (41.6°F) to 9.1°C (48.3°F) (NOAA, 1988). Spring is marked with progressively warmer and drier conditions and by June ambient conditions are hot and dry. Between March and June, 1988, monthly average temperatures at ZION increased from 10.4°C (50.7°F) to 26.4°C (79.5°F) (NOAA, 1988). Generally, the warmest month in ZION is July, followed by August and June (Gregory, 1950). Summer days are characterized by extreme temperatures, commonly greater than 38°C (100°F), while nights are cool and often accompanied by cool down-canyon drafts. Daily fluctuations are easily twenty to thirty degrees Celsius and daytime summer heat usually drops suddenly upon sunset. In July and August, 1988, the monthly average temperatures at ZION were 30.3°C (86.6°F) and 27.3°C (81.1°F) (NOAA, 1988).

Generally, precipitation in ZION is small with an annual mean of 36.8 cm (14.5 inches NOAA, 1988). It is characterized by great annual and seasonal variation in place as well as time (Gregory, 1950). Average annual precipitation within the drainage basin varies from about 25 cm in the southwest portion to slightly over 50 cm in the highest regions (Turner, 1949). Generally, April through June tends to be dry while July and August are considered wet months (Gregory, 1950). Late July and August are characterized by violent convective storms which are locally distributed and result in flash flood events. The wettest months of the year tend to be February and March (Gregory, 1950).

A characteristic feature for both precipitation and temperature within this region is wide annual, seasonal, monthly, and daily variations.

3.3 The Study Reach

The study reach begins 1.3 km below the east boundary of ZION. The beginning of the study reach was not placed along the east boundary because of access difficulties; a large waterfall of approximately 25 m vertical drop prevented access from downstream and presented a substantial hazardous traverse from the upstream end. Thus, the upstream site was selected at the first cross section below the water fall which allowed a valid discharge measurement, Virgin River Mile (VRM) 163.1. The flow from VRM 163.1 to VRM 162.2 is quite turbulent. It cascades from pool to rapids to pool around large, up to thirty foot in axis boulders. This section appears to have a significant influx of groundwater as several springs discharge into the main stem. In addition, the surrounding vegetation though not tall, is fairly dense and appears more lush than downstream reaches. From VRM 162.2 to VRM 160.0, the stream sequences between pools, riffles, and runs. This section also has discrete spring discharges but not with the frequency of the upstream section. The vegetation gradually changes from a lush green to the more sparse, typical semi-arid scene. Cottonwoods, willows, ash, and boxelder form narrow bands along the floodplain. Grasses, scrub brush, and various species of cactus also grow along the sandy banks. The following section, VRM 160.0 to VRM 159.5 appears to have an increased gradient with small steady rapids and a few protruding boulders, and small pools. The last section from VRM 159.5 to VRM 157.3 is characterized by flow sequencing between riffles and runs with only one or two pools. Generally, the run sections are long, 150 m to 300 m, and dominate over the short, 5 m to 30 m, riffle sections.

The downstream end of the study reach was selected based on where the Aquatic Habitat study section was placed for studies being conducted by Water Rights Branch, Water Resources Division, National Park Service.

The streambed substrate throughout the study reach is primarily cobbles interspersed with sand, gravels, and boulders. Sand dominates over cobbles and boulders in the pools. The substrate on the streambanks and floodplain is dominated by sand with a few interspersed cobbles and boulders.

Chapter 4. Field Data Collection

TEMP-84, the model chosen for this study requires data to describe site, stream, and shading characteristics. Data collection techniques and equipment are discussed in the following sections. Further description and calibration procedures for the equipment is presented in Appendix A.

A preliminary sensitivity analysis of TEMP-84, based on data from reconnaissance and professional judgment, was conducted during the early stages of data collection. TEMP-84 sensitivity of modeled maximum and minimum stream temperature to changes in the value of input variables was integral in the development of the various sampling schemes. The preliminary sensitivity analysis was limited to those variables for which sampling schemes were required. Table B.1 in Appendix B documents the results of the preliminary sensitivity analysis.

4.0 General Site Characteristics

Latitude, longitude, longitude of the center of the local time zone, stream aspect, length of stream sections, mean elevation, and stream gradient are all variables which remain constant and were read from tables or measured from USGS topographic maps. Relative humidity and windspeed were measured by ZION employees at the official NOAA weather station located near the ZION visitor center, approximately 5 km northwest of VRM 157.3. Average and 1400 hr relative humidities were calculated from wet and dry bulb temperature measurements taken in the evening, morning, and at 1400 hr. Windspeed measurements were made each day at 1400 hr utilizing a stationary anemometer.

4.1 Stream Characteristics

The study reach was broken into four stream characteristic reaches to describe width, velocity, and percent of the stream bed less than 20 cm deep and with bed material greater than 25 cm in axis. Stream characteristic reach boundaries were defined corresponding to the stream reaches described in Section 3.3. Velocity and width data were collected four and five times respectively between early June and late July. The percent of the stream less than 20 cm in depth and with bed material greater than 25 cm in axis was described once and assumed to remain constant during the study period.

4.1.1 Velocity

According to the preliminary sensitivity analysis, an increase in velocity of 100 percent resulted in less than one percent (0.29°C) increase in the maximum stream temperature and less than 0.3 percent (0.05°C) decrease in minimum temperature. As the sensitivity of the model did not warrant a rigorous sampling scheme, the float method was chosen for describing the average velocity. Student-t test calculations demonstrated that two float lengths per reach were required to calculate a sample average within +/- 0.3 m/s (1 ft/s) (approx. 50 percent) of the population mean. Only one float length was employed in the section between VRM 159.5 and VRM 160.0 as the section was only 0.8 km long and there appeared to be very little variance in velocity within the reach.

Float tests were conducted using oranges thrown in at different points across a cross section and above the starting point of the float length. Float lengths were straight sections with flow velocities representative of the reach in which they were located. The path of each orange was observed carefully so that the time period during which the oranges were controlled by eddies could be subtracted from the travel time. Six floats were initiated within each float length.

4.1.2 Width

Stream width was found to be a critical variable in modeling the stream temperature with TEMP-84. The preliminary sensitivity analysis illustrated that a 10 percent increase in width resulted in a 3.3 percent (1.11°C) increase in the maximum stream temperature while the minimum temperature decreased by 1.4 percent (0.24°C). Student-t test calculations were used to determine the number of width measurements required such that the sample average would be within 10 percent of the population mean. Discrete width measurements were made at 30.5 m (100 ft) intervals around and within the float lengths. Width was measured by stretching a nylon clad steel tape perpendicular to the flow from the right to left edge of water. In the uppermost section, VRM 163.1 to VRM 162.2, width measurements were made at 15.2 m (50 foot) intervals as the width varied noticeably within small distances.

4.1.3 Heat Transfer Across the Streambed

Heat transfer can occur at the streambed when the water depth is less than 20 cm deep and has bed material comprised of bedrock and non-protruding boulders greater than twenty five centimeters in diameter (Beschta, 1984). It was determined from the preliminary sensitivity analysis that this variable had very little effect on the stream temperature. Moreover, a change of 100 percent for each of the sections resulted in less than one percent change in the stream temperature at the end of the study reach. The lack of sensitivity of the stream temperature to this variable justified measurement by estimation techniques. Accordingly, the percentage of streambed which could transfer heat was estimated by eye at each cross section for which a width measurement was made.

4.2 Air Temperature

Hygrothermographs were employed to measure a continuous record of air temperature near the beginning, VRM 163.0, and end, VRM 157.5, of the study reach. Use of standard, white, instrument shelters was not permitted on this project as the study reach was located within a wilderness study area and a national park; white shelters presented a significant visual impairment. As a result, each instrument was placed in a tree which satisfied the following criteria: provided shading by vegetation but did not inhibit natural canyon wind currents, included a crook in which to place the instrument which was accessible, located out of the line of vision of hikers, and located in an area that was representative of the ambient air temperature. White roofs and white plastic louver side panels were installed on the east and west sides of each instrument to provide further shading. Each hygrothermograph was calibrated to a mercury maximum/minimum thermometer mounted alongside the instrument. The instruments were calibrated whenever the chart was changed. In addition to the hygrothermograph, two maximum/minimum thermometers were placed at VRM 159.7 and VRM 161.1 to describe the gradient of ambient air temperature along the study reach. These thermometers were mounted on tree trunks under heavy vegetation to ensure complete shading.

4.3 Stream Temperature

Stream temperatures which vary diurnally as well as seasonally were measured with continuous recording instruments. Ryan submersible thermographs were placed at the upstream end, VRM 163.1, and at the downstream end, VRM 157.3, of the study reach. Criteria for stream thermograph site selection was as follows: representative of depth and temperature, within definite streamlines of the flow, and protected from debris and saltating boulders which are transported during flood events. Assurance of a well mixed stream with regard to temperature at each selected site was confirmed by making several point temperature measurements with a hand held mercury thermometer across the cross section.

4.4 Groundwater Accretion

Groundwater accretion was determined by utilizing a mass balance analysis. In addition to the upstream and downstream ends of the study reach, discharge measurements were made at study section boundaries which appeared to separate reaches of differing groundwater inflow. For instance, discharge was measured at VRM 162.2 above which there was a significant amount of groundwater activity from springs which surfaced above the stream elevation. A discharge measurement was also made at VRM 161.5 below which there appeared to be very little groundwater activity. On one sampling trip a discharge measurement was made at VRM 160.0 as this marked the change from Kayenta to Moenave Formation along the stream.

4.5 Groundwater Temperature

Groundwater temperature was determined by measuring with a hand held mercury thermometer, the temperature of several springs at their respective sources. Spring sources measured were located within 20 ft, vertically, from the stream surface and were assumed representative of the groundwater temperature near the stream. In addition to spring sources above the stream surface, two small artesian flows which bubbled through the sand in very shallow water were measured for a description of groundwater temperature.

4.6 Shading Characteristics for Each Section

The study reach was broken into seven shading characteristic reaches to describe topographic and vegetation shading angles, hillslope angles, tree height, canopy coefficients, buffer strip widths, vegetation overhang and percent of bedrock. Shading characteristic reach boundaries were defined within the stream characteristic reach boundaries (described in Section 3.3) such that topographic and vegetative shading characteristics were uniform. Shading characteristic data were defined only once as they were assumed to remain constant during the study period.

4.6.1 Topographic Shading

TEMP-84 requires the average angles of topographic shading for southeast, south, and southwest directions. Topographic shading during the day was not considered critical as the study reach is oriented in an east-west direction and the sun travels at a high altitude.

Sample variance information for topographic shading angles was calculated from reconnaissance data documented in Table B.2. Student-t test calculations with a confidence level of 90 percent demonstrated that five measurements at each azimuth were required to calculate a sample average within +/- five degrees of the population mean. The five degree error range was selected because it is within 50 percent of the magnitude of the angles measured; according to the sensitivity analysis, a 50 percent change in topographic angle results in small if any change of the maximum and minimum stream temperatures. Five measurement sites for topographic descriptions were established at approximately equal intervals within each reach. Southeast angles, required to determine topographic shading at sunrise, were measured at ten degree intervals between azimuths of 45 to 115 degrees. Southwest angles, required to determine topographic shading during sunset hours, were measured at intervals of ten degrees between azimuths of 240 to 310 degrees. South angles, required to determine topographic shading during the day, were measured at intervals of ten degrees between azimuths of 150 to 210 degrees. All angles were measured from horizontal at the water surface to the rim of the topography with a hand held abney level.

4.6.2 Vegetation Shading

TEMP-84 requires average angles of forest shading perpendicular to the stream and in the south, southeast, and southwest directions. According to the preliminary sensitivity analysis, vegetation variables play a minor role in affecting the stream temperature along this study reach. This is due to the relatively sparse vegetation in addition to the often dominating topographic angles. As a result, the sampling scheme for the topographic shading data was used for the vegetation characteristic data to facilitate efficiency in data collection. Vegetation angles were measured perpendicular to the stream axis as well as at the southeast, south, and southwest azimuths. Angle measurements were made with an abney level from horizontal in the middle of the stream to the top of the vegetation.

4.6.3 Tree Height

Tree height was calculated indirectly from measurements of the angle between horizontal at eye level and the top of the tree, the distance between where the angle measurement was taken and the tree trunk, and the vertical distance from the base of the tree to eye level.

4.6.4 Hillslope Angle

The hill slope angle from horizontal was measured with the hand held abney level or otherwise estimated.

4.6.5 Canopy Coefficient

The portion of solar radiation blocked from reaching the stream by surrounding canopy is described by a canopy coefficient which ranges from zero to one; a coefficient value of zero represents no trees while a value of one represents a dense forest which provides complete shading. This coefficient was estimated at each data collection site.

4.6.6 Percentage of Overhanging Vegetation

The percentage of overhanging vegetation was determined by measuring the portion of the stream width at the shading data collection sites which had overhanging branches or debris.

4.6.7 Buffer Strip Width

The buffer strip width was considered to be continuous as no explicitly defined buffer strip existed alongside the stream.

4.7 Hypothetical Flow Data

Additional data collection was required to calculate velocity and width for hypothetical flow conditions. To obtain this data, the channel profile and water surface slope were surveyed at each float length using an automatic level, tripod, and leveling rod. The channel profile was placed at a cross section within the float length where uniform flow could be assumed reasonably. A discharge measurement was made at the time of the channel profile so that Manning's n could be determined through calculation. The channel profile and water surface elevation surveys were then implemented in Manning's equation to solve for the velocity and width for a given discharge.

Chapter 5. Data Analysis

Field data was collected during June, July, and August, 1988. It was analyzed and managed for input to the stream temperature model TEMP-84. Following are discussions of the analyses required to prepare the data for model input.

5.1 Study Period

The study period for this research was defined to be that time period during which maximum stream temperatures occur. Figure 5.1 portrays maximum, minimum, and mean stream temperatures between 6-3-88 and 8-2-88 at the downstream end of the study reach, Virgin River Mile (VRM) 157.3.

The stream temperature rose gradually through June which is described by Espinosa (1978) to be the spawning period for the Virgin spinedace. By 6-29-88 the stream temperature ceased rising and thus initiated the time period during which maximum temperatures occur. The end of the stream temperature study period was selected as July 23, 1988 because this was the last day the thermograph at VRM 163.1 was working; on July 23 the instrument seal broken and the instrument incurred water damage. This date was close to the initiation of the flood season as the first major precipitation event in July occurred 7-27-88.

The study period was broken into four time periods corresponding to calendar weeks: 6-29-88 through 7-2-88, 7-3-88 through 7-9-88, 7-10-88 through 7-16-88, and

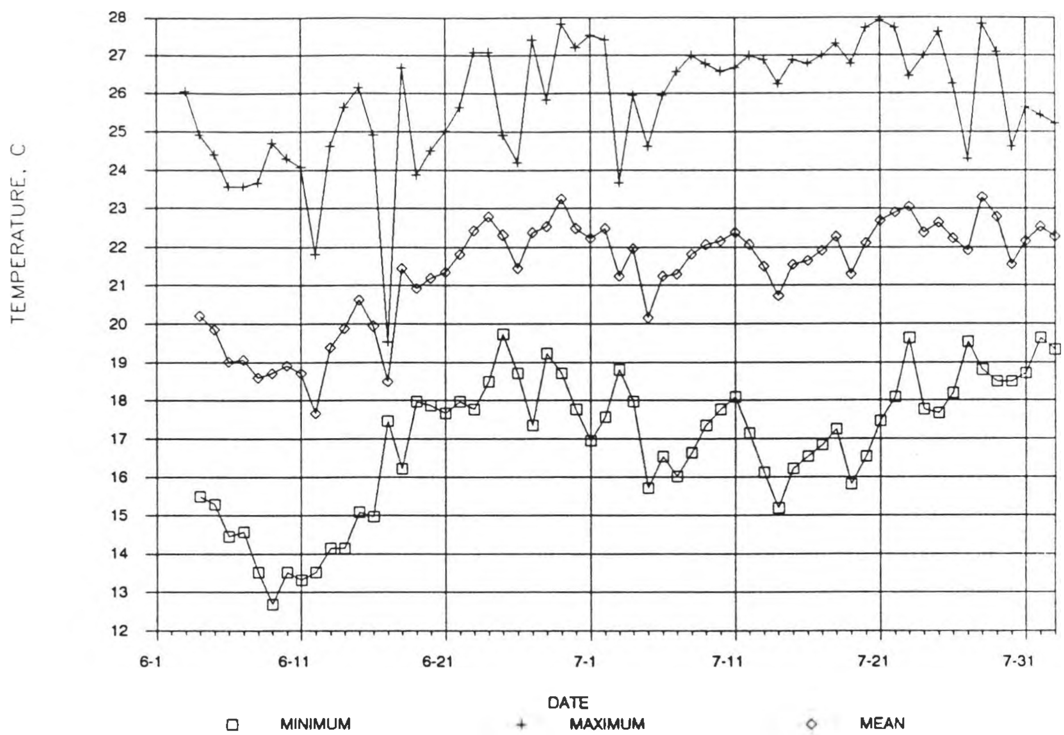

Fig. 5.1 Maximum, minimum, and mean stream temperature measured at Virgin River Mile 157.3 between 6-3-88 and 8-2-88.

7-17-88 through 7-23-88. One day from each week was selected for modeling. If stream characteristic data was collected during the week, the day on which it was collected was modeled. If stream characteristic data was not collected, the day on which the weekly maximum stream temperature at VRM 157.3 occurred was modeled. Accordingly, 6-30-88 and 7-15-88 were selected for modeling from the first and third weeks as stream characteristic data was collected on these days. For the second and fourth weeks, 7-8-88 and 7-21-88 were selected as the weekly maximum stream temperature occurred on these days. Table 5.1 documents the maximum, minimum, and mean stream temperature at VRM 157.3 for each of the days selected for modeling.

Table 5.1 Maximum, minimum, and mean stream temperatures measured at Virgin River Mile 157.3 for 6-30-88, 7-08-88, 7-15-88, and 7-21-88.

DATE	MAXIMUM TEMP. C	MINIMUM TEMP. C	MEAN TEMP. C
6-30-88	27.2	17.8	22.0
7-08-88	27.0	16.7	21.5
7-15-88	26.9	16.2	21.2
7-21-88	27.8	17.5	22.4

5.2 Stream Temperature

Continuous records of stream temperature were collected from 6-3-88 through the 8-18-88. The record collected between 8-2-88 and 8-18-88 was not included in the analysis because the thermograph sensing probes were often buried as a result of active sediment transport during precipitation events. While the record stationed at VRM 157.3 was complete, the record stationed at VRM 163.1 was missing data between 6-3-88 through 6-24-88 and 7-22-88 through 8-02-88. The latter missing data was a result of a broken seal on the instrument allowing water into the inner workings. Data missing between 6-3-88 and 6-24-88 resulted from forgetting to initiate the battery when the instrument was first mounted.

Figures 5.2, 5.3, and 5.4 depict maximum, minimum, and mean, respectively, stream temperatures for VRM 157.3 and VRM 163.1 for the study period of 6-29-88 through 7-22-88. Table C.1 in Appendix C documents daily maximum, minimum, and mean stream temperature readings for VRM 163.1 and VRM 157.3.

The average difference in maximum stream temperature between VRM 157.3 and VRM 163.1 was 5.7°C. At VRM 157.3, the maximum temperature ranged from

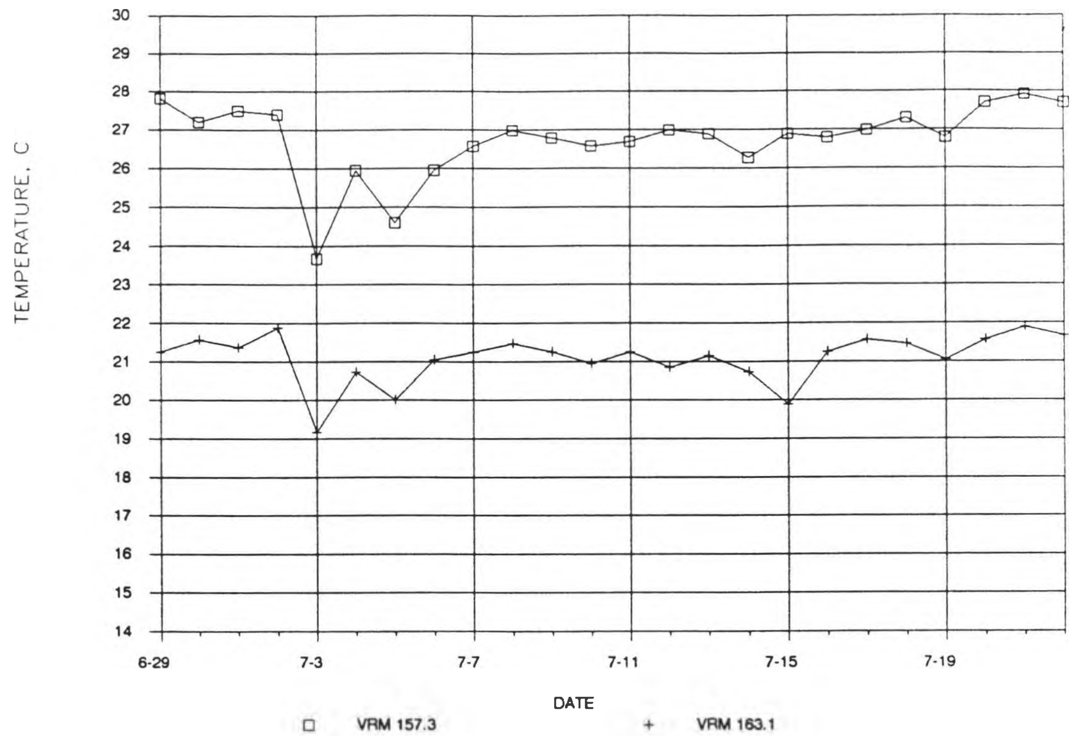

Fig. 5.2 Measured daily maximum stream temperature at Virgin River Mile 157.3 and Virgin River Mile 163.1 between 6-29-88 and 7-22-88.

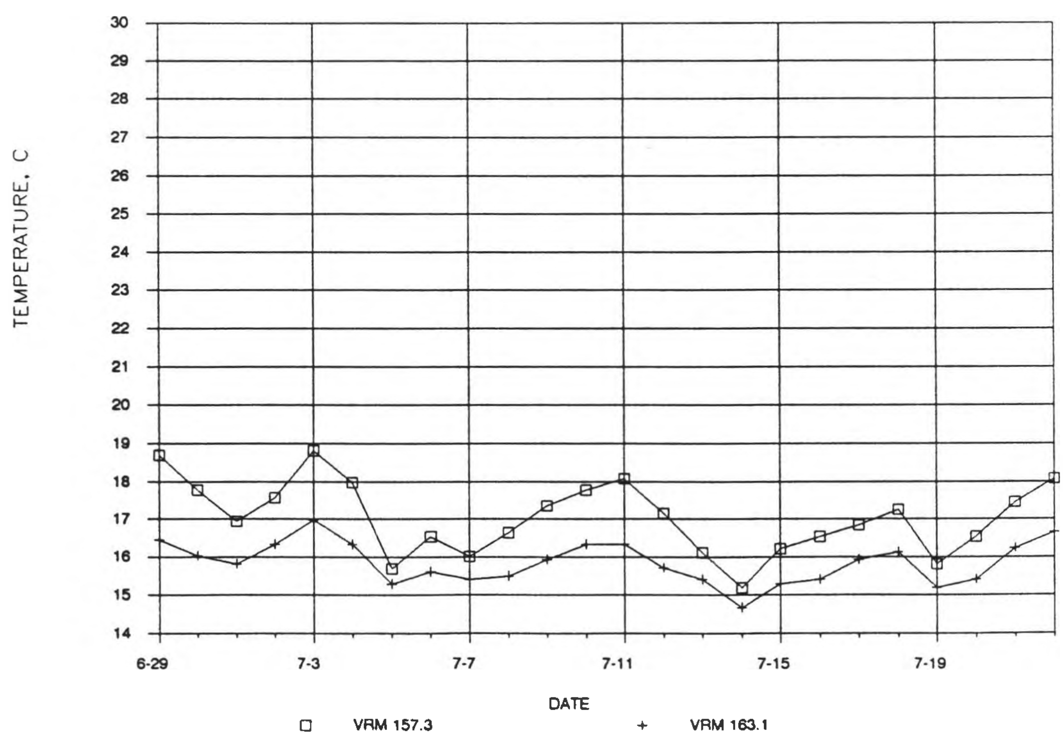

Fig. 5.3 Measured daily minimum stream temperature at Virgin River Mile 157.3 and Virgin River Mile 163.1 between 6-29-88 and 7-22-88.

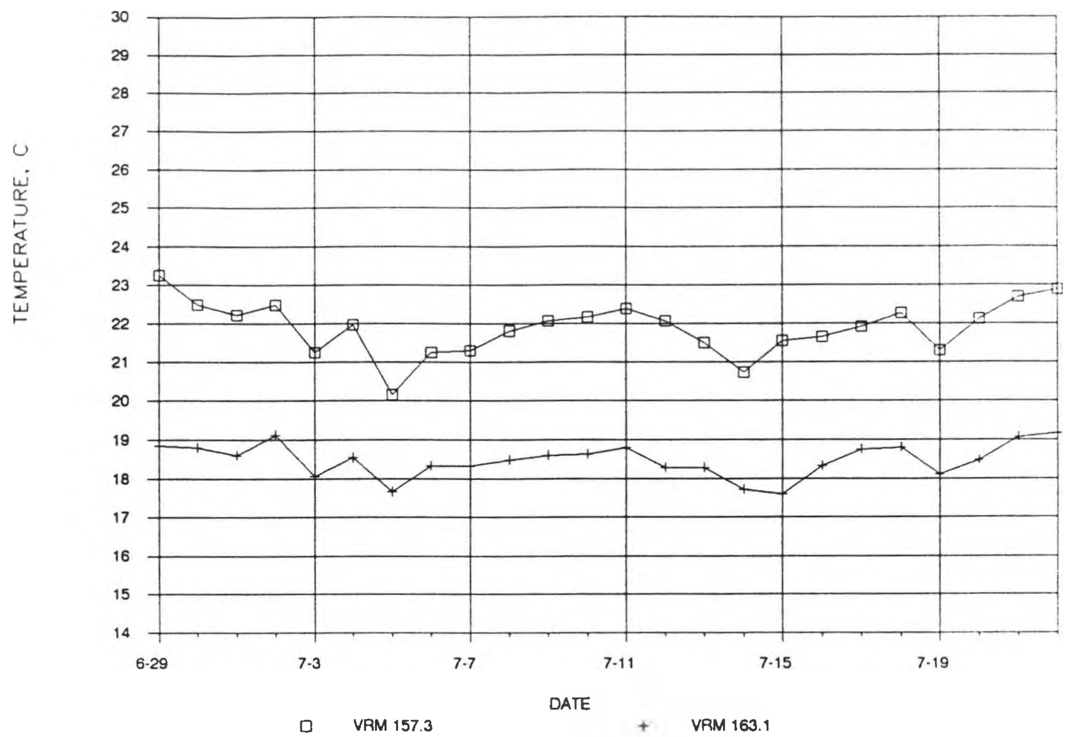

Fig. 5.4 Measured daily mean stream temperature at Virgin River Mile 157.3 and Virgin River Mile 163.1 between 6-39-88 and 7-22-88.

23.7°C to 27.8°C with an average of 26.7°C. At VRM 163.1 the range was 19.2°C to 21.9°C with an average of 21.1°C.

The average difference in minimum stream temperature between VRM 157.3 and VRM 163.1 was 1.2°C with a standard deviation of 0.5°C. At VRM 157.3, the minimum temperature ranged from 15.2°C to 18.8°C with an average of 17.0°C while at VRM 163.1 it ranged from 14.7°C to 17.0°C with an average of 15.8°C.

The average difference in mean stream temperature between VRM 157.3 and VRM 163.1 was 3.4°C with a standard deviation of 0.4°C. Mean stream temperatures ranged from 20.2°C to 23.3°C with an average of 21.8°C at VRM 157.3 and from 17.6°C to 19.2°C with an average of 18.5°C at VRM 163.1.

Hourly stream temperatures were read from the charts at VRM 163.1 for the days selected for modeling (Table C.2). The calibrated hourly values were used for the modeled inflow stream temperature.

5.3 Air Temperature

Continuous recorded air temperature data was first corrected for the difference between the hygrothermograph temperature and the adjacent mercury thermometer temperature which was recorded each time the hygrothermograph was serviced. The difference in temperature was assumed to result from a systematic error of the instrument and was applied proportionally over the chart record.

Data collected at VRM 157.5 between 6-4-88 and 6-21-88 was impossible to adjust due to inconsistencies in field calibration techniques. Thus, this data was not available for use in the analysis.

After making the required adjustments, the air temperatures were calibrated to the standard temperature through calibration curves for the respective maximum/minimum thermometer. Tables C.3 and C.4 document the recorded, adjusted, and calibrated air temperature data for VRM 163.0 and VRM 157.5, respectively. Figures 5.5 and 5.6 show the calibrated record of maximum and minimum air temperature, respectively, at VRM 163.1 and VRM 157.5. Tables C.5 through C.12 document the calibrated hourly air temperature readings from the hygrothermographs at VRM 163 and VRM 157.5 for the days selected for modeling.

The average difference between maximum temperatures at VRM 163.0 and VRM 157.5 was calculated to be 1.35°C for 6-29-88 through 7-22-88 while the average difference between minimum temperatures was calculated to be 0.01°C.

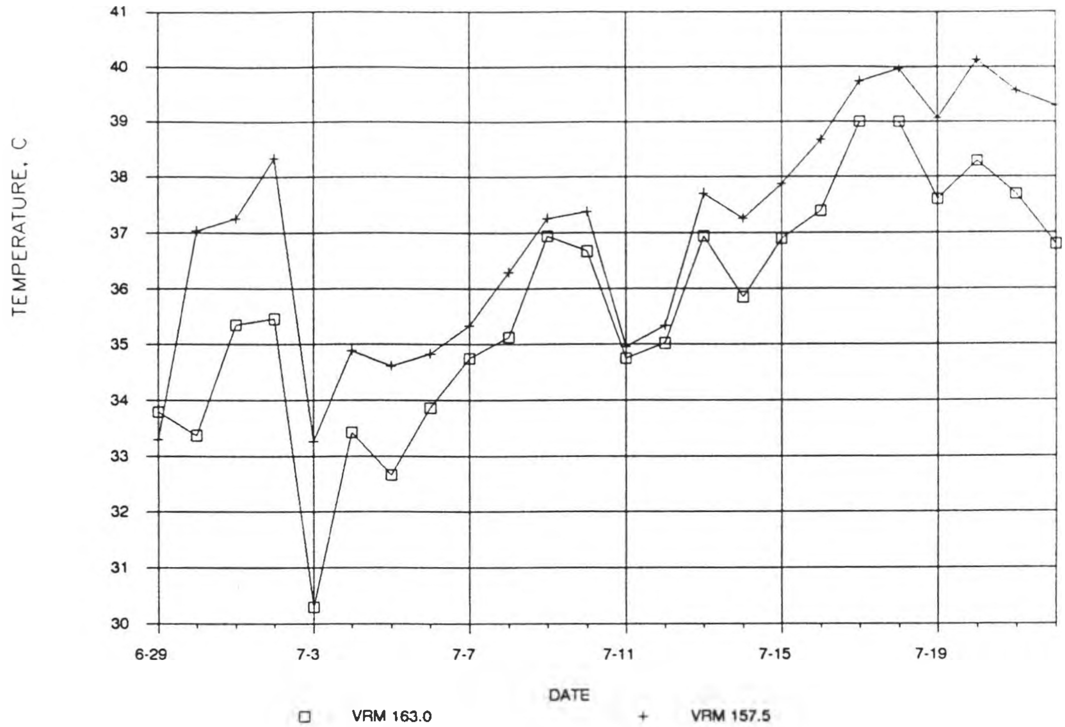

Fig. 5.5 Measured daily maximum air temperatures at Virgin River Mile 157.5 and Virgin River Mile 163.0 between 6-29-88 and 7-22-88.

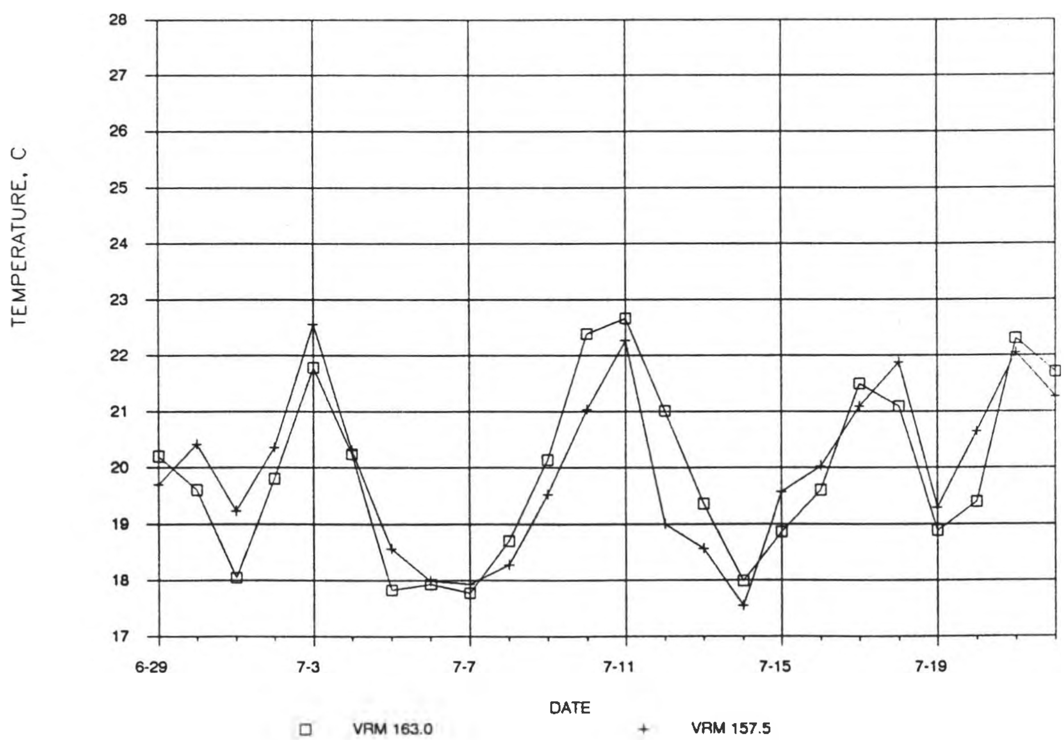

Fig. 5.6 Measured daily minimum air temperatures at Virgin River Mile 157.5 and Virgin River Mile 163.0 between 6-29-88 and 7-22-88.

Contrary to what was expected, the air temperature regime at VRM 163.0 did not differ greatly from that recorded at VRM 157.5.

To lend credibility to the collected air temperature records, a linear regression analysis was conducted between the air temperature record collected utilizing standard techniques by Zion National Park (ZION) and those records collected along the study reach which were valid. Comparisons were made for air temperature readings at 1400 hr as this was the time that the actual air temperature was recorded at the ZION station. Table C.13 documents the 1400 hr air temperature data recorded at VRM 157.5 and VRM 163.0 and by ZION. Figure 5.7 and 5.8 illustrate 1400 hr air temperature of VRM 157.5 and VRM 163.0, respectively, plotted against 1400 hr air temperature recorded at ZION. The square of the correlation coefficient for these relationships was 0.94 for VRM 157.5 and 0.96 for VRM 163.0. While some scatter exists, a definite relationship between air temperature recorded along the study reach and at ZION is evident. Some scatter is expected considering the differences in microclimate between the sites.

The purpose of the maximum/minimum thermometers located at VRM 159.7 and VRM 161.5 was to document changes in the air temperature regime along the study reach. Data from the maximum/minimum thermometers was difficult to utilize as they were read at different times in the day due to the travel time between sites. Furthermore, poor site selection prevented representative data. Accordingly, data collected by the maximum/minimum thermometers set between the hygrothermographs was not used in the analysis. Based on qualitative assessment of the study reach surroundings, it was decided to utilize the air temperature record logged at VRM

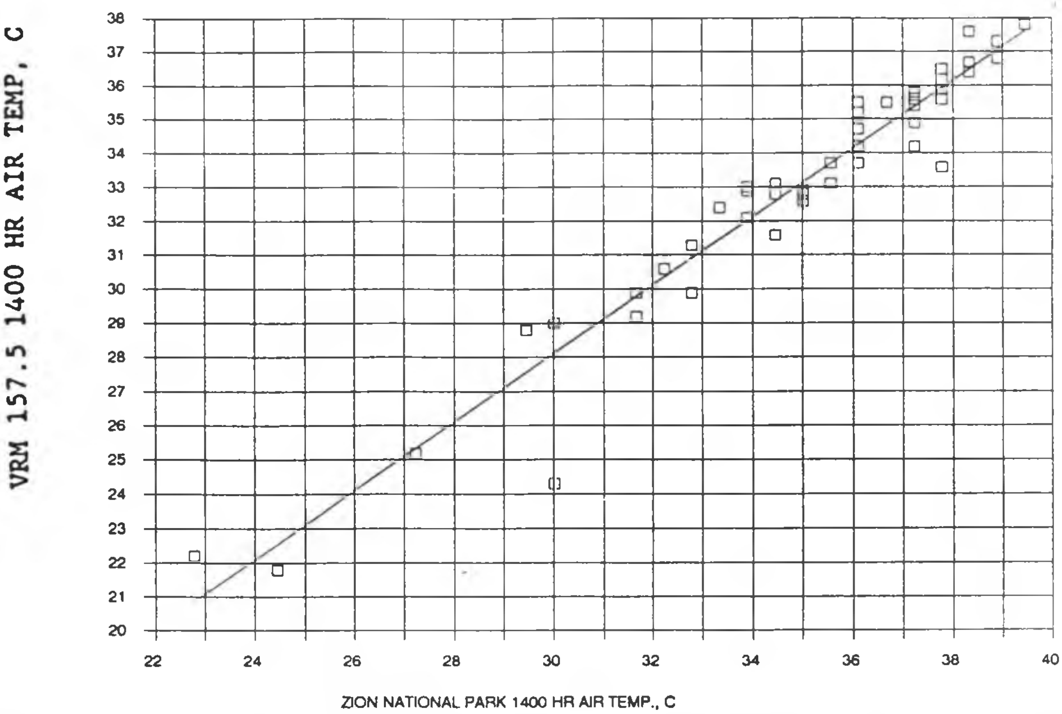

Fig. 5.7 Air temp. measured at 1400 hr at Virgin River Mile 157.5 plotted against official Zion National Park 1400 hr air temp. for 6-22-88 through 8-19-88.

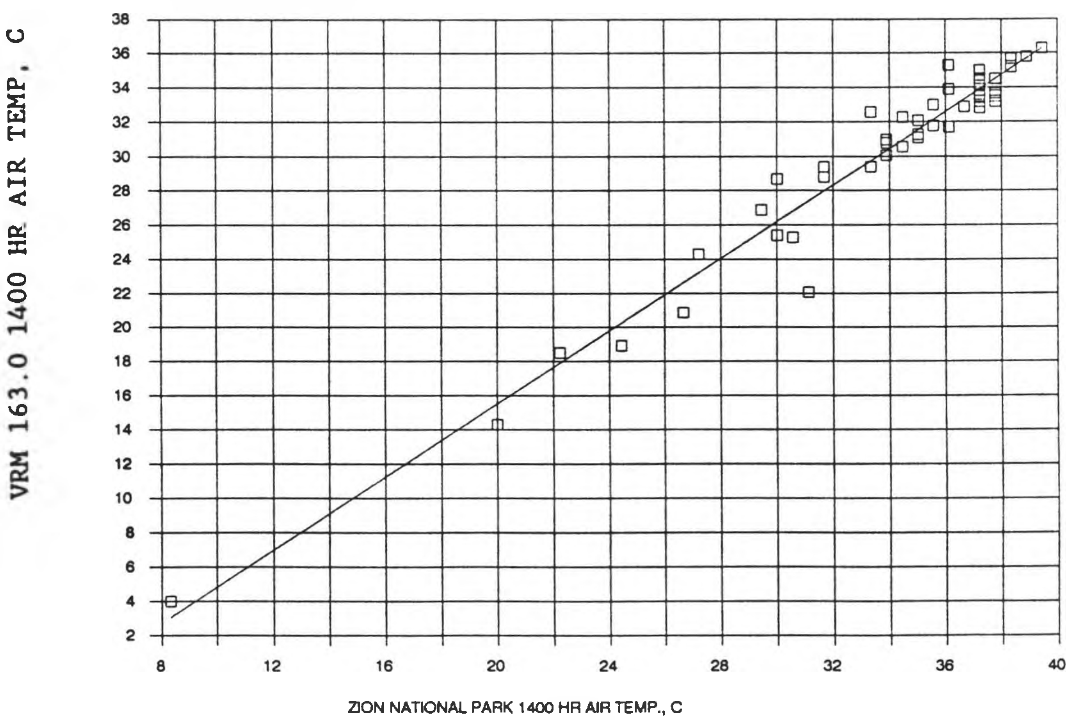

Fig. 5.8 Air temp. measured at 1400 hr at Virgin River Mile 163.0 plotted against official Zion National Park 1400 hr air temp. for 5-28-88 through 8-18-88.

163.0 between VRM 163.1 and 161.5. Downstream of VRM 161.5, the canyon widens and more closely represents the characteristics of the hygrothermograph site at VRM 157.5.

5.4 Topographic Shading Angles

The angle from horizontal at the stream surface to the top of the surrounding topography was measured for specified azimuths at five sampling sites within each reach delineated for shading characteristic data. The average of the five measurements for a given azimuth was calculated along with the sample variance and confidence interval defining, according to the Student-t test, the range within which the calculated sample average represents the population average with a level of confidence of 90 percent. Table 5.2 documents the field collected data and calculated average topographic shading angle for southeast azimuths. Topographic shading data for south and southwest azimuths (Tables C.14 and C.15) are listed in Appendix C. Eighty-three percent of the collected 161 data sets satisfied the sampling scheme design error range of +/- five degree. Ninety-nine percent of the data sets produced an error range within +/- ten degrees.

TEMP-84 requires southeast, south, and southwest topographic angle inputs for each stream section. The orientation of the study reach, ie., east-west, is such that the southeast angle is important for determining the time of the local sunrise while the southwest angle is important for determining the time of the local sunset. The south angle is not critical as the sun travels on a path approximately parallel to the stream axis at an altitude greater than the topographic angles.

Table 5.2. Topographic shading data collected between Virgin River Mile (VRM) 163.1 and VRM 157.3 for southeast azimuths.

	AZIMUTH							
SAMPLE	45 (deg)	55 (deg)	65 (deg)	75 (deg)	85 (deg)	95 (deg)	105 (deg)	115 (deg)
VRM 163.1 - VRM 162.2								
1	43.0	40.0	22.0	22.5	26.0	28.5	27.5	27.0
2	41.5	29.5	29.0	18.5	22.0	23.0	35.0	39.5
3	53.0	50.0	48.0	45.0	43.0	20.5	15.0	19.0
4	33.0	28.0	26.5	24.0	20.0	13.0	20.0	32.5
5	22.0	20.0	18.0	16.0	20.0	28.0	33.0	40.0
AVERAGE:	38.5	33.5	28.7	25.2	26.2	22.6	26.1	31.6
VARIANCE:	135.5	135.8	134.2	132.6	94.2	40.2	72.3	78.4
90%C.I.*:	8.0	8.0	7.9	7.9	6.6	4.3	5.8	6.1
VRM 162.2 - VRM 161.5								
1	29.5	19.0	14.0	12.0	18.5	23.0	33.5	37.0
2	32.0	27.0	15.5	12.0	12.0	18.5	22.0	23.5
3	27.0	22.0	15.0	11.0	14.5	18.5	22.0	28.5
4	36.0	35.0	22.0	14.5	9.5	13.0	15.5	24.0
5	29.5	28.5	27.0	14.5	15.0	21.5	26.5	37.5
AVERAGE:	30.8	26.3	18.7	12.8	13.9	18.9	23.9	30.1
VARIANCE:	11.6	38.2	31.5	2.6	11.4	14.7	44.2	46.4
90%C.I.*:	2.3	4.2	3.8	1.1	2.3	2.6	4.5	4.7
VRM 161.5 - VRM 160.7								
1	21.0	20.0	19.5	9.5	4.5	12.0	22.0	24.0
2	20.5	18.0	17.0	7.5	21.0	22.5	35.0	38.0
3	21.5	15.0	12.5	11.0	14.5	19.5	31.0	32.0
4	25.5	17.5	12.0	6.5	11.0	23.5	27.0	34.0
5	23.0	23.5	24.5	26.0	25.0	24.0	21.0	39.0
AVERAGE:	22.3	18.8	17.1	12.1	15.2	20.3	27.2	33.4
VARIANCE:	4.1	10.1	26.9	63.4	65.6	24.6	35.2	35.8
90%C.I.*:	1.4	2.2	3.6	5.4	5.5	3.4	4.1	4.1
VRM 160.7 - VRM 160.0								
1	10.0	6.0	16.0	23.0	33.5	36.0	37.0	36.5
2	15.0	11.0	9.0	16.0	25.0	31.0	31.0	26.0
3	13.0	10.5	7.5	18.5	25.5	27.5	24.5	23.0
4	12.0	9.0	12.0	21.0	27.5	31.5	29.5	31.5
5	9.5	7.5	6.0	11.5	22.5	22.0	28.0	36.0
AVERAGE:	11.9	8.8	10.1	18.0	26.8	29.6	30.0	30.6
VARIANCE:	5.1	4.3	15.8	20.1	17.2	27.2	21.1	35.9
90%C.I.*:	1.5	1.4	2.7	3.1	2.8	3.6	3.1	4.1

* +/- Confidence Interval for a 90% level of significance.

Table 5.2 (cont'd). Topographic shading data collected between Virgin River Mile (VRM) 163.1 and VRM 157.3 for southeast azimuths.

	AZIMUTH							
SAMPLE	45 (deg)	55 (deg)	65 (deg)	75 (deg)	85 (deg)	95 (deg)	105 (deg)	115 (deg)
VRM 160.0 - VRM 159.5								
1	14.5	5.0	9.0	16.5	18.0	25.5	34.0	30.5
2	13.0	7.5	8.0	15.5	15.5	25.5	28.5	33.5
3	17.0	10.5	7.0	12.5	15.5	14.0	25.5	28.0
4	14.5	16.0	18.0	21.0	24.0	28.0	31.0	34.0
5	35.0	22.0	9.0	14.0	21.0	27.0	27.0	31.0
AVERAGE:	18.8	12.2	10.2	15.9	18.8	24.0	29.2	31.4
VARIANCE:	84.1	46.8	19.7	10.4	13.6	32.4	11.3	5.9
90%C.I.* :	6.3	4.7	3.0	2.2	2.5	3.9	2.3	1.7
VRM 159.5 - VRM 158.4								
1	10.0	6.5	8.5	13.5	19.5	24.5	31.0	36.0
2	8.5	8.0	11.0	19.0	27.5	33.0	34.5	35.5
3	8.5	7.0	13.0	19.0	25.0	28.0	27.0	35.0
4	8.5	5.5	10.0	15.5	22.5	22.5	38.5	35.0
5	25.0	21.0	14.5	14.0	18.0	20.0	28.0	29.0
AVERAGE:	12.1	9.6	11.4	16.2	22.5	25.6	31.8	34.1
VARIANCE:	52.4	41.4	5.7	7.1	15.1	25.7	22.6	8.3
90%C.I.* :	5.0	4.4	1.6	1.8	2.7	3.5	3.3	2.0
VRM 158.4 - VRM 157.3								
1	18.5	16.0	7.0	8.0	14.0	20.5	20.5	24.5
2	16.5	12.5	7.5	10.0	15.0	18.5	20.5	21.0
3	8.5	5.5	6.0	9.5	16.0	27.0	29.0	29.0
4	19.0	12.0	11.0	8.0	14.0	14.0	15.5	26.5
5	14.5	11.0	14.5	15.5	18.5	25.5	34.0	37.0
AVERAGE:	15.4	11.4	9.2	10.2	15.5	21.1	23.9	27.6
VARIANCE:	18.1	14.4	12.3	9.6	3.5	27.9	55.4	36.2
90%C.I.*:	3.3	2.6	2.4	2.1	1.3	3.6	5.1	4.1

* +/- Confidence Interval for a 90% level of significance.

Accordingly, the azimuth at which the local sunrise and sunset occurred was figured by comparing for corresponding azimuths, sun altitude calculated by TEMP-84 to the average topographic altitude calculated from the field data. It was then determined between which two azimuths, for which fielddata was collected, the sun would rise or set. The average topographic angles for the two azimuths which bounded the local sunrise or local sunset were averaged for model input. In cases where a topographic altitude angle calculated from field data was within one degree of the sun's altitude, the topographic angle itself was used for model input. This analysis was conducted for southeast and southwest topographic angles for each section on each day modeled.

TEMP-84 establishes the south topographic angle to be representative of azimuths between 150 degrees and 210 degrees, clockwise from north. The average topographic angles calculated for these azimuths were averaged to obtain a south topographic shading angle for each section. Table 5.3 documents the southeast, south, and southwest topographic shading angles implemented for each section on each day selected for modeling.

Table 5.3. Average southwest, south, and southeast topographic shading angles for each of the delineated Virgin River stream reaches.

DATE	VRM 163.1 - 162.2			VRM 162.2 - 161.5			VRM 161.5 - 160.7			VRM 160.0 - 159.5		
	SE deg	S deg	SW deg	SE deg	S deg	SW deg	SE deg	S deg	SW deg	SE deg	S deg	SW deg
6-30-88	25.7	44.3	24.0	15.8	41.8	24.2	14.6	25.7	27.6	13.1	26.5	28.7
7-08-88	25.7	44.3	24.0	15.8	41.8	24.2	14.6	25.7	27.7	13.1	26.5	28.7
7-15-88	25.7	44.3	21.6	15.8	41.8	24.2	14.6	25.7	27.7	15.9	26.5	28.7
7-21-88	25.7	44.3	21.6	15.8	41.8	24.2	14.6	25.7	27.7	17.4	26.5	28.7

DATE	VRM 159.4 - 158.4			VRM 158.4 - 157.3		
	SE deg	S deg	SW deg	SE deg	S deg	SW deg
6-30-88	13.8	26.2	25.0	9.7	24.1	21.4
7-08-88	13.8	26.2	25.0	9.7	24.1	21.4
7-15-88	16.2	26.2	22.7	9.7	24.1	21.4
7-21-88	19.4	26.2	20.7	9.7	24.1	21.4

5.5 Vegetation Shading Angles

In addition to describing the shading resulting from surrounding topography, TEMP-84 requires data describing shading resulting from surrounding vegetation. This includes data for vegetation shading angles, hillslope angles, forest angles perpendicular to the stream axis, buffer width, canopy cover coefficients, percent of stream directly shaded, and tree height.

The vegetation shading angle was measured from horizontal at the stream surface to the top of the surrounding vegetation at the same azimuths and sampling sites for which topographic shading data was collected. For a given azimuth, the average of the five measurements within a section was calculated along with the sample variance and confidence interval defining, as calculated by the Student-t test, the range within which the calculated sample average represents the population average with a level of confidence of 90 percent. Table 5.4 documents the field collected data and calculated average vegetation shading angle for southeast azimuths. Vegetation shading data for south and southwest azimuths (Tables C.16 and C.17) are listed in Appendix C. Eighty percent of the collected 161 data sets satisfied a range of +/- ten degrees. Ninety-seven percent of the data sets produced an error range of less than or equal to +/- fifteen degrees.

TEMP-84 requires southeast, south, and southwest vegetation shading angle inputs for each stream section. Vegetation angles are potentially important throughout the day in contrast to the topographic angles which are primarily important during local sunrise and sunset. The calculated average vegetation shade angles for azimuths from 75 degrees, which is approximately sunrise, to 115 degrees, clockwise from

Table 5.4. Vegetation shading data collected between Virgin River Mile (VRM) 16.31 and VRM 157.3 for southeast azimuths.

	AZIMUTH							
SAMPLE	45 (deg)	55 (deg)	65 (deg)	75 (deg)	85 (deg)	95 (deg)	105 (deg)	115 (deg)
VRM 163.1 - VRM 162.2								
1	19.5	12.0	18.0	17.0	16.5	0.0	12.5	18.0
2	0.0	30.0	29.5	13.0	22.5	38.0	35.0	37.0
3	33.5	0.0	0.0	0.0	0.0	0.0	0.0	11.5
4	45.5	44.5	34.0	27.0	21.5	13.0	21.5	26.5
5	21.5	17.0	18.0	12.5	25.5	30.5	31.0	37.0
AVERAGE:	24.0	20.7	19.9	13.9	17.2	16.3	20.0	26.0
VARIANCE:	288.8	292.7	173.6	94.3	103.0	303.7	201.1	129.1
90%C.I.*:	11.6	11.7	9.0	6.6	6.9	11.9	9.7	7.8
VRM 162.2 - VRM 161.5								
1	27.0	16.0	14.0	13.5	19.0	8.0	14.0	13.0
2	33.5	22.0	22.0	12.0	12.5	7.0	12.0	23.0
3	22.5	20.0	21.5	22.5	29.5	25.5	19.0	14.0
4	18.5	22.0	26.5	20.0	8.0	8.0	7.5	14.5
5	35.5	33.0	28.0	13.0	16.0	28.0	30.0	38.5
AVERAGE:	27.4	22.6	22.4	16.2	17.0	15.3	16.5	20.6
VARIANCE:	51.6	39.8	29.9	22.3	65.6	110.2	74.0	116.2
90%C.I.*:	4.9	4.3	3.7	3.2	5.5	7.2	5.9	7.4
VRM 161.5 - VRM 160.7								
1	11.0	0.0	0.0	6.0	8.0	14.0	21.0	26.0
2	14.0	13.5	17.0	28.5	30.0	40.5	35.0	21.5
3	18.5	18.0	9.5	7.0	8.0	6.0	8.0	14.5
4	14.5	13.5	15.0	10.0	4.0	10.0	33.0	44.0
5	33.0	34.5	35.0	34.5	29.0	34.0	37.5	41.0
AVERAGE:	18.2	15.9	15.3	17.2	15.8	20.9	26.9	29.4
VARIANCE:	75.6	153.7	164.7	177.1	159.2	236.1	151.8	160.9
90%C.I.*:	5.9	8.5	8.8	9.1	8.6	10.5	8.4	8.7
VRM 160.7 - VRM 160.0								
1	22.0	27.0	15.0	9.5	15.5	17.5	21.0	20.0
2	10.5	6.5	9.0	13.0	18.0	19.5	49.5	59.0
3	10.0	16.0	7.0	20.0	22.0	28.5	29.0	26.0
4	11.5	18.0	28.0	36.0	39.5	38.0	39.0	39.5
5	23.0	18.5	13.5	16.5	0.0	13.0	30.0	32.5
AVERAGE:	15.4	17.2	14.5	19.0	19.0	23.3	33.7	35.4
VARIANCE:	42.4	53.6	67.5	105.6	200.9	99.3	118.7	226.9
90%C.I.*:	4.5	5.0	5.6	7.0	9.7	6.8	7.5	10.3

* +/- Confidence Interval for a 90% level of significance.

Table 5.4 (cont'd). Vegetation shading data collected between Virgin River Mile (VRM) 163.1 and VRM 157.3 for southeast azimuths.

SAMPLE	45 (deg)	55 (deg)	65 (deg)	75 (deg)	85 (deg)	95 (deg)	105 (deg)	115 (deg)
	AZIMUTH							
VRM 160.0 - VRM 159.5								
1	11.5	24.0	13.0	14.0	19.0	0.0	16.0	18.5
2	5.0	9.5	14.5	19.5	23.5	25.5	24.0	25.0
3	0.0	12.0	8.5	5.5	6.0	14.0	22.0	29.0
4	15.5	18.0	23.0	30.5	30.5	34.0	35.5	36.0
5	37.0	24.5	10.0	8.0	5.0	0.0	8.0	0.0
AVERAGE:	13.8	17.6	13.8	15.5	16.8	14.7	21.1	21.7
VARIANCE:	203.6	46.4	32.1	99.9	123.3	230.5	103.6	187.5
90%C.I.*:	9.8	4.7	3.9	6.8	7.6	10.4	7.0	9.4
VRM 159.5 - VRM 158.4								
1	8.5	8.0	18.0	20.0	20.0	26.0	34.0	32.0
2	5.5	12.5	18.0	23.0	32.0	34.5	30.5	45.0
3	10.0	10.0	13.5	0.0	14.0	17.5	16.5	28.5
4	9.0	5.5	3.0	6.5	17.0	11.5	0.0	0.0
5	27.5	21.0	15.0	0.0	11.0	26.0	13.5	0.0
AVERAGE:	12.1	11.4	13.5	9.9	18.8	23.1	18.9	21.1
VARIANCE:	76.9	35.4	38.3	120.3	65.7	78.2	188.7	408.8
90%C.I.*:	6.0	4.1	4.2	7.5	5.5	6.0	9.4	13.8
VRM 158.4 - VRM 157.3								
1	0.0	16.5	8.5	9.0	9.0	10.0	19.5	13.0
2	14.5	9.5	5.5	23.0	17.0	21.0	23.5	27.5
3	5.5	8.0	7.5	10.0	17.0	27.0	29.5	32.0
4	49.5	35.5	31.0	26.0	25.0	20.0	0.0	11.0
5	9.5	19.5	17.5	20.0	24.5	30.0	28.5	29.0
AVERAGE:	15.8	17.8	14.0	17.6	18.5	21.6	20.2	22.5
VARIANCE:	383.2	120.7	111.5	59.3	43.3	59.3	143.7	95.0
90%C.I.*:	13.4	7.5	7.2	5.3	4.5	5.3	8.2	6.7

* +/- Confidence Interval for a 90% level of significance.

North, were averaged for the southeast angle. The average shading angles for azimuths between 150 and 210 degrees were averaged to obtain a representative south vegetative shading angle. The average shading angles between azimuths of 240 degrees to approximately sunset at 290 degrees were averaged for the southwest vegetative angle. Table 5.5 documents southeast, south, and southwest vegetation shading angles implemented in TEMP-84 simulations.

Table 5.5. Average southwest, south, and southeast vegetation shading angles for each of the delineated Virgin River stream reaches.

ANGLE	VRM 163.1 - 162.2 deg	VRM 162.2 - 161.5 deg	VRM 161.5 - 160.7 deg
SE	18.9	18.0	20.9
S	38.9	32.9	20.2
SW	22.1	17.3	17.4

ANGLE	VRM 160.0 - 159.5 deg	VRM 159.4 - 158.4 deg	VRM 158.4 - 157.3 deg
SE	17.3	17.6	19.1
S	20.2	22.1	19.3
SW	13.5	15.2	14.4

Hillslope angles for the left and right side of the stream were either measured with the abney level or estimated by eye at each of the five data collection sites within a section. The five data points for the left and right side of the stream respectively, were then averaged for model input. Hillslope angles ranged from 41.9 degrees at the upstream end of the reach to 0.0 degrees at the downstream end. Hillslope data and calculated averages are listed in Table C.18.

Forest angles perpendicular to the stream axis for the left and right side of the stream were measured at the five data collection sites in each section. Similar to topographic and vegetation shading angles, the forest angle was measured with an abney level from horizontal at the stream surface to the estimated average forest vegetation height alongside the stream. The five measurements per section on the right and left side of the stream respectively, were averaged for model input. Perpendicular forest angles ranged from 42.7 degrees at the upstream end of the study reach to 27.6 degrees towards the downstream end. Forest angle data and calculated averages are listed in Table C.18.

Model documentation stated that the buffer width should be considered continuous unless it is well defined. Since there is no well defined buffer width along the study reach a value of -1 was input which depicts a continuous buffer width.

The canopy cover coefficient represents the canopy density. According to the TEMP-84 model documentation it "reflects the amount of energy that is allowed to pass directly through the forest canopy without being intercepted by the canopy." A value of 0 represents no canopy while a value of 1 represents a dense forest. Values for canopy cover coefficients at each of the data collection sites were estimated based on the degree to which the vegetation blocked the background from view. Estimated canopy cover coefficients within each section were averaged for model input. Canopy cover coefficients ranged from 0.65 to 0.35. Table C.18 documents the collected data and the calculated canopy cover coefficient for each section.

The percentage of stream directly shaded by overhanging vegetation was determined at each of the five data collection sites within each section. It was calculated by dividing the length of stream width directly shaded by the total stream width. The average percent of stream directly shaded ranged from 3.3 percent to 0.0 percent over the seven sections. Table C.18 documents the calculated percent of stream directly shaded for each section.

Forest vegetation height or tree height was determined by indirect means. The vertical distance from eye level to the top of the tree was determined through trigonometric calculations. The vertical distance from eye level to the tree base was added to obtain the total tree height. The five calculated tree height values, for each side of the stream within each section, were averaged to obtain tree height values for model input. Tree height ranged from 12.7 m to 4.9 m. Table C.19 documents field collected data and computations for tree height for the right and left, facing upstream, side of the stream.

5.6 Groundwater Accretion

A mass balance analysis was conducted to determine the groundwater accretion. Discharge measurements made along the study reach were subtracted to quantify the accretion occurring between the two measurement sites. All discharge measurements were made within five hours of each other except for the specific measurements cited in the following paragraph.

Table 5.6 documents the groundwater accretion data collected for the East Fork of the Virgin River within ZION. It delineates the discharge measured at each site and the time at which it was taken. Note that on 6-30-88, the discharge at VRM 157.4 was measured on 7-1-88 rather than 6-30-88. Considering that base flow conditions existed throughout 6-30-88 and 7-1-88, this discharge measurement was assumed acceptable for the analysis. A similar situation exists for the data collected on 6-3-88. Due to time constraints, the discharge at VRM 162.2 was not measured until the morning of 6-4-88. Again, flow conditions did not change and removing the measurement from the analysis was not warranted.

Accretion data collected on 5-27-88 was collected by other members of the National Park Service field crew as were the discharge measurements taken at VRM 157.4. All field crew members were thoroughly trained and experienced in taking discharge measurements. The accretion data set on 5-27-88 was collected for purposes other than the stream temperature study. It incorporates a discharge at VRM 163.9, ie., the East ZION boundary, while the discharge at VRM 162.2 was omitted.

Table 5.6. Groundwater accretion data collected along the reach between Virgin River Mile (VRM) 163.1 and VRM 157.3.

SITE	DAY	TIME	DISCHARGE l/s	DIFF l/s
VRM 163.9	5-27-88	1411	954	
VRM 163.1	5-27-88	1656	957	3
VRM 161.5	5-27-88	1853	1056	99
VRM 157.4	5-27-88	1610	1175	119
TOTAL ACC				221

SITE	DAY	TIME	DISCHARGE l/s	DIFF l/s
VRM 163.1	6-30-88	1126	957	
VRM 162.2	6-30-88	0950	1017	60
VRM 161.5	6-30-88	0844	1096	79
VRM 157.4	7-01-88	0948	1005	-91
TOTAL ACC				48

SITE	DAY	TIME	DISCHARGE l/s	DIFF l/s
VRM 163.1	6-03-88	1644	1076	
VRM 162.2	6-04-88	0814	1113	37
VRM 161.5	6-03-88	1400	1204	91
VRM 157.4	6-03-88	1700	1252	48
TOTAL ACC				176

SITE	DAY	TIME	DISCHARGE l/s	DIFF l/s
VRM 163.1	7-15-88	1130	926	
VRM 162.2	7-15-88	1010	991	65
VRM 160.0	7-15-88	0802	1056	65
VRM 157.4	7-15-88	1230	1107	51
TOTAL ACC				181

SITE	DAY	TIME	DISCHARGE l/s	DIFF l/s
VRM 163.1	6-24-88	1222	1085	
VRM 162.2	6-24-88	1037	1054	-31
VRM 161.5	6-24-88	0920	1127	74
VRM 157.4	6-24-88	1111	1263	136
TOTAL ACC				178

The data set of 7-15-88 incorporated a discharge at VRM 160.0 where a change in the geologic formation bounding the alluvium streambed occurs. The discharge at VRM 161.5 was omitted. On afterthought, it was realized that omission of the discharge at VRM 161.5 prevented comparison of accretion in the individual reaches calculated for 7-15-88 to accretion in the individual reaches of the other data sets. No other groundwater accretion data sets were collected for which to compare the groundwater accretion upstream and downstream of VRM 160.0.

It was evident for the individual reaches, that neither a trend or consistency in groundwater accretion could be deciphered due to fluctuations in the groundwater accretion measured and the lack of consistency in site location. The groundwater accretion from VRM 163.1 to VRM 162.2 ranged from -31 l/s (-1.1 cfs) to 65 l/s (2.3 cfs). Accretion from VRM 162.2 to VRM 161.5 seemed to be slightly more stable ranging from 74 l/s (2.6 cfs) to 91 l/s (3.2 cfs) while the accretion from VRM 161.5 to VRM 157.4 ranged from -91 l/s (-3.2 cfs) to 136 l/s (4.8 cfs).

In contrast to the sporadic nature of the data for groundwater accretion of individual segments, the groundwater accretion for the entire study reach, from VRM 163.1 to VRM 157.4, was somewhat consistent. Figure 5.9 illustrates the groundwater accretion measured between VRM 163.1 and VRM 157.4 plotted against time. Three of the five data points have a range of 5.7 l/s (0.2 cfs). The accretion calculated for 5-27-88 was slightly higher at a value of 221 l/s (7.8 cfs). Accretion for 6-20-88 appears to be an outlying point but is within the precision of the measurement, i.e., approximately +/- 170 l/s (6 cfs). The five data points were averaged to arrive at a groundwater accretion of 161 l/s (5.7 cfs) for the entire study reach. This accretion was distributed evenly along the study reach as no justification existed for weighting it otherwise. In reality, this calculated accretion represents the difference between the total flow accretion through groundwater and overland spring flow and the total loss of water through infiltration, evaporation, and evapotranspiration.

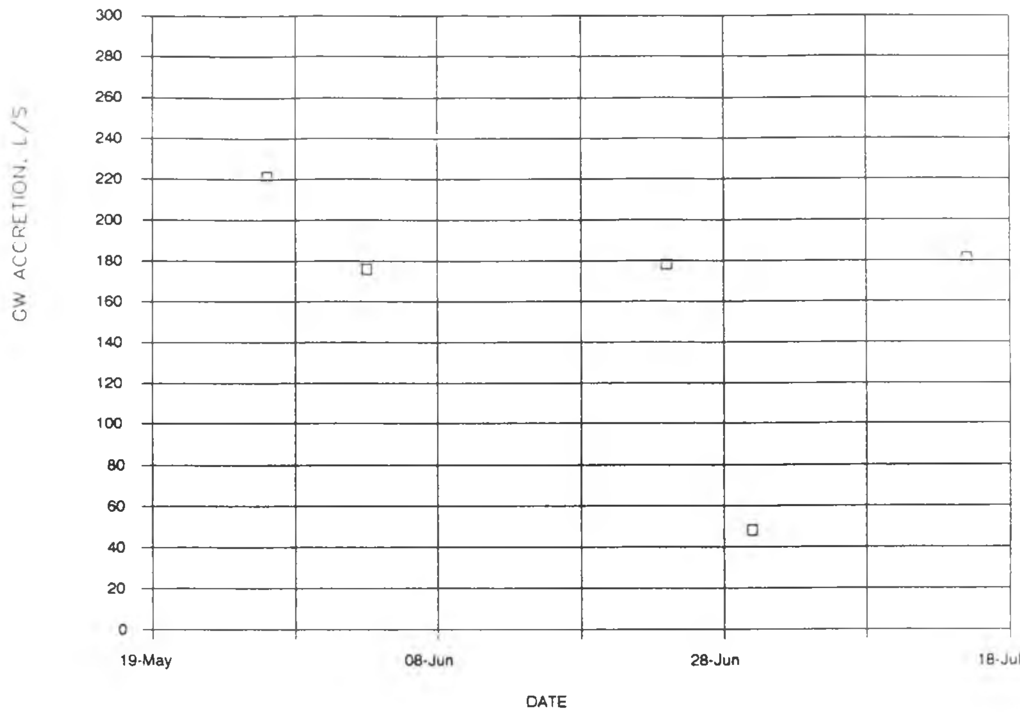

Fig. 5.9 Discrete groundwater accretion measurements for the reach of Virgin River Mile (VRM) 163.1 to VRM 157.3.

5.7 Groundwater Temperature

Groundwater temperature data collected on 6-3-88 and 7-15-88 was averaged to produce groundwater temperature estimates of 14.9°C and 14.5°C respectively. Table 5.7 documents spring temperatures measured at the spring source and the calculated averages. Data collected on 6-24-88 and 6-30-88 was not valid for analysis as a separation in the mercury fluid of the thermometer existed during this time. The average groundwater temperature values of 14.9°C and 14.5°C from 6-3-88 and 7-15-88 respectively, were averaged to 14.7°C for model input.

5.8 Discharge

Discharge was quantified throughout the 1988 field season for purposes other than the stream temperature study by direct measurement with pygmy or Price AA vertical axis current meter at a selected cross section located at VRM 157.4. Base flow conditions depicted by a stage value of 0.33 m to 0.34 m, existed throughout the stream temperature study period. Between 6-29-88 and 7-22-88, three discharge measurements were made: 991 l/s (35 cfs) on 7-1-88, 1048 l/s (37 cfs) on 7-5-88, and 1104 l/s (39 cfs) on 7-15-88. The three measurements were averaged at 1076 l/s (38 cfs) for a baseflow discharge value at VRM 157.3.

Table 5.7. Groundwater temperature measured at the source of springs entering the East Fork between Virgin River Mile (VRM) 163.1 and VRM 157.3.

SPRING #	DATE	SPRING TEMP C	CALIB TEMP C	SPRING#	DATE	SPRING TEMP C	CALIB TEMP C
7-S-1-R	6-3-88	16.7	15.6	7-S-1-R	7-15-88	15.3	14.1
7-S-3-R	6-3-88	15.6	14.4	7-S-3-R		-	-
6-S-1-R	6-4-88	16.9	15.9	6-S-1-R	7-15-88	15.3	14.1
4-S-1-L	6-4-88	15.0	13.8	4-S-1-L	7-15-88	17.2	16.2
3-S-1-R		-	-	3-S-1-R	7-15-88	15.0	13.8
AVERAGE:			14.9	AVERAGE:			14.5

5.9 Topographic Map Data

Stream section aspect, stream section gradient, stream section length, and mean elevation of the entire study reach are model inputs characterizing the study reach. They were determined from the Springdale East, Utah and Barracks, Utah USGS quadrangle maps. Both maps were to the scale of 1:24,000.

The length of each delineated section was measured with a map wheel which was precise to +/- 61 m (200 ft). Each section boundary was assigned a river mile which conformed to the Pacific Southwest Inter-Agency Committee (PSIC) River Mile Index. Table 5.8 documents each section length measured from USGS quadrangle maps and the corresponding river mile.

Table 5.8. Lengths of the delineated Virgin River reaches as measured from USGS quadrangle maps.

SECTION	LENGTH feet	LENGTH meters	LENGTH mile	RIVER MILE
1	5768	1758.0	1.09	VRM 157.3 - VRM 158.4
2	5600	1706.9	1.06	VRM 158.4 - VRM 159.5
3	2411	734.9	0.46	VRM 159.5 - VRM 160.0
4	3500	1066.8	0.66	VRM 160.0 - VRM 160.7
5	4028	1227.7	0.76	VRM 160.7 - VRM 161.5
6	3600	1097.3	0.68	VRM 161.5 - VRM 162.2
7	4564	1391.0	0.86	VRM 162.2 - VRM 163.1

The stream aspect of each section was estimated on the map and measured with a protractor. The aspect was selected such to represent the general direction of the stream section; the sinuosity around the general direction was neglected. The model requires the aspect to be quantified by the number degrees clockwise from North to an imaginary vector directed downstream. Stream aspects were described to the nearest degree and are estimated to be accurate within +/- 5 degrees. Table 5.9 documents the stream aspect of each section as determined from USGS quadrangle maps.

Table 5.9. Gradient and aspect for the delineated Virgin River reaches as determined from USGS quadrangle maps. Aspect represents the angle clockwise from North to the vector pointed downstream.

SECTION	GRADIENT m/m (ft/ft)	ASPECT degrees
VRM 157.3 - VRM 158.4	0.0091	259
VRM 158.4 - VRM 159.5	0.0097	248
VRM 159.5 - VRM 160.0	0.0098	251
VRM 160.0 - VRM 160.7	0.0101	247
VRM 160.7 - VRM 161.5	0.0105	253
VRM 161.5 - VRM 162.2	0.0159	275
VRM 162.2 - VRM 163.1	0.0323	277

The stream gradient for each study reach section was determined by first measuring the length between adjacent contour lines crossed by the stream and calculating the corresponding gradient. It was assumed that the gradient between two contour lines was constant. Each gradient represented within a given section was then weighted by the length to which it corresponded. The weighted gradients were then summed and divided by the total length of the given section. Table 5.9 documents the gradient of each section as determined from USGS quadrangle maps.

The mean elevation of the study reach was determined in a manner similar to that used to calculate study reach stream gradients. The mean elevation between adjacent contour lines was calculated and weighted by the distance between the corresponding contours. The weighted elevations were summed and divided by the total distance between the upstream and downstream contour lines which encompassed the study reach. The mean elevation, calculated by this technique was determined to be 1241 m.

5.10 Width

The model requires for each section a representative stream width. Width measurements were made six times (6-4-88, 6-24-88, 6-30-88, 7-9-88, 7-15-88, and 7-23-88) throughout the field season. Theoretically, width measurements were repeated to establish the variance of the stream width during the study period. However, since base flow conditions existed throughout the study period, repeated measurements illustrated discrepancies due to different interpretations of which cross section was perpendicular to the stream, inconsistency in defining the stream edge, and inconsistency in subtracting the width of protruding rocks in the stream surface. To alleviate this problem, data collection trips on 7-23-88 and 8-5-88 incorporated defining consistent criteria for which to calibrate all width measurements, i.e., what length of protruding rocks to subtract and where the edge of water should be defined. Calibration of previous measurements was possible for those measurements which were well documented in terms of what was included in and subtracted from the width. Measurements which were not documented clearly were deleted from the analysis. It was assumed that for each measurement, the cross section was correctly judged to be perpendicular to the stream flow. All calibrated width measurements for each cross section were averaged in order to balance the random errors in the measurements as well as determine one width value for each cross section. Table C.20 documents the width measurements at designated cross sections and the calculated averages. Average stream widths were then grouped according to the section in which they were located and averaged again to obtain a section average stream width.

Table 5.10 documents for each section, the average width, variance, and confidence interval, defining, according to the Student-t test, the range within which the calculated sample average represents the population average with a level of confidence of 90 percent. All sections had a confidence interval less than 10 percent of the width which is consistent with the sampling scheme design. Average section width ranged from 6.4 m for the most upstream section to 8.6 m for the most downstream section.

Table 5.10. Calculated average width and computed statistics from stream width data collected within the delineated Virgin River Mile reaches.

SECTION	COUNT	AVERAGE m	VARIANCE m^2	90%C.I.* m
VRM 163.1 - 162.2	22	6.4	8.0	0.4
VRM 162.2 - 160.0	19	8.1	3.9	0.3
VRM 160.9 - 159.5	10	7.5	4.6	0.5
VRM 159.5 - 157.3	22	8.6	12.0	0.5

* Confidence interval for a 90% level of significance.

5.11 Percent Bedrock

Data for determining the percent of streambed which is at a depth of less than twenty centimeters and comprised of bedrock greater than twenty-five centimeters in axis was estimated with an approximated precision of +/- 0.15 m. The cross section's percentage meeting the stated criteria was determined by dividing the measured width of bedrock by the average width of the cross section as determined from the width analysis. Bedrock percentages within each study reach section were averaged for an appropriate value for model input. The largest calculated percentage of bedrock was 12.7 percent for the section from VRM 158.4 to VRM 159.5. Table C.21 documents the calculated percentage of streambed for each section comprised of depth less than twenty centimeters and bedrock greater than twenty-five centimeters in axis.

5.12 Velocity

Stream velocity was characterized by float test measurements utilizing oranges as floats on several float lengths throughout the study reach. Float test data represents the surface velocity of the stream. To obtain an average stream velocity, a coefficient of 0.85 was applied to the calculated average surface velocity (Buchanan, 1969).

Velocity data was collected on 6-4-88, 6-24-88, 6-30-88, and 7-15-88. Data collected on 6-4-88 was omitted from the data set due to inconsistent measuring techniques in implementing the float test. Data points from the remaining data sets were also omitted if the delay time due to the influence of eddies on the float was not recorded and thus could not be subtracted from the float time. The travel time for each float through designated float sections is documented in Table C.22.

Six float tests were conducted within each float length. The travel times for each float length were averaged and divided by the distance to obtain an average surface velocity for that day. The average surface velocity for each float length, for each day, was then grouped according to the section in which it was located and averaged for an average velocity per section per day. Table 5.11 documents the average surface velocity for each section on each day.

Table 5.11. Average surface velocity as calculated from velocity data collected within the delineated Virgin River reaches.

	6-24-88	6-30-88	7-15-88	AVERAGE
SECTION	AVERAGE VELOCITY m/s	AVERAGE VELOCITY m/s	AVERAGE VELOCITY m/s	AVERAGE VELOCITY m/s
VRM 163.1 - 162.2	0.76	0.88	0.78	0.81
VRM 162.2 - 160.0	0.91	0.89	0.91	0.90
VRM 160.0 - 159.5	0.90	0.81	0.97	0.89
VRM 159.5 - 157.3	0.99	0.84	0.88	0.90
AVERAGE SURFACE VELOCITY FOR ENTIRE STUDY REACH:				0.88

The average surface velocities calculated for 6-24-88, 6-30-88, and 7-15-88, for a given section were within 0.18 m/s of each other. This change in velocity approximates a maximum of 24 percent of the measured velocity while the rated precision of the measurement is 25 percent (Buchanan, 1969). In addition, the flow throughout the three data collection trips was at base flow condition as depicted by the staff plate reading of 0.33 m for each day. Upon consideration of the precision of the measurements and the base flow conditions, the average surface velocities from the three data collection trips were averaged to obtain, for each section, an average surface velocity for base flow conditions. The average surface velocity for each section differed by less than 0.15 m/s from the average surface velocity of any other section. Again, it was decided that delineation with respect to surface velocity between sections was not warranted. Accordingly, the average surface velocities from the individual sections were combined to obtain an average surface velocity for the study reach of 0.88 m/s. Applying the correction factor of 0.85 for surface velocity produces an average stream velocity of 0.76 m/s.

5.13 Relative Humidity and Wind

Model input requires a single relative humidity value measured at 1300 hour. Relative humidity point samples were taken around 1300 hour with a sling psychrometer but the data is sporadic with respect to the time it was taken, the location at which it was taken, and the measuring technique. Due to these inconsistencies in addition to the overall lack of data, relative humidity data collected by the ZION weather station was used for model input. Table C.23 documents the average, which was calculated by ZION from the maximum and minimum relative humidity readings, and 1400 hr relative humidity values measured at the ZION weather station. From 6-29-88 through 7-22-88 the measured 1400 hr relative humidity ranged from 8 percent to 34 percent with an average of 15.0 percent. Values measured at 1400 hr were used for model input as they were measured relatively close in time to the desired 1300 hr.

Windspeed data was collected with a hand held anemometer in a similar fashion to the relative humidity. Moreover, it was collected sporadically with respect to time and location of the measurements. The maximum wind speed measured along the study reach was 19 km/hr. The majority of windspeeds measured did not reach the minimum 8 km/hr mark on the scale of the hand held anemometer. As with the relative humidity data, official windspeed data collected at the ZION weather station was utilized for model input. Windspeed measurements by ZION were taken as a point sample at 1400 hr with a stationary anemometer. The ZION wind data should only be considered a rough estimate of the daily average windspeed along the study reach. Table C.24 documents the wind data collected by ZION. Windspeed ranged from 0.0 to 24 km/hour between 6-29-88 and 7-22-88. The average windspeed was 7.1 km/hour.

5.14 Stream Characteristics under Hypothetical Conditions

Since TEMP-84 does not model flow through the study system, representative width and velocity values were simulated for hypothetical flow simulations. The computer program, NEWCHAN (BLM, 1985) developed by the Bureau of Land Management (BLM), was utilized on channel profile and water surface slope data to develop relationships between flow and stream width and stream velocity. Tables C.25 through C.27 document the channel profile data of the seven cross sections profiled and C.28 documents the water surface slope data. The Manning's "n" roughness coefficient was solved for empirically from flow, channel profile, and water surface slope data for existing conditions. Table 5.12 documents the discharge, water surface slope, channel area, and Manning's n value modeled for existing conditions at each cross section .

Utilizing a constant Manning's n value and water surface slope, a range of stage values were input for which the BLM program computed the velocity, channel area, hydraulic radius, top width, and wetted perimeter. Tables C.29 through C.36 document the rating tables with respect to discharge, width, and velocity developed for each cross section for flow greater than and less than 2832 l/s (100 cfs). Figure 5.10 and 5.11 show for cross section one, which is located between VRM 157.3 and VRM 158.4, plots of width versus discharge and velocity versus discharge, respectively. Similar plots were constructed for the remaining six cross sections and were utilized for flow greater than 2832 l/s. Plots were also developed for flow less than 2832 l/s.

Table 5.12. Measured discharge and NEWCHAN (BLM, 1985) modeled values for discharge, water surface slope, channel area, and Manning's "n" values for existing conditions on the delineated Virgin River reaches.

CROSS-SECTION	LOCATION	MEAS. DISCHARGE l/s	CALC. DISCHARGE l/s	WATER SURFACE SLOPE m/m	CHANNEL AREA m^2	MANNING'S "n"
#1	VRM 157.3 - 158.4	1033.7	1047.8	0.0042	1.5	0.031
#2	VRM 158.4 - 159.5	1053.5	1062.0	0.0084	1.6	0.046
#3	VRM 159.5 - 160.0	1016.7	1008.2	0.0028	2.0	0.045
#4	VRM 160.0 - 160.7	1030.8	1028.0	0.0046	1.7	0.039
#5	VRM 160.7 - 161.5	1127.1	1107.3	0.0046	1.8	0.034
#6	VRM 161.5 - 162.2	1036.5	1045.0	0.0047	1.7	0.036
#7	VRM 162.2 - 163.1	0923.2	0917.6	0.0022	2.1	0.042

Width and velocity values were then read off the respective figure for the selected hypothetical flow value. Similar to data analysis for baseflow conditions, width and velocity values were grouped according to the section in which the respective cross section was located and then averaged for a representative section value. Table 5.13 documents the width and velocity values determined for the selected hypothetical flows.

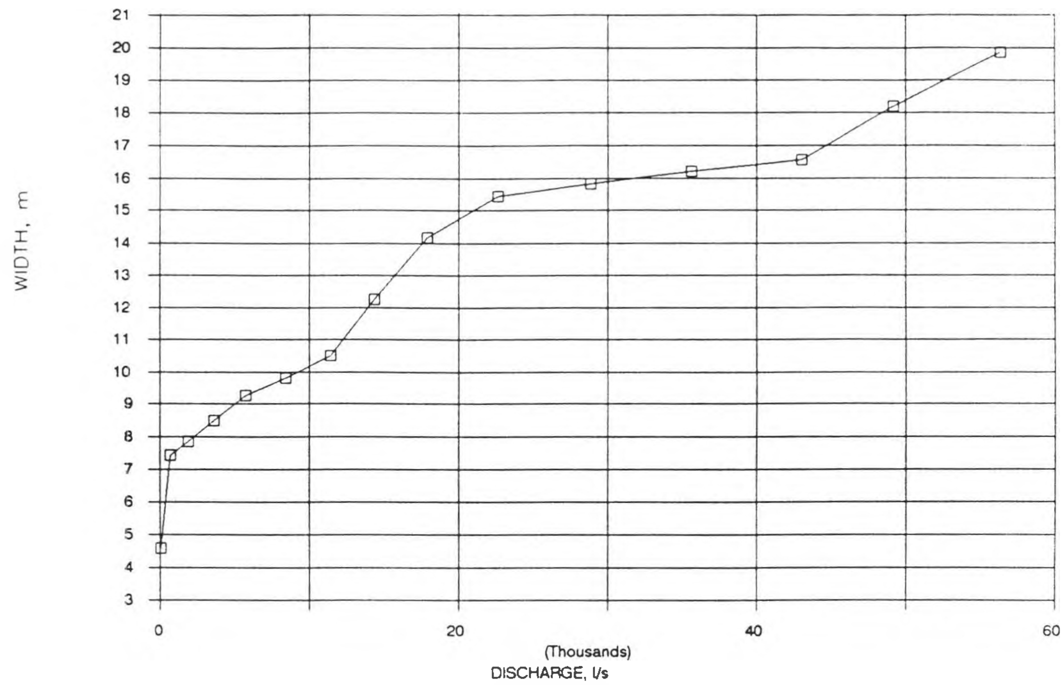

Fig. 5.10 NEWCHAN (BLM, 1985) modeled width values plotted against discharge values for the reach between Virgin River Mile (VRM) 157.3 and VRM 158.4.

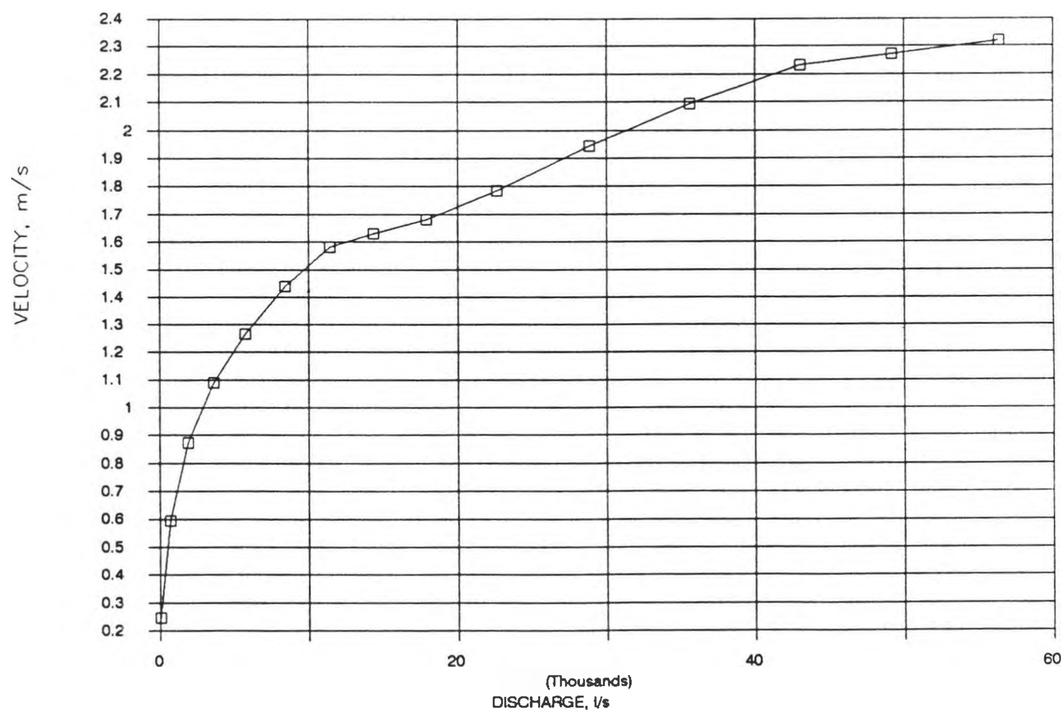

Fig. 5.11 NEWCHAN (BLM, 1985) modeled velocity values plotted against discharge for the reach between Virgin River Mile (VRM) 157.3 and VRM 158.4.

Table 5.13. NEWCHAN (BLM, 1985) modeled average width and velocity values for the delineated Virgin River reaches.

SECTION	28,320 l/s (1000 cfs) AVERAGE VELOCITY m/s	AVERAGE WIDTH m	14,160 l/s (500 cfs) AVERAGE VELOCITY m/s	AVERAGE WIDTH m	2,832 l/s (100 cfs) AVERAGE VELOCITY m/s	AVERAGE WIDTH m
VRM 162.2 - 163.1	1.3	15.6	1.0	14.3	0.6	10.3
VRM 160.0 - 162.2	1.8	14.9	1.5	12.4	0.9	9.3
VRM 159.5 - 160.0	1.2	18.5	1.0	16.0	0.7	8.1
VRM 157.3 - 159.5	1.9	16.6	1.5	13.5	0.9	9.1

SECTION	2,124 l/s (75 cfs) AVERAGE VELOCITY m/s	AVERAGE WIDTH m	906 l/s (32 cfs) AVERAGE VELOCITY m/s	AVERAGE WIDTH m	566 l/s (20 cfs) AVERAGE VELOCITY m/s	AVERAGE WIDTH m
VRM 162.2 - 163.1	0.6	9.8	0.4	8.0	0.4	7.0
VRM 160.0 - 162.2	0.8	9.1	0.6	8.6	0.5	8.2
VRM 159.5 - 160.0	0.6	7.6	0.5	6.9	0.4	6.5
VRM 157.3 - 159.5	0.9	8.4	0.6	7.5	0.5	7.3

SECTION	283 l/s (10 cfs) AVERAGE VELOCITY m/s	AVERAGE WIDTH m
VRM 162.2 - 163.1	0.3	6.2
VRM 160.0 - 162.2	0.4	7.6
VRM 159.5 - 160.0	0.3	5.6
VRM 157.3 - 159.5	0.4	7.0

The percent of the stream that is less than twenty centimeters deep and comprised of bedrock greater than twenty-five centimeters in axis was also affected by hypothetical flows. For all flows greater than baseflow, this distance was set to zero as the flow becomes deep and the amount of bedrock on existing banks is negligible. For flows less than or equal to baseflow, it was assumed that this distance was the same as that calculated for baseflow conditions. This distance was then divided by the hypothetical stream width for a corresponding discharge.

Table 5.14 documents percent bedrock and percent overhanging vegetation data for the selected hypothetical flows. The percent of stream that is directly shaded by overhanging vegetation was assumed to be zero for the smallest hypothetical flow of 283 l/s (10 cfs). For all other flows, the distance estimated for overhanging vegetation was assumed to remain constant equal to that measured for baseflow conditions. This distance was then divided by the hypothetical stream width for the corresponding discharge.

Table 5.14. TEMP-84 model input for percent bedrock and percent direct shade for the delineated Virgin River reaches for the selected hypothetical flows.

	28,320 l/s (1000 cfs)		14,160 l/s (500 cfs)		2,832 l/s (100 cfs)	
SECTION	% BEDROCK	% DIRECT SHADE	% BEDROCK	% DIRECT SHADE	% BEDROCK	% DIRECT SHADE
VRM 162.2 - 163.1	0.0	0.0	0.0	0.0	0.0	0.0
VRM 160.0 - 162.2	0.0	1.1	0.0	1.3	0.0	1.7
VRM 159.5 - 160.0	0.0	0.7	0.0	0.8	0.0	1.5
VRM 157.3 - 159.5	0.0	1.4	0.0	1.7	0.0	2.5

	2,124 l/s (75 cfs)		906 l/s (32 cfs)		566 l/s (20 cfs)	
SECTION	% BEDROCK	% DIRECT SHADE	% BEDROCK	% DIRECT SHADE	% BEDROCK	% DIRECT SHADE
VRM 162.2 - 163.1	0.0	0.0	2.6	0.0	3.0	0.0
VRM 160.0 - 162.2	0.0	1.8	5.6	1.9	5.9	2.0
VRM 159.5 - 160.0	0.0	1.6	14.3	1.8	15.2	1.9
VRM 157.3 - 159.5	0.0	2.7	9.5	3.0	9.8	3.1

Table 5.14 (cont'd). TEMP-84 model input for percent bedrock and percent direct shade for the delineated Virgin River reaches for the selected hypothetical flows.

	283 l/s (10 cfs)	
SECTION	% BEDROCK	% DIRECT SHADE
VRM 162.2 - 163.1	3.4	0.0
VRM 160.0 - 162.2	6.3	0.0
VRM 159.5 - 160.0	17.5	0.0
VRM 157.3 - 159.5	10.2	0.0

Chapter 6. Simulation of Existing Conditions

6.1 Simulation of the Time of Peak Temperature

The initial simulations of existing conditions for 6-30-88, 7-08-88, 7-15-88, and 7-21-88, depicted a consistent one to two hour lag of the modeled peak temperature behind measured. A detailed sensitivity analysis demonstrated a one hour forward shift in the modeled time of peak temperatures and a 5.5 percent (1.8°C) drop in the maximum temperature with a 50 percent decrease in velocity. To determine if a 50 percent decrease in the velocity input would be justified, the accuracy of the velocity field data was evaluated. Moreover, velocities measured by the floating chip method were compared to velocities measured by a vertical axis current meter. Table D.1 in Appendix D documents this comparison. Where the floating chip method measured an average velocity of 0.85 m/s, the 30 member set of point velocity measurements collected with a vertical axis current meter measured an average velocity of 0.57 m/s. The average velocity measured by the vertical axis current meter was 32 percent less than the average velocity measured by the floating chip method. Considering that the floating chip measurement is accurate to +/-25 percent (Buchanan, 1969) and the velocity measurements by the vertical axis current meters are considered accurate to +/- 15 percent, a decrease in the velocity input value of 50 percent is not unreasonable. Accordingly, the value of the velocity component utilized in simulation of existing conditions, 0.38 m/s, is 50 percent less than the value of 0.76 m/s determined from data analysis of the field collected velocity measurements. As a result, the peak temperatures of the final simulations of existing conditions occur within one hour of those measured.

6.2 Simulation of Existing Stream Temperature

TEMP-84 is a physical process model which uses equations to describe the heat flux between the stream and surrounding media. It does not incorporate regression equations, rating curves, or calibration coefficients. As a result, calibration "tools" other than the input data set are not available. Furthermore, clear justification must be made for modifying the model input data set. For a model such as TEMP-84, simulation of existing conditions serves as a measure of "how well" TEMP-84 simulates the respective study reach rather than an exercise by which to match modeled output to measured values.

Figures 6.1, 6.2, 6.3, and 6.4 depict the modeled and measured diurnal fluctuation of the stream temperature at VRM 157.3. Hourly stream temperature values for both measured and modeled regimes are logged in Table D.2. In all cases, the modeled stream temperature regime illustrated a greater diurnal fluctuation than measured. The maximum, mean, and minimum stream temperature for each curve is documented in Table D.3. The difference between modeled and measured maximum stream temperature ranged from 0.3°C (1.1 percent) on 7-21-88 to 2.0°C (7.4 percent) on 6-30-88. The difference between minimum stream temperature values ranged from 1.1oC (6.3 percent) on 7-21-88 to 1.8oC (10.1 percent) on 6-30-88. Modeled mean temperatures were always less than the measured mean temperatures with a difference

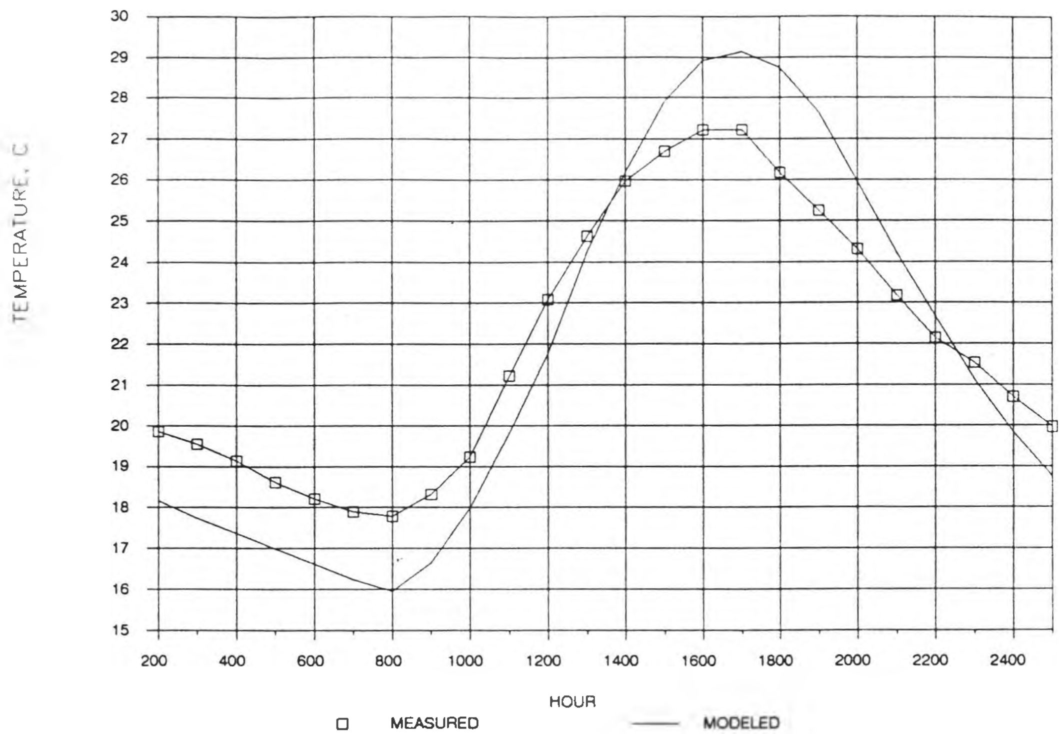

Fig. 6.1 Measured and TEMP-84 modeled diurnal fluctuation in stream temperature at Virgin River Mile 157.3 on 6-30-88.

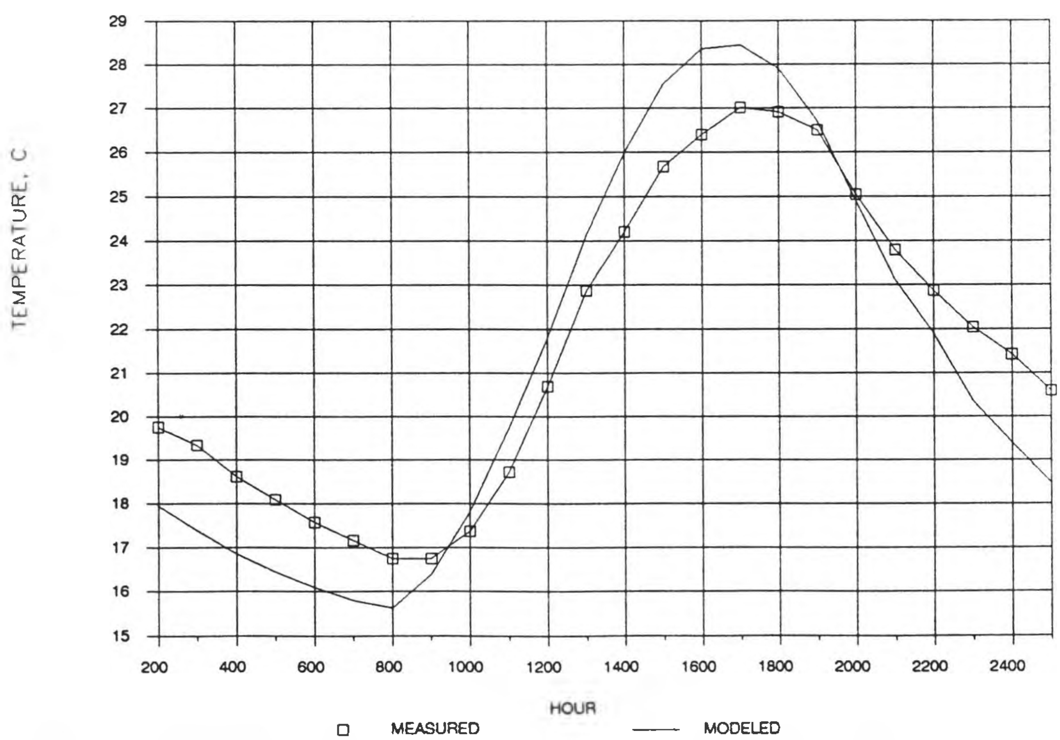

Fig. 6.2 Measured and TEMP-84 modeled diurnal fluctuation in stream temperature at Virgin River Mile 157.3 on 7-08-88.

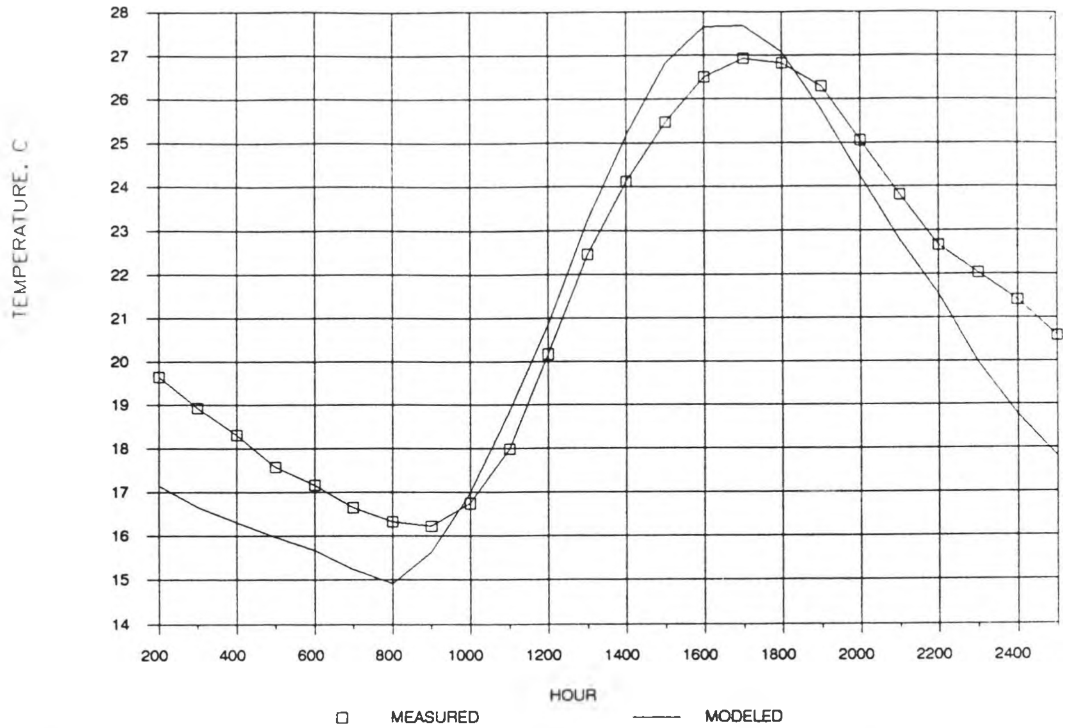

Fig. 6.3 Measured and TEMP-84 modeled diurnal fluctuation in stream temperature at Virgin River Mile 157.3 on 7-15-88.

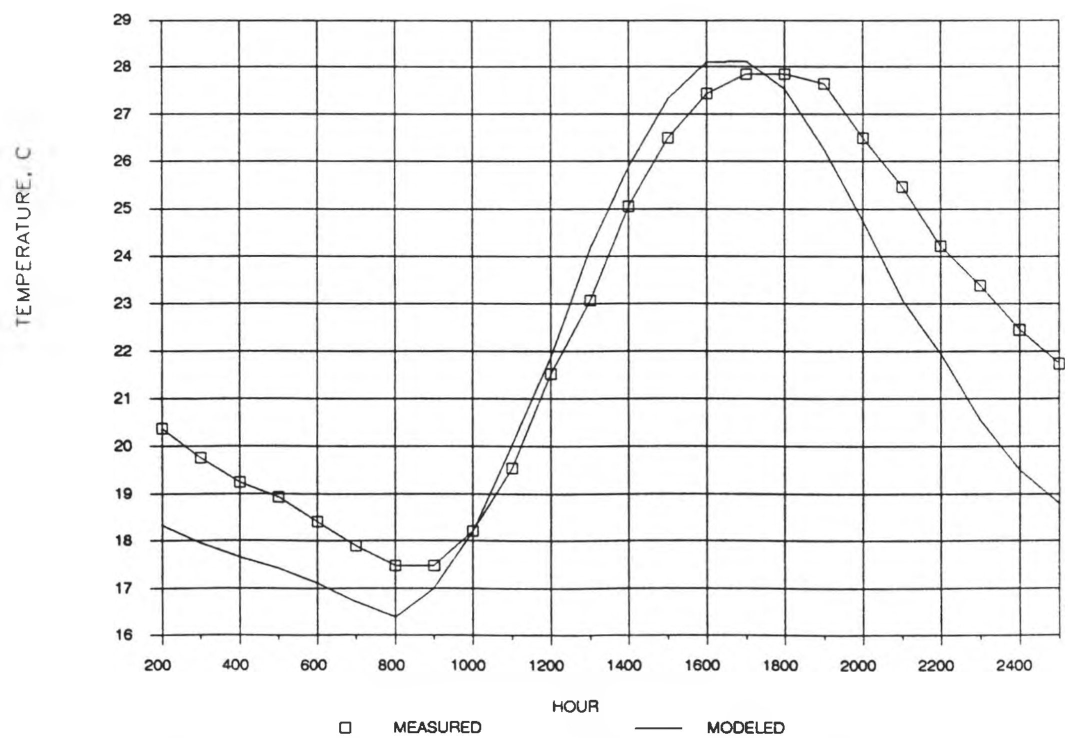

Fig. 6.4 Measured and TEMP-84 modeled diurnal fluctuation in stream temperature at Virgin River Mile 157.4 on 7-21-88.

ranging from 0.3°C (1.4 percent) on 6-30-88 and 7-08-88 to 1.0°C (4.5 percent) on 7-21-88.

6.3 Simulation of Heat Flux Components

The difference between each simulation lies in the modeling of the heat flux components. Figure 6.5, which was constructed from the modeled heat flux components of 6-30-88, shows that the dominating heat flux component is the net solar radiation. It is also evident from this figure that heat loss results primarily from the evaporative heat flux. Table D.4 documents the hourly values in Ly/min for each of the heat transfer components. Figure 6.6 illustrates that the most significant change in the individual modeled heat flux components between the four days simulated was an increase in the evaporative heat loss. On 6-30-88 the evaporative heat loss was 292 Ly/day (approx. 0.50 cm/day); on 7-08-88 it was 364 Ly/day (approx. 0.63 cm/day); on 7-15-88 it was 442 Ly/day (approx. 0.76 cm/day) and on 7-21-88 it was 480 Ly/day (approx. 0.83 cm/day). Table D.5 documents the energy transfer rate in Ly/day for each component on each day. A large increase in evaporative heat loss with a relatively small change in heat transfer from the other components results in a lower simulated stream temperature as depicted on 7-15-88 and 7-21-88. The modeled evaporation rates were compared to NOAA published evaporation rates for the nearest station, Saint George, Utah (NOAA station #7516) at N37.7, E113.3 approximately 97 km southeast of Zion National Park (ZION). The evaporation rates for Saint George and the study reach cannot be expected to match identically because the Saint George station location is 393 m lower than that of ZION and in a different topographic setting. Despite these differences, the comparison does give a rough

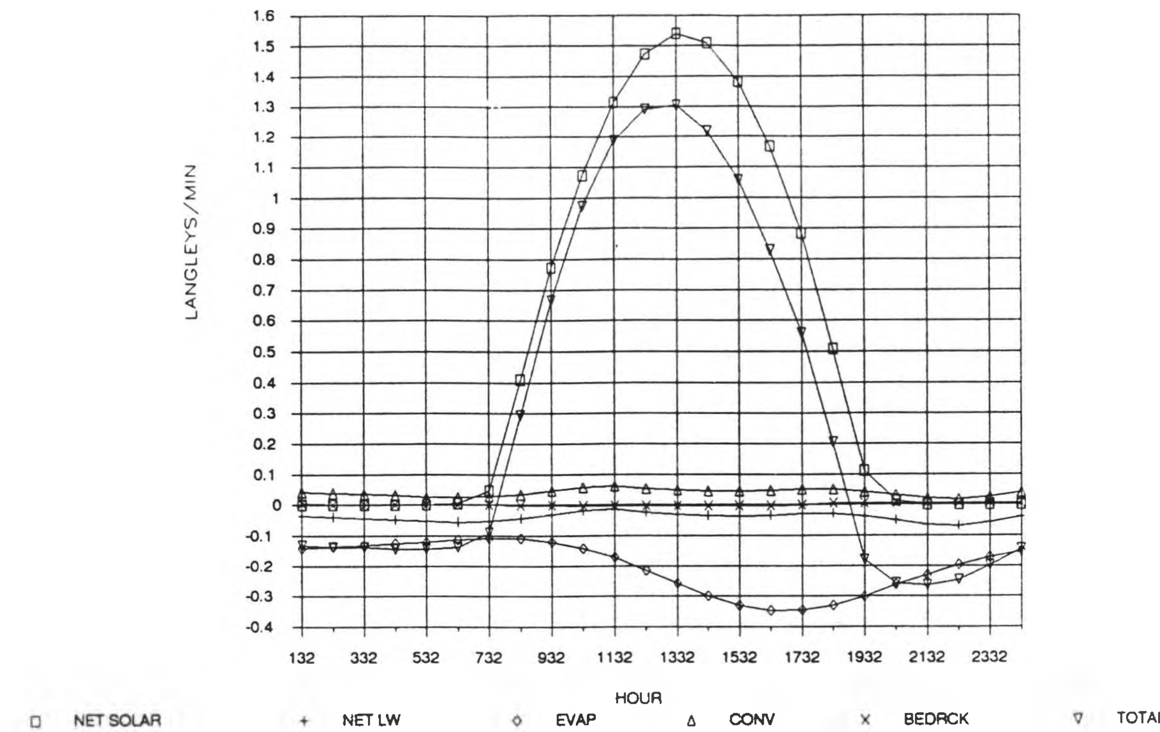

Fig. 6.5 Diurnal fluctuation in TEMP-84 modeled energy budget components for existing conditions at Virgin River Mile 157.3 on 6-30-88.

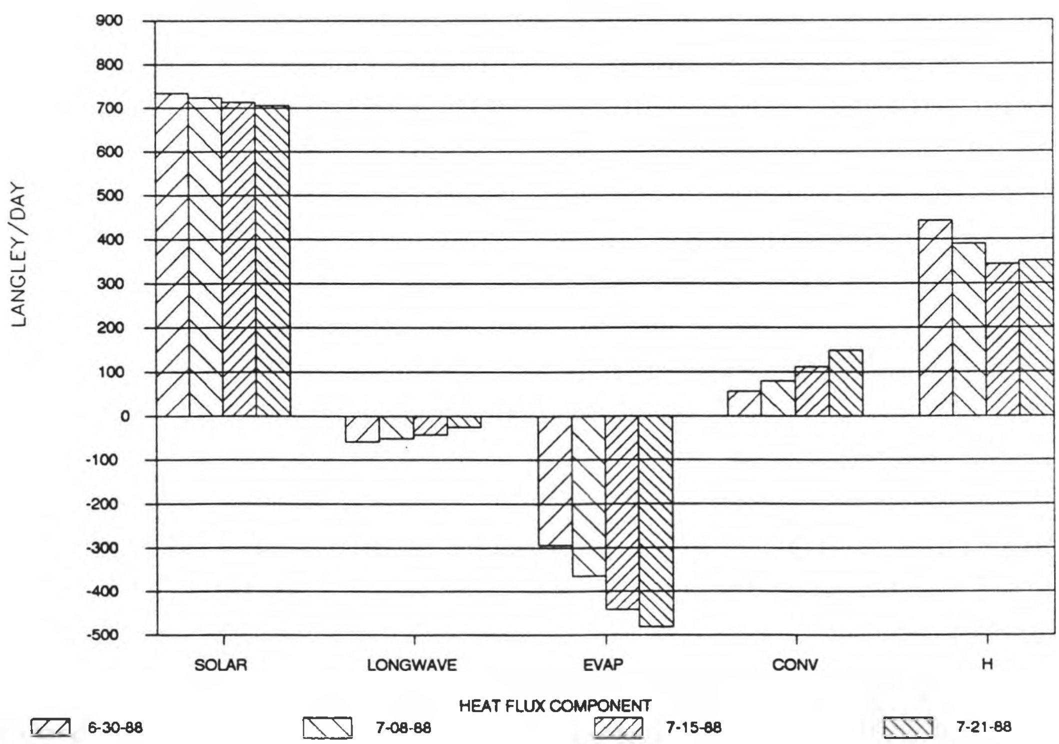

Fig. 6.6 TEMP-84 modeled daily heat flux at Virgin River Mile 157.3 for existing conditions on 6-30-88, 7-08-88, 7-15-88, and 7-21-88.

indication as to whether the modeled evaporation rates resemble realistic values. On 7-15-88 and 7-21-88 the modeled evaporation rates were approximately 0.05 cm/day and 0.30 cm/day higher respectively, than that measured at Saint George. Conversely, on 7-08-88 and 6-30-88, the modeled evaporation was 0.16 cm/day and 0.44 cm/day lower respectively, than measured at Saint George.

The convective heat transfer component, a heat input, is directly related to the evaporative heat transfer and thus also increases in magnitude over the consecutive modeled days. Resulting in heat gain, it counters the evaporative heat loss by a proportion determined from air temperature and vapor pressure gradients.

The net solar heat flux decreases as the Julian day increases. After the summer solstice, approximately June 20, the solar declination decreases, the zenith angles increase, and the days get shorter which results in less available solar radiation. The nearest solar radiation data collection stations were located at Las Vegas, NV, N36.05, E115.10 at an elevation of 664 m (NCDC station #23169) and Grand Junction, CO, N39.1, E108.3 at an elevation of 1475 m (NCDC station #23066). Modeled results for net solar radiation decreased from 733 Ly/day on 6-30-88 to 705 Ly/day on 7-21-88. Comparatively, the average daily global radiation for July recorded by the National Climatic Data Center was 770 Ly/day at Las Vegas and 625 Ly/day at Grand Junction. Considering that ZION lies almost directly between these two solar radiation collection stations and the average study reach elevation is also between those of the two stations, it seems reasonable that the modeled net solar radiation flux is between the measured radiation values.

Heat transfer studies by Anderson (1954) at Lake Hefner portrayed an atmospheric longwave radiation rate at the lake surface of 800 Ly/day, a reflected loss of 26 Ly/day and a water body emission rate of 900 Ly/day. This results in a net heat loss of 126 Ly/day which is greater than the TEMP-84 modeled longwave radiation heat loss of 58 Ly/day on 6-30-88, 51 Ly/day on 7-08-88, 42 Ly/day on 7-15-88, and 24 Ly/day on 7-21-88.

6.4 Sensitivity Analysis

Knowledge of the input data precision and model sensitivity to the various input components allows a better understanding of the existing condition simulations. Table 6.1 delineates estimates of the precision associated with each of the TEMP-84 input variables. A detailed sensitivity analysis was conducted on TEMP-84 utilizing the data input set compiled for 6-30-88.

In conducting the sensitivity analysis, TEMP-84 input variables were divided in two groups based on results from the preliminary sensitivity analysis: (1) those thought to have a large effect and (2) those thought to have little effect on the modeled stream temperature.

Input variables thought to have a large effect on the modeled stream temperature were varied by a consistent +/- 15 percent to allow a comparative study as to which variables the model was most sensitive. The results show that TEMP-84 was most sensitive to the inflow stream temperature followed by, in decreasing order of sensitivity, width, discharge, air temperature, length, and velocity. The remaining variables resulted in less than 0.5°C change in the outflow temperature with a 15 percent perturbation in the input value. These variables were also perturbed by their respective rated precision to describe the modeled stream temperature regime with respect to the precision of the input data. Results from the sensitivity analysis are documented in Table 6.2 and Figures D.1 through D.20 in Appendix D.

Table 6.1. Estimated precision of data collected between Virgin River Mile (VRM) 157.3 and VRM 161.0 for input to the stream temperature model TEMP-84.

SITE CHARACTERISTICS	PRECISION	STREAM CHARACTERISTICS	PRECISION
Latitude	+/- .1 deg	Stream aspect	+/- 5.0 deg
Longitude	+/- .1 deg	Stream gradient	+/- 20 %
Mean Elevation	+/- 1 %	Length	+/- 10 %
Relative humidity	+/- 50 %	Width	+/- 10 %
Windspeed	+/- 50 %	Velocity	+/- 15 %
		Flowrate	+/- 10 %
SHADING CHARACTERISTICS	**PRECISION**	Inflow temperature	+/- 5 %
Average topographic angle	+/- 25 %	Groundwater temperature	+/- 7 %
Average vegetation angle	+/- 50 %	Groundwater inflow	+/- 100 %
Canopy cover coefficient	+/- 25 %	Air temperature	+/- 10 %
Average hillslope angle	+/- 10 %	Percent bedrock	+/- 15 %
Tree height	+/- 25 %		
Percent directly shaded	+/- 10 %		
Perpendicular forest angle	+/- 30 %		

Input variables thought to have little effect on the stream temperature were varied by a range which encompassed the rated precision of the measured data. It was evident that for each variable except the hillslope angle, a large, ie., greater than or equal to 50 percent, change in input was required to make even a 0.5°C change in the modeled stream temperature. In fact, tree height, canopy cover, buffer width, latitude, longitude, topographic shading, stream gradient, percent bedrock, stream

Table 6.2. Arithmetic and percent change in TEMP-84 modeled maximum and minimum stream temperature with the specified change in the designated variable.

	GW TEMP EXISTING - PERTURBED				LENGTH EXISTING - PERTURBED				STREAM TEMPERATURE EXISTING - PERTURBED			
	+15%	-15%	+7%	-7%	+15%	-15%	+10%	-10%	+15%	-15%	+5%	-5%
MIN TEMP DIFF, C	-0.28	0.29	-0.10	0.10	-0.21	-0.09	-0.13	0.02	-1.64	1.68	-0.53	-0.53
MAX TEMP DIFF, C	-0.27	0.27	-0.10	0.10	-0.61	0.89	-0.48	0.55	-1.47	1.52	-0.48	0.48
MIN TEMP DIFF, %	-1.8	1.8	-0.6	0.6	-1.3	-0.6	-0.8	0.1	-10.1	10.3	-3.3	3.3
MAX TEMP DIFF, %	-0.9	0.9	-0.3	0.3	-2.1	3.1	-1.6	1.9	-4.8	5.0	-1.6	1.6

	AIR TEMPERATURE EXISTING - PERTURBED				WIND EXISTING - PERTURBED				RELATIVE HUMIDITY EXISTING - PERTURBED			
	+15%	-15%	+10%	-10%	+15%	-15%	+50%	-50%	+15%	-15%	+50%	-50%
MIN TEMP DIFF, C	-0.83	0.74	-0.54	0.50	0.04	-0.04	0.13	-0.13	-0.20	0.21	-0.60	0.67
MAX TEMP DIFF, C	-1.09	0.97	-0.71	0.66	0.08	-0.07	0.26	-0.26	-0.20	0.21	-0.58	0.66
MIN TEMP DIFF, %	-5.2	4.6	-3.4	3.1	0.3	-0.3	0.8	-0.8	-1.3	1.3	-3.8	4.2
MAX TEMP DIFF, %	-3.7	3.3	-2.4	2.2	0.3	-0.2	0.9	-0.9	-0.7	0.7	-2.0	2.3

	DISCHARGE EXISTING - PERTURBED				WIDTH EXISTING - PERTURBED				VELOCITY EXISTING - PERTURBED			
	+15%	-15%	+10%	-10%	+15%	-15%	+10%	-10%	+15%	-15%	+50%	-50%
MIN TEMP DIFF, C	-0.19	0.23	-0.13	0.15	0.18	-0.19	0.12	-0.12	0.21	-0.43	0.35	-2.10
MAX TEMP DIFF, C	1.19	-1.42	0.82	-0.92	-1.51	1.63	-1.02	1.08	-0.53	0.59	-1.16	3.55
MIN TEMP DIFF, %	-1.2	1.4	-0.8	0.9	1.1	-1.2	0.8	-0.8	1.3	-2.7	2.2	-13.2
MAX TEMP DIFF, %	4.1	-4.9	2.8	-3.2	-5.2	5.6	-3.5	3.7	-1.8	2.0	-4.0	12.2

	GW FLOW EXISTING - PERTURBED			
	+15%	-15%	+100%	-100%
MIN TEMP DIFF, C	0.02	-0.02	0.14	-0.17
MAX TEMP DIFF, C	0.27	-0.28	1.63	-2.10
MIN TEMP DIFF, %	0.1	-0.1	0.9	-1.1
MAX TEMP DIFF, %	0.9	-1.0	5.6	-7.2

aspect, direct shading and vegetation shading angle variables demonstrated essentially no effect on the modeled stream temperature when perturbed by a relatively large amount. The hillslope angle was somewhat sensitive to the modeled stream temperature as a 20 degree (approx. 50 percent) increase resulted in a 1.1°C decrease in the maximum stream temperature. Results from the sensitivity analysis for these variables are documented in Table 6.3 and Figures D.21 through D.45.

Table 6.3. Arithmetic and percent change in TEMP-84 modeled maximum and minimum stream temperature with the specified change in the designated variable.

	HILLSLOPE ANGLE EXISTING - PERTURBED				PERPENDICULAR FOREST ANGLE EXISTING - PERTURBED				- DIRECT SHADING EXISTING - PERTURBED	
	-5 deg	+5 deg	+10 deg	+20 deg	+5 deg	-5 deg	+10 deg	-10 deg	+50%	+100%
MIN TEMP DIFF, C	0.0	0.3	0.3	0.9	0.0	0.3	0.0	0.3	0.0	0.0
MAX TEMP DIFF, C	0.0	0.4	0.4	1.1	0.1	0.3	0.1	0.2	0.2	0.4
MIN TEMP DIFF, %	0.0	1.9	2.1	5.3	0.0	1.8	0.0	1.8	-0.1	-0.1
MAX TEMP DIFF, %	0.0	1.1	1.3	3.2	0.2	0.8	0.4	0.6	0.7	1.3

	TREE HEIGHT EXISTING - PERTURBED				CANOPY COVER EXISTING - PERTURBED				BUFFER WIDTH EXISTING - PERTURBED		
	-10 ft	+10 ft	+15 ft	+20 ft	+25%	-25%	+50%	-50%	+20 ft	+40 ft	+60 ft
MIN TEMP DIFF, C	0.0	0.0	0.0	0.0	0.0	0.0	0.0	0.1	0.1	0.0	0.0
MAX TEMP DIFF, C	0.0	0.0	0.0	0.0	0.0	0.0	0.0	0.1	0.0	0.0	0.0
MIN TEMP DIFF, %	0.0	0.0	0.0	0.0	-0.2	0.3	-0.3	0.8	0.6	0.3	0.1
MAX TEMP DIFF, %	0.0	0.0	0.0	0.0	0.0	0.0	0.0	0.1	0.1	0.0	0.0

	VEGETATION SHADING ANGLE EXISTING - PERTURBED				STREAM ASPECT EXISTING - PERTURBED				LONGITUDE EXISTING - PERTURBED	
	+15 deg	-15 deg	+25 deg	+35 deg	+5 deg	-5 deg	+10 deg	-10 deg	+0.1 deg	-0.1 deg
MIN TEMP DIFF, C	0.0	-0.3	0.0	0.0	0.0	-0.2	0.0	0.0	0.0	0.0
MAX TEMP DIFF, C	0.0	0.0	0.0	0.0	0.0	0.0	0.0	0.0	0.0	0.0
MIN TEMP DIFF, %	0.0	-2.1	0.0	0.0	0.0	-0.9	0.0	0.0	0.0	0.0
MAX TEMP DIFF, %	0.0	0.0	0.0	0.0	0.0	0.0	0.0	0.0	0.0	0.0

	TOPOGRAPHIC SHADING ANGLE EXISTING - PERTURBED				MEAN ELEVATION EXISTING - PERTURBED				LATITUDE EXISTING - PERTURBED	
	+10 deg	-10 deg	+20 deg	-20 deg	+10%	-10%	+20%	-20%	+0.1 deg	-0.1 deg
MIN TEMP DIFF, C	0.0	0.0	0.0	0.0	0.0	0.0	0.0	0.0	0.0	0.0
MAX TEMP DIFF, C	0.0	0.0	0.0	0.0	-0.1	0.1	-0.1	0.1	0.0	0.0
MIN TEMP DIFF, %	0.0	-0.2	0.0	-0.2	-0.1	0.0	-0.1	0.0	0.0	0.0
MAX TEMP DIFF, %	0.0	0.0	0.0	0.0	-0.2	0.2	-0.3	0.4	0.0	0.0

	STREAM GRADIENT EXISTING - PERTURBED				PERCENT BEDROCK EXISTING - PERTURBED		
	+10%	-10%	+30%	-30%	+50	-50%	+100%
MIN TEMP DIFF, C	0.0	0.0	0.0	0.0	0.0	0.0	0.0
MAX TEMP DIFF, C	0.0	0.0	0.0	0.0	0.0	0.0	0.0
MIN TEMP DIFF, %	0.0	0.0	0.0	0.0	0.0	0.0	0.0
MAX TEMP DIFF, %	0.0	0.0	0.0	0.0	0.1	-0.1	0.2

Chapter 7. Simulation of Hypothetical Conditions

The purpose of this study is to describe the change in stream temperature regime at VRM 157.3 with changes in flow and inflow temperature. Hypothetical flow conditions and hypothetical inflow stream temperatures were simulated using TEMP-84.

7.1 Hypothetical Flow Simulation

Hypothetical flows of 28,320 l/s (1000 cfs), 14,160 l/s (500 cfs), 2,832 l/s (100 cfs), 2,124 l/s (75 cfs), 906 l/s (32 cfs), 566 l/s (20 cfs), and 283 l/s (10 cfs) were selected for simulation. The maximum flow of 28,320 l/s represents the magnitude of flow for flash flood events as measured during the 1987 and 1988 field seasons. The minimum flow, 283 l/s, approximates a low flow for which the stream can remain active year round. Width and velocity stream characteristics for hypothetical flows were empirically derived as a function of flow. In order to make valid comparisons between hypothetical flow and existing flow stream temperature regimes, the baseflow rate of 906 l/s (32 cfs) at VRM 163.1 was also modeled using empirically derived width and velocity data.

Table 7.1 documents a comparison between empirically derived width and velocity values and those developed from field data for baseflow conditions of 906 l/s. Empirically derived width values were within twenty-five percent of those determined from field data with three of the comparisons being within fifteen percent. Empirically derived velocity differed by a maximum of 0.3 m/s (75 percent) and minimum of 0.1 m/s (25 percent). While velocity values from the empirical relationships were consistently larger than those calculated from field data, empirically derived width values fluctuated between being greater than and less than field data.

Table 7.1. Comparison of NEWCHAN (BLM, 1985) modeled width and velocity values to those calculated from field data for the delineated Virgin River reaches.

	WIDTH		VELOCITY	
	FIELD DATA m	EMPIRICAL FORMULA m	FIELD DATA m/s	EMPIRICAL FORMULA m/s
VRM 157.3 - VRM 159.5	8.7	7.5	0.4	0.6
VRM 159.5 - VRM 160.0	7.5	6.9	0.4	0.5
VRM 160.0 - VRM 162.2	8.1	8.6	0.4	0.6
VRM 162.2 - VRM 163.1	6.4	8.0	0.4	0.5

Figure 7.1 illustrates the difference in modeled stream temperature between when field data and empirical data were used for width and velocity input. Similar figures for 7-08-88, 7-15-88, and 7-21-88 are filed as Figure E.1, E.2, and E.3 in Appendix E. Table E.1 documents the maximum, minimum, and mean stream temperature for each simulation. Simulations utilizing empirical width and velocity values resulted in a maximum stream temperature approximately 1°C greater, a minimum temperature within 0.5°C, and a mean temperature within 0.1°C of that modeled with field data. Any difference in peak time between simulated diurnal regimes resulted from the difference in velocity input.

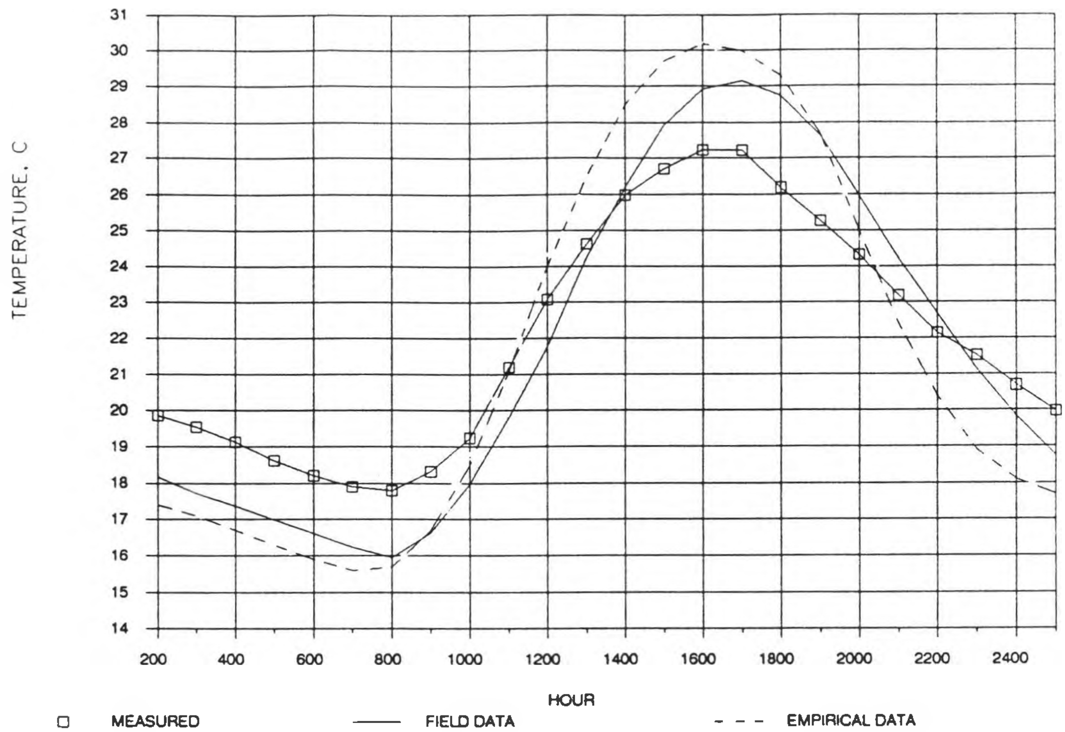

Fig. 7.1 Measured and TEMP-84 modeled diurnal fluctuation in stream temperature for 6-30-88 at Virgin River Mile 157.3 utilizing field collected data and empirically derived data.

The largest flow for simulation was chosen to be 28,320 l/s as it is the order of magnitude for flood events measured during the field seasons of 1987 and 1988. Figure 7.2 illustrates the diurnal fluctuation in stream temperature for 6-30-88 for hypothetical flows greater than baseflow. Also depicted is the measured inflow stream temperature at VRM 163.1. Because the modeled stream temperature for both 14,160 l/s and 28,320 l/s approach the measured inflow stream temperature at VRM 163.1, the maximum simulated flow for 7-08-88, 7-15-88, and 7-21-88 was chosen to be 14,160 l/s. Figures 7.3, 7.4, and 7.5 show, for these days, the modeled diurnal fluctuation in stream temperature for hypothetical flows greater than baseflow.

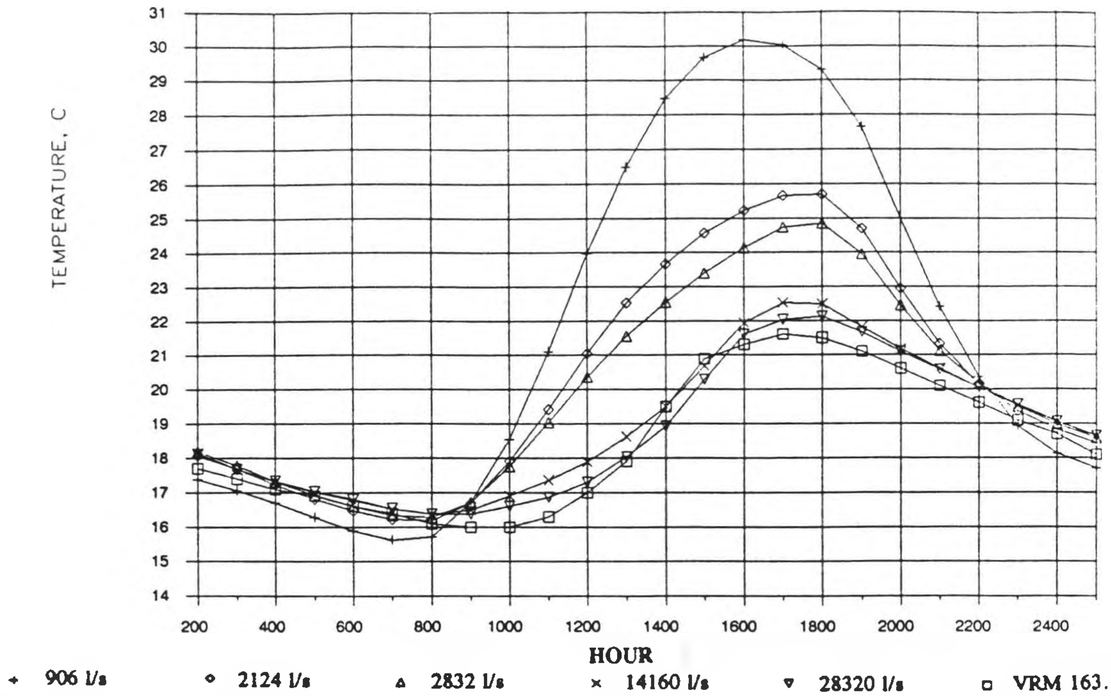

Fig. 7.2 TEMP-84 modeled stream temperature at Virgin River Mile (VRM) 157.3 for flow greater than and equal to baseflow and measured stream temperatures at VRM 163.1 on 6-30-88.

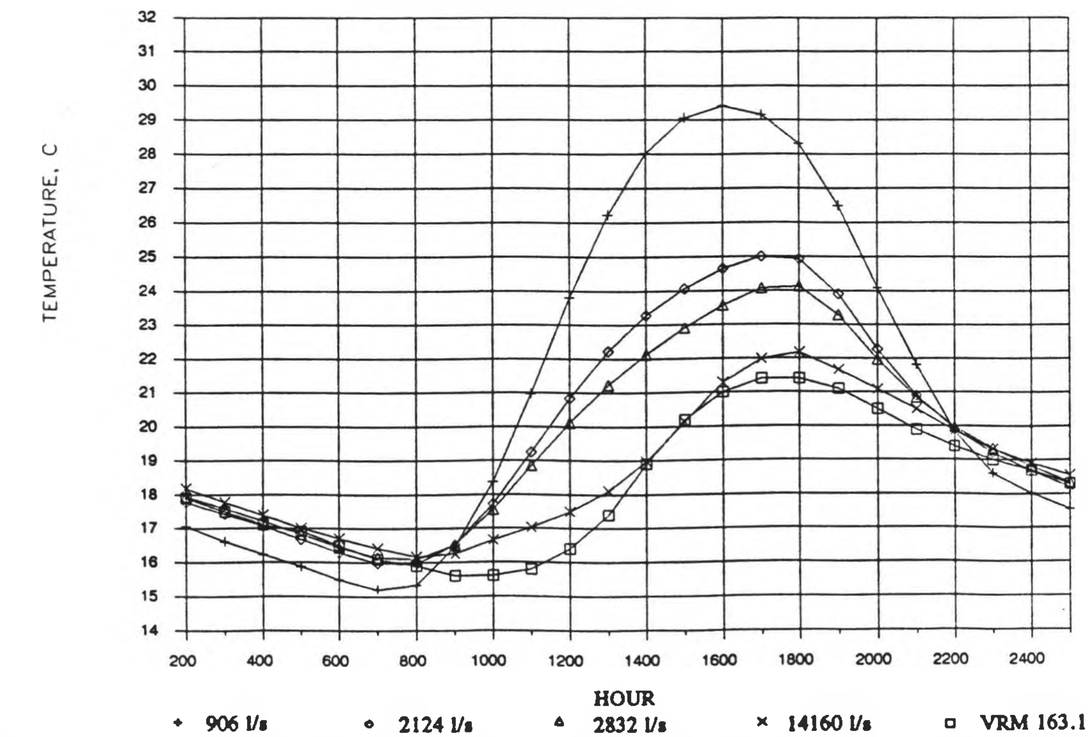

Fig. 7.3 TEMP-84 modeled stream temp. at Virgin River Mile (VRM) 157.3 for flow greater than and equal to baseflow and measured stream temp. at VRM 163.1 on 7-08-88.

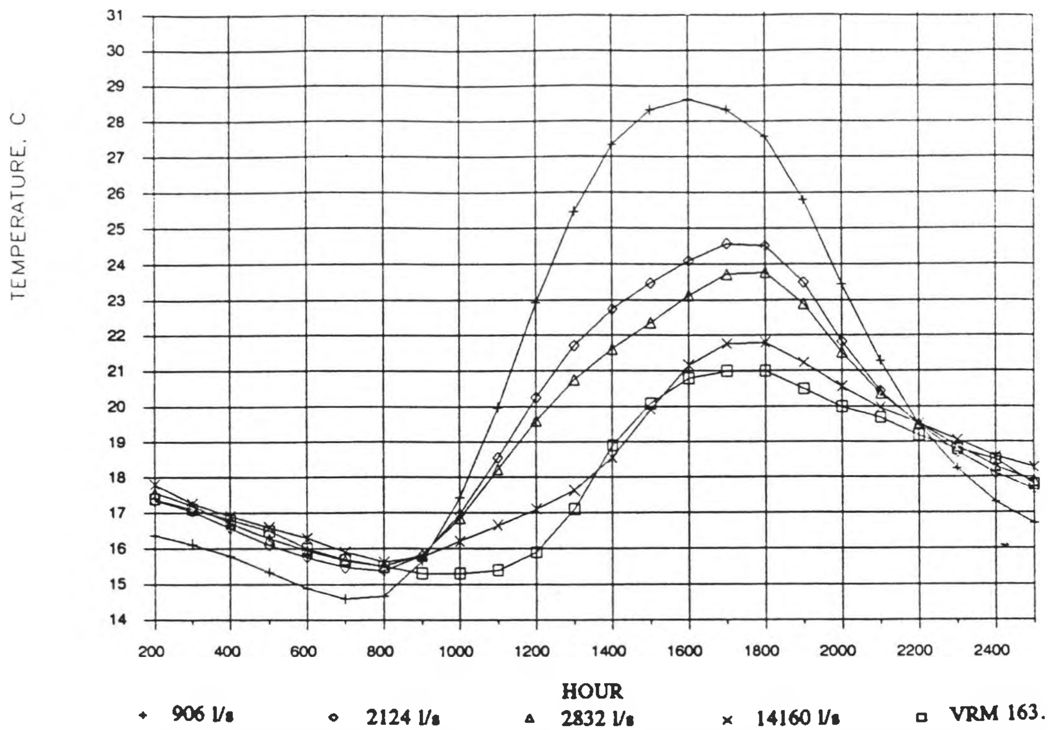

Fig. 7.4 TEMP-84 modeled stream temp. at Virgin River Mile (VRM) 157.3 for flow greater than and equal to baseflow and measured stream temp. at VRM 163.1 on 7-15-88.

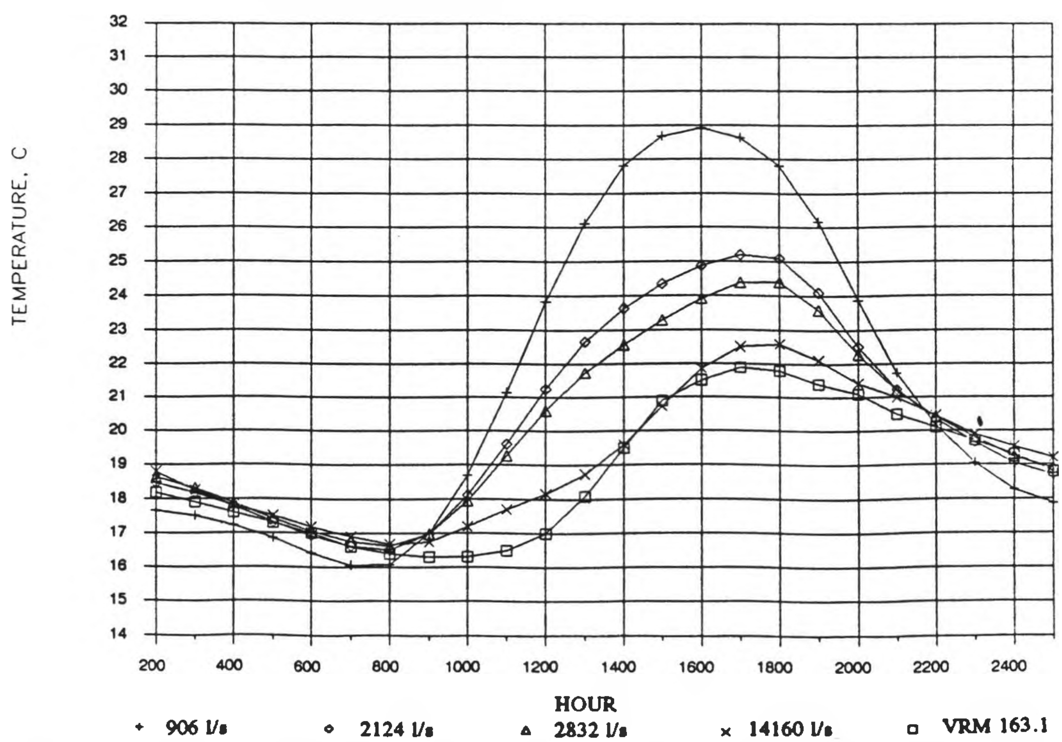

Fig. 7.5 TEMP-84 modeled stream temp. at Virgin River Mile (VRM) 157.3 for flow greater than and equal to baseflow and measured stream temp. at VRM 163.1 on 7-21-88.

The simulated stream temperature regime for the flows greater than baseflow are similar between the days selected for modeling. In each case, the stream temperature drops as the flow increases and the 14,160 l/s diurnal temperature regime approximates that of the inflow stream temperature regime.

Figures 7.6, 7.7, 7.8, and 7.9 illustrate the diurnal fluctuation in stream temperature for hypothetical flows less than baseflow. These simulations show a significant increase in stream temperature with a decrease in flow. Also, a greater variance between modeled stream temperature regimes is evident for a given hypothetical condition. Table E.2, E.3, E.4, and E.5 document the hourly stream temperature for all simulations of hypothetical flow conditions.

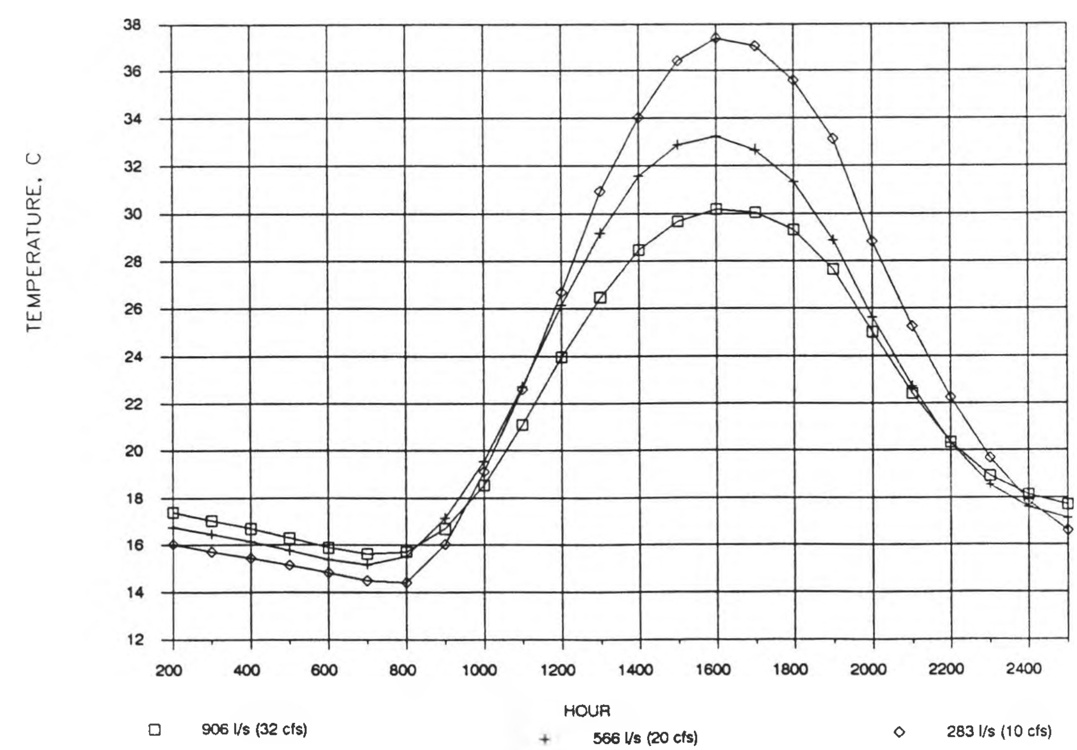

Fig. 7.6 TEMP-84 modeled stream temperature at Virgin River Mile 157.3 for flow less than and equal to baseflow on 6-30-88.

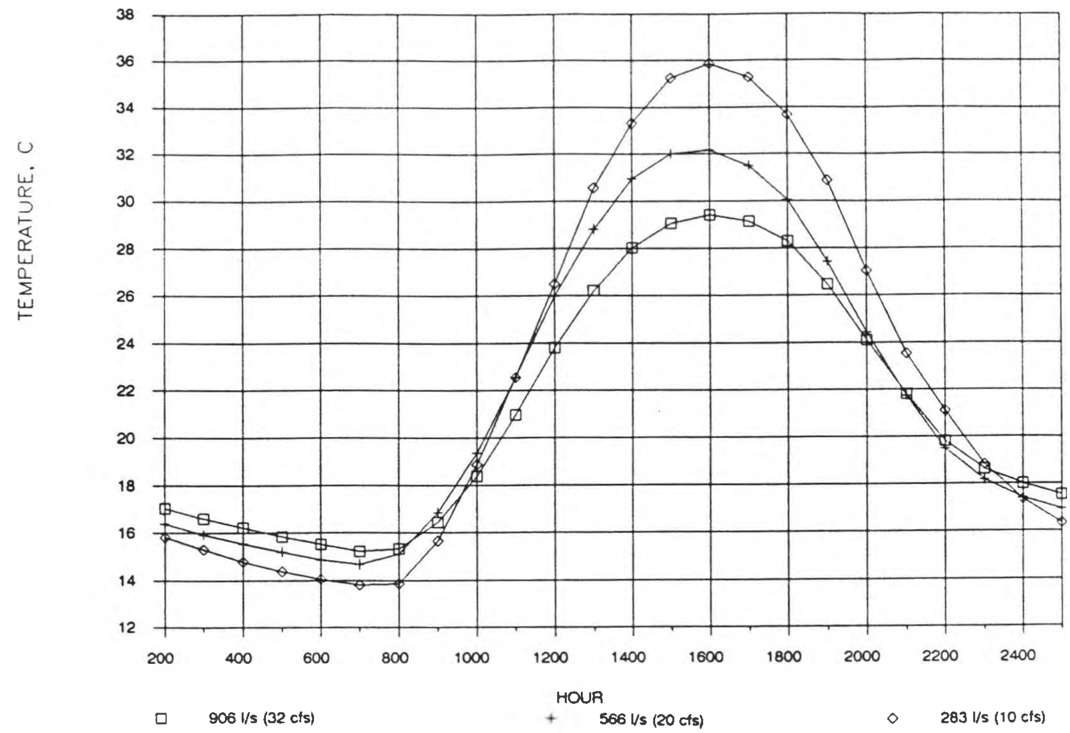

Fig. 7.7 TEMP-84 modeled stream temperature at Virgin River Mile 157.3 for flow less than and equal to baseflow on 7-08-88.

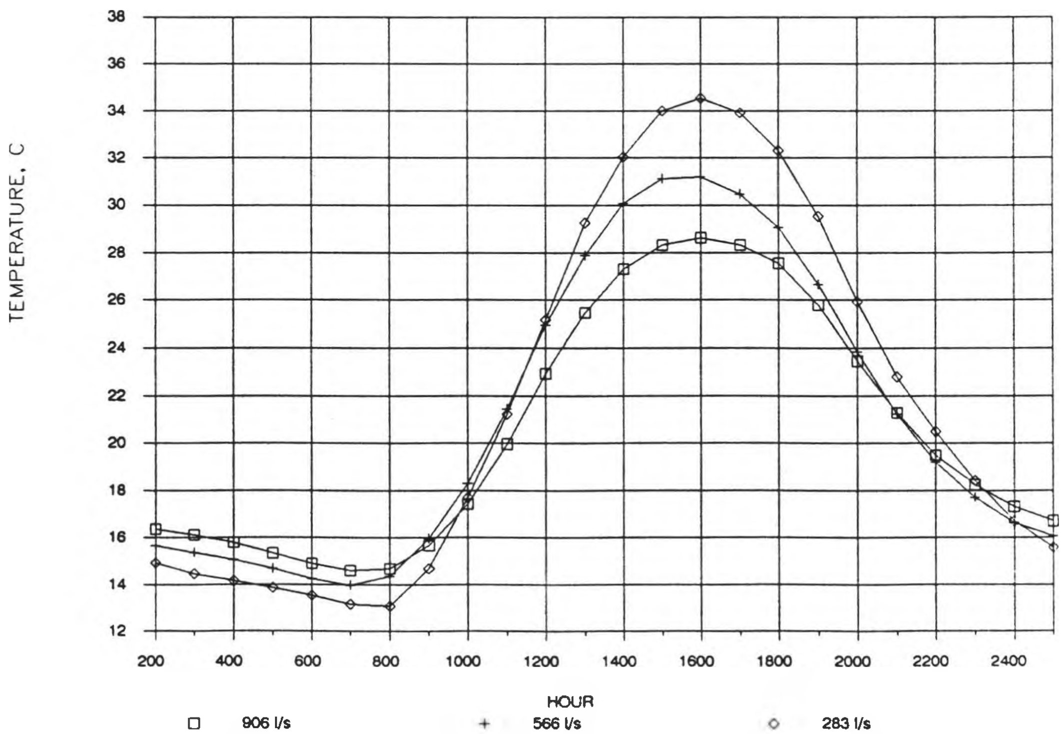

Fig. 7.8 TEMP-84 modeled stream temperature at Virgin River Mile 157.3 for flow less than and equal to baseflow on 7-15-88.

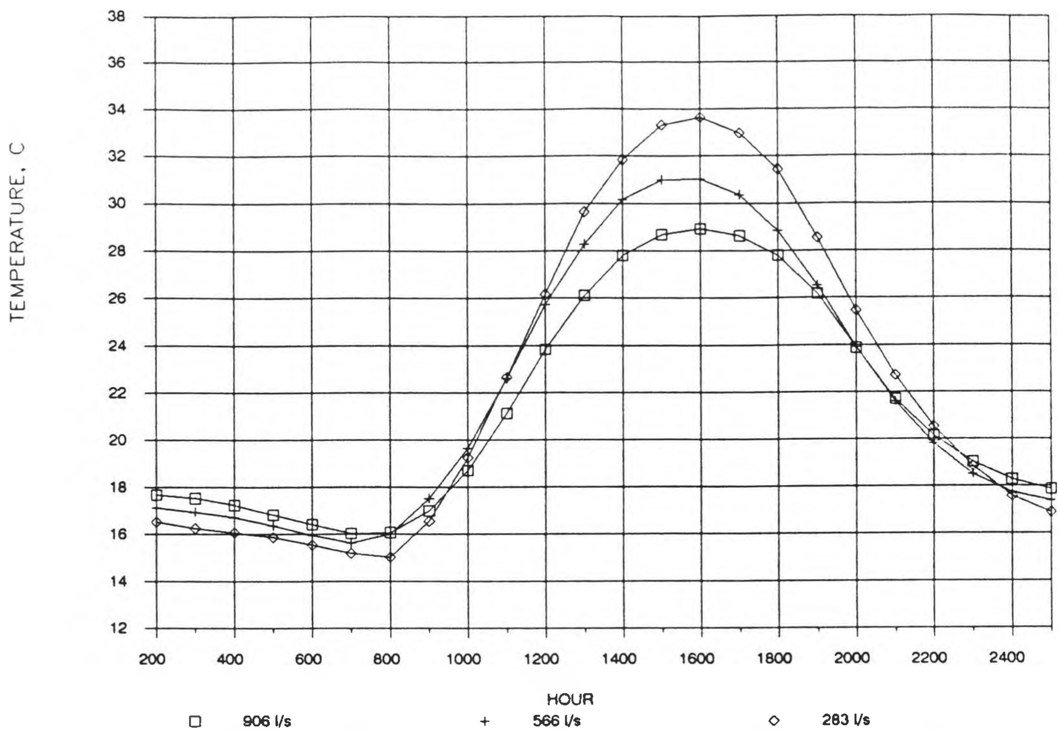

Fig. 7.9 TEMP-84 modeled stream temperature at Virgin River Mile 157.3 for flow less than and equal to baseflow on 7-21-88.

Because TEMP-84 was not calibrated to simulate existing stream temperatures at VRM 157.3, the modeled stream temperatures under hypothetical conditions should be viewed in terms of a relative change from those modeled for existing conditions and not for the actual stream temperatures produced. Accordingly, the percent change from that modeled for baseflow conditions, ie., 906 l/s was calculated for the maximum, mean, and minimum stream temperature for each hypothetical simulation (Table E.6, E.7, and E.8).

To simulate actual stream temperatures for the selected hypothetical conditions, the average percent change for each stream temperature characteristic, i.e., maximum, mean, and minimum, under each hypothetical flow simulation, was applied to measured stream temperatures at VRM 157.3 (Table 7.2, 7.3, and 7.4).

Table 7.2. Maximum stream temperature as calculated from the TEMP-84 simulated percent change applied to existing conditions.

	FLOW					
	EXISTING	14,160 l/s (500 cfs)	2,832 l/s (100 cfs)	1,124 l/s (75 cfs)	566 l/s (20 cfs)	283 l/s (10 cfs)
DATE	MAX STR TEMP C	MAX STR TEMP C	MAX STR TEMP C	MAX STR TEMP C	MAX STR TEMP C	MAX STR TEMP C
6-30-88	27.2	20.3	22.4	23.1	29.9	33.7
7-08-88	27.0	20.4	22.1	23.0	29.6	33.0
7-15-88	26.9	20.5	22.4	23.1	29.4	32.5
7-21-88	27.8	21.7	23.5	24.2	29.9	32.4
MEAN	27.2	20.7	22.6	23.4	29.7	32.9
VAR	0.16	0.43	0.38	0.32	0.06	0.35
STD DEV	0.40	0.66	0.62	0.57	0.24	0.59

Table 7.3. Mean stream temperature as calculated from the TEMP-84 simulated percent change applied to existing conditions.

	FLOW					
	EXISTING	14,160 l/s (500 cfs)	2,832 l/s (100 cfs)	1,124 l/s (75 cfs)	566 l/s (20 cfs)	283 l/s (10 cfs)
DATE	MEAN STR TEMP C	MEAN STR TEMP C	MEAN STR TEMP C	MEAN STR TEMP C	MEAN STR TEMP C	MEAN STR TEMP C
6-30-88	22.0	19.3	20.4	20.7	22.8	24.1
7-08-88	21.5	19.0	20.0	20.2	22.1	23.0
7-15-88	21.2	18.9	19.9	20.1	21.7	22.5
7-21-88	22.4	20.2	21.0	21.3	22.9	23.5
MEAN	21.8	19.4	20.3	20.6	22.4	23.3
VAR	0.28	0.35	0.25	0.30	0.33	0.47
STD DEV	0.53	0.59	0.50	0.55	0.57	0.68

Table 7.4. Minimum stream temperature as calculated from the TEMP-84 simulated percent change applied to existing conditions.

	FLOW					
	EXISTING	14,160 l/s (500 cfs)	2,832 l/s (100 cfs)	1,124 l/s (75 cfs)	566 l/s (20 cfs)	283 l/s (10 cfs)
DATE	MIN STR TEMP C	MIN STR TEMP C	MIN STR TEMP C	MIN STR TEMP C	MIN STR TEMP C	MINSTR TEMP C
6-30-88	17.8	18.7	18.6	18.5	17.3	16.4
7-08-88	16.7	17.8	17.7	17.6	16.2	15.2
7-15-88	16.2	17.3	17.2	17.1	15.5	14.5
7-21-88	17.5	18.2	18.0	17.9	17.0	16.3
MEAN	17.1	18.0	17.9	17.8	16.5	15.6
VAR	0.54	0.35	0.34	0.34	0.66	0.83
STD DEV	0.73	0.59	0.59	0.59	0.81	0.91

The resulting stream temperatures were quite agreeable between the four days modeled; the standard deviation for each set of maximum, mean, and minimum temperatures under each hypothetical condition was always less than 1.0°C.
Seeing as the modeled results have inherent errors and each of the four days selected represents only a small sample from the population of stream temperatures, the results were averaged to provide an estimate of the maximum, mean, and minimum stream temperatures expected for each hypothetical condition. Average maximum stream temperatures from the four days modeled ranged from 32.9°C at 283 l/s to 20.7°C at 14,160 l/s. Average minimum stream temperatures ranged from 15.6°C at 283 l/s to 18.0°C at 14,160 l/s while average mean stream temperatures ranged from 23.3°C at 283 l/s to 19.4°C at 14,160 l/s.

Figure 7.10 shows for hypothetical flows, the percent change of modeled maximum stream temperature from that modeled for baseflow conditions. The percent change in maximum stream temperature for each simulation on each day is tabulated in Table E.6. The percent change represents the change in stream temperature from existing and thus was calculated by subtracting the modeled hypothetical temperature from the modeled existing temperature and then dividing by the modeled existing temperature. Accordingly, a positive percent change represents a decrease in maximum temperature while a negative percent change represents an increase. The average percent change in maximum stream temperature for each flow was 23.9 percent for 14,160 l/s, 17.0 percent for 2,832 l/s, 14.2 percent for 2,124 l/s, -9.0 percent for 566 l/s, and -20.9 percent for 283 l/s. Corresponding standard deviations associated with each set were 1.56 percent, 1.06 percent, 1.02 percent, 1.01 percent, and 3.07 percent for 14,160 l/s, 2,832 l/s, 2,214 l/s, 566 l/s, and 283 l/s respectively.

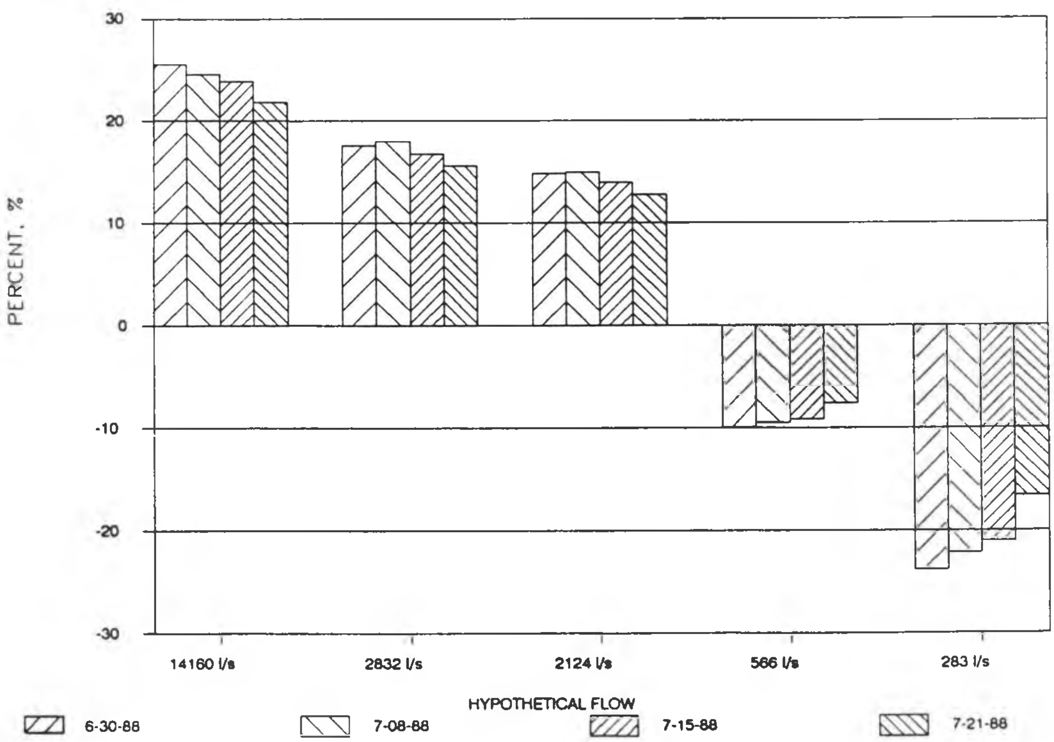

Fig 7.10 Percent change in maximum stream temperature at Virgin River Mile 157.3 for TEMP-84 modeled hypothetical flows from that modeled for baseflow on 6-30-88, 7-08-88, 7-15-88, and 7-21-88.

Figure 7.11 portrays for hypothetical flows, the percent change of modeled mean stream temperature from that modeled for baseflow conditions. The percent change in mean stream temperature for each simulation on each day is tabulated in Table E.7. Again, positive values represent a decrease in mean stream temperature while negative values represent an increase. The percent change in mean stream temperature is significantly reduced from the percent change calculated for maximum stream temperature. The average percent change in mean temperature for each flow was 11.2 percent for 14,160 l/s, 6.7 percent for 2,832 l/s, 5.6 percent for 2,124 l/s, -2.8 percent for 566 l/s, and -6.8 percent for 283 l/s. The standard deviations associated with each set were 1.19 percent, 0.62 percent, 0.65 percent, 0.64 percent, and 1.96 percent for 14,160 l/s, 2,832 l/s, 1,124 l/s, 566 l/s, and 283 l/s.

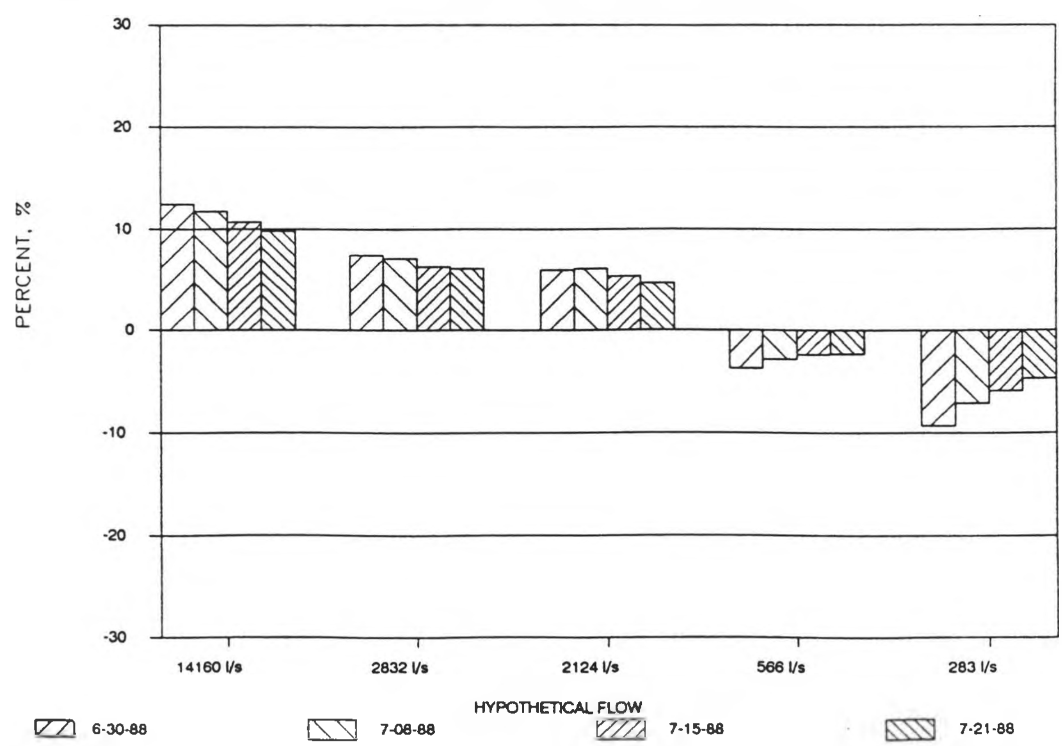

Fig 7.11 Percent change in mean stream temperature at Virgin River Mile 157.3 for TEMP-84 modeled hypothetical flows from that modeled for baseflow on 6-30-88, 7-08-88, 7-15-88, and 7-21-88.

Figure 7.12 illustrates for hypothetical flows, the percent change of modeled minimum stream temperature from that modeled for baseflow conditions. The percent change in minimum stream temperature for each simulation on each day is tabulated in Table E.8. In contrast to simulated maximum and mean stream temperatures, flows greater than baseflow illustrated an increase in minimum stream temperature while flows less than baseflow illustrated a decrease. The average percent change in minimum stream temperature for each flow was -5.6 percent for 14,160 l/s, -4.9 percent for 2,832 l/s, -4.3 percent for 1,124 l/s, 3.3 percent for 566 l/s, and 8.5 percent for 283 l/s. The standard deviations associated with each set were 1.45 percent, 1.43 percent, 1.41 percent, 0.62 percent, and 1.56 percent for 14,160 l/s, 2,832 l/s, 1,124 l/s, 566 l/s, and 283 l/s, respectively.

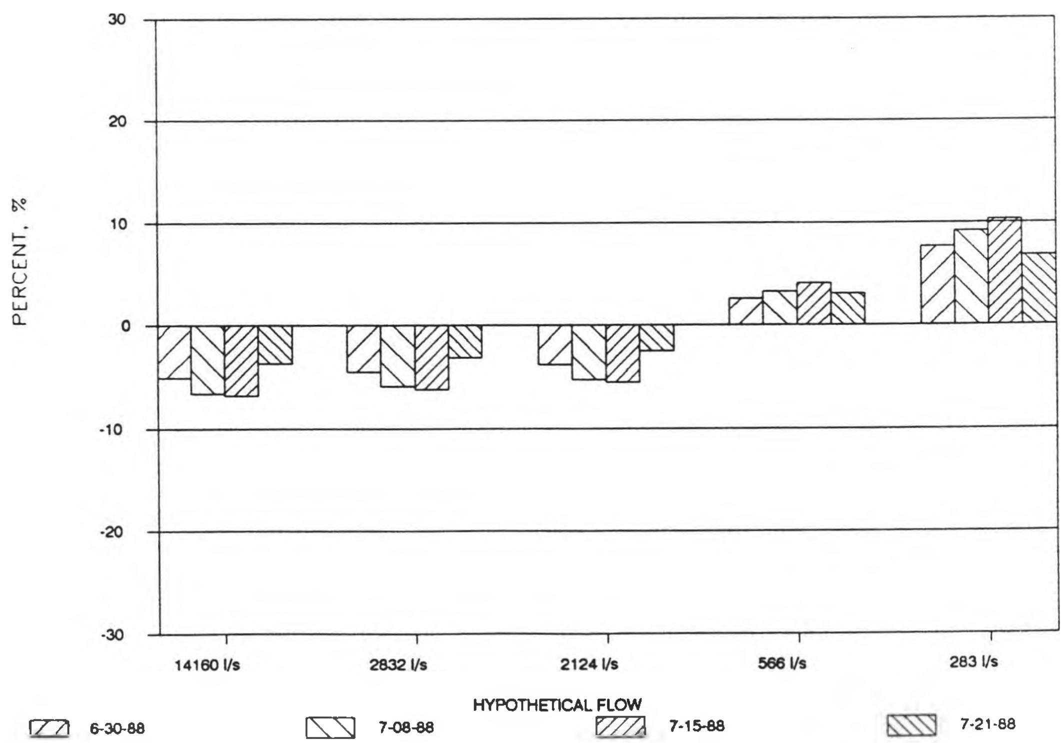

Fig 7.12 Percent change in minimum stream temperature at Virgin River Mile 157.3 for TEMP-84 modeled hypothetical flows from that modeled for baseflow on 6-30-88, 7-08-88, 7-15-88, and 7-21-88.

The time at which peak stream temperatures occur ranges a maximum of two hours between the various flows. The stream temperature regime for 14,160 l/s consistently lags at least one hour behind the those for lower flows with the maximum stream temperature occurring at approximately 1600 hr and minimum stream temperature occurring at approximately 0700 hr. The maximum peak temperatures for the remaining flows occur between 1700 and 1800 hr while the minimum stream temperatures occur at approximately 0800.

7.2 Hypothetical Inflow Stream Temperature Simulation

The average ambient temperature at VRM 163.0 and the groundwater temperature were delineated for simulation of hypothetical inflow temperature conditions. In order to make valid comparisons, existing conditions were simulated utilizing an average inflow stream temperature in contrast to the hourly defined diurnal stream temperature regime used in modeling existing conditions. All other input variables remained constant. Figure 7.13 compares, for 6-30-88, modeled stream temperature utilizing a daily average inflow stream temperature versus an hourly defined diurnal stream temperature inflow. Figures E.4 through E.6 illustrate similar comparisons for 7-08-88, 7-15-88, and 7-21-88. Table E.9 documents the maximum, mean, and minimum stream temperature for each simulation. Simulations utilizing an average inflow stream temperature depicted maximum stream temperatures 1.0oC to 1.5°C higher than those modeled with a diurnal stream temperature inflow. Minimum and mean stream temperatures were within 0.3°C and 0.1°C, respectively.

Figure 7.14, 7.15, 7.16, and 7.17, illustrate the diurnal fluctuation in stream temperature on 6-30-88, 7-08-88, 7-15-88, and 7-21-88, at VRM 157.3 for existing

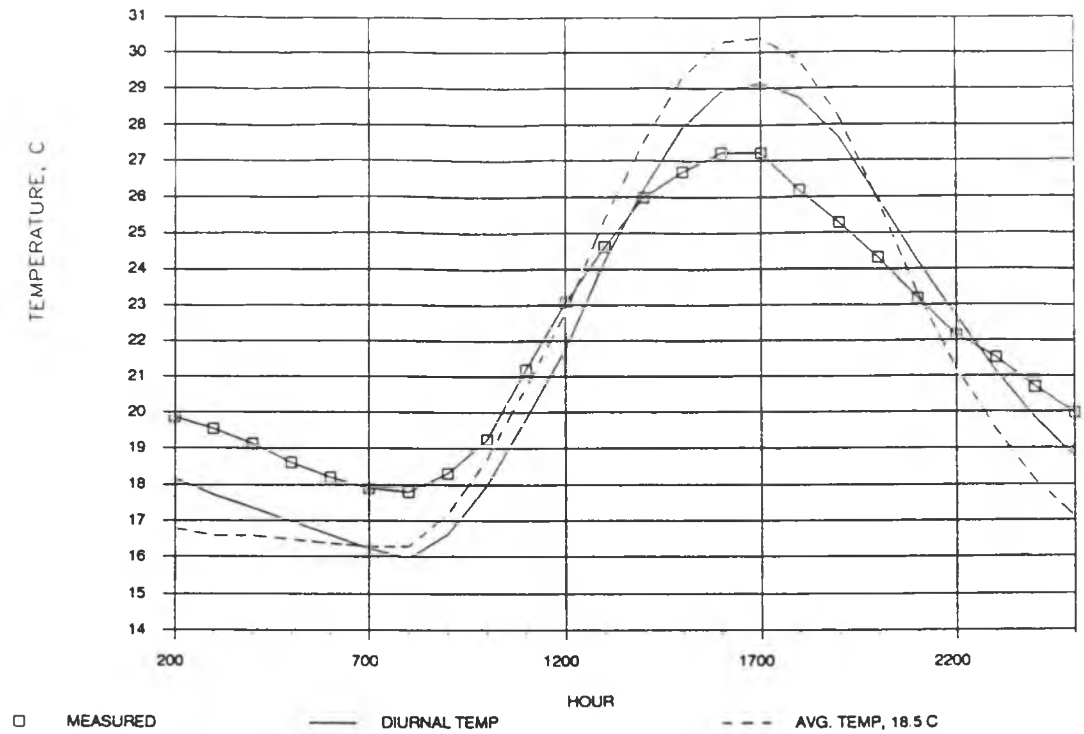

Fig. 7.13 Measured and TEMP-84 modeled stream temp. for Virgin River Mile 157.3 utilizing diurnal and average inflow stream temperatures on 6-30-88.

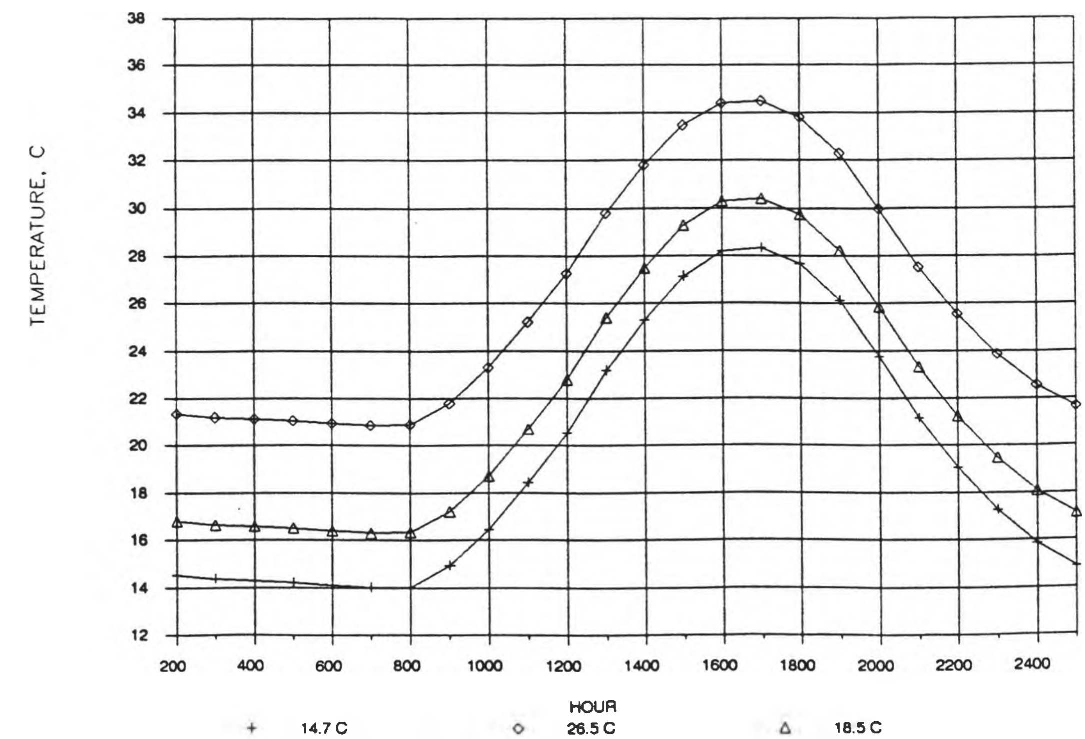

Fig. 7.14 TEMP-84 modeled stream temp. for Virgin River Mile 157.3 on 6-30-88 with inflow at existing, groundwater, and average ambient temperature.

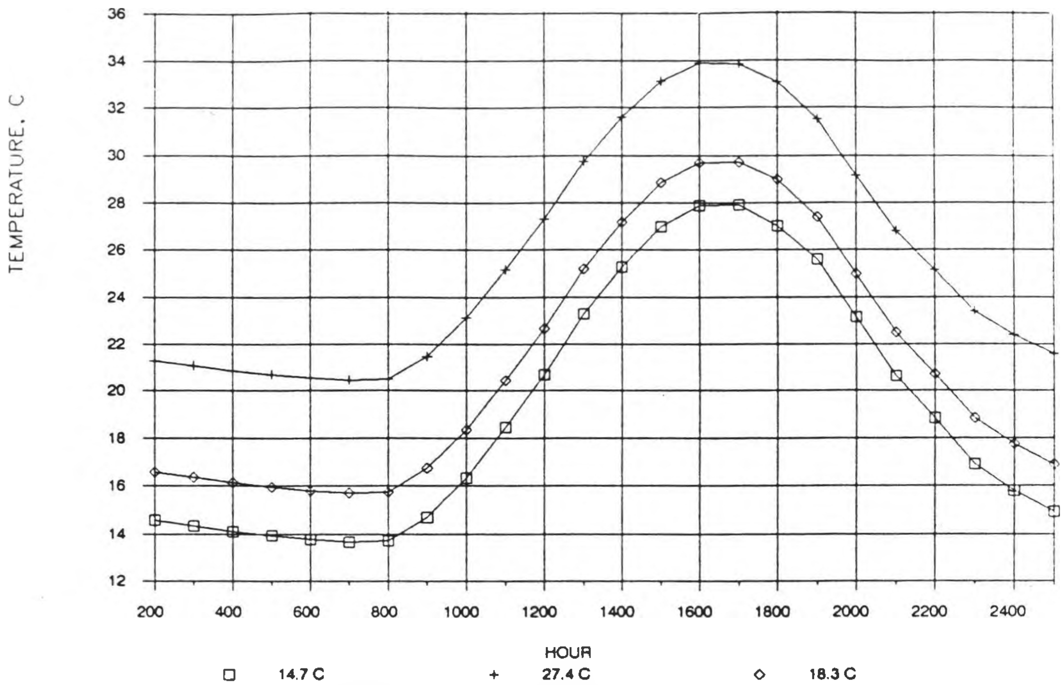

Fig. 7.15 TEMP-84 modeled stream temp. for Virgin River Mile 157.3 on 7-08-88 with inflow at existing, groundwater, and average ambient temperature.

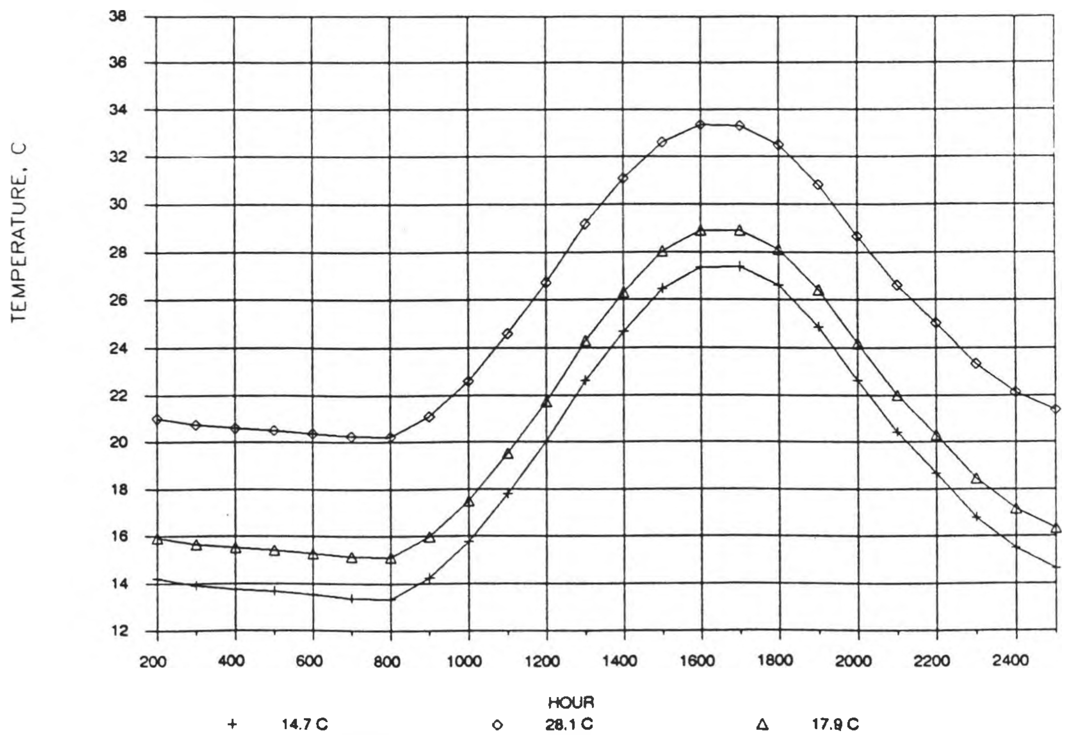

Fig. 7.16 TEMP-84 modeled stream temp. for Virgin River Mile 157.3 on 7-15-88 with inflow at existing, groundwater, and average ambient temperature.

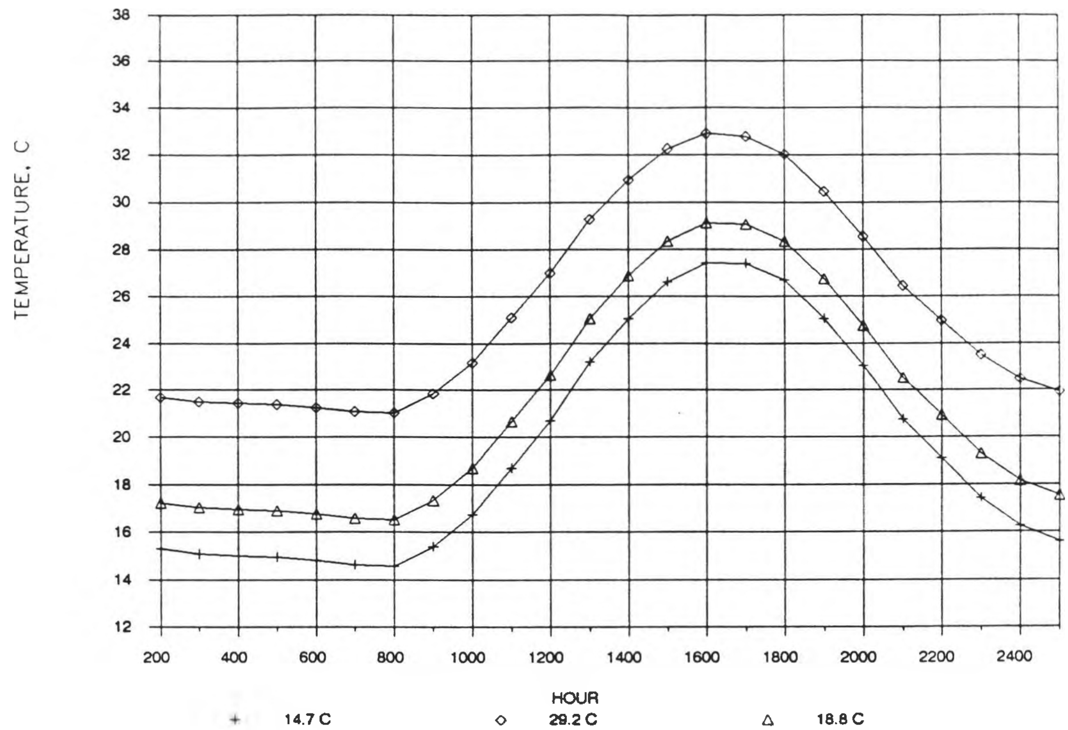

Fig. 7.17 TEMP-84 modeled stream temp. for Virgin River Mile 157.3 on 7-21-88 with inflow at existing, groundwater, and average ambient temperature.

conditions and the selected hypothetical inflow temperature conditions. Table E.10 and E.11 document the hourly stream temperatures for each simulation on each day.

In contrast to modeled stream temperature regimes for hypothetical flows, the entire twenty-four hour diurnal stream temperature regime for hypothetical inflow temperature conditions was shifted by nearly a constant interval from that modeled for existing conditions. Inflow at the average ambient temperature, which is 8 to 10°C greater than existing inflow temperature, illustrated an increase in modeled stream temperature at VRM 157.3 of approximately 4°C to 5°C. Inflow at groundwater temperature, which is approximately 4°C less than existing inflow temperature, illustrated a decrease in modeled stream temperature at VRM 157.3 of approximately

2°C. In both cases, an approximate change in stream temperature of 1°C occurred at VRM 157.3 for every 2°C change in the inflow stream temperature.

As discussed with hypothetical flow simulations, TEMP-84 was not calibrated to simulate existing conditions at VRM 157.3. Thus, the results from modeling hypothetical inflow temperature conditions should be viewed in terms of the relative change from that modeled for existing conditions and not for the actual temperatures produced. For each simulation, the percent change in maximum, mean, and minimum stream temperatures was calculated from that modeled for existing average inflow stream temperatures (Table E.12).

To simulate stream temperatures for the selected hypothetical conditions, the average percent change for each stream temperature characteristic, i.e., maximum, mean, and minimum, under each hypothetical inflow condition was applied to the measured stream temperature at VRM 157.3 (Table 7.5).

The resulting stream temperatures between the four days modeled were similar; the standard deviation for each set of maximum, mean, and minimum temperatures under each hypothetical conditions was less than 0.55°C. Because the results have inherent errors from the modeling process and each simulation represents only a small sample from the population of stream temperatures, the results were averaged to provide an estimate of maximum, mean, and minimum stream temperatures for each hypothetical condition. Maximum stream temperature ranged from an average of 31.1°C for average ambient inflow temperatures to 25.6°C under groundwater temperature inflow conditions. Mean stream temperatures ranged from an average of 26.4°C to 19.8°C for average ambient inflow temperature and groundwater temperature inflow conditions, respectively. Minimum stream temperatures ranged from an average of 22.2°C for average ambient temperature inflow to 15.0°C for groundwater temperature inflow.

Figure 7.18 depicts for hypothetical inflow stream temperatures, the percent change of modeled maximum stream temperature from that modeled for existing

Table 7.5. Maximum, mean, and minimum stream temperature as calculated from the TEMP-84 simulated percent change applied to existing conditions.

	INFLOW TEMPERATURE			INFLOW TEMPERATURE		
	EXISTING	GW TEMP	AVG. AMBIENT	EXISTING	GW TEMP	AVG. AMBIENT
DATE	MAX STR TEMP C	MAX STR TEMP C	MAX STR TEMP C	MEAN STR TEMP C	MEAN STR TEMP C	MEAN STR TEMP C
6-30-88	27.2	25.4	30.9	22.0	19.8	26.5
7-08-88	27.0	25.4	30.8	21.5	19.6	26.1
7-15-88	26.9	25.5	31.1	21.2	19.4	26.3
7-21-88	27.8	26.2	31.4	22.4	20.5	26.8
MEAN	27.2	25.6	31.1	21.8	19.8	26.4
VARIANCE	0.16	0.15	0.07	0.28	0.23	0.09
STD DEV	0.40	0.39	0.27	0.53	0.48	0.30

	INFLOW TEMPERATURE		
	EXISTING	GW TEMP	AVG. AMBIENT
DATE	MIN STR TEMP C	MIN STR TEMP C	MIN STR TEMP C
6-30-88	17.8	15.3	22.8
7-08-88	16.7	14.6	21.8
7-15-88	16.2	14.4	21.7
7-21-88	17.5	15.5	22.3
MEAN	17.1	15.0	22.2
VARIANCE	0.54	0.28	0.26
STD DEV	0.74	0.53	0.51

conditions. The percent change for each simulation on each day is tabulated in Table E.12. Again, the percent change represents the change from existing conditions and a positive percent change represents a decrease in stream temperature while a negative percent change represents an increase. Inflow at the groundwater temperature resulted in an average decrease in maximum stream temperature of 5.9 percent. The standard deviation associated with this average was 0.58 percent. In contrast, an inflow at the daily average ambient temperature resulted in an average increase in maximum stream temperature of -14.1 percent. The standard deviation associated with this average is 1.10 percent.

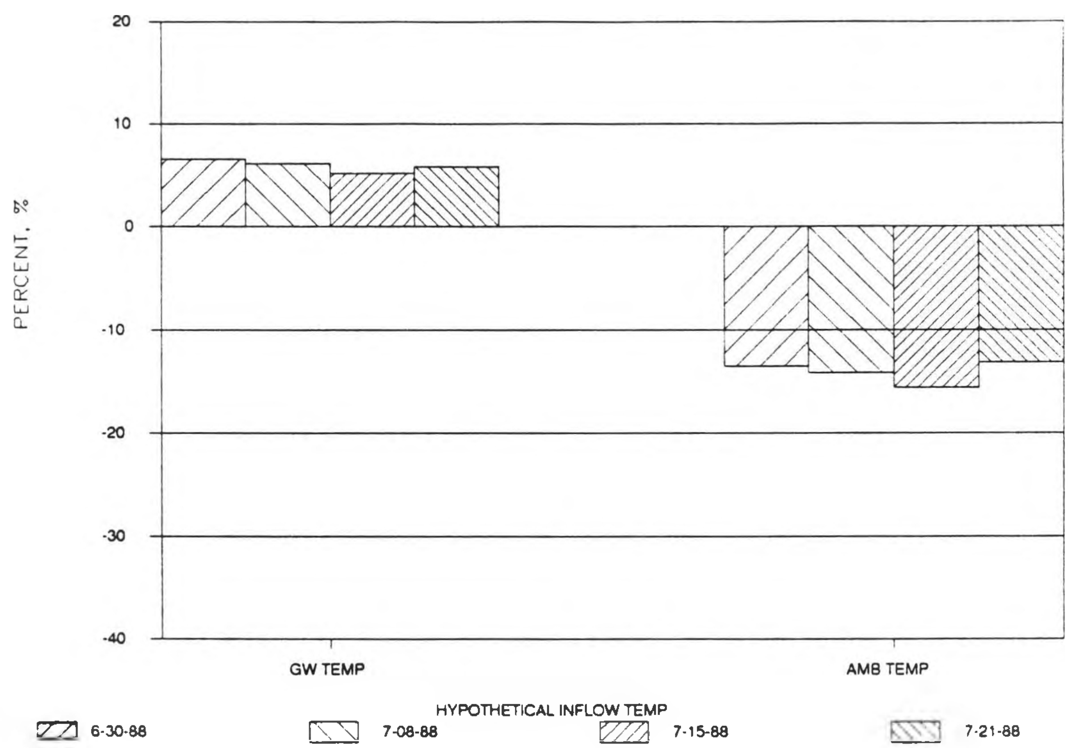

Fig 7.18 Percent change in maximum stream temp. at Virgin River Mile 157.3 for TEMP-84 modeled hypothetical inflow temps. from that modeled for existing conditions on 6-30-88, 7-08-88, 7-15-88, and 7-21-88.

Figure 7.19 portrays the percent change in the mean stream temperature. The percent change for each simulation on each day is tabulated in Table E.12. The average percent decrease in mean stream temperature with groundwater temperature inflow was 9.0 percent with an associated standard deviation of 0.83 percent. The average percent increase in mean stream temperature with inflow at the average ambient temperature was -21.3 percent with an associated standard deviation of 1.88 percent.

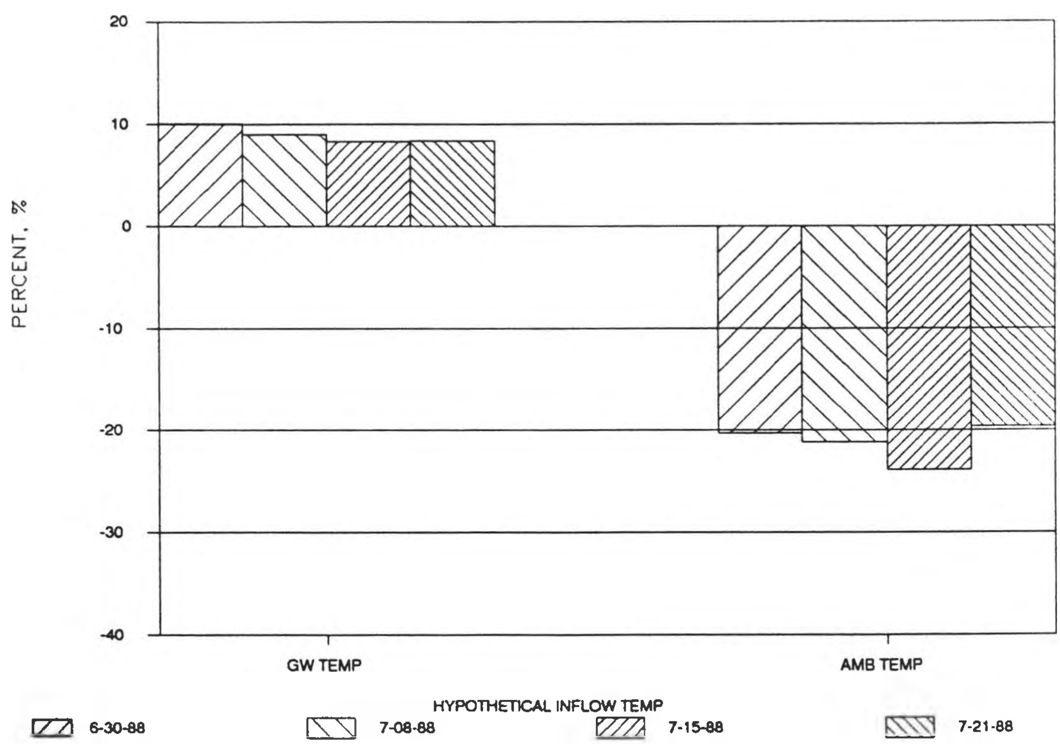

Fig 7.19 Percent change in mean stream temp. at Virgin River Mile 157.3 for TEMP-84 modeled hypothetical inflow temps. from that modeled for existing conditions on 6-30-88, 7-08-88, 7-15-88, and 7-21-88.

Finally, figure 7.20 illustrates the percent change in minimum stream temperature for the hypothetical inflow temperature simulations. The percent change for each simulation on each day is tabulated in Table E.12. The average decrease in minimum stream temperature with an inflow at the groundwater temperature was 12.4 percent with an associated standard deviation of 1.29 percent. The average increase in minimum stream temperature with inflow at the average ambient stream temperature was -30.0 percent with an associated standard deviation of 2.91 percent.

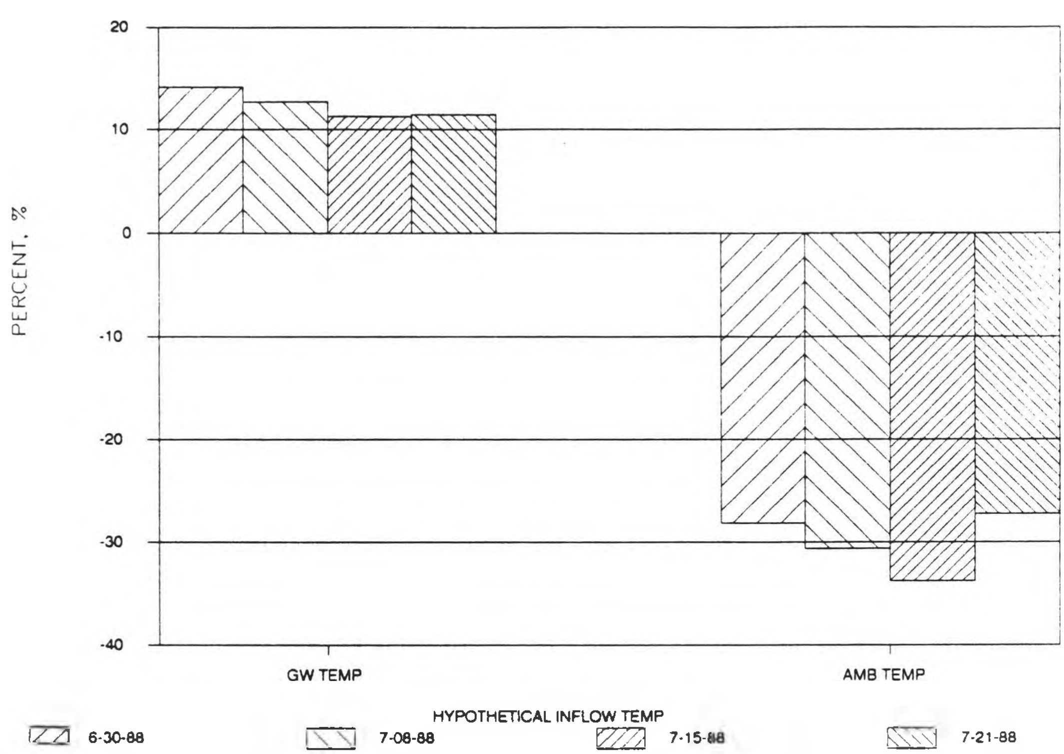

Fig 7.20 Percent change in minimum stream temp. at Virgin River Mile 157.3 for TEMP-84 modeled hypothetical inflow temps. from that modeled for existing conditions on 6-30-88, 7-08-88, 7-15-88, and 7-21-88.

Chapter 8. Discussion

The stream temperature of the East Fork of the Virgin River is dynamic over a twenty-four hour period. At VRM 157.3 maximum stream temperatures varied between 26°C and 28°C during the month of July while minimum stream temperatures varied between 18°C to 16°C. A diurnal fluctuation of 10°C was common. Increased solar exposure towards the downstream end of the study reach is the probable cause for the average 5.7°C increase between the daily maximum stream temperature at VRM 157.3 and that a VRM 163.1. Flow at VRM 163.1 was cooler most likely because of the severe vertical canyon walls which provided shading upstream and at VRM 163.1 as well as the influx of groundwater upstream of the study reach. Downstream from VRM 163.1, the canyon widens and the stream is openly exposed to solar radiation; solar radiation is a dominant heat source and effectively heats the stream. The solar radiation component, which has a strong effect during the day is absent between sunset and sunrise.

It appears from the small difference between minimum temperatures at VRM 157.3 and VRM 163.1 that the energy transfer rate during the night is nearly the same throughout the study reach. Slight differences in minimum stream temperatures were likely due to small differences in air temperatures.

A sensitivity analysis was conducted to determine the relative effect of the respective input variables on the modeled stream temperature. Based on sensitivity analysis results, each variable was rated with respect to a large, moderate, small, or negligible effect on the modeled stream temperature for this study reach (Table 8.1). A large effect was defined for Table 8.1 as greater than 1°C change in either maximum or minimum stream temperature with a 15 percent change in the input value. A moderate effect was defined as a 0.5°C to 1.0°C change with a 15 percent change in the input value. Similarly, a small effect was defined as a 0.1°C to 0.5°C change with an approximate 15 percent change in input value. A negligible effect was defined as 0.0°C to 0.1°C change in modeled stream temperature with a relatively large, ie., greater than 50 percent or well outside the precision boundaries of the measurement, change in the input value.

TEMP-84 was most sensitive to the inflow stream temperature followed by, in decreasing order of sensitivity, the variables of width, discharge, and air temperature all of which had a large effect on the resulting modeled stream temperature. TEMP-84 was also quite responsive to the variables of length and velocity which had moderate effects on the modeled stream temperature. The remaining variables resulted in less than 0.5°C change in the outflow temperature with a 15 percent perturbation in the input value. The inflow stream temperature is important because it establishes the reference temperature to which the modeled change in temperature is applied. Width and length values are important because they are used to calculate the surface area over which the heat transfer occurs. Discharge quantifies the size of the stream and thus establishes the thermal inertia of the system. Air temperature plays a large

Table 8.1. Sensitivity of TEMP-84 input variables in terms of large, moderate, small, and ngeligible effect on the modeled stream tmeperature.

Input Variable	Change in Input Variable	Response of Stream Temp. (Existing - Perturbed) Maximum Temp.	Minimum Temp.	Rated Effect
Stream Temperature	+15%	-1.5	-1.6	LARGE
	-15%	1.5	1.7	
Width	+15%	-1.5	0.2	LARGE
	-15%	1.6	-0.2	
Discharge	+15%	1.2	-0.2	LARGE
	-15%	-1.4	0.2	
Air Temperature	+15%	-1.1	-0.8	LARGE
	-15%	1.0	0.7	
Velocity	+15%	-0.5	0.2	MODERATE
	-15%	0.6	-0.4	
Length	+15%	-0.6	-0.2	MODERATE
	-15%	0.9	-0.1	
Hillslope Angle	+5 deg (>10%)	0.4	0.3	SMALL
	-5 deg (>10%)	0.0	0.0	
Relative Humidity	+15%	-0.2	-0.2	SMALL
	-15%	0.2	0.2	
Groundwater Temp.	+15%	-0.3	-0.3	SMALL
	-15%	0.3	0.3	
Groundwater Flow	+15%	0.3	0.0	SMALL
	-15%	-0.3	0.0	
Perpendicular Forest Angle	+5 deg (>15%)	0.1	0.0	SMALL
	-5 deg (>15%)	0.3	0.3	
Wind	+15%	0.1	0.0	SMALL
	-15%	-0.1	0.0	
Mean Elevation	+10%	-0.1	0.0	SMALL
	-10%	0.1	0.0	
Tree Height	+6.1 m (>50%)	0.0	0.0	NEGLIGIBLE
Canopy Cover	+50%	0.0	0.0	NEGLIGIBLE
	-50%	0.1	0.1	
Buffer Width	+20 ft	0.0	0.1	NEGLIGIBLE
Latitude	+0.1	0.0	0.0	NEGLIGIBLE
	-0.1	0.0	0.0	
Longitude	+0.1	0.0	0.0	NEGLIGIBLE
	-0.1	0.0	0.0	
Topographic Angle	+20 deg (>45%)	0.0	0.0	NEGLIGIBLE
	-20 deg (>45%)	0.0	0.0	
Stream Gradient	+30%	0.0	0.0	NEGLIGIBLE
	-30%	0.0	0.0	
Percent Bedrock	+100%	0.0	0.0	NEGLIGIBLE
Stream Aspect	+10 deg (>5%)	0.0	0.0	NEGLIGIBLE
	-10 deg (>5%)	0.0	0.0	
Direct Shading	+100%	0.4	0.0	NEGLIGIBLE
Vegetation Angle	+35 deg (>90%)	0.0	0.0	NEGLIGIBLE
	-15 deg (>40%)	0.0	0.0	

role in regulating the stream temperature as it is encompassed either directly or indirectly in all the heat transfer processes except net solar radiation and advection. Velocity was the only variable found to affect the time of the modeled stream temperature peak as well as the peak values. Velocity is utilized to calculate the travel time of an individual water parcel and thus also serves to determine the start time for the parcel. Corresponding to the start time is a start inflow stream temperature which directly affects the time and value of the peak temperatures.

The majority of shading characteristic data had a negligible effect on the resulting stream temperature. The two variables of hillslope angle and perpendicular forest angle demonstrated a small effect. Small to negligible effects were expected for these variables as the study reach is oriented in an east-west direction, the sun rides at a high altitude, and the vegetation is relatively sparse.

Somewhat surprising was the small effect of wind and relative humidity on the modeled stream temperature. The reason for this apparent small effect are the small input values of 18 percent input for relative humidity and 3.2 km per hour for wind on 6-30-88. A 15 percent change in these variables results in only small changes of 2.7 percent and 0.5 km per hour for relative humidity and wind, respectively. Not surprisingly, a 15 percent change has only a small effect on the stream temperature. While the value of relative humidity seems reasonable, 3.2 km seems low for the study reach wind component especially with respect to morning and evening time periods during which strong convective winds are common. It is likely that the stream temperature is more sensitive to windspeed than illustrated in this analysis.

In simulating existing conditions, the model predicted greater diurnal fluctuations in stream temperature with minimum temperatures lower than existing by 1.1°C to 1.8°C and maximum temperatures greater than existing by 0.3°C to 2.0°C. Elevated modeled maximum temperatures may be due to a number of reasons. For one, TEMP-84 does not incorporate cloud cover effects and is documented as a model to simulate maximum possible stream temperature. Cloud cover was shown by Tennessee Valley Authority (1972) to effectively attenuate the solar radiation reaching the stream. On 6-30-88 the sky was rated by Zion National Park (ZION) to be 1/10 to 5/10 cloud covered. On 7-08-88, 7-15-88, and 7-21-88, it was rated at less than 1/10 cloud cover. Neglecting the effect of cloud cover in modeling would have the greatest consequence for 6-30-88.

Another cause of elevated maximum stream temperatures could be inaccurate modeling of the evaporative heat flux. Evaporation is the most dominating heat loss variable in the energy balance. Evaporative flux has been studied for many years resulting in a large number of empirically derived formulae (Ryan and Harleman, 1973). Applying empirical formulae to sites other than for which they were derived creates a degree of uncertainty in the resulting evaporative flux calculation. Duttweiler's evaporative heat loss equation which provided the best fit to official NOAA evaporation data collected in Saint George, UT, possibly underestimates the evaporative heat loss occurring in the ZION system.

Cooling from the net longwave flux may also be underestimated. While the Stefan Boltzman Radiation Law used in TEMP-84 is an accepted technique for modeling longwave flux (TVA, 1972), the emissivities assumed and calculated for air, canopy, and water may not be representative of the emissivities for air, canopy, and water in ZION. TEMP-84 also assumes a constant density of riparian vegetation for calculating longwave radiation emitted from canopy. In ZION the vegetation is not of a constant density but rather spotty with trees and bushes located sporadically along the study reach. As result, the longwave radiation emitted from the canopy is likely overestimated. This overestimate would result in an underestimate of the net longwave flux thus underestimating the cooling effect of net longwave flux.

In addition to the inaccuracies of modeling, discrepancies between simulated and existing stream temperatures may also be due to a lack of precision in input data. Part of the sensitivity analysis was conducted to determine the uncertainty in modeled stream temperature resulting from input data imprecision. This analysis displayed that the greatest uncertainty in the modeled maximum stream temperature resulted from the imprecision of groundwater flow and stream width data. The precision range for width data allowed for greater than 1.0°C increase in maximum temperature. The precision range of groundwater data allowed a 2.1°C increase. Also causing uncertainty in the modeled maximum stream temperature were the variables of stream temperature, velocity, relative humidity, air temperature, and discharge. Perturbation by their respective rated precision resulted in an increase in maximum stream temperature by 0.5°C, 0.5°C, 0.6°C, 0.7°C, and 0.9°C, respectively. Input data error meeting the precision range for a combination of these variables could have easily caused the over prediction of the maximum temperature of 0.3°C to 2.0°C.

Explanation of why TEMP-84 modeled minimum stream temperatures at values less than measured is not clear. During early morning hours to about 0730, the energy transfer components, except solar radiation which is zero, were all calculated at low rates without any one dominating over the others. During these hours net longwave and evaporative flux were cooling while convective heat transfer was warming the stream. Evaporative cooling may have been over predicted at night due to the lack of site specific empirical coefficients. Or possibly the empirical constant utilized in the Bowen ratio does not accurately depict the relationship between evaporative and convective heat flux for the ZION system.

Error in input data equal to the precision range of a combination of variables could accumulate and also account for the difference of 1.1°C to 1.8°C between modeled and measured minimum stream temperatures. The sensitivity analysis depicted that the precision in stream temperature and relative humidity data allowed for the greatest uncertainty in the modeled minimum stream temperatures. Perturbation of the stream temperature by its precision allowed for a 0.5°C decrease in minimum temperature while the precision range of relative humidity allowed for a 0.7°C decrease. Also contributing to the uncertainty of the modeled minimum stream temperature was the precision range in air temperature which allowed for a 0.5°C decrease in minimum stream temperature.

The difference between modeled and measured mean temperatures ranged from 0.3°C to 1.0°C. All mean temperatures were determined by calculating the time weighted average from the hourly defined record. The mean temperature for 6-30-88 most closely matched the measured mean temperature because the difference between modeled and measured maximum values was balanced by the difference between minimum values.

Statistical applications are difficult to apply to the four simulations as the hourly measured and modeled stream temperatures for a twenty-four hour period were not random in nature. Thus, it is difficult to determine which of the four simulations best models existing conditions.

Simulation of 7-21-88 and 6-30-88 most accurately modeled the measured maximum and mean stream temperature, respectively. Minimum temperatures were modeled most accurately by simulations of 7-08-88 and 7-21-88. After evaluating the four simulations it appeared that the simulation of 7-21-88 most closely modeled diurnal fluctuations while 6-30-88 most closely simulated mean stream temperatures.

The timing of modeled peaks for the diurnal fluctuation also indicates of how well the measured stream temperature regime was simulated. Lag in the modeled diurnal fluctuations likely resulted from a culmination of: imprecision in the time corresponding to modeled and measured data points depicted in Figure 6.1 through 6.4, inaccuracy in the modeled velocity component, and assumptions and simplification in the model solution theory itself. Simulation on 6-30-88 depicted peak times modeled most closely to measured peak times. Peak times for 7-08-88, 7-15-88, and 7-21-88 differ from measured by thirty minutes to one hour.

Hypothetical conditions were simulated for each of the four days selected for modeling. Width, velocity, discharge, percent bedrock, and percent direct shade had the same input values over the four days modeled for a given hypothetical condition. Differences in simulated diurnal fluctuations for a given hypothetical condition resulted from differing meteorological conditions and inflow stream temperatures.

Because each hypothetical simulation represents the change in stream temperature from that at baseflow condition and no one hypothetical simulation can be judged as absolute, an average percent change in maximum, mean, and minimum stream temperature was determined for each hypothetical condition.

The average percent change for maximum, minimum, and mean values applied to measured stream temperatures at VRM 157.3 provides an estimate of the stream temperatures expected under the selected hypothetical condition. Table 8.2 tabulates the resulting average maximum, mean and minimum stream temperatures calculated for each hypothetical condition as well as the diurnal fluctuation.

Table 8.2. Estimates of the maximum, mean, and minimum stream temperatures expected during July at Virgin River Mile 157.3 for the selected hypothetical flow conditions.

Flow Condition	Maximum Temp. deg C	Mean Temp. deg C	Minimum Temp. deg C	Diurnal Fluct. deg C
14,160 l/s	20.7	19.4	18.0	2.7
2,832 l/s	22.6	20.3	17.9	4.7
2,124 l/s	23.4	20.6	17.8	5.6
566 l/s	29.7	22.4	16.5	13.2
283 l/s	32.9	23.3	15.6	17.3

The maximum stream temperatures changed dramatically for flows differing from that of baseflow. For a flow of 283 l/s (10 cfs), the estimated maximum stream temperature reached a level of 32.9°C which is at least 5°C higher than that measured for baseflow conditions. In contrast, for a flow of 14,160 l/s (500 cfs), the estimated maximum stream temperature, 20.7°C, decreased at least 6°C from than that measured for baseflow. A shift in stream temperature can dramatically change the existing ecological balance and change the character of the aquatic habitat. Often important in characterizing aquatic habitat is the maximum stream temperature as aquatic organisms frequently have thermal maximum temperatures above which they cannot exist. The maximum stream temperatures estimated for 566 l/s (20 cfs) and 283 l/s (10 cfs) might be such to prevent existing organisms from further livelihood. Similarly, maximum stream temperatures as low as that expected for 2,124 l/s (75 cfs), 2,832 l/s (100 cfs), and 14,160 l/s (500 cfs) might also alter the selection of aquatic life which currently exists.

Mean stream temperatures follow the same pattern as maximum stream temperatures, ie., increasing with decreased flow and decreasing with increased flow. The mean stream temperature depicted for 283 l/s, 23.3°C, is at least 0.9°C higher and the mean stream temperature estimated for 14,160 l/s, 19.4°C, is at least 1.8°C lower than that measured for baseflow conditions.

Minimum stream temperatures increased with increased flow while they decreased for decreased flow. The minimum stream temperature estimated for 283 l/s, 15.6°C, is at least 0.6°C lower than that measured for existing conditions. The minimum stream temperature estimated for 14,160 l/s, 18.0°C, is at least 0.2°C higher than that measured. Minimum stream temperatures did not differ as much as maximum stream temperatures because of the low heat transfer rate that occurs during the night for all flows.

As expected, the diurnal fluctuation dampens for larger flows with relatively low maximum and high minimum stream temperatures. This result corresponds to Sullivan's (1989) work illustrating decreased diurnal fluctuation with increased stream size. The larger stream illustrates a greater thermal inertia and is less responsive to fluctuations in atmospheric conditions. Equation 2.1, TEMP-84's simplified basic solution theory, predicts this response. As the discharge increases, the increase in surface area becomes small compared to the increase in discharge. Accordingly, the ratio of surface area to discharge becomes small. As a result, the net heat transfer multiplied by a decreasing surface area to discharge ratio produces smaller change in temperature and dampened diurnal fluctuations. Eventually, the surface area to discharge ratio approaches zero and thus the calculated change in temperature approaches zero. When this happens, the modeled stream temperature approximates that of the inflow stream temperature; this occurred at approximately 14,160 l/s for the study reach. In contrast, for low flows, the surface area to discharge value tends to be large producing large temperature changes and increased diurnal fluctuations.

Figure 8.1 depicts a plot of the diurnal fluctuation with respect to flow. Change in the diurnal fluctuation transpired most dramatically within the first 2,832 l/s and then gradually decreased to 2.7°C by 14,160 l/s. In contrast, as the flow decreased from baseflow, the diurnal fluctuation increases quickly towards infinity. Of course this cannot happen in reality. The probable stream temperature and diurnal fluctuation for near zero flow would be equal to the surrounding air temperature and its diurnal fluctuation.

The percent change in stream temperature from that modeled for baseflow condition is fairly consistent between the four days modeled for the respective hypothetical condition. The standard deviation for the average percent change in maximum, mean, and minimum stream temperature, respectively, was less than two percent for all cases except simulation of maximum stream temperature at 283 l/s.

For this hypothetical condition, the percent change in maximum stream temperature ranged from -23.8 percent to -16.6 percent over the four days selected for modeling. The standard deviation was 3.07 percent. The percent change in temperature varies more for low flow conditions because the flow component is less dominating and the change in temperature is more responsive to fluctuations in the heat transfer components.

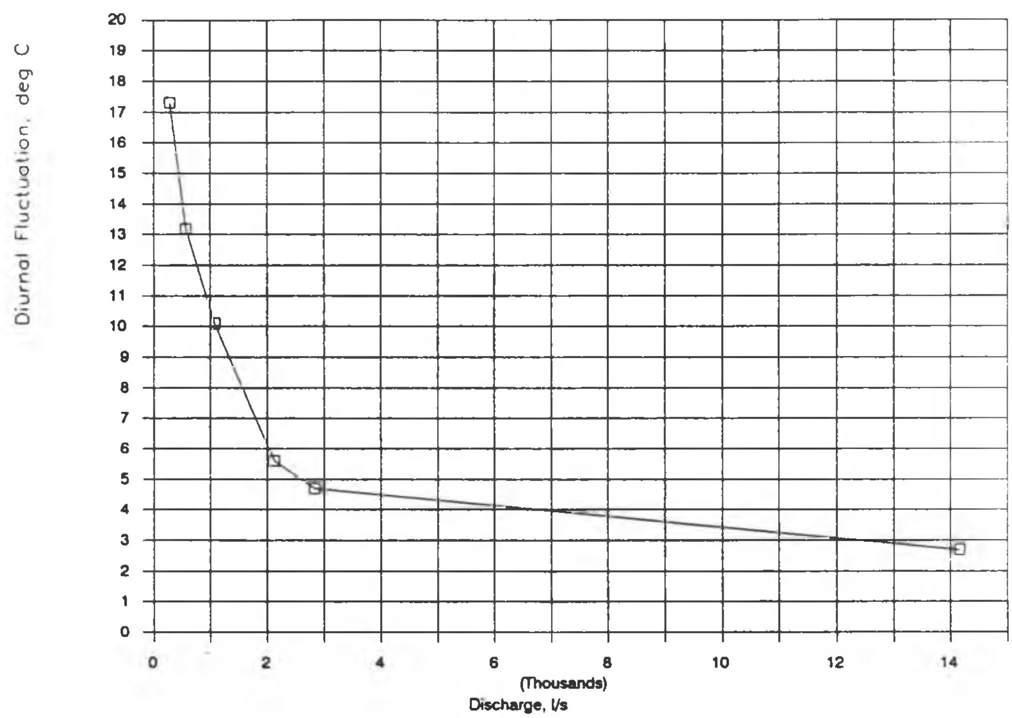

Fig. 8.1. Trend in diurnal fluctuation of stream temperature at Virgin River Mile 157.3 with respect to flow.

With a decrease in flow from 14,160 l/s to 283 l/s, the average percent change in maximum stream temperature decreased from 23.9 percent to -20.9 percent while the average percent change in mean stream temperature decreased from 11.2 percent to -6.8 percent. In contrast, the average percent change for minimum stream temperature increased from -5.6 percent to 8.5 percent. Figure 8.2 illustrates the trend of the average percent change in maximum, mean, and minimum stream temperature with respect to flow. Each curve decreases in slope with increased discharge showing that the increase/decrease in average percent change for minimum, mean, and maximum temperatures becomes small with additional increases in discharge. The range in the average percent change for minimum, mean, and maximum temperatures occurs to a large degree between 283 l/s and 2,832 l/s. Between 2,832 l/s and 14,160 l/s, the absolute value of the average percent change for minimum, mean, and maximum stream temperature increased by 0.6 percent, 4.5 percent and 7.0 percent, respectively. Simulations of 28,320 l/s (1000 cfs) for 6-30-88 indicated an increase in the percent change of maximum temperature of 1.3 percent from that modeled for 14,160 l/s and no increase/decrease in the percent change for mean and minimum stream temperatures. Small increases in the percent change in stream temperatures with a large increase in discharge infer that a limiting percent change in stream temperature exists beyond which discharge will not affect. An estimate for this limiting percent change in temperature can be made from the simulated results for 14,160 l/s seeing as the increase in percent change in temperature between 14,160 l/s and 28,320 l/s on 6-30-88 was less than 1.5 percent ie., 0.5°C. The average percent change of 23.9 percent for maximum stream temperature, 11.2 percent for mean stream temperature, and -5.6 percent for minimum stream temperature reached at 14,160 l/s approximates a boundary percent change beyond which increases in discharge will not affect.

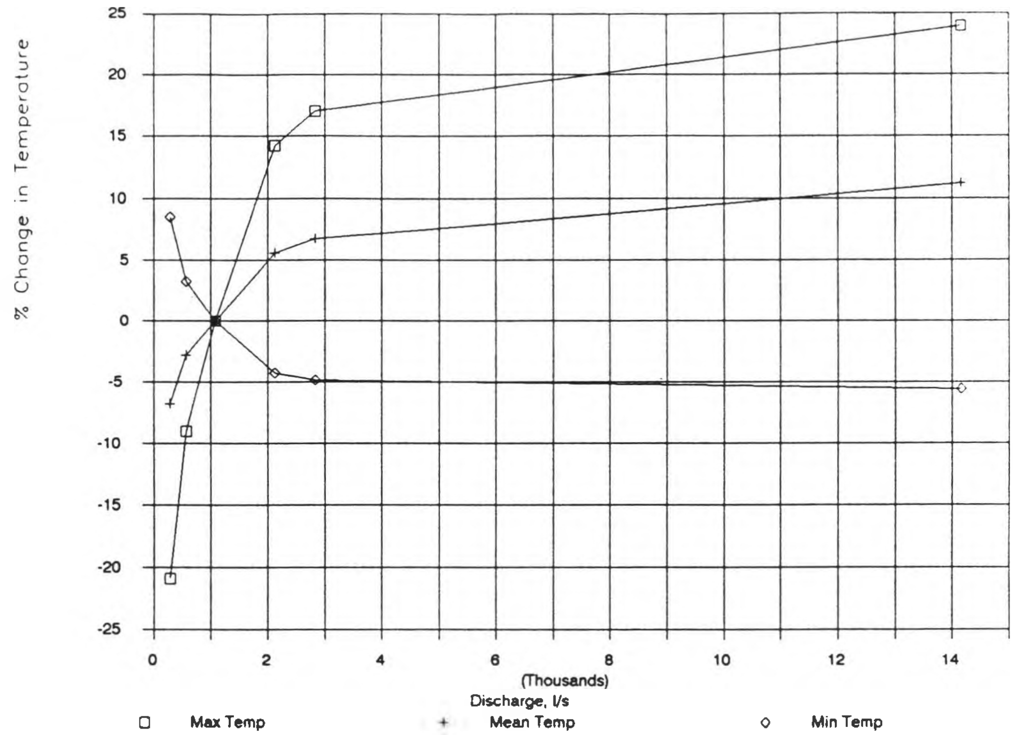

Fig. 8.2 Average percent change in maximum, mean, and minimum stream temperature at Virgin River Mile 157.3 with respect to flow.

As with the diurnal fluctuation, the average percent change in maximum, mean, and minimum temperatures increase in an exponential fashion for flows less than baseflow. It is obvious that stream temperature cannot reach infinity as the flow approaches zero. It is most probable that as the flow decreases from 283 l/s, the maximum, mean, and minimum stream temperatures will approach values equal to those of the surrounding air temperature.

The difference in time for peak temperatures is largely due to the change in velocity for the different flows. Another factor is that stream temperature output from TEMP-84 was reported at hourly intervals. Output values for hypothetical conditions were interpolated to delineate stream temperature values within +/- 15 minutes of those output for baseflow conditions. Therefore, the times logged for the stream temperature values delineated in Figures 7.2 through 7.9 and Tables E.2 through E.5 are precise to +/- 15 minutes. In addition, the inflow temperature regime at VRM 163.1 also has inherent error in the time logged on the chart as a result of the imprecision of the instrument.

Modeled results for hypothetical conditions are not absolute but rather have an inherent error due to a lack of precision in model input data as well as model shortcomings, assumptions, and simplifications. Specifically, for hypothetical flow conditions, a lack of precision exists for width and velocity values as they were estimated as function of flow based on empirical relationships. The relationships for these variables were determined from Manning's equation assuming a constant Manning's n roughness coefficient and a constant energy slope. While it is known that neither the "n" value nor the energy slope remain constant for varying flows, it was the best information available. Furthermore, no data are available for which to compare to the empirically derived values to estimate their accuracy. Accordingly, the results from modeling the hypothetical conditions should be judged as an indication of the response of stream temperature in contrast to an absolute answer.

Simulating the hypothetical inflow stream temperature conditions required altering the single variable of inflow stream temperature. While the inherent inaccuracies of the model are still present, any inaccuracies from estimated values by means other than measured data is averted.

Results from modeling the hypothetical inflow temperature represent the change in stream temperature from that of baseflow conditions. Since each individual simulation has inherent errors and inaccuracies, the percent change in maximum, mean, and minimum stream temperatures from the four modeled days were averaged for a better overall indication of the response of stream temperature to the respective hypothetical inflow temperature condition.

The average percent change for maximum, mean, and minimum stream temperature values applied to the measured stream temperatures at VRM 157.3 provides an estimate for stream temperatures expected under the selected hypothetical conditions. Table 8.3 tabulates the resulting average maximum, mean, and minimum stream temperatures for each hypothetical condition.

Table 8.3. Estimates of the maximum, mean, and minimum stream temperatures for the selected hypothetical inflow temperature conditions at Virgin River Mile 157.3.

Inflow Temperature Condition	Maximum Temperature deg C	Mean Temperature deg C	Minimum Temperature deg C	Diurnal Fluctuation deg C
Groundwater Temperature	25.6	19.8	15.0	10.6
Average Ambient Temperature	31.1	26.4	22.2	8.9

As expected, cooler inflow stream temperatures resulted in cooler downstream temperatures while warmer inflow stream temperatures resulted in warmer downstream temperatures. For average ambient inflow stream temperatures, the maximum stream temperature reached 31.1°C which is at least 3.3°C higher than that measured for baseflow conditions. Similarly, the mean stream temperature of 26.4°C is at least 4.0°C higher and the minimum stream temperature of 22.2°C is at least 4.4°C higher than those measured. In contrast, for groundwater temperature inflow, the maximum stream temperature of 25.6°C is at least 1.3°C lower, the mean stream temperature of

19.8°C is at least 1.4°C lower, and the minimum stream temperature of 15.0°C is at least 1.2°C lower than those measured for baseflow conditions.

The stream temperature regime over the twenty-four hour period for the different inflow temperature conditions were very uniform in shape; each regime appeared to differ from the others and existing conditions by a consistent number of degrees throughout the twenty-four hours. This results because the inflow stream temperature for each simulation serves as a reference temperature around which the diurnal fluctuation is modeled. Comparing the absolute temperature difference between the individual hypothetical simulations and existing conditions indicated that an average stream temperature change of 0.5°C occurred at VRM 157.3 for every one degree perturbation in inflow stream temperature at VRM 163.1.

The percent change in maximum, minimum, or mean stream temperature from that modeled for existing conditions was quite similar over the four days for a given hypothetical inflow temperature condition. The standard deviation for each average was less than two percent except for the percent change in minimum stream temperature under average ambient inflow temperature conditions. The percent change for this hypothetical condition ranged from -27.3 percent to -33.8 percent. The standard deviation over the four days modeled was 2.91 percent. Contrary to what was seen previously, minimum stream temperatures depicted the largest percent change between hypothetical and existing conditions. This is because minimum temperatures are less in absolute value than mean or maximum temperatures while the temperature difference between hypothetical and existing maximum, mean, and minimum stream temperatures, respectively, are the same. Moreover a smaller number is divided into the same difference producing a larger percent change.

Overall, the percent change in maximum, mean, and minimum stream temperature was greater in absolute value for ambient inflow conditions than groundwater temperature inflow conditions. This was expected because the ambient inflow temperatures differed by 8°C to 10°C while the groundwater temperature only differed by 3°C to 4°C from inflow stream temperatures for existing conditions; as depicted by the results, a greater difference in inflow stream temperatures produced a greater difference in outflow stream temperature.

Conclusion

The East Fork of the Virgin River flows at an average base rate of 1,076 l/s (38 cfs) through a widening canyon in southwest Utah. Ambient conditions are typical of the Southwest with high afternoon temperatures and cool evening and night temperatures.

The first objective of this study was to describe the existing stream temperature regime of the East Fork of the Virgin River within Zion National Park during the summer of 1988. Diurnal fluctuations of 10°C at Virgin River Mile (VRM) 157.3 were common during the study period, June 29 through July 22, 1988. Daily maximum stream temperature recorded at VRM 157.3 ranged between 23.7°C and 27.8°C. Daily minimum stream temperature ranged from 15.2°C to 18.8°C and daily mean stream temperatures ranged from 21.2°C to 22.9°C. Average maximum, mean, and minimum stream temperatures at VRM 157.3 during the study period were 26.7°C, 21.8°C, and 17.0°C, respectively. The above documented stream temperatures were all recorded during base flow conditions.

The second objective was to predict the response of the daily fluctuations and mean daily stream temperature to hypothetical flow and inflow temperature conditions. To accomplish this objective, TEMP-84 was utilized to model existing conditions and selected hypothetical conditions. Modeled results were viewed in terms of the relative change in stream temperature from that modeled for existing conditions.

The average percent change in maximum, mean, and minimum stream temperature modeled for each hypothetical flow was applied to measured stream temperatures to estimate the stream temperatures expected for the selected hypothetical flow condition. Table 9.1 documents the resulting stream temperatures.

Table 9.1. Estimates of the maximum, mean, and minimum stream temperatures expected during July for the selected hypothetical flow conditions at Virgin River Mile 157.3.

Flow Condition	Maximum Temperature deg C	Mean Temperature deg C	Minimum Temperature deg C	Diurnal Fluct. deg C
14,160 l/s	20.7	19.4	18.0	2.7
2,832 l/s	22.6	20.3	17.9	4.7
2,124 l/s	23.4	20.6	17.8	5.6
566 l/s	29.7	22.4	16.5	13.2
283 l/s	32.9	23.3	15.6	17.3

The change in maximum, mean, and minimum stream temperatures for hypothetical flows greater than baseflow depicted decreasing maximum and mean stream temperatures and increasing minimum stream temperatures. The percent change in modeled maximum, mean, and minimum stream temperatures from that modeled for existing conditions increases/decreases dramatically between baseflow and 2,832 l/s (100 cfs). Beyond 2,832 l/s, the percent change in stream temperature increases/decreases gradually up to 14,160 l/s (500 cfs) and then only slightly between 14,160 l/s and 28,320 l/s (1000 cfs). These results indicate that a limiting percent change in stream temperature exists beyond which increases in discharge will not affect. A decrease in maximum stream temperature of 23.9 percent, decrease in mean stream temperature of 11.2 percent, and increase in minimum stream temperature of 5.6 percent, as simulated for 14,160 l/s, is an estimate of the limiting percent change in maximum, mean, and minimum stream temperatures for increasing flows. These respective percent changes applied to measured stream temperatures result in an average maximum stream temperature of 20.7°C, average mean of 19.4°C, and average minimum of 18.0°C.

The response of stream temperatures to hypothetical flows decreasing from that of baseflow depicted sharp increases in maximum and mean temperatures and decreases in minimum stream temperatures. For 283 l/s (10 cfs), the maximum stream temperature increased from the existing maximum stream temperature by 20.9 percent resulting in a stream temperature of 32.9°C. Mean stream temperatures increased by 6.8 percent resulting in a stream temperature of 23.3°C while minimum stream temperatures decreased by 8.5 percent resulting in stream temperature of 15.6°C.

Increasing hypothetical flow conditions produced decreased diurnal fluctuations in stream temperature. For flow greater than baseflow, the diurnal fluctuation dropped sharply between baseflow and 2,832 l/s and then gradually decreased to 2.7°C by 14,160 l/s. In contrast, a decrease in flow from that of baseflow produced an increase in the diurnal fluctuation. For flow less than baseflow, the diurnal fluctuation increased quickly from an average of 10.2°C at baseflow to 17.3°C at 283 l/s.

Modeled results illustrate that the surface area to flow ratio plays a large role in the simulated stream temperature. As flow increases, it eventually becomes great enough to drive the ratio of surface area to discharge towards zero and thus cause the calculated change in stream temperature to approach zero. For these conditions, variations in meteorological conditions have a minimum effect and the outflow stream temperatures approach that of the inflow values. For the East Fork of the Virgin River, a flow of 14,160 l/s was great enough to result in only small changes as the modeled stream temperature was simulated within 1°C of the inflow stream temperature values. In contrast, for low flows, the surface area to discharge ratio becomes large thus producing relatively large changes in stream temperatures. Because the flow is less dominating, the calculated change in stream temperature for low flows is much more responsive to variations in the net heat flux and thus shows a greater variance between simulations.

Modeled results for hypothetical inflow temperature conditions show that the stream temperature at VRM 157.3 will respond dynamically in the direction corresponding to the direction of change in the inflow temperature at VRM 163.1. Furthermore, each modeled diurnal fluctuation at the downstream end of the study reach was offset from the modeled existing diurnal fluctuation by an average of 0.5°C for every 1°C difference in inflow temperature.

Again, applying the average percent change in maximum, mean, and minimum stream temperature for each hypothetical condition to measured stream temperatures provides an estimate of stream temperatures expected for the selected inflow temperature condition. Table 9.2 documents the resulting stream temperatures.

Average ambient inflow temperatures modeled increases in maximum, mean, and minimum stream temperature of 14.1 percent, 21.3 percent, and 30.0 percent, respectively, from that modeled for existing conditions.

Table 9.2. Estimates of the maximum, mean, and minimum stream temperatures expected during July for the selected hypothetical inflow temperature conditions at Virgin River Mile 157.3.

Inflow Temperature Condition	Maximum Temperature deg C	Mean Temperature deg C	Minimum Temperature deg C	Diurnal Fluctuation deg C
Groundwater Temperature	25.6	19.8	15.0	10.6
Average Ambient Temperature	31.1	26.4	22.2	8.9

Inflow at groundwater inflow temperature modeled decrease in maximum, mean, and minimum stream temperature of 5.9 percent, 9.0 percent and 12.4 percent, respectively, from that modeled for existing conditions.

Recommendations for Future Research

In carrying out this research, several problematic situations occurred which could be avoided in the future. For instance, forgetting to turn on the Ryan stream thermograph battery resulting in no data collection and the broken stream thermograph seal resulting in instrument flooding and damage could have been avoided if more attention had been given to the instrument conditions during servicing an double checking settings and thermograph assembly prior to remounting in the stream.

Further data collection problems were incurred as a result of instrument site selection. Data from maximum/minimum mercury thermometers was useless due to the unrepresentative site selection. It is difficult to find adequate shading for a mercury thermometer while at the same time measuring accurate air temperatures. For future research, it is recommended that artificial shade be constructed for the thermometers to allow siting in an open location representative of surrounding air temperatures. Another problem related to instrument site selection arose when the probe to the submersible stream thermograph became buried with sediment deposition from flood flow. This situation can be avoided by allowing room for sediment deposition when siting the instrument. In this East Fork study reach, at least eight inches should have been left between the tip of the probe and the elevation of the streambed.

Problems arose in analysis of air temperature data due to calibrating the instrument with different thermometers at the beginning and end of each chart record. This can easily be avoided by calibrating the instrument to only one thermometer.

Some data analysis complications arose because of inadequate planning on how the data will be analyzed prior to data collection. It is essential that the method for data analysis be clearly set thus allowing proper planning for data collection to meet data analysis needs. Proper planning could have prevented the sporadic collection of relative humidity and wind data which was useless in the analysis. It also would have prevented the lack of consistency in site location for discharge measurements which made groundwater accretion analysis difficult.

Finally, it is important that the field crew collecting data for the study be informed thoroughly on the importance of the data and the guidelines by which it should be collected. More complete direction and emphasis to the crew on the importance of taking the downstream discharge at VRM 157.3 on the same day as that for which the upstream discharge measurements were made would have prevented the need for assuming the same flow over two consecutive days for groundwater accretion analysis.

In future research, TEMP-84 can most efficiently be used by placing emphasis on those variables for which the model was most sensitive, i.e., inflow stream temperature, width, air temperature, discharge, velocity, and length. For systems that differ greatly from that of the East Fork of the Virgin River, a thorough sensitivity analysis should be conducted prior to data collection using site representative data to re-evaluate the sensitive variables in the system.

This research indicated that the velocity component is fairly important as it controls the time of the modeled peak temperatures. Because the velocity component is utilized for tracking and calculating the travel time of the individual water parcels, one might implement a dye time test to determine appropriate velocity values. This method would describe the travel time from the upstream to the downstream end of the study reach.

According to the modeled results, the evaporative flux represents the greatest heat transfer from the stream. Because the evaporative heat flux is potentially very important, one should determine site specific evaporation coefficients for the empirical evaporative flux equation. This would allow more confidence that the evaporative heat transfer was being modeled accurately.

Describing the stream characteristics of width, velocity, etc. was found to be labor intensive as well as time consuming. One might look into utilizing aerial photographs as a possible means to collect stream characteristic data.

Research is needed in modeling the response of stream temperature to perturbations in natural conditions during the different time periods of the year. This research addressed that time period during which maximum stream temperatures occur. Another important time period with respect to fisheries is that time period during which spawning occurs.

A future research project exists in modeling the flow regime along with the stream temperature regime for a short study reach. This would provide for a more accurate accounting of stream characteristics corresponding to flows differing from baseflow. It would be interesting to note the differences between results simulated with empirically developed data versus those simulated with hydraulically modeled data.

Another future research project would be to attempt to measure for the East Fork of the Virgin River or a similar stream, stream temperatures for the ranges of flow and inflow temperature implemented for hypothetical conditions in this research. Measured and modeled results could then be compared.

One could also research the role of air temperature versus solar radiation in controlling the stream temperature. Literature is unclear on which of these two variables plays a larger role in regulating the stream temperature.

Use of the results from this study for systems other than the study site on which this research was conducted, should only be considered upon comparison of the system under question to that of the East Fork of the Virgin River within Zion National Park. If the system under question differs noticeably with respect to shading characteristics, stream characteristics, or meteorological characteristics from that of the East Fork, application of results from this research would not be appropriate as the relationship of stream temperature to the variables in TEMP-84 would likely change.

References

Adams, T.N. and K. Sullivan, 1988. The Physics of Forest Stream Heating: A Simple Model, Submitted to Water Resources Research, March, 1988.

Anderson, E.R., 1954. Energy-Budget Studies of the Water-Loss Investigations: Lake Hefner Studies, Technical Report, USGS Prof Paper #269, pp. 71-118.

Beschta, R.L., 1984. Temp-84, A Computer Model for Predicting Stream Temperature Resulting from the Management of Streamside Vegetation, USDA-Forest Serv, WSDG-AD-00009, 76 pp.

Beschta, R.L., R.E. Bilby, G.W. Brown, L.B. Holtby, and T.D. Hofstra, 1987. Stream Temperature and Aquatic Habitat: Fisheries and Forestry Interactions, in Streamside Management: Forestry and Fishery Interactions, College of Forest Resources, Univ of Washington, pp. 191-232.

Bureau of Land Management, 1985. Stream Channel Cross Section Surveys and Data Analysis, USBLM TR-4341-1, 48 pp.

Bowen, I.S., 1926. The Ratio of Heat Losses By Conduction and by Evaporation from any Water Surface, Physical Review, Vol 27, pg. 779.

Brocard, D.N. and D.R.F. Harleman, 1976. One-Dimensional Temperature Predictions in Unsteady Flows, J. Hydraul. Div., A.S.C.E., 102(HY3):227-239.

Brooks, F.A., 1959. An Introduction to Physical Microclimatology, Univ. of California, Davis, 264 pp.

Brown, G.W., 1969. Predicting Temperatures of Small Streams, Water Resour. Res., 5(1):68-75.

Brown, G.W., and J.T. Krygier, 1970. Effects of Clear-Cutting on Stream Temperature, Water Resour. Res., 6(4):1133-1139.

Brown, G.W., G.W. Swank, and J. Rothacher, 1971. Water Temperature in the Steamboat Drainage, USDA-Forest Serv., Pacific NW For. and Range Exp. Sta., Res. Paper PNW-119, 17 pp.

Brown, L.C. and T.O. Barnwell, Jr, 1987. The Enhanced Stream Water Quality Models QUAL2E and QUAL2E-UNCAS: Documentation and User Manual, Prepared for U.S. Environmental Protection Agency, Athens, GA, EPA/600/3-87/007, 189 pp.

Buchanan, T.J., and W.P. Somers, 1969. Discharge Measurements at Gaging Stations, Techniques of Water Resources Investigations, Chapter A8, Book 3, U.S. Geological Survey.

Busch D.E., and S.G. Fisher, 1981. Metabolism of a Desert Stream, Freshwater Biology, 11:301-307.

Cluis, D.A., 1972. Relationship Between Stream Water Temperature and Ambient Air Temperature, Nordic Hydrology, 3:65-71.

Crisp, D.T., and E.D. Le Cren, 1970. The Temperature of Three Different Small Streams in Northwest England, Hydrobiology, 35: 305-323.

Crittenden, R.N., 1978. Sensitivity Analysis of a Theoretical Energy Balance Model for Water Temperatures in Small Streams, Ecological Modeling, 5:207-224.

Crittenden, R.N., 1977. The Prediction of the Temperature of Small Clear Streams, Masters Thesis, University of the Pacific, 74 pp.

Currier, J.B., and D. Hughes, 1980. An Approach to Water Resources Evaluation of Non-Point Silvicultural Sources, Chapter VII, EPA-600/8-80-012.

Deacon J.E., P.B. Schumann, and E.L. Stuenkel, 1987. Thermal Tolerances and Preferences of Fishes of the Virgin River System (Utah, Arizona, Nevada), Great Basin Naturalist, 47(4):538-546.

Deacon, J.e., 1988. Letter of 3-28-88 and Verbal Communication, UNLV, Dept of Biology, Las Vegas, Nevada.

Delay, W.H., and J. Seaders, 1966. Predicting Temperatures in Rivers and Reservoirs, J. Sanitary Eng. Div., A.S.C.E., 92(SA1):115-133.

Doesken, N., 1988. Verbal Communication, CSU, Dept. of Atmospheric Sciences, Ft. Collins, Colorado.

Edinger, J.E., D.W. Duttweiler, and J.C.Geyer, 1968. The Response of Water Temperatures to Meteorological Conditions, Water Resour. Res., 4(5):1137-1143.

Ellis, S., 1981. A Temperature Model for Small Mountain Streams, Masters Thesis, Colorado State University, 56 pp.

Espinosa, F.A., and J.E. Deacon, 1978. Rearing Bait Fish in the Desert Southwest, UNLV, Federal Aid in Commercial Fisheries Research and Development, Project No. 6-9-D, 29 pp.

Fowler, W.B., J.D. Helvey, and E.N. Felix, 1987. Hydrologic and Climatic Changes in Three Small Watersheds After Timber Harvest, USDA-Forest Serv. Pacific NW For. and Range Exp. Sta., Res. Paper PNW-RP-379, 13pp.

Fry, F.E.J., 1947. Effects of the Environment on Animal Activity, U. Toronto Stud., Biol. Ser., 55:1-62.

Gregory, H.E., 1950. Geology and Geography of the Zion Park Region Utah and Arizona, USGS Professional Paper No 220, 200 pg.

Hauser G.E., 1987. User's Manual for One-Dimensional, Unsteady Flow and Water Quality Modeling in River Systems with Dynamic Tributaries, Tennessee Valley Authority, Report No. WR28-3-590-135, 60 pp.

Hauser, G.E., 1987. DYNOCS-RQUAL, River Water Quality Modeling System, Presentation Material from Engineering Laboratory Seminar, March 17, 60pp.

Holtby, B., and C.P. Newcombe, 1982. A Preliminary Analysis of Logging-Related Temperature Changes in Carnation Creek, British Columbia, Proceedings of the Carnation Creek Workshop, Malaspina College, pp. 81-99.

Hsueh S.F., 1972. Thermal Dispersion in a Stream Model, Master's Thesis, Rutgers University, 66pp.

Jobson, H.E. and T.N. Keefer, 1979. Modeling Highly Transient Flow, Mass, and Heat Transport in the Chattahoochee River near Atlanta, Georgia, USGS Professional Paper No. 1136, 41 pp.

Jobson, H.E., 1973. The Dissipation of Excess Heat From Water Systems, J. Power Div., A.S.C.E., 99(PO1):89-103.

Johns, A., 1987. Trip Report of meeting at UNLV, Water Rights Branch, Water Resources Division, National Park Service.

Klock, G.O., and W. Lopushinsky, 1980. Soil Water Trends After Clearcutting in the Blue Mountains of Oregon, USDA-Forest Serv., Pacific NW For. and Range Exp. Sta., PNW Research Note-361, 8 p.

Kothandaraman, V., 1972. Air-Water Temperature Relationship in Illinois River, Water Resour. Bull., 8(1):38-45.

Levno, A., and J. Rothacher, 1967. Increases in Maximum Stream Temperatures, USDA-Forest Serv., Pacific NW For. and Range Exp. Sta., PNW Research Note-65, 12pp.

Macan T.T., 1959. The Temperature of a Small Stony Stream, Hydrobiologia, Vol.12:89-106.

Martin, J.L., 1986. Simplified, Steady-State Temperature and Dissolved Oxygen Model: User's Guide, Instruction Report E-86-4, US Army Waterways Experiment Station, Vicksburg, Miss, 25 pp.

Mitchell, J.M., 1958. Effect of Changing Observation Time on Mean Temperature, Bulletin American Meteorological Society, 39(2):83.

Moore, A.M., 1967. Correlation and Analysis of Water-Temperature Data for Oregon Streams, USGS Water Supply Paper #1819-K, 53 pp.

Morse, W.L., 1978. The Dishonest Method in Stream Temperature Modeling, Water Resour. Res., 14(1):45-51.

Morse, W.L., 1970. Stream Temperature Prediction Model, Water Resour. Res., 6(1):290-302.

Morse, W.L., 1972. Stream Temperature Prediction Under Reduced Flow, J. Hydraul. Div., A.S.C.E., 98(HY6):1031-1047.

National Climatic Data Center, 1988. Direct and Global Radiation Data for Las Vegas, NV, and Grand Junction, CO, Asheville North Carolina.

National Oceanic and Atmospheric Administration, 1988. Climatological Data for Utah in June and July, 1988.

Nicks, A.D., and J.F. Harp, 1980. Stochastic Generation of Temperature and Solar Radiation Data, J. of Hydrology, 48:1-17.

O'Brien, J.S., and W.J. Miller, 1984. Yampa and Green Rivers Water Temperature Simulation, WRFSL Report No. 84-1, 27 pp.

Pacific Southwest Inter-Agency Committee, 1974. River Mile Index, Virgin River Basin, Arizona, Nevada, Utah, Report of the Water Management Technical Subcommittee.

Paily, P.P., E.O. Macagno, and J.F. Kennedy, 1974. Winter-Regime Surface Heat Loss From Heated Streams, Institute of Hydraulic Research, IIHR Report No. 155, Univ of Iowa, 98 pp.

Pluhowski, E.J., 1970. Urbanization and Its Effect on the Temperature of the Streams on Long Island, New York, USGS Professional Paper No. 627D, 110 pp.

Quigley, T.M., 1981. Estimating Contribution of Overstory Vegetation to Stream Surface Shade, Wildlife Soc. Bulletin, 9(1):22-27.

Raphael, J.M., 1962. Prediction of Temperature in Rivers and Reservoirs, J. Power Div., A.S.C.E., 88(PO2):157.

Reifsnyder, W.E., and H.W. Lull, 1965. Radiant Energy in Relation to Forests. USDA-Forest Service, Technical Bulletin No. 1344, 111 pp.

Ryan, P.J., and D.R.F. Harleman, 1973. An Analytical and Experimental Study of Transient Cooling Pond Behavior, Ralph M. Parsons Laboratory for Water Resources and Hydrodynamics, Dept. of Civil Eng., Mass. Institute of Tech., Report No. 161, 91 pp.

Satterlund, D.R., 1979. An Improved Equation for Estimating Long-Wave Radiation From the Atmosphere, Water Resour. Res., 15(6):1649-1650.

Schoellhamer, D.H., and H.E. Jobson, 1986. Programmers Manual for a One-Dimensional Lagrangian Transport Model, Water Resources Investigation Report 86-4144, U.S. Geological Survey, NSTL, Miss.

Schoellhamer, D.H., and H.E. Jobson, 1986. Users Manual for a One-Dimensional Lagrangian Transport Model, Water Resources Investigation Report 86-4145, U.S. Geological Survey, NSTL, Miss.

Sellers, W.D., 1965. Physical Climatology, Univ of Chicago Press, Chicago, 272 pp.

Stevens, H.H., J.F. Ficke, and G.F. Smoot, 1975. Water Temperature-Influential Factors, Field Measurement, and Data Presentation, Techniques of Water-Resources Investigations, Chapter D1, Book 1, US Geological Survey, 65 pp.

Sullivan, K., and T.N. Adams, 1988. Temperature Patterns in Natural Stream Environments: An Analysis Based on Principles of Stream Heating and Field Data, Submitted to Water Resour. Res, March 1988, 46 pp.

Swift, L.W. Jr., and J.B. Messer, 1971. Forest Cuttings Raise Temperatures of Small Streams in the Southern Appalachians, J. of Soil and Water Conservation, May-June:111-116.

Tennessee Valley Authority, 1972. Heat and Mass Transfer Between a Water Surface and the Atmosphere. Water Resources Research, Lab Report No. 14, Norris, Tenn.

Theurer, F.D., K.A. Voos, and C.G. Prewitt, 1982. Application of IFG'S Instream Water Temperature Model in the Upper Colorado River, International Symposium on Hydrometeorology, AWRA, June:287-292.

Theurer, F.D., K.A. Voos, and W.J. Miller, 1984. Instream Water Temperature Model, Instream Flow Information Paper 16, U.S. Fish and Wildl. Serv., FWS/OBS-84/15.

US Fish and Wildlife Service, National Ecology Research Center, 1987. Training Course Notes for IF 215 - Problem Solving with the Instream Flow Incremental Methodology.

Turner, W.V., 1949. Watershed Conditions in the Upper Virgin River Basin, Utah, U.S. BOR, Boulder City, Nevada.

Vugts, H.F., 1974. Calculation of Temperature Variations of Small Mountain Streams, J. of Hydrology, 23:267-278.

Ward, J.V., 1974. A Temperature-Stressed Stream Ecosystem Below a Hypolimnial Release Mountain Reservoir, Arch. Hydrobiol., 74(2):247-275.

Ward, J.V. and J.A. Stanford, 1979. Ecological Factors Controlling Stream Zoobenthos with Emphasis on Thermal Modification of Regulated Streams, in The Ecology of Regulated Streams. Plenum Press, New York, pp 35-55.

A variety of instruments were used for collecting data. Ryan Model "J" Thermographs which are continuous recording and submersible, were mounted in the stream to record the stream temperature. Hygrothermographs which were calibrated in the field to maximum/minimum mercury thermometers were utilized to measure the air temperature along the study reach. Hand held mercury and alcohol thermometers were utilized to measure the temperature of spring flow. An abney level was used to measure shading angles while discharge measurements were made utilizing a vertical axis current meter.

A.1 Ryan Model "J" Stream Thermographs

Battery powered Ryan Model "J" Thermographs used to record stream temperature, were mounted on fence posts which were driven into the streambed. Each instrument is 4.8 inches in diameter and 8.3 inches in length and has a sensor, 2.9 inches in length, comprised of a liquid system within a fast response Teflon coated probe. The sensor response time is rated at seventy-five seconds for 2/3 span of the chart. Full span of the chart can be sensed within eight minutes. Each chart spans thirty degrees centigrade and is marked at one degree intervals. Accuracy is rated at +/- 2 percent (+/- 0.6°C) for temperature and +/- 0.2 percent (+/- 3 minutes/day) for time.

Ryan stream thermographs and the various thermometers were calibrated at ZION because the instruments had not been received prior to departure for the field season. Guidance on calibration techniques was provided by Mr. Gale Murphy, an instrument specialist at the Engineering Research Center (ERC) at Colorado State University (CSU). To calibrate, the instruments were hung in a water bath contained in a one and a half foot diameter, two foot tall rubber bucket. A mercury, total immersion, precision thermometer which was factory rated to read within 0.1°C was hung in the "bath" to measure a standard water temperature. The precision thermometer was calibrated by ERC prior to use to verify the 0.1°C rating. The bath was manually stirred and the temperature was altered by means of adding ice or hot water. At least fifteen minutes was allowed for the bath temperature to stabilize and the instruments to come to equilibrium after the bath temperature was altered. The relationship between sensed and standard temperatures for each of the instruments was developed through linear regression analyses. Field calibration data for the stream thermographs are listed in Table A.1.

Table A.1 Field calibration data for Ryan Submersible Thermographs #64624 and #64622.

STANDARD TEMP C	#64624 THERM. C	#64622 THERM. C
22.3	22.0	21.4
20.8	21.9	21.0
21.2	21.8	21.0
22.0	22.2	21.3
28.2	28.0	26.5
27.6	28.0	26.7
29.9	29.6	
17.8	18.8	17.8
6.9	8.7	7.3
7.3	8.5	7.2
7.6	8.6	7.2
12.9	13.3	11.7
13.0	13.3	11.9
13.4	13.8	12.2
29.9	30.3	28.8
30.9	31.1	29.4

Upon completion of the field season, the Ryan stream thermographs and various thermometers which had not been damaged in the field were submitted to the ERC for professional calibration. The instruments were hung in a temperature bath of ethylene glycol and water. The temperature of the bath was mechanically controlled and the resulting temperatures sensed by the instruments were read and recorded. The relationship between sensed and standard temperatures for each of the instruments was developed through linear regression analyses. ERC calibration data for Ryan stream thermograph #64622 are listed in Table A.2.

Table A.2 Engineering Research Center calibration data for Ryan Stream Thermograph #64622.

COLORADO STATE UNIVERSITY
CALIBRATED NOVEMBER 3-8, 1988
GALE MURPHY, RODNEY WITLER

TEMPERATURE REPORTED IN DEGREES C.

THERMOGRAPHS BATTERY CHECK: OK

STANDARD	SN 64622
11.5	11.1
16.6	16.0
20.9	20.0
25.3	24.2
30.6	29.6

Instrument #64622 was set at the downstream end of the study reach, VRM 157.3. The calibration data and regression generated by the ERC for this instrument aligned well with the calibration data developed in the field (Figure A.1) and was used to calibrate the data recorded by instrument #64622.

Instrument #64624 was set at the upstream end of the study reach, VRM 163.1. It operated through July 22 at which time the water seal broke and the instrument was damaged beyond repair. As a result, the instrument could not be calibrated at the end of the season by the ERC. Though not verified by the ERC, the linear regression equation developed from field data was assumed to be accurate for the time period between June 3 and July 22. This is based on the assumption that field calibration techniques were acceptable. Similarity between calibration data

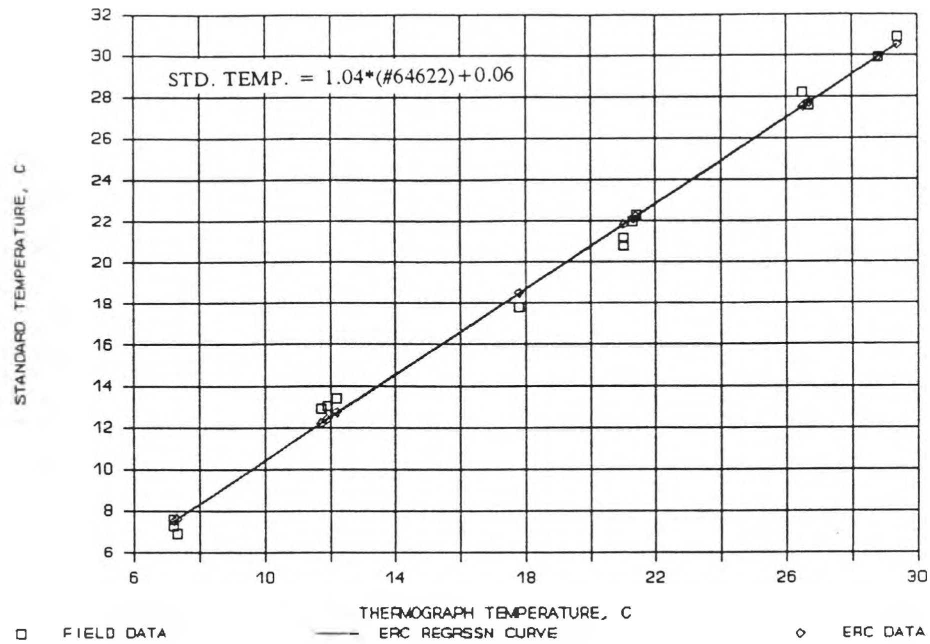

Fig. A.1 Calibration Data and Regression Curve for Ryan Stream Thermograph #64622.

developed in the field and calibration data generated by the ERC for instrument #64622 supports this assumption. Figure A.2 portrays the calibration data and regression line for instrument #64624.

A.2 Hand Held Thermometers

Two mercury hand held thermometers and one alcohol hand held thermometer were utilized throughout the summer to measure the temperature of spring flow. The mercury thermometers were read with a precision of 0.5°F while the alcohol thermometer read with a precision of 0.5°C. Field calibration data are listed in Table A.3.

Mercury thermometer #1 was utilized from the beginning of the field season through 8-5-88 at which time it broke. Prior to 8-5-88, calibration data was generated

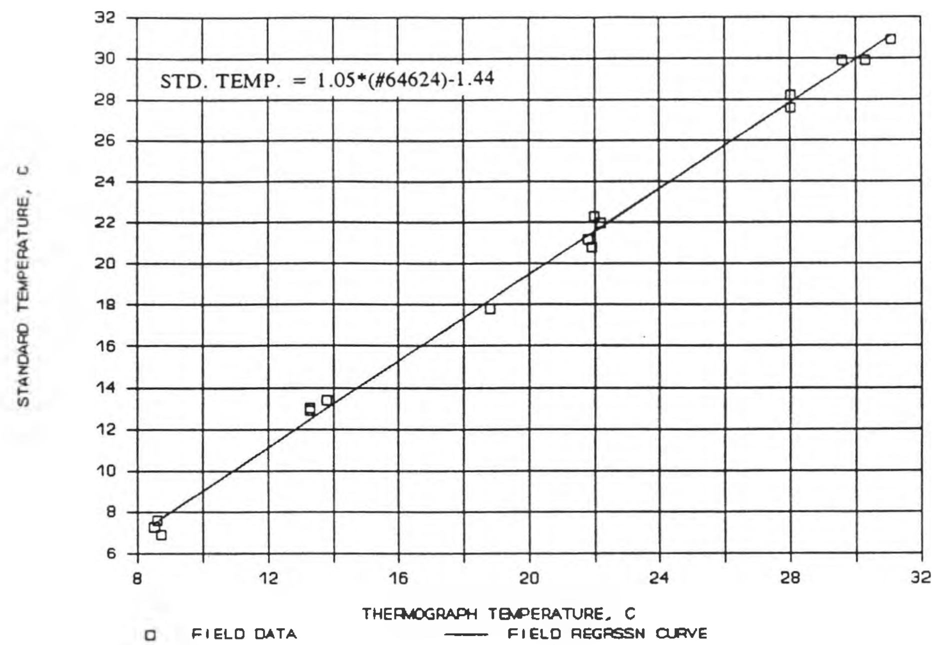

Fig. A.2 Calibration Data and Regression Curve for Ryan Stream Thermograph #64624.

Table A.3 Field calibration data for Mercury #1, Mercury #2, and Alcohol handheld thermometers.

STANDARD TEMP C	ALCOHOL TEMP C	MERCURY#2 TEMP C
29.7	29.8	30.0
27.3	27.5	27.8
25.3	25.5	25.6
24.0	24.2	24.4
22.1	22.5	22.2
32.0	31.8	32.2
28.8	28.9	28.9
29.2	29.1	28.9
27.1	27.3	27.2
22.2	22.5	23.1
30.3		30.8

STANDARD TEMP C	MERCURY#1 TEMP C
31.2	31.4
29.2	29.2
24.9	25.8
30.0	30.3
24.9	25.3
31.9	31.9
24.6	25.0

by placing the thermometer outside, under complete shade, alongside the mercury precision thermometer with care to keep the bulbs of the thermometers suspended in air. The thermometers were read simultaneously at different times of the day over a period of a four days from July 18 through July 21, to obtain data points throughout the diurnal fluctuation of temperature. The resulting regression along with the regression equation is shown in Figure A.3. Field calibration results were applied to data collected by Mercury thermometer #1.

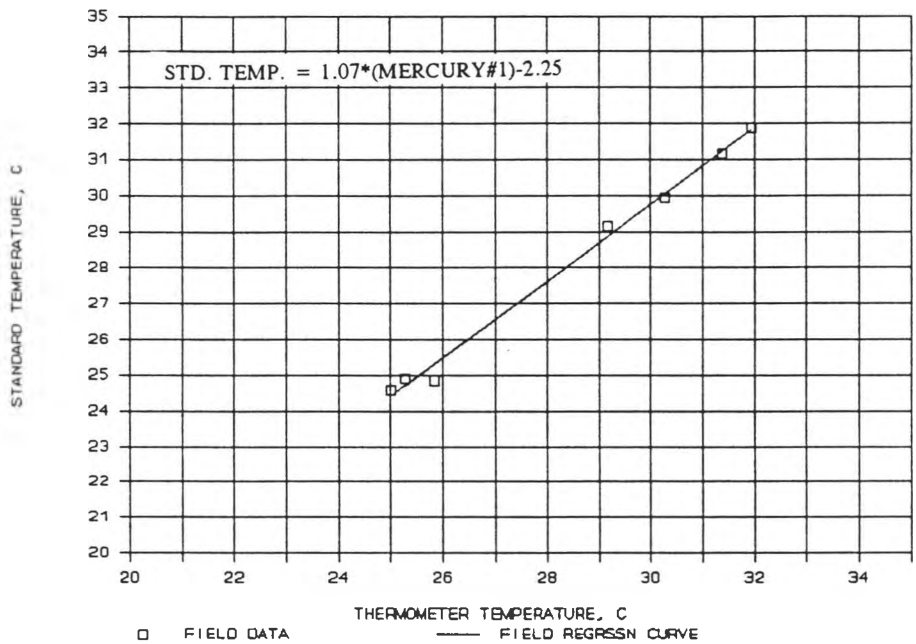

Fig. A.3. Calibration Data and Regression Curve for Hand Held Mercury Thermometer #1.

Mercury thermometer #2 which was of the same make as mercury thermometer #1 was utilized after 8-5-88. This thermometer was calibrated at ZION as well as by the ERC. The field calibration data consisted of air temperature data, as described with the mercury #1 thermometer, as well as water temperature data collected in the water bath. Figure A.4 documents the ERC regression equation and illustrates that the regression curve developed from the ERC data is of slightly lesser slope, resulting in approximately 0.5°C difference from that developed from the field data in the 30°C range. ERC calibration data for both the mercury #2 and alcohol thermometers are listed in Table A.4. Regressions developed from ERC data were implemented for the mercury #2 and alcohol thermometers.

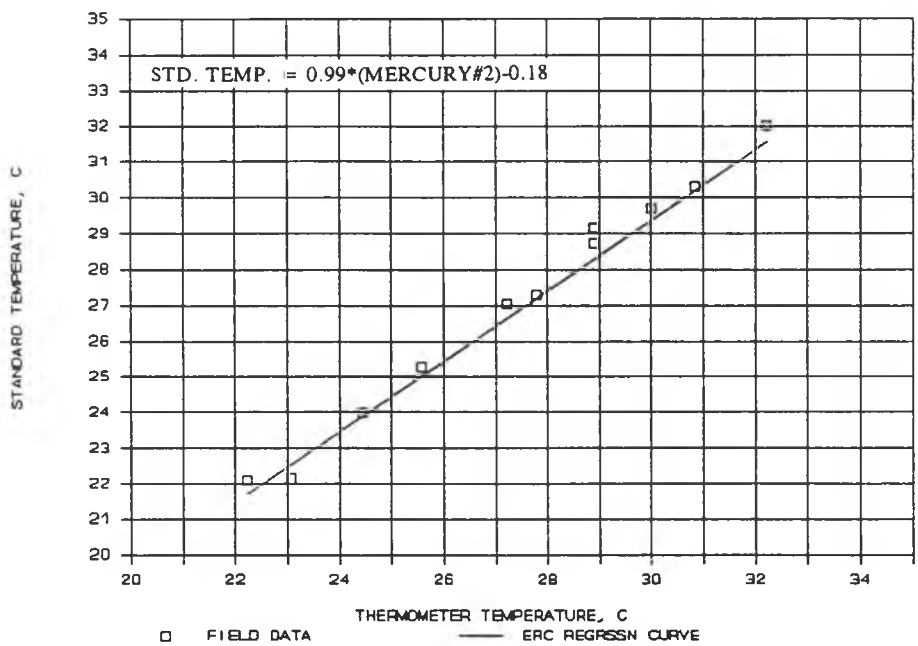

Fig. A.4 Calibration Data and Regression Curve for Hand Held Mercury Thermometer #2.

All data collected by the Mercury #1 thermometer between 6-24-88 and 7-10-88 was omitted from the analysis due to an approximate 3°F separation in the mercury fluid of the thermometer. The separation was noticed on 6-30-88 and corrected on 7-10-88. To determine when the separation in mercury occurred, a study was conducted on the difference between simultaneous readings of the Mercury #1 thermometer and other temperature measuring devices. This analysis illustrated a noticeable increase in the difference between the Mercury #1 thermometer measurement and that of the instrument being compared beginning 6-24-88. It was thus determined that the separation was incurred on 6-24-88 and all data collected between this date and 7-10-88 was not valid.

Table A.4 ERC calibration data for Mercury #2 and Alcohol handheld thermometers.

WEKSLER Alcohol Thermometer (degrees C)		Mercury Pocket Thermometer (degrees C)		
Standard Temp.	Weksler Temp.	Standard Temp.	Total Emersion Temp.	Tip Emersion Temp.
-9	-8	-8.4	-7.8	
-5	-4	1.9	0.6	
1	2	12.1	12.8	
7	8	21.1	21.7	
12	13	29.9	30.6	30.6
17	18	42.6	43.3	43.3
22	23	30.6	31.1	31.1
27	28	20.7	21.1	21.1
33	34	11.9	12.8	
40	41	2.3	2.8	

A.3 Hygrothermographs

Hygrothermographs which were driven by a clock, recorded air temperature on a continuous basis according to the response of a bimetal sensor. Temperature was plotted on a seven day chart which ranged from 10°F to 110°F and marked at intervals of 2°F. The instruments used were fairly old and can only be expected to be accurate to within +/- 2°F (Nolan, 1988). Prior to field implementation, the instruments were thoroughly checked with respect to operation within a temperature controlled environment by Charlie Wilkins, a technician for the Colorado Climate Center in Ft. Collins, CO. In addition, the instruments were set in the CSU weather shelter.

Comparisons to the official CSU weather station hygrothermograph and the standard mercury thermometer were made during the period of 5-3-88 to 5-15-88. Table A.5 documents simultaneous air temperature readings from standard mercury thermometer, CSU official hygrothermograph and the field implemented hygrothermographs. Point readings depicted that the hygrothermographs measured within 2°F of the actual temperature measured by the mercury thermometer. Comparisons between the CSU hygrothermograph chart and the charts recorded by instrument #63518 and #60516 document that each of the field instruments read peak temperatures within 2°F of those read by the official CSU hygrothermograph (Figure A.5 and A.6).

Table A.5 Simultaneous air temperature readings from standard mercury thermometer, CSU official hygrothermograph, and field implemented hygrothermographs.

DATE	TIME	STANDARD TEMP C	CSU HYGRO. C	HYGRO. #63518 C	HYGRO. #60758 C	HYGRO. #63516 C
5-10-88	11:10	15.6		14.4	15.6	14.4
5-10-88	16:15	17.5			17.2	17.7
5-11-88	15:15	23.3	23.6		23.3	23.4
5-12-88	12:00	26.7			26.7	27.2
5-12-88	19:00	27.2	28.3	25.6		27.8
5-13-88	7:30	13.9	14.4	14.4		13.9
5-13-88	morning low		11.1	11.1		10.6
5-13-88	16:15	30.0	31.1	31.1		30.6
5-15-88	-	20.6	20.6	21.1		20.8

NOTE: All instruments were located in CSU weather shelter.

A.4 Mercury Maximum/Minimum Thermometers

Weather Measure Model TM45 Minimum-Maximum Thermometers were implemented to serve as a reference by which to calibrate hygrothermographs. These thermometers consisted of a glass "U" tube filled with mercury, two metal indices, one to indicate the maximum temperature and one to indicate the minimum temperature, a magnet to reset the indices, and minimum and maximum temperature

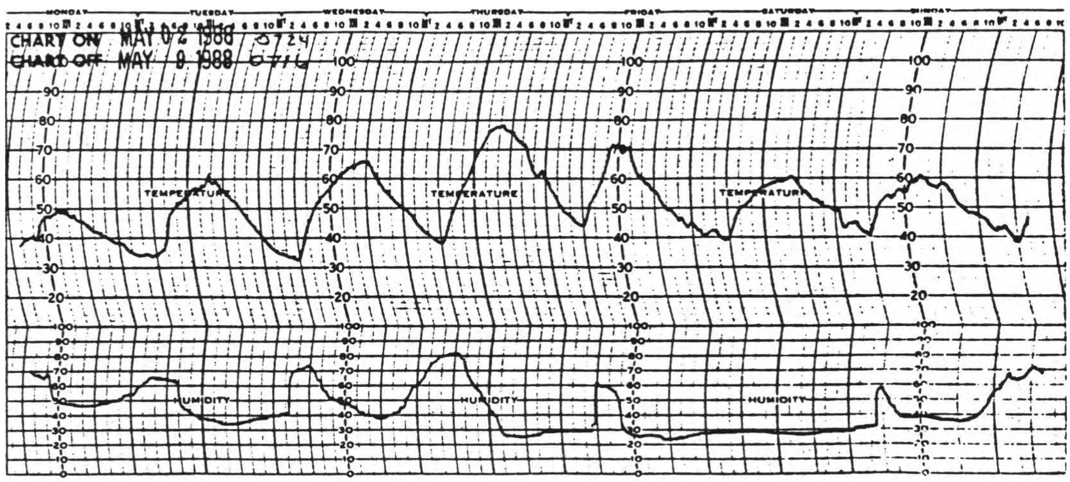

CSU Hygrothermograph Chart

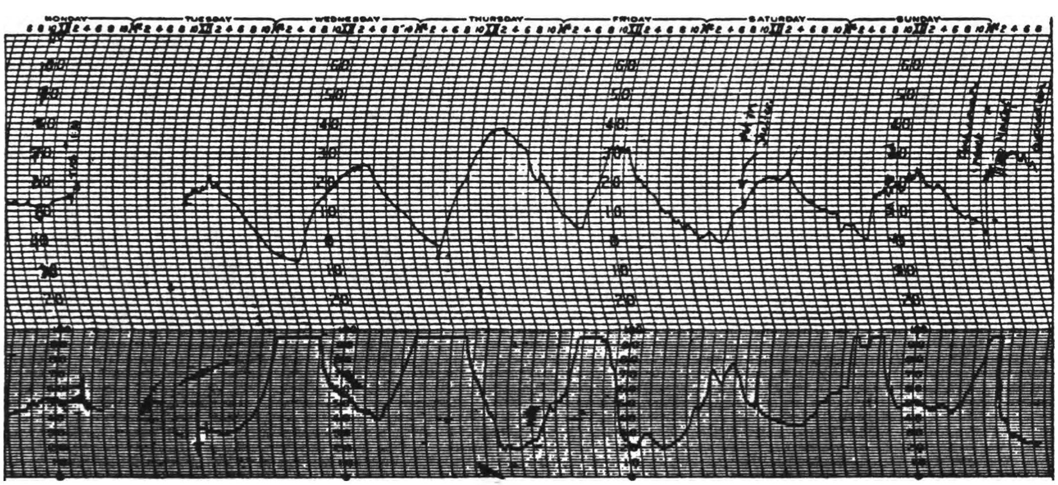

Field Hygrothermograph #63518 Chart

Figure A.5. Comparison of charts recorded by CSU hygrothermograph and field hygrothermograph #63518 chart between 5-3-88 and 5-6-88.

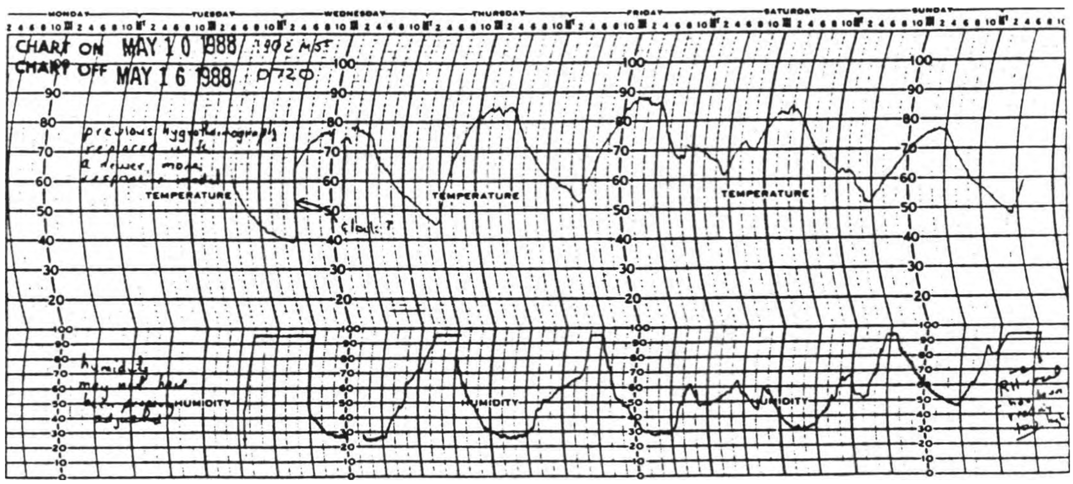

CSU Hygrothermograph Chart

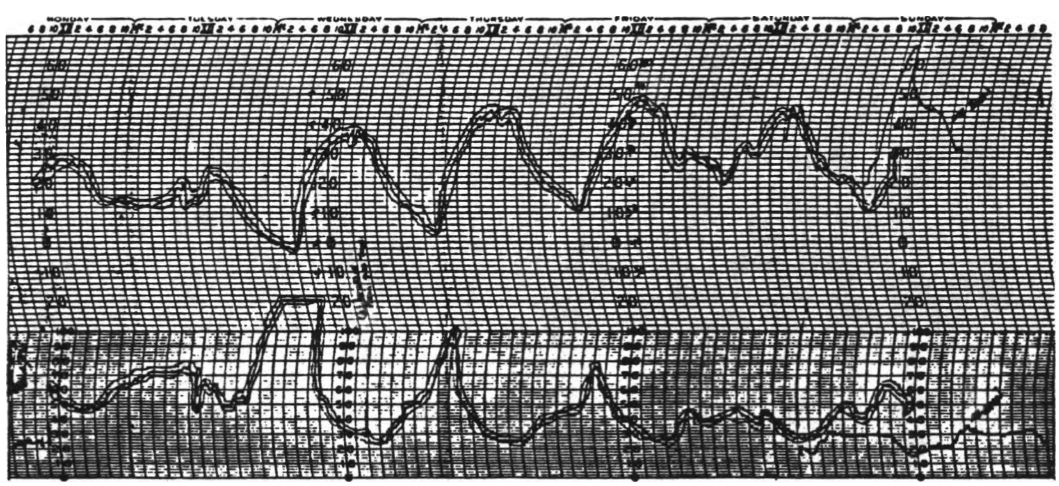

Field Hygrothermograph #63516 Chart

Figure A.6. Comparison of charts recorded by CSU hygrothermograph and field hygrothermograph #63516 chart between 5-11-88 and 5-14-88.

scaling. The precision in reading the instruments was +/- 1°C. One of the two minimum-maximum thermometers was calibrated in the field as well as professionally by the ERC. Regressions developed from the ERC and field collected data are shown in Figures A.7 and A.8. For the one comparison available (Figure A.8), little difference between the ERC and field data regression existed thus adding support to the validity of the field calibration techniques. In all cases, the ERC regression equation, which is documented on each figure, was implemented in the data analysis. ERC and field calibration data are listed in Tables A.6 and A.7.

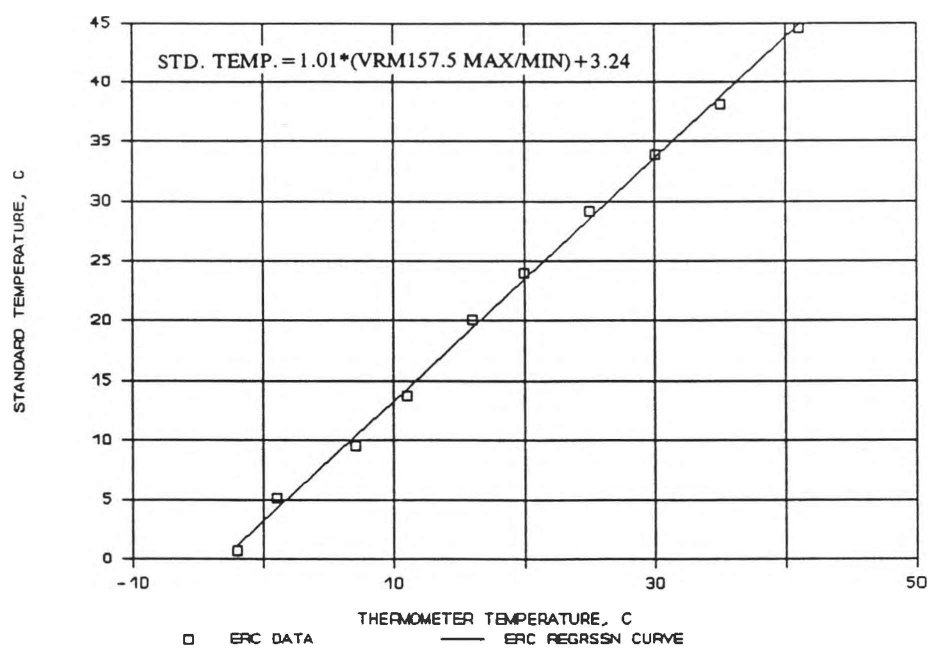

Fig. A.7 Calibration Data and Regression Curves for Virgin River Mile 157.5 Maximum/Minimum Thermometer.

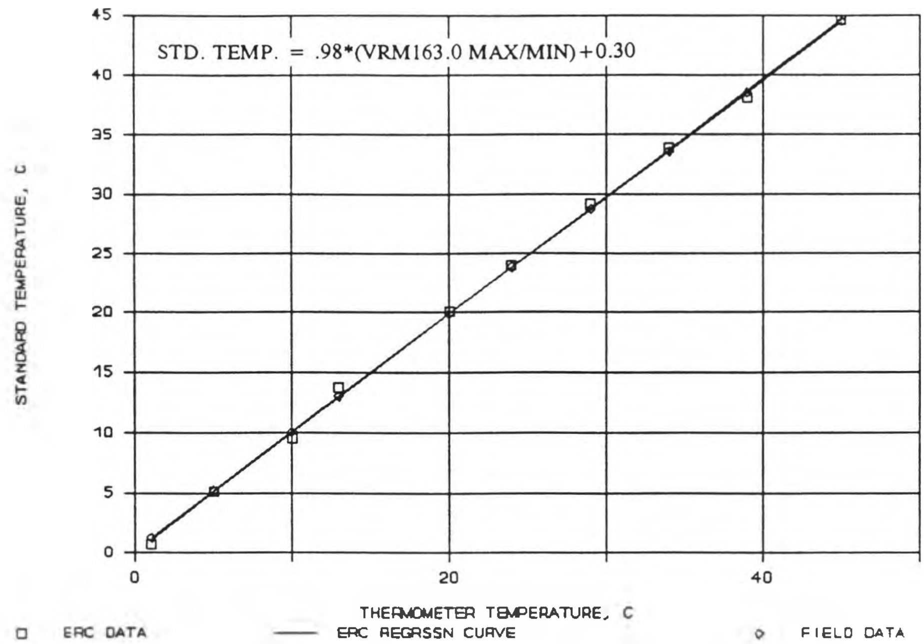

Fig. A.8 Calibration Data and Regression Curve for Virgin River Mile 163.0 Maximum/Minimum Thermometer.

Table A.6 Engineering Research Center calibration data for maximum/minimum mercury thermometers.

Calibration of Min/Max thermometers.

Standard: Platinum resistance thermometer probe.
Doric DS-100-T5 probe readout.

ALL READING IN DEGREES CELSIUS

Standard Reading (+)	N. Fork (column)		161.1 (column)		UES (column)		Sec. 3 (column)		LEF (column)	
	Min.	Max.	Min.	Max.	Min.	Max.	Min.	Max.	Min.	Max.
0.7	1	1	5	3	2	1	3	3	-1	-2
5.1	5	5	9	7	6	5	7	7	3	1
9.5	9	9	12	12	11	10	10	11	6	7
13.8	13	13	17	15	14	13	15	14	11	11
20.1	19	19	23	21	20	20	21	20	16	16
24.0	23	23	26	25	23	24	24	24	20	20
29.2	27	28	32	30	29	29	29	29	25	25
33.9	33	34	37	35	34	34	34	34	30	30
38.1	37	38	41	40	38	39	39	38	34	35
44.6	45	45	49	46	45	45	45	44	42	41

Table A.7. Field calibration data for maximum/minimum mercury thermometers.

STANDARD TEMP C	MAX/MIN VRM 161.1 C	MAX/MIN VRM 159.7 C	MAX/MIN VRM 163.0 C
31.7	33.5	31.8	32.0
29.7	31.0	29.0	30.0
27.3	29.0	27.0	27.5
25.3	27.2	25.2	25.5
24.0	26.0	24.0	24.2
22.1	24.0	22.0	22.2

A.5 Abney Level

A hand held abney level was used for all angle measurements. The precision in reading this instrument was +/- 0.5 degrees.

A.6 Discharge Equipment

A pygmy vertical axis current meter mounted to a top-setting wading rod was used to measure discharge. A nylon coated steel tape strung across the stream was used to delineate the location of each velocity measurement. Discharge measurements were made according the midsection method outlined by the USGS (Buchanan, 1969) which are generally accepted to be precise to within ten percent of the calculated measurement.

Table B.1 . Pre-data results of the percent change in the modeled maximum and minimum stream temperature (deg C) at VRM 157.3 with the specified increase in the designated model input variable.

	BASE	WIDTH			BUFFER			CANOPY COVER		
	TEMP	WID10%	WID50%	WID100%	BUF10%	BUF50%	BUF100%	CC10%	CC60%	CC90%
MIN TEMP	17.4	17.16	16.29	15.33	17.37	17.39	17.41	17.41	17.54	17.58
MAX TEMP	34.05	35.16	39.08	42.92	34.03	34.03	34.04	34.06	33.98	33.95
%CHG MIN		-1.38	-6.38	-11.90	-0.17	-0.06	0.06	0.06	0.80	1.03
%CHG MAX		3.26	14.77	26.05	-0.06	-0.06	-0.03	0.03	-0.21	-0.29

	BASE	GW TEMP			GW FLOW			LENGTH		
	TEMP	10DEG	13DEG	20DEG	GW10%	GW50%	GW100%	LEN10%	LEN50%	LEN100%
MIN TEMP	17.4	16.87	17.09	17.62	17.4	17.39	17.38	17.13	16.35	15.38
MAX TEMP	34.05	33.56	33.77	34.26	33.93	33.43	32.85	35.09	37.77	40.71
%CHG MIN		-3.05	-1.78	1.26	0.00	-0.06	-0.11	-1.55	-6.03	-11.61
%CHG MAX		-1.44	-0.82	0.62	-0.35	-1.82	-3.52	3.05	10.93	19.56

	BASE	L/R VEGE ANGLES			TREE HEIGHT			TOPO ANGLES		
	TEMP	L/RVEG10%	L/RVEG50%	L/RVE100%	TREE10%	TREE50%	TREE100%	TOPO10%	TOPO50%	TOPO100%
MIN TEMP	17.4	17.39	17.38	17.38	17.39	17.39	17.38	17.4	17.4	17.4
MAX TEMP	34.05	34.04	33.99	33.95	34.06	34.06	34.06	34.05	34.05	32.44
%CHG MIN		-0.06	-0.11	-0.11	-0.06	-0.06	-0.11	0.00	0.00	0.00
%CHG MAX		-0.03	-0.18	-0.29	0.03	0.03	0.03	0.00	0.00	-4.73

	BASE	VEGE ANGLES			BEDROCK			VELOCITY		
	TEMP	VEG10%	VEG50%	VEG100%	BED10%	BED50%	BED100%	VEL10%	VEL50%	VEL100%
MIN TEMP	17.4	17.4	17.4	17.4	17.4	17.4	17.4	17.39	17.36	17.35
MAX TEMP	34.05	34.05	34.05	34.05	34.03	33.97	33.89	34.12	34.34	34.34
%CHG MIN		0.00	0.00	0.00	0.00	0.00	0.00	-0.06	-0.23	-0.29
%CHG MAX		0.00	0.00	0.00	-0.06	-0.23	-0.47	0.21	0.85	0.85

Table B.2 . Data collected during reconnaisance of study reach on 5-19-88.

TIME	WIDTH ft	DEPTH ft	TOPO. ANGLE SE deg	TOPO. ANGLE S deg	TOPO. ANGLE SW deg
10:05	37	0.7	27	32	13
10:30	26	1.1	35	25	13
10:50	22	1.2	20	34	16
11:05	23	1.2	20	34	14
11:20	33	0.8	21	27	16
11:38	26	1.0	21	21	19
11:55	29	1.1	23	29	27
12:12	40	0.5	26	31	23
12:48	34	0.8	25	35	16
13:03	24	1.5	33	31	25
13:20	28	0.9	21	26	23
13:35	28	1.0	20	48	16
13:50	23	1.2	15	45	13
14:08	25	1.2	25	37	14

NOTE: Measurements were taken at approximately 15 minute intervals as the reach between VRM 157.5 and VRM 162.0 was traversed.

Table C.1. Daily maximum and minimum stream temperature values at VRM 163.1 and VRM 157.3. Mean temperatures are calculated from maximum and minimum values.

	VRM 157.3					VRM 163.1				
DATE	MAX STR TEMP C	CALIB MAX TEMP C	MIN STR TEMP C	CALIB MIN TEMP C	CALIB MEAN TEMP C	MAX STR TEMP C	CALIB MAX TEMP C	MIN STR TEMP C	CALIB MIN TEMP C	CALIB MEAN TEMP C
6-4	24.0	24.9	14.9	15.5	20.2					
6-5	23.5	24.4	14.7	15.3	19.8					
6-6	22.7	23.6	13.9	14.5	19.0					
6-7	22.7	23.6	14.0	14.6	19.1					
6-8	22.8	23.7	13.0	13.5	18.6					
6-9	23.8	24.7	12.2	12.7	18.7					
6-10	23.4	24.3	13.0	13.5	18.9					
6-11	23.2	24.1	12.8	13.3	18.7					
6-12	21.0	21.8	13.0	13.5	17.7					
6-13	23.7	24.6	13.6	14.1	19.4					
6-14	24.7	25.6	13.6	14.1	19.9					
6-15	25.2	26.2	14.5	15.1	20.6					
6-16	24.0	24.9	14.4	15.0	19.9					
6-17	18.8	19.5	16.8	17.5	18.5					
6-18	25.7	26.7	15.6	16.2	21.5					
6-19	23.0	23.9	17.3	18.0	20.9					
6-20	23.6	24.5	17.2	17.9	21.2					
6-21	24.1	25.0	17.0	17.7	21.3					
6-22	24.7	25.6	17.3	18.0	21.8					
6-23	26.1	27.1	17.1	17.8	22.4					
6-24	26.1	27.1	17.8	18.5	22.8	22.2	21.8			
6-25	24.0	24.9	19.0	19.7	22.3	20.0	19.5	18.0	17.4	18.4
6-26	23.3	24.2	18.0	18.7	21.5	19.5	19.0	17.3	16.7	17.8
6-27	26.4	27.4	16.7	17.4	22.4	21.1	20.6	16.3	15.6	18.1
6-28	24.9	25.9	18.5	19.2	22.5	20.9	20.4	17.4	16.8	18.6
6-29	26.8	27.8	18.0	18.7	23.3	21.7	21.3	17.1	16.4	18.9
6-30	26.2	27.2	17.1	17.8	22.5	22.0	21.6	16.7	16.0	18.8
7-1	26.5	27.5	16.3	16.9	22.2	21.8	21.4	16.5	15.8	18.6
7-2	26.4	27.4	16.9	17.6	22.5	22.3	21.9	17.0	16.3	19.1
7-3	22.8	23.7	18.1	18.8	21.2	19.7	19.2	17.6	17.0	18.1
7-4	25.0	26.0	17.3	18.0	22.0	21.2	20.7	17.0	16.3	18.5
7-5	23.7	24.6	15.1	15.7	20.2	20.5	20.0	16.0	15.3	17.6
7-6	25.0	26.0	15.9	16.5	21.2	21.5	21.0	16.3	15.6	18.3
7-7	25.6	26.6	15.4	16.0	21.3	21.7	21.3	16.1	15.4	18.3
7-8	26.0	27.0	16.0	16.6	21.8	21.9	21.5	16.2	15.5	18.5
7-9	25.8	26.8	16.7	17.4	22.1	21.7	21.3	16.6	15.9	18.6
7-10	25.6	26.6	17.1	17.8	22.2	21.4	20.9	17.0	16.3	18.6
7-11	25.7	26.7	17.4	18.1	22.4	21.7	21.3	17.0	16.3	18.8
7-12	26.0	27.0	16.5	17.2	22.1	21.3	20.8	16.4	15.7	18.3
7-13	25.9	26.9	15.5	16.1	21.5	21.6	21.2	16.1	15.4	18.3
7-14	25.3	26.3	14.6	15.2	20.7	21.2	20.7	15.4	14.7	17.7
7-15	25.9	26.9	15.6	16.2	21.6	20.4	19.9	16.0	15.3	17.6
7-16	25.8	26.8	15.9	16.5	21.7	21.7	21.3	16.1	15.4	18.3
7-17	26.0	27.0	16.2	16.8	21.9	22.0	21.6	16.6	15.9	18.7
7-18	26.3	27.3	16.6	17.3	22.3	21.9	21.5	16.8	16.1	18.8
7-19	25.8	26.8	15.2	15.8	21.3	21.5	21.0	15.9	15.2	18.1
7-20	26.7	27.7	15.9	16.5	22.1	22.0	21.6	16.1	15.4	18.5

Table C.1 (cont'd). Daily maximum and minimum stream temperature values at VRM 163.1 and VRM 157.3. Mean temperatures are calculated from maximum and minimum values.

	VRM 157.3					VRM 163.1				
DATE	MAX STR TEMP C	CALIB MAX TEMP C	MIN STR TEMP C	CALIB MIN TEMP C	CALIB MEAN TEMP C	MAX STR TEMP C	CALIB MAX TEMP C	MIN STR TEMP C	CALIB MIN TEMP C	CALIB MEAN TEMP C
7-21	26.8	27.8	16.8	17.5	22.6	22.3	21.9	16.9	16.2	19.1
7-22	26.7	27.7	17.4	18.1	22.9	22.1	21.7	17.3	16.7	19.2
7-23	25.5	26.5	18.9	19.6	23.1					
7-24	26.0	27.0	17.1	17.8	22.4					
7-25	26.6	27.6	17.0	17.7	22.6					
7-26	25.3	26.3	17.5	18.2	22.2					
7-27	23.4	24.3	18.8	19.5	21.9					
7-28	26.8	27.8	18.1	18.8	23.3					
7-29	26.1	27.1	17.8	18.5	22.8					
7-30	23.7	24.6	17.8	18.5	21.6					
7-31	24.7	25.6	18.0	18.7	22.2					
8-1	24.5	25.4	18.9	19.6	22.5					
8-2	24.3	25.2	18.6	19.3	22.3					

Table C.2 . Hourly readings from stream thermograph at VRM 163.1 on 6-30-88, 7-08-88, 7-15-88, and 7-21-88.

TIME	6-30-88 STREAM TEMP C	CALIB STREAM TEMP C	7-8-88 STREAM TEMP C	CALIB STREAM TEMP C	7-15-88 STREAM TEMP C	CALIB STREAM TEMP C	7-21-88 STREAM TEMP C	CALIB STREAM TEMP C
100	18.7	18.1	18.9	18.3	18.4	17.8	19.3	18.8
200	18.3	17.7	18.5	17.9	18.0	17.4	18.8	18.2
300	18.0	17.4	18.1	17.5	17.7	17.1	18.5	17.9
400	17.7	17.1	17.7	17.1	17.4	16.8	18.2	17.6
500	17.5	16.9	17.5	16.9	17.1	16.5	17.9	17.3
600	17.2	16.6	17.1	16.5	16.7	16.0	17.6	17.0
700	17.0	16.4	16.8	16.1	16.4	15.7	17.2	16.6
800	16.8	16.1	16.6	15.9	16.2	15.5	17.0	16.4
900	16.7	16.0	16.3	15.6	16.0	15.3	16.9	16.3
1000	16.7	16.0	16.3	15.6	16.0	15.3	16.9	16.3
1100	16.9	16.3	16.5	15.8	16.1	15.4	17.1	16.5
1200	17.6	17.0	17.0	16.4	16.6	15.9	17.6	17.0
1300	18.5	17.9	18.0	17.4	17.7	17.1	18.7	18.1
1400	20.0	19.5	19.4	18.9	19.4	18.9	20.0	19.5
1500	21.3	20.9	20.7	20.2	20.6	20.1	21.3	20.9
1600	21.7	21.3	21.4	21.0	21.2	20.8	21.9	21.5
1700	22.0	21.6	21.8	21.4	21.4	21.0	22.3	21.9
1800	21.9	21.5	21.8	21.4	21.4	21.0	22.2	21.8
1900	21.5	21.1	21.5	21.1	21.0	20.5	21.8	21.4
2000	21.1	20.6	21.0	20.5	20.5	20.0	21.5	21.1
2100	20.6	20.1	20.4	19.9	20.2	19.7	21.0	20.5
2200	20.1	19.6	19.9	19.4	19.7	19.2	20.6	20.1
2300	19.6	19.1	19.5	19.0	19.3	18.8	20.2	19.7
2400	19.2	18.7	19.2	18.7	20.0	19.5	19.8	19.3

Table C.3. Daily maximum and minimum air temperature readings from hygrothermograph located at VRM 163.0. Mean temperatures are calculated from maximum and minimum values.

	VRM 163.0								
DATE	MAX AIR TEMP F	ADJUSTED MAX AIR F	ADJUSTED MAX AIR C	CALIB MAX AIR C	MIN AIR TEMP F	ADJUSTED MIN AIR F	ADJUSTED MIN AIR C	CALIB MIN AIR C	CALIB MEAN AIR C
5-29-88	69.0	68.5	20.3	19.4	41.5	41.0	5.0	3.1	11.2
5-30-88	52.5	51.5	10.8	9.3	41.0	40.0	4.4	2.5	5.9
5-31-88	66.5	65.0	18.3	17.3	39.5	38.0	3.3	1.3	9.3
6-1-88	77.0	75.0	23.9	23.2	46.0	44.0	6.7	4.9	14.1
6-2-88	86.0	83.5	28.6	28.3	51.5	49.0	9.4	7.8	18.1
6-3-88	92.5	89.5	31.9	31.8	56.5	53.5	11.9	10.5	21.2
6-25-88	90.0	90.2	32.3	32.2	72.0	72.2	22.3	21.6	26.9
6-26-88	88.0	88.3	31.3	31.1	70.0	70.3	21.3	20.5	25.8
6-27-88	89.0	89.5	31.9	31.8	63.5	64.0	17.8	16.7	24.3
6-28-88	92.0	92.6	33.7	33.7	71.0	71.6	22.0	21.2	27.4
6-29-88	92.0	92.8	33.8	33.8	69.0	69.8	21.0	20.2	27.0
6-30-88	92.0	92.5	33.6	33.4	68.0	68.9	20.5	19.6	26.5
7-1-88	95.5	96.1	35.6	35.4	64.0	64.6	18.1	18.0	26.7
7-2-88	95.5	96.3	35.7	35.5	67.0	67.8	19.9	19.8	27.6
7-3-88	86.0	86.9	30.5	30.3	70.5	71.4	21.9	21.8	26.0
7-4-88	91.5	92.6	33.7	33.4	67.5	68.6	20.3	20.2	26.8
7-5-88	90.0	91.2	32.9	32.7	63.0	64.2	17.9	17.8	25.2
7-6-88	92.0	93.4	34.1	33.9	63.0	64.4	18.0	17.9	25.9
7-7-88	93.5	95.0	35.0	34.8	62.5	64.1	17.8	17.8	26.3
7-8-88	94.0	95.7	35.4	35.1	64.0	65.8	18.8	18.7	26.9
7-9-88	99.0	99.0	37.2	36.9	66.5	68.4	20.2	20.1	28.5
7-10-88	99.0	98.5	36.9	36.7	73.0	72.5	22.5	22.4	29.5
7-11-88	96.0	95.0	35.0	34.8	74.0	73.0	22.8	22.7	28.7
7-12-88	97.0	95.5	35.3	35.0	71.5	70.0	21.1	21.0	28.0
7-13-88	101.0	99.0	37.2	36.9	69.0	67.0	19.4	19.4	28.2
7-14-88	99.5	97.0	36.1	35.8	67.0	64.5	18.1	18.0	26.9
7-15-88	99.0	99.0	37.2	36.9	69.0	66.1	18.9	18.9	27.9
7-16-88	100.0	99.9	37.7	37.4	67.5	67.4	19.7	19.6	28.5
7-17-88	103.0	102.8	39.3	39.0	71.0	70.8	21.6	21.5	30.2
7-18-88	103.0	102.7	39.3	39.0	70.5	70.2	21.2	21.1	30.1
7-19-88	100.5	100.1	37.8	37.6	66.5	66.1	18.9	18.9	28.2
7-20-88	102.0	101.5	38.6	38.3	67.5	67.0	19.4	19.4	28.8
7-21-88	101.0	100.4	38.0	37.7	73.0	72.4	22.4	22.3	30.0
7-22-88	99.5	98.8	37.1	36.8	72.0	71.3	21.8	21.7	29.3
7-23-88	97.5	96.7	35.9	35.7	77.5	76.7	24.8	24.7	30.2
8-6-88	79.0	79.1	26.2	26.0	58.5	58.6	14.8	14.8	20.4
8-7-88	86.0	86.2	30.1	29.9	58.0	58.2	14.6	14.5	22.2
8-8-88	89.5	89.8	32.1	31.9	55.0	55.3	12.9	12.9	22.4
8-9-88	90.0	90.4	32.4	32.2	58.0	58.4	14.7	14.6	23.4
8-10-88	91.5	92.0	33.3	33.1	59.0	59.5	15.3	15.2	24.2
8-11-88	73.0	73.6	23.1	23.0	61.0	61.6	16.4	16.4	19.7
8-12-88	89.5	89.5	31.9	31.7	60.0	60.0	15.6	15.5	23.6
8-13-88	92.0	92.0	33.3	33.1	60.0	60.0	15.6	15.5	24.3

Table C.3 (cont'd).

Daily maximum and minimum air temperature readings from hygrothermograph located at VRM 163.0. Mean temperatures are calculated from maximum and minimum values.

VRM 163.0									
DATE	MAX AIR TEMP F	ADJUSTED MAX AIR F	ADJUSTED MAX AIR C	CALIB MAX AIR C	MIN AIR TEMP F	ADJUSTED MIN AIR F	ADJUSTED MIN AIR C	CALIB MIN AIR C	CALIB MEAN AIR C
8-14-88	95.0	95.0	35.0	34.8	59.5	59.5	15.3	15.2	25.0
8-15-88	92.5	92.5	33.6	33.4	66.0	66.0	18.9	18.8	26.1
8-16-88	92.5	92.4	33.6	33.3	57.0	56.9	13.8	13.8	23.6
8-17-88	94.5	94.4	34.7	34.4	60.0	59.9	15.5	15.5	24.9
8-18-88	96.5	96.4	35.8	35.5	65.5	65.4	18.6	18.5	27.0

Table C.4. Daily maximum and minimum air temperature readings from hygrothermograph located at VRM 157.5. Mean temperatures are calculated from maximum and minimum values.

	VRM 157.5								
DATE	MAX AIR TEMP F	ADJUSTED MAX AIR F	ADJUSTED MAX AIR C	CALIB MAX AIR C	MIN AIR TEMP F	ADJUSTED MIN AIR F	ADJUSTED MIN AIR C	CALIB MIN AIR C	CALIB MEAN AIR C
6-22-88	101.0	100.6	38.1	38.4	68.5	68.1	20.1	19.1	28.8
6-23-88	104.0	103.2	39.6	40.0	72.0	71.2	21.8	21.0	30.5
6-24-88	104.0	102.8	39.3	39.7	74.0	72.8	22.7	21.9	30.8
6-25-88	95.0	93.4	34.1	34.1	77.0	75.4	24.1	23.5	28.8
6-26-88	91.5	89.5	31.9	31.8	71.0	69.0	20.6	19.7	25.8
6-27-88	97.0	94.6	34.8	34.9	67.0	64.6	18.1	17.1	26.0
6-28-88	97.5	94.7	34.8	34.9	74.0	71.2	21.8	21.0	28.0
6-29-88	95.0	95.0	35.0	35.1	72.0	69.0	20.6	19.7	27.4
6-30-88	99.5	92.0	33.3	37.0	69.0	61.5	16.4	19.9	28.4
7-1-88	100.0	92.4	33.6	37.3	68.0	60.4	15.8	19.2	28.3
7-2-88	102.0	94.3	34.6	38.3	70.0	62.4	16.9	20.4	29.3
7-3-88	93.0	85.3	29.6	33.3	74.0	66.3	19.1	22.6	27.9
7-4-88	96.0	88.2	31.2	34.9	70.0	62.3	16.8	20.3	27.6
7-5-88	95.5	87.7	30.9	34.6	67.0	59.2	15.1	18.6	26.6
7-6-88	96.0	88.1	31.2	34.8	66.0	58.2	14.6	18.0	26.4
7-7-88	96.0	89.0	31.7	35.3	66.0	58.1	14.5	17.9	26.6
7-8-88	97.5	90.7	32.6	36.3	65.5	58.7	14.8	18.3	27.3
7-9-88	99.0	92.4	33.6	37.3	67.5	60.9	16.1	19.5	28.4
7-10-88	99.0	92.6	33.7	37.4	70.0	63.6	17.6	21.0	29.2
7-11-88	94.5	88.3	31.3	35.0	72.0	65.8	18.8	22.3	28.6
7-12-88	95.0	89.0	31.7	35.3	66.0	60.0	15.6	19.0	27.2
7-13-88	99.0	93.2	34.0	37.7	65.0	59.2	15.1	18.6	28.1
7-14-88	98.0	92.4	33.6	37.3	63.0	57.4	14.1	17.5	27.4
7-15-88	93.5	93.5	34.2	37.9	61.0	61.0	16.1	19.6	28.7
7-16-88	95.0	94.9	34.9	38.7	62.0	61.8	16.6	20.0	29.3
7-17-88	97.0	96.8	36.0	39.7	64.0	63.7	17.6	21.1	30.4
7-18-88	97.5	97.2	36.2	40.0	65.5	65.1	18.4	21.9	30.9
7-19-88	96.0	95.6	35.3	39.1	61.0	60.5	15.8	19.3	29.2
7-20-88	98.0	97.5	36.4	40.1	63.5	62.9	17.2	20.6	30.4
7-21-88	97.5	96.5	35.8	39.6	66.0	65.4	18.6	22.1	30.8
7-22-88	97.0	96.0	35.6	39.3	65.0	64.0	17.8	21.3	30.3
7-23-88	91.5	90.4	32.4	36.1	69.5	68.4	20.2	23.7	29.9
7-24-88	95.5	94.4	34.7	38.4	63.0	61.9	16.6	20.1	29.2
7-25-88	94.5	93.3	34.1	37.8	65.5	64.3	17.9	21.4	29.6
7-26-88	91.5	90.3	32.4	36.1	65.0	63.8	17.7	21.2	28.6
7-27-88	83.5	82.2	27.9	31.5	59.0	57.7	14.3	17.7	24.6
7-28-88	86.0	86.0	30.0	33.7	60.5	59.2	15.1	18.6	26.1
7-29-88	88.5	88.4	31.3	35.0	60.0	59.9	15.5	19.0	27.0
7-30-88	87.5	87.4	30.8	34.4	64.0	63.9	17.7	21.2	27.8
7-31-88	86.0	85.9	29.9	33.6	58.0	57.9	14.4	17.8	25.7
8-1-88	85.5	85.3	29.6	33.3	57.0	56.8	13.8	17.2	25.2
8-2-88	84.0	83.8	28.8	32.4	61.5	61.3	16.3	19.7	26.1
8-3-88	85.0	84.8	29.3	33.0	57.0	56.8	13.8	17.2	25.1
8-4-88	88.0	87.8	31.0	34.7	62.0	61.8	16.6	20.0	27.3
8-5-88	75.5	75.4	24.1	27.7	63.0	62.9	17.2	20.6	24.2
8-6-88	79.0	78.9	26.1	29.7	57.0	56.9	13.8	17.3	23.5
8-7-88	85.0	84.8	29.3	33.0	54.0	53.8	12.1	15.5	24.3

Table C.4 (cont'd).

Daily maximum and minimum air temperature readings from hygrothermograph located at VRM 157.5. Mean temperatures are calculated from maximum and minimum values.

DATE	MAX AIR TEMP F	ADJUSTED MAX AIR F	ADJUSTED MAX AIR C	CALIB MAX AIR C	MIN AIR TEMP F	ADJUSTED MIN AIR F	ADJUSTED MIN AIR C	CALIB MIN AIR C	CALIB MEAN AIR C
	VRM 157.5								
8-8-88	87.5	87.3	30.7	34.4	52.0	51.8	11.0	14.4	24.4
8-13-88	88.0	87.7	30.9	34.6	53.5	53.2	11.8	15.2	24.9
8-14-88	91.5	90.9	32.7	36.4	53.0	52.4	11.3	14.7	25.6
8-15-88	89.0	88.1	31.2	34.8	61.0	60.1	15.6	19.1	27.0
8-16-88	90.0	88.8	31.6	35.2	52.0	50.8	10.4	13.8	24.5
8-17-88	92.5	91.0	32.8	36.5	56.5	55.0	12.8	16.2	26.3
8-18-88	94.5	92.7	33.7	37.4	62.0	60.2	15.7	19.1	28.3
8-19-88	93.0	90.9	32.7	36.4	64.0	61.9	16.6	20.1	28.3

Table C.5 Hourly readings from hygrothermograph at VRM 163.0 on 6-30-88.

TIME	AIR TEMP F	ADJUSTED TEMP F	ADJUSTED TEMP C	CALIB. TEMP C
100	75.5	76.0	24.4	24.3
200	75.0	75.5	24.2	24.0
300	74.0	74.5	23.6	23.5
400	73.0	73.5	23.1	22.9
500	71.5	72.0	22.2	22.1
600	70.0	70.5	21.4	21.3
700	69.0	69.5	20.8	20.7
800	68.0	68.5	20.3	20.2
900	71.0	71.5	21.9	21.8
1000	76.5	77.0	25.0	24.9
1100	82.0	82.5	28.1	27.9
1200	83.5	84.0	28.9	28.7
1300	86.0	86.5	30.3	30.1
1400	88.0	88.5	31.4	31.2
1500	89.0	89.5	31.9	31.7
1600	90.0	90.5	32.5	32.3
1700	92.0	92.5	33.6	33.4
1800	92.0	92.5	33.6	33.4
1900	90.0	90.5	32.5	32.3
2000	88.0	88.5	31.4	31.2
2100	78.0	78.5	25.8	25.7
2200	76.0	76.5	24.7	24.6
2300	75.0	75.5	24.2	24.0
2400	76.0	76.5	24.7	24.6

Table C.6 . Hourly readings from hygrothermograph at VRM 163.0 on 7-08-88.

TIME	AIR TEMP F	ADJUSTED TEMP F	ADJUSTED TEMP C	CALIB. TEMP C
100	75.5	77.3	25.2	25.0
200	73.5	75.3	24.1	23.9
300	71.0	72.8	22.7	22.6
400	69.0	70.8	21.6	21.5
500	68.0	69.8	21.0	20.9
600	66.5	68.3	20.2	20.1
700	65.0	66.8	19.3	19.3
800	64.0	65.8	18.8	18.7
900	66.0	67.8	19.9	19.8
1000	73.5	75.3	24.1	23.9
1100	78.0	79.8	26.6	26.4
1200	85.5	87.3	30.7	30.5
1300	87.5	89.3	31.8	31.6
1400	90.5	92.3	33.5	33.3
1500	91.5	93.3	34.1	33.8
1600	93.0	94.8	34.9	34.6
1700	93.0	94.8	34.9	34.6
1800	93.5	95.3	35.2	34.9
1900	93.5	95.3	35.2	34.9
2000	94.0	95.8	35.4	35.2
2100	89.5	91.3	32.9	32.7
2200	79.5	81.3	27.4	27.2
2300	77.5	79.3	26.3	26.1
2400	78.0	79.8	26.6	26.4

Table C.7 . Hourly readings from hygrothermograph at VRM 163.0 on 7-15-88.

TIME	AIR TEMP F	ADJUSTED TEMP F	ADJUSTED TEMP C	CALIB. TEMP C
100	81.0	78.1	25.6	25.5
200	78.5	75.6	24.2	24.1
300	76.5	73.6	23.1	23.0
400	74.0	71.1	21.7	21.6
500	72.5	69.6	20.9	20.8
600	71.0	68.1	20.1	20.0
700	70.0	67.1	19.5	19.4
800	69.0	66.1	18.9	18.9
900	74.0	71.1	21.7	21.6
1000	82.0	79.1	26.2	26.0
1100	85.5	82.6	28.1	27.9
1200	92.5	89.6	32.0	31.8
1300	94.5	91.6	33.1	32.9
1400	96.0	93.1	33.9	33.7
1500	96.0	96.0	35.6	35.3
1600	98.0	98.0	36.7	36.4
1700	99.0	99.0	37.2	36.9
1800	97.5	97.5	36.4	36.1
1900	98.0	98.0	36.7	36.4
2000	96.0	96.0	35.6	35.3
2100	85.0	85.0	29.4	29.3
2200	81.5	81.5	27.5	27.3
2300	80.0	80.0	26.7	26.5
2400	80.0	80.0	26.7	26.5

Table C.8 . Hourly readings from hygrothermograph at VRM 163.0 on 7-21-88.

TIME	AIR TEMP F	ADJUSTED TEMP F	ADJUSTED TEMP C	CALIB. TEMP C
100	82.5	81.9	27.7	27.6
200	81.0	80.4	26.9	26.7
300	79.5	78.9	26.1	25.9
400	77.0	76.4	24.7	24.5
500	76.0	75.4	24.1	24.0
600	73.5	72.9	22.7	22.6
700	73.0	72.4	22.4	22.3
800	73.0	72.4	22.4	22.3
900	73.0	72.4	22.4	22.3
1000	80.0	79.4	26.3	26.2
1100	85.5	84.9	29.4	29.2
1200	87.5	86.9	30.5	30.3
1300	90.5	89.9	32.2	31.9
1400	92.0	91.4	33.0	32.8
1500	94.0	93.4	34.1	33.9
1600	97.0	96.4	35.8	35.5
1700	100.0	99.4	37.4	37.2
1800	99.5	98.9	37.2	36.9
1900	100.5	99.9	37.7	37.4
2000	100.0	99.4	37.4	37.2
2100	88.0	87.4	30.8	30.6
2200	83.5	82.9	28.3	28.1
2300	82.5	81.9	27.7	27.6
2400	84.5	83.9	28.8	28.7

Table C.9 . Hourly readings from hygrothermograph at VRM 157.5 on 6-30-88.

TIME	AIR TEMP F	ADJUSTED TEMP F	ADJUSTED TEMP C	CALIB. TEMP C
100	77.0	71.5	21.9	25.5
200	75.5	70.0	21.1	24.6
300	74.0	68.5	20.3	23.8
400	72.0	66.5	19.2	22.7
500	69.5	64.0	17.8	21.3
600	68.5	63.0	17.2	20.7
700	69.0	61.5	16.4	19.9
800	71.0	63.5	17.5	21.0
900	74.5	67.0	19.4	23.0
1000	81.0	73.5	23.1	26.6
1100	86.0	78.5	25.8	29.4
1200	88.5	81.0	27.2	30.8
1300	90.0	82.5	28.1	31.7
1400	92.5	85.0	29.4	33.1
1500	95.0	87.5	30.8	34.5
1600	96.5	89.0	31.7	35.3
1700	98.0	90.5	32.5	36.2
1800	99.5	92.0	33.3	37.0
1900	95.0	87.5	30.8	34.5
2000	90.0	82.5	28.1	31.7
2100	83.0	75.5	24.2	27.7
2200	77.5	70.0	21.1	24.6
2300	75.5	68.0	20.0	23.5
2400	79.0	71.5	21.9	25.5

Table C.10. Hourly readings from hygrothermograph at VRM 157.5 on 7-08-88.

TIME	AIR TEMP F	ADJUSTED TEMP F	ADJUSTED TEMP C	CALIB. TEMP C
100	75.5	68.7	20.4	23.9
200	73.0	66.2	19.0	22.5
300	70.5	63.7	17.6	21.1
400	69.0	62.2	16.8	20.3
500	67.5	60.7	15.9	19.4
600	66.0	59.2	15.1	18.6
700	67.5	60.7	15.9	19.4
800	71.0	64.2	17.9	21.4
900	78.0	71.2	21.8	25.3
1000	86.0	79.2	26.2	29.8
1100	91.5	84.7	29.3	32.9
1200	93.0	86.2	30.1	33.8
1300	93.5	86.7	30.4	34.1
1400	95.0	88.2	31.2	34.9
1500	95.5	88.7	31.5	35.2
1600	96.0	89.2	31.8	35.5
1700	97.5	90.7	32.6	36.3
1800	97.5	90.7	32.6	36.3
1900	91.5	84.7	29.3	32.9
2000	90.0	83.2	28.4	32.1
2100	79.0	72.2	22.3	25.9
2200	76.0	69.2	20.7	24.2
2300	80.0	73.2	22.9	26.4
2400	79.5	72.7	22.6	26.2

Table C.11. Hourly readings from hygrothermograph at VRM 157.5 on 7-15-88.

TIME	AIR TEMP F	ADJUSTED TEMP F	ADJUSTED TEMP C	CALIB. TEMP C
100	72.5	72.4	22.4	26.0
200	71.0	70.9	21.6	25.2
300	68.5	68.4	20.2	23.7
400	66.0	65.9	18.8	22.3
500	64.0	63.9	17.7	21.2
600	63.0	62.9	17.2	20.6
700	61.0	61.0	16.1	19.6
800	63.5	63.5	17.5	21.0
900	67.0	67.0	19.4	23.0
1000	75.0	75.0	23.9	27.5
1100	83.0	83.0	28.3	32.0
1200	87.5	87.5	30.8	34.5
1300	88.5	88.5	31.4	35.1
1400	90.0	90.0	32.2	35.9
1500	91.5	91.5	33.1	36.8
1600	91.5	91.5	33.1	36.8
1700	93.0	93.0	33.9	37.6
1800	93.0	93.0	33.9	37.6
1900	89.0	89.0	31.7	35.3
2000	86.5	86.5	30.3	33.9
2100	85.0	85.0	29.4	33.1
2200	80.0	80.0	26.7	30.3
2300	70.0	70.0	21.1	24.6
2400	68.0	68.0	20.0	23.5

Table C.12. Hourly readings from hygrothermograph at VRM 157.5 on 7-21-88.

TIME	AIR TEMP F	ADJUSTED TEMP F	ADJUSTED TEMP C	CALIB. TEMP C
100	78.5	77.9	25.5	29.1
200	77.0	76.4	24.7	28.3
300	75.0	74.4	23.6	27.1
400	73.0	72.4	22.4	26.0
500	71.5	70.9	21.6	25.2
600	68.5	67.9	19.9	23.5
700	66.5	65.9	18.8	22.3
800	67.5	66.9	19.4	22.9
900	70.5	69.9	21.1	24.6
1000	76.0	75.4	24.1	27.7
1100	83.0	82.4	28.0	31.6
1200	84.5	83.9	28.8	32.5
1300	86.5	85.9	29.9	33.6
1400	87.5	86.9	30.5	34.2
1500	90.0	89.4	31.9	35.6
1600	93.5	92.5	33.6	37.3
1700	95.0	94.0	34.4	38.2
1800	97.5	96.5	35.8	39.6
1900	90.0	89.0	31.7	35.3
2000	87.5	86.5	30.3	33.9
2100	85.5	84.5	29.2	32.8
2200	78.0	77.0	25.0	28.6
2300	70.0	69.0	20.6	24.1
2400	76.0	75.0	23.9	27.5

Table C.13. Daily 1400 hr temperature readings from field hygrothermographs and Zion National Park.

DATE	VRM 157.5 1400 AIR TEMP F	VRM 157.5 ADJUSTED 1400 AIR F	VRM 157.5 ADJUSTED 1400 AIR C	VRM 157.5 CALIB 1400 AIR C	VRM 163.0 1400 AIR TEMP F	VRM 163.0 ADJUSTED 1400 AIR F	VRM 163.0 ADJUSTED 1400 AIR C	VRM 163.0 CALIB 1400 AIR C	ZNP 1400 AIR TEMP F	ZNP 1400 AIR TEMP C
5-28-88					73.0	73.0	22.8	22.1	88.0	31.1
5-29-88					43.0	42.5	5.8	4.0	47.0	8.3
5-30-88									56.0	13.3
5-31-88					61.5	60.0	15.6	14.3	68.0	20.0
6-1-88					73.0	71.0	21.7	20.9	80.0	26.7
6-2-88					81.0	78.5	25.8	25.3	87.0	30.6
6-3-88					89.5	86.5	30.3	30.1	93.0	33.9
6-21-88									94.0	34.4
6-22-88	96.0	95.6	35.3	35.5					97.0	36.1
6-23-88	100.0	99.2	37.3	37.6					101.0	38.3
6-24-88	100.0	98.8	37.1	37.3					102.0	38.9
6-25-88	86.0	84.4	29.1	28.8	81.0	81.2	27.3	26.9	85.0	29.4
6-26-88	87.0	85.0	29.4	29.2	84.0	84.3	29.1	28.8	89.0	31.7
6-27-88	94.0	91.6	33.1	33.1					94.0	34.4
6-28-88	94.0	91.2	32.9	32.8	88.0	88.6	31.4	31.3	95.0	35.0
6-29-88					86.0	86.8	30.4	30.2		
6-30-88	92.5	85.0	29.4	33.1	88.5	89.5	31.9	31.8	96.0	35.6
7-1-88	97.0	89.4	31.9	35.6	91.5	92.1	33.4	33.2	100.0	37.8
7-2-88	97.5	89.8	32.1	35.8	92.0	92.8	33.8	33.5	99.0	37.2
7-3-88	77.0	69.3	20.7	24.3	77.0	77.9	25.5	25.4	86.0	30.0
7-4-88	92.0	84.2	29.0	32.6	89.0	90.1	32.3	32.1	95.0	35.0
7-5-88	92.5	84.7	29.3	32.9	87.0	88.2	31.2	31.0	93.0	33.9
7-6-88	92.5	84.6	29.2	32.9	87.0	88.4	31.3	31.1	95.0	35.0
7-7-88	93.0	86.0	30.0	33.7	88.0	89.5	31.9	31.7	97.0	36.1
7-8-88	96.0	89.2	31.8	35.5	90.0	91.7	33.2	32.9	98.0	36.7
7-9-88	96.0	89.4	31.9	35.6	92.0	93.9	34.4	34.1	99.0	37.2
7-10-88	95.5	89.1	31.7	35.4	96.0	95.5	35.3	35.0	99.0	37.2
7-11-88									95.0	35.0
7-12-88	90.5	84.5	29.2	32.8	92.0	90.5	32.5	32.3	94.0	34.4
7-13-88	94.5	88.7	31.5	35.2	98.0	96.0	35.6	35.3	97.0	36.1
7-14-88	95.0	89.4	31.9	35.6	97.0	94.5	34.7	34.5	99.0	37.2
7-15-88	90.0	90.0	32.2	35.9	96.0	93.1	33.9	33.7	100.0	37.8
7-16-88	91.5	91.4	33.0	36.7	96.0	95.9	35.5	35.2	101.0	38.3
7-17-88	93.5	93.3	34.1	37.8	98.0	97.8	36.6	36.3	103.0	39.4
7-18-88					97.0	96.7	35.9	35.7	101.0	38.3
7-19-88	91.0	90.6	32.6	36.2	95.0	94.6	34.8	34.5	100.0	37.8
7-20-88	92.0	91.5	33.1	36.8	97.5	97.0	36.1	35.8	102.0	38.9
7-21-88	87.5	86.9	30.5	34.2	92.0	91.4	33.0	32.8	99.0	37.2
7-22-88	92.0	91.0	32.8	36.5	93.5	92.8	33.8	33.5	100.0	37.8
7-23-88	90.5	89.4	31.9	35.6	93.0	92.2	33.4	33.2	99.0	37.2
7-24-88	90.5	89.4	31.9	35.6					100.0	37.8
7-25-88									102.0	38.9
7-26-88	92.0	90.8	32.7	36.4					101.0	38.3
7-27-88	67.0	65.7	18.7	22.2					73.0	22.8
7-28-88	80.5	80.5	26.9	30.6					90.0	32.2
7-29-88	88.0	87.9	31.1	34.7					97.0	36.1
7-30-88	82.5	82.4	28.0	31.6					94.0	34.4

Table C.13 (cont'd).

Daily 1400 hr temperature readings from field hygrothermographs and Zion National Park.

DATE	VRM 157.5 1400 AIR TEMP F	VRM 157.5 ADJUSTED 1400 AIR F	VRM 157.5 ADJUSTED 1400 AIR C	VRM 157.5 CALIB 1400 AIR C	VRM 163.0 1400 AIR TEMP F	VRM 163.0 ADJUSTED 1400 AIR F	VRM 163.0 ADJUSTED 1400 AIR C	VRM 163.0 CALIB 1400 AIR C	ZNP 1400 AIR TEMP F	ZNP 1400 AIR TEMP C
7-31-88	79.5	79.4	26.3	29.9					91.0	32.8
8-1-88									85.0	29.4
8-2-88	82.0	81.8	27.7	31.3					91.0	32.8
8-3-88	78.0	77.8	25.4	29.0					86.0	30.0
8-4-88	85.0	84.8	29.3	33.0					93.0	33.9
8-5-88	71.0	70.9	21.6	25.2	76.0	76.0	24.4	24.3	81.0	27.2
8-6-88	65.0	64.9	18.3	21.8	66.0	66.1	18.9	18.9	76.0	24.4
8-7-88	79.5	79.3	26.3	29.9	85.0	85.2	29.6	29.4	89.0	31.7
8-8-88					85.0	85.3	29.6	29.4	92.0	33.3
8-9-88					87.0	87.4	30.8	30.6	94.0	34.4
8-10-88					87.0	87.5	30.8	30.6	94.0	34.4
8-11-88					65.5	65.5	18.6	18.5	72.0	22.2
8-12-88					84.0	84.0	28.9	28.7	86.0	30.0
8-13-88	84.0	83.7	28.7	32.4	91.0	91.0	32.8	32.6	92.0	33.3
8-14-88	87.5	86.9	30.5	34.2	93.5	93.5	34.2	33.9	97.0	36.1
8-15-88									96.0	35.6
8-16-88	84.5	83.3	28.5	32.1	88.0	87.9	31.1	30.8	93.0	33.9
8-17-88	87.5	86.0	30.0	33.7	92.0	91.9	33.3	33.0	96.0	35.6
8-18-88	90.0	88.2	31.2	34.9	93.0	92.9	33.8	33.6	99.0	37.2
8-19-88	88.0	85.9	29.9	33.6					100.0	37.8

Table C.14. Field collected data and calculated average topographic shading angle for South azimuths.

SAMPLE	AZIMUTH 150 (deg)	160 (deg)	170 (deg)	180 (deg)	190 (deg)	200 (deg)	210 (deg)
VRM 163.1 - VRM 162.2							
1	55.0	55.0	56.5	56.0	44.0	40.0	33.0
2	43.5	46.5	50.5	50.5	47.0	44.0	45.5
3	24.5	32.0	45.5	48.0	49.8	38.5	37.0
4	43.5	45.5	46.5	47.0	44.5	38.0	31.5
5	51.5	52.0	51.0	46.5	38.0	38.0	33.0
AVERAGE:	43.6	46.2	50.0	49.6	44.7	39.7	36.0
VARIANCE:	139.3	78.3	19.0	15.2	19.2	6.5	32.4
90%C.I.*:	8.1	6.1	3.0	2.7	3.0	1.7	3.9
VRM 162.2 - VRM 161.5							
1	37.0	33.5	35.5	38.5	33.0	34.5	34.0
2	41.0	42.0	43.5	44.0	38.0	38.5	37.0
3	43.0	41.0	44.0	45.0	46.5	47.0	49.5
4	36.0	41.0	46.5	48.0	42.5	41.0	33.5
5	45.5	46.0	47.5	49.0	47.5	45.0	47.5
AVERAGE:	40.5	40.7	43.4	44.9	41.5	41.2	40.3
VARIANCE:	16.0	20.5	22.3	17.1	36.6	25.1	58.3
90%C.I.*:	2.7	3.1	3.2	2.8	4.1	3.4	5.2
VRM 161.5 - VRM 160.7							
1	35.0	39.0	38.0	35.0	28.0	17.5	17.0
2	44.5	42.0	38.0	32.5	24.0	20.0	11.5
3	41.0	32.0	24.5	24.5	20.0	22.0	18.0
4	28.0	22.0	9.5	19.5	22.0	19.0	8.5
5	30.0	30.0	28.0	23.5	27.0	21.0	6.5
AVERAGE:	35.7	33.0	27.6	27.0	24.2	19.9	12.3
VARIANCE:	49.5	62.0	138.4	42.3	11.2	3.1	25.8
90%C.I.*:	4.8	5.4	8.1	4.4	2.3	1.2	3.5
VRM 160.7 - VRM 160.0							
1	34.0	25.5	26.0	29.0	31.0	24.5	16.5
2	24.0	29.0	34.0	32.5	27.0	19.5	15.0
3	38.5	40.0	37.0	33.0	31.0	21.0	19.0
4	42.5	40.0	38.0	35.0	26.0	24.0	20.0
5	39.5	39.0	35.5	29.0	28.5	23.0	19.0
AVERAGE:	35.7	34.7	34.1	31.7	28.7	22.4	17.9
VARIANCE:	52.1	48.0	22.8	7.0	5.2	4.4	4.3
90%C.I.*:	4.9	4.7	3.3	1.8	1.6	1.4	1.4
VRM 160.0 - VRM 159.5							
1	29.5	33.5	31.5	30.0	33.5	22.5	8.0
2	34.5	29.5	32.5	32.5	22.5	18.0	15.0
3	33.0	34.5	30.0	23.0	24.0	14.5	13.5
4	38.5	39.5	31.0	27.5	28.0	24.0	15.5
5	37.0	31.0	26.5	29.5	26.0	15.5	13.0
AVERAGE:	34.5	33.6	30.3	28.5	26.8	18.9	13.0
VARIANCE:	12.4	14.8	5.3	12.6	18.3	17.7	8.9
90%C.I.*:	2.4	2.6	1.6	2.4	2.9	2.9	2.0

* +/- Confidence Interval for a 90% level of significance.

Table C.14 (cont'd). Field collected data and calculated average topographic shading angle for South azimuths.

SAMPLE	150 (deg)	160 (deg)	170 (deg)	180 (deg)	190 (deg)	200 (deg)	210 (deg)
	AZIMUTH						
VRM 159.5 - VRM 158.4							
1	28.5	32.5	33.5	30.0	20.0	18.5	13.5
2	38.0	37.0	32.5	27.5	20.5	22.0	16.0
3	38.0	35.5	31.0	26.0	26.5	22.0	18.0
4	30.0	25.5	29.5	31.5	26.0	23.5	19.5
5	29.0	29.0	25.5	20.5	21.0	21.0	19.5
AVERAGE:	32.7	31.9	30.4	27.1	22.8	21.4	17.3
VARIANCE:	23.7	22.2	9.8	18.2	10.1	3.4	6.6
90%C.I.*:	3.3	3.2	2.1	2.9	2.2	1.3	1.8
VRM 158.4 - VRM 157.3							
1	21.5	19.0	27.0	28.0	28.5	18.5	18.0
2	28.0	32.0	31.0	24.0	20.5	20.5	10.5
3	41.0	41.0	39.0	33.5	26.5	23.0	19.0
4	15.0	21.0	23.0	24.5	19.0	9.5	4.0
5	32.0	30.0	34.5	29.5	24.5	16.0	11.0
AVERAGE:	27.5	28.6	30.9	27.9	23.8	17.5	12.5
VARIANCE:	98.8	79.3	39.1	15.2	16.0	26.6	37.8
90%C.I.*:	6.8	6.1	4.3	2.7	2.7	3.5	4.2

* +/- Confidence Interval for a 90% level of significance.

Table C.15. Field collected data and calculated average topographic shading angle for Southwest azimuths.

SAMPLE	AZIMUTH 240 (deg)	250 (deg)	260 (deg)	270 (deg)	280 (deg)	290 (deg)	300 (deg)	310 (deg)
VRM 163.1 - VRM 162.2								
1	33.5	29.5	26.0	9.0	11.0	16.0	17.5	25.0
2	52.5	51.5	44.0	25.5	22.0	20.5	21.0	21.5
3	12.0	9.0	7.5	18.0	27.0	31.0	35.5	38.0
4	15.0	11.0	16.5	19.0	30.5	33.0	49.0	51.0
5	24.5	22.0	19.0	12.5	17.5	31.5	39.0	45.5
AVERAGE:	27.5	24.6	22.6	16.8	21.6	26.4	32.4	36.2
VARIANCE:	266.6	295.7	186.9	40.3	59.4	58.4	170.2	162.6
90%C.I.*:	11.2	11.8	9.4	4.3	5.3	5.2	8.9	8.7
VRM 162.2 - VRM 161.5								
1	22.5	13.5	11.5	20.0	22.0	30.5	38.5	40.0
2	25.5	13.0	10.5	13.0	18.0	36.5	38.0	43.0
3	24.5	18.5	14.0	14.0	16.0	22.0	22.0	22.0
4	28.0	22.0	16.0	15.5	23.5	27.5	27.5	26.5
5	28.5	17.0	17.5	17.0	18.0	28.0	33.5	32.0
AVERAGE:	25.8	16.8	13.9	15.9	19.5	28.9	31.9	32.7
VARIANCE:	6.2	13.8	8.7	7.6	9.8	27.7	50.2	78.2
90%C.I.*:	1.7	2.5	2.0	1.9	2.1	3.6	4.8	6.1
VRM 161.5 - VRM 160.7								
1	7.5	14.5	23.0	26.5	28.5	32.5	40.0	43.5
2	4.0	13.0	17.0	23.5	21.5	20.0	26.0	30.0
3	3.5	14.5	21.0	26.0	25.5	24.5	22.0	30.0
4	15.5	23.0	29.5	32.0	30.5	29.0	29.0	32.0
5	28.5	8.5	23.5	31.0	32.0	23.5	26.5	23.0
AVERAGE:	11.8	14.7	22.8	27.8	27.6	25.9	28.7	31.7
VARIANCE:	110.2	27.6	20.6	12.8	17.6	23.9	46.2	55.2
90%C.I.*:	7.2	3.6	3.1	2.5	2.9	3.3	4.7	5.1
VRM 160.7 - VRM 160.0								
1	4.0	10.5	15.5	25.0	28.0	34.0	30.5	27.0
2	6.0	11.0	17.0	22.0	32.0	37.5	40.0	37.0
3	4.0	7.0	16.0	18.5	24.0	29.5	36.5	38.5
4	3.0	8.0	19.5	23.5	24.0	27.0	24.0	26.5
5	5.0	8.0	16.0	21.5	22.0	27.0	29.0	26.0
AVERAGE:	4.4	8.9	16.8	22.1	26.0	31.0	32.0	31.0
VARIANCE:	1.3	3.1	2.6	5.9	16.0	21.4	39.9	38.4
90%C.I.*:	0.8	1.2	1.1	1.7	2.7	3.2	4.3	4.2
VRM 160.0 - VRM 159.5								
1	6.0	12.0	20.5	27.0	28.0	26.5	39.5	37.0
2	5.5	9.0	10.5	23.5	28.5	31.0	29.5	37.5
3	19.0	20.0	22.0	25.5	31.5	36.0	32.0	31.5
4	5.5	10.0	11.5	21.0	30.0	33.5	33.5	32.0
5	10.0	13.0	21.5	30.5	41.0	45.5	45.0	44.0
AVERAGE:	9.2	12.8	17.2	25.5	31.8	34.5	35.9	36.4
VARIANCE:	33.6	18.7	32.5	12.9	28.3	50.1	39.4	25.7
90%C.I.*:	4.0	3.0	3.9	2.5	3.6	4.8	4.3	3.5

* +/- Confidence Interval for a 90% level of significance.

Table C.15 (cont'd). Field collected data and calculated average topographic shading angle for Southwest azimuths.

SAMPLE	240 (deg)	250 (deg)	260 (deg)	270 (deg)	280 (deg)	290 (deg)	300 (deg)	310 (deg)
	AZIMUTH							
VRM 159.5 - VRM 158.4								
1	10.0	14.0	22.0	24.0	27.5	35.5	38.0	41.5
2	7.0	16.5	20.0	25.0	26.5	29.5	33.0	37.5
3	6.0	3.5	9.5	16.5	21.5	23.5	26.0	31.0
4	8.5	4.5	10.0	11.0	17.0	23.5	23.0	27.0
5	3.0	7.0	14.0	17.0	21.0	24.0	31.5	31.0
AVERAGE:	6.9	9.1	15.1	18.7	22.7	27.2	30.3	33.6
VARIANCE:	7.1	33.9	32.6	33.7	18.6	28.0	35.0	33.7
90%C.I.*:	1.8	4.0	3.9	4.0	2.9	3.6	4.0	4.0
VRM 158.4 - VRM 157.3								
1	6.5	9.0	13.3	14.0	14.5	24.0	25.0	28.5
2	2.5	1.5	5.0	17.5	16.0	28.0	27.0	27.0
3	5.0	4.5	7.0	17.5	19.0	17.5	19.0	29.0
4	6.5	11.5	17.0	23.5	24.5	27.0	27.0	28.0
5	5.0	5.0	9.0	13.0	18.5	25.0	24.0	20.0
AVERAGE:	5.1	6.3	10.3	17.1	18.5	24.3	24.4	26.5
VARIANCE:	2.7	15.6	23.6	16.9	14.6	17.0	10.8	13.8
90%C.I.*:	1.1	2.7	3.3	2.8	2.6	2.8	2.2	2.5

* +/- Confidence Interval for a 90% level of significance.

Table C.16. Field collected data and calculated average vegetation shading angle for South azimuths.

SAMPLE	AZIMUTH 150 (deg)	160 (deg)	170 (deg)	180 (deg)	190 (deg)	200 (deg)	210 (deg)
VRM 163.1 - VRM 162.2							
1	62.0	55.5	58.5	38.0	40.0	36.5	36.0
2	38.0	34.5	42.5	51.5	58.0	58.5	52.0
3	29.0	30.5	35.5	30.0	35.5	41.0	40.0
4	25.0	35.0	25.0	0.0	25.0	23.5	19.0
5	48.0	44.5	44.0	41.5	41.0	44.0	43.5
AVERAGE:	40.4	40.0	41.1	32.2	39.9	40.7	38.1
VARIANCE:	224.3	101.5	150.9	383.6	142.6	160.3	148.8
90%C.I.*:	10.2	6.9	8.4	13.4	8.2	8.7	8.3
VRM 162.2 - VRM 161.5							
1	19.5	16.0	58.0	58.0	57.0	49.5	46.0
2	28.0	0.0	21.0	27.0	36.0	31.5	16.5
3	16.0	24.0	0.0	0.0	30.0	33.0	31.0
4	37.0	46.0	40.5	39.0	42.5	34.5	30.5
5	47.5	46.0	0.0	48.5	48.5	48.0	44.5
AVERAGE:	29.6	26.4	23.9	34.5	42.8	39.3	33.7
VARIANCE:	166.2	394.8	647.3	503.8	111.1	75.8	145.3
90%C.I.*:	8.8	13.6	17.4	15.4	7.2	6.0	8.2
VRM 161.5 - VRM 160.7							
1	32.0	26.5	26.0	25.5	20.5	27.0	27.5
2	22.0	25.0	25.5	19.5	13.0	6.5	0.0
3	17.0	29.0	20.5	19.0	21.0	16.0	17.0
4	24.0	22.0	26.0	22.0	25.5	26.5	26.5
5	12.5	4.0	7.0	7.0	19.0	16.5	31.5
AVERAGE:	21.5	21.3	21.0	18.6	19.8	18.5	20.5
VARIANCE:	54.5	100.0	66.6	48.7	20.3	72.6	159.6
90%C.I.*:	5.1	6.8	5.6	4.8	3.1	5.8	8.6
VRM 160.7 - VRM 160.0							
1	24.5	28.0	27.0	24.0	22.0	16.0	11.0
2	28.0	31.5	32.0	29.5	18.0	17.0	9.0
3	55.5	61.0	61.0	53.0	25.0	20.5	22.5
4	39.5	38.5	21.0	20.0	12.0	9.0	8.0
5	28.0	20.0	19.0	0.0	26.5	46.5	43.0
AVERAGE:	35.1	35.8	32.0	25.3	20.7	21.8	18.7
VARIANCE:	162.2	242.8	289.0	363.7	34.2	208.1	218.2
90%C.I.*:	8.7	10.7	11.6	13.0	4.0	9.9	10.1
VRM 160.0 - VRM 159.5							
1	28.5	29.5	28.0	20.0	21.0	21.5	15.0
2	30.5	27.0	25.0	25.0	17.0	17.0	18.0
3	17.5	17.5	15.5	15.5	0.0	0.0	0.0
4	0.0	14.0	3.5	25.5	0.0	17.0	16.5
5	24.0	34.0	34.0	32.0	29.5	45.0	44.0
AVERAGE:	20.1	24.4	21.2	23.6	13.5	20.1	18.7
VARIANCE:	151.2	70.2	142.6	38.7	172.3	261.3	252.2
90%C.I.*:	8.4	5.7	8.2	4.3	9.0	11.1	10.9

* +/- Confidence Interval for a 90% level of significance.

Table C.16 (cont'd). Field collected data and calculated average vegetation shading angle for South azimuths.

SAMPLE	150 (deg)	160 (deg)	170 (deg)	180 (deg)	190 (deg)	200 (deg)	210 (deg)
	AZIMUTH						
VRM 159.5 - VRM 158.4							
1	31.5	32.5	0.0	0.0	26.0	25.0	16.0
2	45.0	32.5	22.5	18.0	12.0	13.5	0.0
3	32.5	38.0	39.5	32.0	27.5	19.0	0.0
4	31.0	13.5	14.5	23.5	24.5	0.0	11.0
5	27.0	27.5	29.0	38.5	33.0	21.0	15.0
AVERAGE:	33.4	28.8	21.1	22.4	24.6	15.7	8.4
VARIANCE:	46.4	87.0	222.9	218.4	59.9	94.2	62.3
90%C.I.*:	4.7	6.4	10.2	10.1	5.3	6.6	5.4
VRM 158.4 - VRM 157.3							
1	18.0	17.0	13.0	8.5	7.0	5.5	0.0
2	35.5	36.5	31.5	22.0	27.5	20.5	15.0
3	31.0	20.0	35.0	20.5	19.5	26.0	23.5
4	21.5	17.5	22.0	19.5	22.0	24.0	15.5
5	39.0	27.0	0.0	23.0	0.0	0.0	13.0
AVERAGE:	29.0	23.6	20.3	18.7	15.2	15.2	13.4
VARIANCE:	80.9	67.9	202.5	34.3	128.6	136.8	72.2
90%C.I.*:	6.2	5.6	9.7	4.0	7.8	8.0	5.8

* +/- Confidence Interval for a 90% level of significance.

Table C.17. Field collected data and calculated average vegetation shading angle for Southwest azimuths.

	AZIMUTH							
SAMPLE	240 (deg)	250 (deg)	260 (deg)	270 (deg)	280 (deg)	290 (deg)	300 (deg)	310 (deg)
VRM 163.1 - VRM 162.2								
1	34.0	0.0	13.5	11.0	8.5	12.0	15.0	13.0
2	54.5	60.0	62.0	28.0	25.0	20.5	10.0	8.0
3	23.5	22.5	12.0	7.0	8.0	12.0	26.0	23.0
4	0.0	32.0	31.0	30.5	31.0	40.0	45.0	43.0
5	37.5	34.0	0.0	12.5	0.0	0.0	12.5	21.5
AVERAGE:	29.9	29.7	23.7	17.8	14.5	16.9	21.7	21.7
VARIANCE:	403.7	469.0	580.7	114.1	167.8	220.1	207.0	179.7
90%C.I.*:	13.7	14.8	16.5	7.3	8.9	10.2	9.8	9.2
VRM 162.2 - VRM 161.5								
1	36.5	5.0	19.5	29.5	26.0	0.0	27.0	43.0
2	10.0	19.5	20.0	13.5	19.0	0.0	38.5	44.5
3	23.0	19.0	13.0	9.5	0.0	13.5	17.5	6.0
4	32.0	30.0	18.0	17.5	18.5	13.5	17.0	19.5
5	29.0	18.0	15.5	10.5	20.0	19.0	21.0	20.0
AVERAGE:	26.1	18.3	17.2	16.1	16.7	9.2	24.2	26.6
VARIANCE:	105.1	79.0	8.6	65.8	96.2	75.6	79.8	276.9
90%C.I.*:	7.0	6.1	2.0	5.6	6.7	5.9	6.1	11.4
VRM 161.5 - VRM 160.7								
1	50.0	0.0	10.5	9.0	9.0	22.0	40.0	39.5
2	7.5	10.0	12.0	13.0	23.5	27.0	19.0	15.0
3	7.5	9.5	6.0	6.5	15.0	14.0	14.0	17.0
4	25.5	20.0	0.0	19.5	5.5	17.0	18.0	22.5
5		36.5	20.0	36.5	34.5	31.0	22.5	18.0
AVERAGE:	22.6	15.2	9.7	16.9	17.5	22.2	22.7	22.4
VARIANCE:	405.1	191.8	55.0	144.2	136.9	48.7	102.7	98.9
90%C.I.*:	16.5	9.5	5.1	8.2	8.0	4.8	6.9	6.8
VRM 160.7 - VRM 160.0								
1	5.0	4.0	4.0	9.5	14.5	18.0	19.0	31.0
2	4.0	13.0	18.5	18.5	16.0	15.0	10.5	8.0
3	7.0	7.0	14.0	22.0	13.0	13.0	16.5	20.5
4	10.5	16.5	33.5	34.0	21.5	0.0	0.0	0.0
5	6.5	12.0	12.0	0.0	0.0	14.0	23.0	23.5
AVERAGE:	6.6	10.5	16.4	16.8	13.0	12.0	13.8	16.6
VARIANCE:	6.2	24.8	118.9	165.3	63.1	48.5	80.1	154.9
90%C.I.*:	1.7	3.4	7.5	8.8	5.4	4.8	6.1	8.5
VRM 160.0 - VRM 159.5								
1	8.5	1.5	18.5	0.0	23.0	26.0	14.5	12.0
2	6.5	55.0	9.5	14.0	0.0	0.0	0.0	0.0
3	21.0	24.0	0.0	27.0	29.0	27.0	26.0	22.5
4	0.0	0.0	19.0	0.0	22.0	21.5	26.5	26.5
5	14.0	14.0	23.5	0.0	0.0	0.0	46.0	0.0
AVERAGE:	10.0	18.9	14.1	8.2	14.8	14.9	22.6	12.2
VARIANCE:	62.9	503.3	87.9	147.2	189.7	189.3	287.7	152.1
90%C.I.*:	5.4	15.4	6.4	8.3	9.4	9.4	11.6	8.4

* +/- Confidence Interval for a 90% level of significance.

Table C.17 (cont'd). Field collected data and calculated average vegetation shading angle for Southwest azimuths.

SAMPLE	240 (deg)	250 (deg)	260 (deg)	270 (deg)	280 (deg)	290 (deg)	300 (deg)	310 (deg)
	AZIMUTH							
VRM 159.5 - VRM 158.4								
1	11.0	6.5	8.5	0.0	29.5	33.5	34.5	35.0
2	0.0	0.0	21.0	27.0	29.5	30.0	29.5	29.5
3	4.5	7.5	17.5	19.0	22.0	24.0	26.5	0.0
4	13.0	22.5	24.5	26.0	14.0	25.5	22.5	23.5
5	4.5	3.0	15.0	18.0	0.0	0.0	0.0	0.0
AVERAGE:	6.6	7.9	17.3	18.0	19.0	22.6	22.6	17.6
VARIANCE:	28.2	75.4	37.1	117.5	153.9	173.7	178.8	274.7
90%C.I.*:	3.6	5.9	4.2	7.4	8.5	9.0	9.1	11.3
VRM 158.4 - VRM 157.3								
1	8.5	19.0	20.0	25.0	26.0	38.0	37.5	29.5
2	4.5	6.0	13.0	28.5	31.5	34.0	35.5	36.5
3	8.0	3.5	3.0	14.0	21.0	31.5	33.0	15.5
4	8.0	6.0	0.0	0.0	10.0	11.0	0.0	0.0
5	0.0	10.5	14.0	9.0	10.0	18.0	14.0	10.0
AVERAGE:	5.8	9.0	10.0	15.3	19.7	26.5	24.0	18.3
VARIANCE:	13.1	37.6	68.5	136.0	92.2	131.5	267.9	217.1
90%C.I.*:	2.5	4.2	5.7	8.0	6.6	7.8	11.2	10.1

* +/- Confidence Interval for a 90% level of significance.

Table C.18. Field collected data and calculated averages for characteristic shading.

NOTE: LEFT AND RIGHT SIDES OF STREAM ARE DEFINED FACING DOWNSTREAM.

SITE	HILLSLOPE ANGLE LEFT (deg)	HILLSLOPE ANGLE RIGHT (deg)	PERPENDICULAR FOREST ANGLE LEFT (deg)	PERPENDICULAR FOREST ANGLE RIGHT (deg)	BUFFER WIDTH LEFT (ft)	BUFFER WIDTH RIGHT (ft)	OVERHANG VEGE. (%)	CANOPY COVER COEFFICIENT LEFT	CANOPY COVER COEFFICIENT RIGHT
VRM 163.1 - VRM 162.2									
1	38.0	37.0	53.5	28.0	-1	-1	0.0	0.30	0.30
2	44.0	27.5	57.0	31.0	-1	-1	0.0	0.40	0.30
3	40.0	39.0	35.5	25.0	-1	20	0.0	0.50	0.50
4	40.5	36.0	24.0	57.5	20	-1	0.0	0.40	0.65
5	47.0	25.0	43.5	28.0	-1	-1	0.0	0.50	0.50
AVERAGE:	41.9	32.9	42.7	33.9			0.00	0.42	0.45
VARIANCE:	12.8	38.8	180.8	178.6			0.00	0.01	0.02
90%C.I.*:	2.5	4.3	9.2	9.2			0.00	0.06	0.10
VRM 162.2 - VRM 161.5									
1	21.0	37.5	25.0	41.5	-1	-1	7.9	0.50	0.60
2	0.0	25.0	47.0	48.5	30	40	0.0	0.60	0.50
3	39.0	0.0	33.0	36.0	25	30	0.0	0.30	0.40
4	32.0	0.0	42.0	27.0	-1	30	0.0	0.40	0.30
5	47.5	0.0	47.5	28.0	-1	-1	0.0	0.60	0.50
AVERAGE:	27.9	12.5	38.9	36.2			1.58	0.48	0.46
VARIANCE:	337.6	312.5	94.3	82.8			12.47	0.02	0.01
90%C.I.*:	12.6	12.1	6.7	6.2			2.42	0.09	0.08
VRM 161.5 - VRM 160.7									
1	0.0	0.0	35.0	35.0	-1	30	16.3	0.60	0.40
2	0.0	0.0	34.0	29.0	-1	-1	0.0	0.50	0.40
3	0.0	0.0	19.0	41.0	-1	-1	0.0	0.60	0.10
4	0.0	0.0	27.0	28.5	-1	-1	0.0	0.50	
5	0.0	0.0	30.5	37.0	-1	-1	0.0	0.70	0.50
AVERAGE:	0.0	0.0	29.1	34.1			3.26	0.58	0.35
VARIANCE:	0.0	0.0	41.8	28.6			53.14	0.01	0.03
90%C.I.*:	0.0	0.0	4.4	3.7			5.00	0.06	0.14
VRM 160.7 - VRM 160.0									
1	0.0	0.0	27.5	37.0	-1	-1	3.6	0.60	0.60
2	0.0	0.0	34.0	23.5	-1	-1	0.0	0.40	0.60
3	0.0	0.0	33.0	21.0	-1	-1	0.0	0.40	0.70
4	0.0	0.0	40.0	36.0	20	20	0.0	0.60	0.60
5	0.0	0.0	50.0	32.0	30	30	0.0	0.50	0.60
AVERAGE:	0.0	0.0	36.9	29.9			0.73	0.50	0.62
VARIANCE:	0.0	0.0	73.3	53.1			2.64	0.01	0.00
90%C.I.*:	0.0	0.0	5.9	5.0			1.11	0.07	0.03
VRM 160.0 - VRM 159.5									
1	0.0	0.0	20.0	45.5	30	20	4.7	0.60	0.30
2	0.0	35.0	32.0	31.5	-1	15	0.0	0.60	0.70
3	0.0	11.0	23.0	33.5	15	20	0.0	0.40	0.40
4	38.0	0.0	40.0	28.0	-1	20	0.0	0.60	0.60
5	0.0	10.0	34.5	40.5	30	-1	0.0	0.60	0.60
AVERAGE:	7.6	11.2	29.9	35.8			0.93	0.56	0.52
VARIANCE:	288.8	204.7	68.3	50.2			4.33	0.01	0.03
90%C.I.*:	11.7	9.8	5.7	4.9			1.43	0.06	0.11

* +\- Confidence Interval for a 90% level of significance

Table C.18 (cont'd). Field collected data and calculated averages for characteristic shading.

NOTE: LEFT AND RIGHT SIDES OF STREAM ARE DEFINED FACING DOWNSTREAM.

SITE	HILLSLOPE ANGLE LEFT (deg)	HILLSLOPE ANGLE RIGHT (deg)	PERPENDICULAR FOREST ANGLE LEFT (deg)	PERPENDICULAR FOREST ANGLE RIGHT (deg)	BUFFER WIDTH LEFT (ft)	BUFFER WIDTH RIGHT (ft)	OVERHANG VEGE. (%)	CANOPY COVER COEFFICIENT LEFT	CANOPY COVER COEFFICIENT RIGHT
VRM 159.5 - VRM 158.4									
1	41.0	30.0	37.0	33.5	30	-1	0.6	0.50	0.40
2	0.0	30.0	28.5	43.5	30	-1	0.0	0.60	0.50
3	0.0	30.0	47.5	34.0	30	-1	0.0	0.75	0.40
4	0.0	0.0	30.5	46.0	30	30	8.0	0.70	0.40
5	0.0	30.0	37.0	40.5	25	-1	0.0	0.70	0.60
AVERAGE:	8.2	24.0	36.1	39.5			1.72	0.65	0.46
VARIANCE:	336.2	180.0	55.2	31.4			12.39	0.01	0.01
90%C.I.*:	12.6	9.2	5.1	3.8			2.41	0.07	0.06
VRM 158.4 - VRM 157.3									
1	0.0	0.0	14.4	30.0	30	40	0.0	0.50	0.60
2	0.0	0.0	33.0	36.0	40	30	7.7	0.40	0.80
3	31.0	0.0	40.0	33.5	25	30	0.0	0.60	0.60
4	0.0	0.0	19.0	58.0	30	30	0.0	0.70	0.60
5	0.0	0.0	31.5	19.5	20	30	0.0	0.60	0.55
AVERAGE:	6.2	0.0	27.6	35.4			1.54	0.56	0.63
VARIANCE:	192.2	0.0	111.6	199.2			11.83	0.01	0.01
90%C.I.*:	9.5	0.0	7.2	9.7			2.36	0.08	0.07

* +\- Confidence Interval for a 90% level of significance

Table C.19. Field collected data and computations for tree height.

	RIGHT - FACING UPSTREAM					LEFT - FACING UPSTREAM				
SAMPLE	DIST ft	ANGLE deg	CONSTANT	TREE HT ft	TREE HT m	DIST ft	ANGLE deg	CONSTANT	TREE HT ft	TREE HT m
VRM 163.1 - VRM 162.2										
1	32	38.0	5.15	30.2	9.2	25	43.0	5.15	28.5	8.7
2	25	48.5	5.15	33.4	10.2	18	43.0	5.15	21.9	6.7
3	24	46.0	5.15	30.0	9.1	17	20.0	5.15	11.3	3.5
4	17	44.5	5.15	21.9	6.7				25.0	7.6 **
5	13	37.5	5.15	15.1	4.6	25	28.5	5.15	18.7	5.7
AVERAGE:				26.1	8.0				21.1	6.4
VARIANCE:				55.9	5.2				42.8	4.0
90%C.I.*:				5.1	1.6				4.8	1.5
** TREE HEIGHT WAS ESTIMATED BY EYE										
VRM 162.2 - VRM 161.5										
1	70	47.0	5.15	80.2	24.4	20	29.0	5.15	16.2	4.9
2	42	24.5	5.15	24.3	7.4	29	33.0	5.15	24.0	7.3
3	35	26.5	5.15	22.6	6.9	42	24.0	5.15	23.8	7.3
4	38	34.0	5.15	30.8	9.4	25	21.5	5.15	15.0	4.6
5	28	9.5	5.15	9.8	3.0	28	38.0	5.15	27.0	8.2
AVERAGE:				33.5	10.2				21.2	6.5
VARIANCE:				369.2	68.6				28.0	2.6
90%C.I.*:				13.1	5.7				3.6	1.1
VRM 161.5 - VRM 160.7										
1	38	39.0	5.15	35.9	10.9	35	45.0	5.15	40.2	12.2
2	21	34.5	5.15	19.6	6.0	27	45.0	5.15	32.2	9.8
3	24	34.5	5.15	21.6	6.6	46	51.0	5.15	62.0	18.9
4	21	31.0	5.15	17.8	5.4	25	41.0	5.15	26.9	8.2
5	22	44.0	5.15	26.4	8.0	33	52.0	5.15	47.4	14.4
AVERAGE:				24.3	7.4				41.7	12.7
VARIANCE:				52.9	4.9				189.0	17.6
90%C.I.*:				3.5	1.1				9.4	2.9
VRM 160.7 - VRM 160.0										
1	33	31.0	5.15	25.0	7.6	12	30.0	5.15	12.1	3.7
2	43	55.5	5.15	67.7	20.6	39	40.5	5.15	38.5	11.7
3	57	39.5	5.15	52.1	15.9	25	31.0	5.15	20.2	6.1
4	22	49.0	5.15	30.5	9.3	28	26.5	5.15	19.1	5.8
5	50	30.5	5.15	34.6	10.5	43	27.0	5.15	27.1	8.2
AVERAGE:				42.0	12.8				23.4	7.1
VARIANCE:				310.4	28.8				99.3	9.2
90%C.I.*:				12.1	3.7				6.8	2.1
VRM 160.0 - VRM 159.5										
1	24	37.0	5.15	23.2	7.1	20	49.5	5.15	28.6	8.7
2	20	36.0	5.15	19.7	6.0	28	32.0	5.15	22.6	6.9
3	36	37.0	5.15	27.1	8.3	26	35.0	5.15	23.4	7.1
4	17	24.5	5.15	12.9	3.9	37	48.0	5.15	46.2	14.1
5	40	34.5	5.15	32.6	9.9	28	24.5	5.15	17.9	5.5
AVERAGE:				23.1	7.0				27.7	8.5
VARIANCE:				55.8	5.2				121.2	11.3
90%C.I.*:				5.1	1.6				7.5	2.3

* +/- Confidence Interval for a 90% level of significance.

Table C.19 (cont'd). Field collected data and computations for tree height.

SAMPLE	RIGHT - FACING UPSTREAM DIST ft	ANGLE deg	CONSTANT	TREE HT ft	TREE HT m	LEFT - FACING UPSTREAM DIST ft	ANGLE deg	CONSTANT	TREE HT ft	TREE HT m
VRM 159.5 - VRM 158.4										
1	32	46.0	5.15	38.3	11.7	31	25.5	5.15	19.9	6.1
2	35	48.0	5.15	41.4	12.6	23	26.0	5.15	16.4	5.0
3	35	26.5	5.15	22.6	6.9	24	10.0	5.15	9.4	2.9
4	44	43.5	5.15	46.9	14.3	20	45.0	5.15	25.2	7.7
5	43	28.5	5.15	28.5	8.7	21	12.0	5.15	9.6	2.9
AVERAGE:				35.5	10.8				16.1	4.9
VARIANCE:				96.9	9.0				46.0	4.3
90%C.I.*:				6.7	2.1				4.6	1.4
VRM 158.4 - VRM 157.3										
1	30	22.0	5.15	17.3	5.3	17	27.5	5.15	14.0	4.3
2	65	33.0	5.15	47.4	14.4	35	33.0	5.15	27.9	8.5
3	24	33.5	5.15	15.9	4.8	23	18.5	5.15	12.8	3.9
4	50	32.5	5.15	33.4	10.2	42	33.0	5.15	32.4	9.9
5	23	40.5	5.15	24.8	7.6	33	26.5	5.15	21.6	6.6
AVERAGE:				27.7	8.5				21.8	6.6
VARIANCE:				168.8	15.7				72.7	6.8
90%C.I.*:				8.9	2.7				5.8	1.8

* +/- Confidence Interval for a 90% level of significance.

Table C.20. Width measurements at designated cross sections within the study reach.

CROSS-SECTION	6-4-88 WIDTH FT	6-24-88 WIDTH FT	6-30-88 WIDTH FT	7-9-88 WIDTH FT	7-15-88 WIDTH FT	7-23-88 WIDTH FT	AVERAGE
VRM 163.1 - VRM 162.2							
SECTION #1							
450					24.5		24.5
400					18.0		18.0
350					20.0		20.0
300		17.5	18.0		17.0		17.5
250		30.0	24.5		24.5		26.3
200	22.0	22.5	21.0	19.0			21.1
150	23.5		20.5	23.0			22.3
100	35.0	33.5	33.0	32.5			33.5
50	29.5		30.0				29.8
0	23.5	23.5	19.0	23.0			22.3
PROFILE				25.0			25.0
SECTION #2							
E					18.0		18.0
D					20.0		20.0
C					14.0		14.0
B					24.0		24.0
A					21.0		21.0
0	28.0	26.5	26.5		26.0		26.8
25	27.0	17.0	20.5		18.0		20.6
70	10.5		12.5		13.0		12.0
115	14.0	13.0	15.5		13.5		14.0
165	18.5	19.0	18.5		19.0		18.8
230		16.0	18.5		18.5		17.7
280		23.0	23.0		23.0		23.0
VRM 162.2 - VRM 160.0							
SECTION #1							
0	30.5	28.0	29.0	28.5			29.0
100	34.5	35.0	34.0	33.0			34.1
200	24.5	24.5	24.5	24.0			24.4
300	28.0	26.5	26.5	27.0			27.0
400	25.5	29.5	29.0	28.5			28.1
500		26.0	25.5	25.5			25.7
PROFILE				28.5			28.5
SECTION #2							
0	33.0	29.5	28.0			28.0	29.6
100	27.0	27.0	25.5	24.5		24.5	25.7
200	25.0	25.0	23.5	23.5		23.5	24.1
300	21.0	23.0	21.5	21.0			21.6
400		25.0	24.5	23.5		24.0	24.3
500		24.5	24.0	23.5			24.0
PROFILE				32.0			32.0
SECTION #3							
0	32.0	31.0	32.0	32.1			31.8
100	21.0	20.0	19.0	18.5		18.5	19.4
200	26.5	26.5	25.5	26.0			26.1
300	30.0	29.0	26.5	29.0		28.0	28.5
400		22.0	24.0	25.0		25.0	24.0
500		29.5	29.5	31.5		31.5	30.5
PROFILE				25.5			25.5

Table C.20 (cont'd). Width measurements at designated cross sections within the study reach.

CROSS-SECTION	6-4-88 WIDTH FT	6-24-88 WIDTH FT	6-30-88 WIDTH FT	7-9-88 WIDTH FT	7-15-88 WIDTH FT	7-23-88 WIDTH FT	AVERAGE
VRM 160.0 - VRM 159.5							
SECTION #1							
C					22.0	21.0	21.5
B					17.5	18.0	17.8
A					28.5	28.0	28.3
0	30.0	28.5	26.5	26.0		26.0	27.4
100	26.0	26.0	24.5			25.5	25.5
200	22.0	23.0	22.5	22.5			22.5
300	32.0		31.5			30.5	31.3
400		22.0	23.5	21.5		22.0	22.3
500						25.5	25.5
PROFILE				23.0			23.0
VRM 159.5 - VRM 157.3							
SECTION #1							
0	36.0	35.5	35.0		34.5		35.3
100	30.0	30.0	28.5		28.5		29.3
200	21.5		25.0		22.5	26.0	23.8
300	32.5	31.5	32.0		27.5		30.9
400	40.0	40.5	38.5		39.5		39.6
500		44.0	43.0		43.5	42.0	43.1
600					31.0		31.0
700					32.5	32.0	32.3
A					36.5		36.5
B					28.0		28.0
PROFILE						25.4	25.4
SECTION #2							
0		26.5	26.5		26.0		26.3
100		23.5	24.0		24.0		23.8
200		23.0	23.5		23.0		23.2
300		24.5	24.0		24.0		24.2
400		22.0	21.0		21.5		21.5
500		25.5	25.0		25.0		25.2
A					24.0		24.0
B					16.5		16.5
600					25.5	26.0	25.8
700					29.5		29.5
PROFILE						24.6	24.6

Table C.21. Calculated percentage of streambed for each section comprised of depth less than twenty centimeters and bedrock greater than twenty-five centimeters in axis.

VRM 163.1 - VRM 162.2

CROSS-SECTION	AVERAGE WIDTH FT	LENGTH OF BDRCK FT	BEDROCK %
450	24.5	0.0	0.0
400	18.0	0.0	0.0
350	20.0	0.5	2.5
300	17.5	0.0	0.0
250	26.3	3.0	11.4
200	21.1	3.0	14.2
150	22.3	3.0	13.4
100	33.5	0.0	0.0
50	29.8	4.5	15.1
0	22.3	0.0	0.0
E	18.0	0.0	0.0
D	20.0	1.0	5.0
C	14.0	0.0	0.0
B	24.0	0.0	0.0
A	21.0	0.0	0.0
0	26.8	0.0	0.0
25	20.6	0.0	0.0
70	12.0	0.0	0.0
115	14.0	0.0	0.0
165	18.8	0.0	0.0
230	17.7	0.0	0.0
280	23.0	0.0	0.0
COUNT			22
AVERAGE			2.8

VRM 160.0 - VRM 159.5

CROSS-SECTION	AVERAGE WIDTH FT	LENGTH OF BDRCK FT	BEDROCK %
C	21.5	7.0	32.6
B	17.8	0.0	0.0
A	28.3	1.5	5.3
0	27.4	0.0	0.0
100	25.5	4.0	15.7
200	22.5	3.0	13.3
300	31.3	8.0	25.5
400	22.3	0.5	2.2
500	25.5	5.0	19.6
COUNT			9.0
AVERAGE			12.7

VRM 162.2 - VRM 160.0

CROSS-SECTION	AVERAGE WIDTH FT	LENGTH OF BDRCK FT	BEDROCK %
0	29.0	1.0	3.4
100	34.1	0.0	0.0
200	24.4	1.0	4.1
300	27.0	1.0	3.7
400	28.1	7.0	24.9
500	25.7	2.5	9.7
0	29.6	2.0	6.8
100	25.7	0.0	0.0
200	24.1	3.0	12.4
300	21.6	1.0	4.6
400	24.3	1.5	6.2
500	24.0	0.5	2.1
0	31.8	2.5	7.9
100	19.4	1.5	7.7
200	26.1	1.5	5.7
300	28.5	0.0	0.0
400	24.0	0.0	0.0
500	30.5	2.5	8.2
COUNT			18.0
AVERAGE			6.0

VRM 159.5 - VRM 157.3

CROSS-SECTION	AVERAGE WIDTH FT	LENGTH OF BDRCK FT	BEDROCK %
0	35.3	6.0	17.0
100	29.3	1.5	5.1
200	23.8	2.0	8.4
300	30.9	3.0	9.7
400	39.6	2.5	6.3
500	43.1	4.0	9.3
600	31.0	3.0	9.7
700	32.3	6.0	18.6
A	36.5	4.0	11.0
B	28.0	4.0	14.3
0	26.3	1.5	5.7
100	23.8	4.5	18.9
200	23.2	1.0	4.3
300	24.2	0.0	0.0
400	21.5	0.0	0.0
500	25.2	0.0	0.0
A	24.0	1.0	4.2
B	16.5	3.0	18.2
600	25.8	0.0	0.0
700	29.5	0.0	0.0
COUNT			20.0
AVERAGE			8.0

Table C.22. Travel time (seconds) and calculated velocity through designated float sections.

		FLOAT #	6-24-88 seconds	6-30-88 seconds	7-15-88 seconds
VRM 163.1 - VRM 162.2					
FLOAT SECTION #1 LENGTH: 205 FT		1	-	75	86
		2	62	74	68
		3	-	60	65
		4	86	72	68
		5	89	61	92
		6	-	62	87
	VELOCITY:		2.59	3.04	2.64
FLOAT SECTION #2 LENGTH: 165 FT		1	91	65	62
		2	72	66	74
		3	70	50	67
		4	55	60	59
		5	53	64	67
		6	-	-	73
	VELOCITY:		2.42	2.70	2.46
VRM 162.2 - VRM 160.0					
FLOAT SECTION #1 LENGTH: 392 FT		1	143	131	131
		2	130	122	143
		3	-	126	120
		4	121	115	118
		5	127	152	120
		6	117	176	130
	VELOCITY:		3.07	2.86	3.09
FLOAT SECTION #2 LENGTH: 500 FT		1	170	143	171
		2	170	126	170
		3	153	161	180
		4	170	149	184
		5	198	164	178
		6	170	242	114
	VELOCITY:		2.91	3.05	3.01
FLOAT SECTION #3 LENGTH: 268 FT		1	76	77	127
		2	91	76	83
		3	85	102	101
		4	77	95	87
		5	115	98	79
		6	-	107	92
	VELOCITY:		3.02	2.90	2.83
VRM 160.0 - VRM 159.5					
FLOAT SECTION #1 LENGTH: 309 FT		1	108	93	105
		2	136	114	99
		3	94	118	104
		4	99	109	110
		5	93	111	96
		6	97	156	70
	VELOCITY:		2.96	2.64	3.17

Table C.22 (cont'd). Travel time (seconds) and calculated velocity through designated float sections.

	FLOAT #	6-24-88 seconds	6-30-88 seconds	7-15-88 seconds
VRM 159.5 - VRM 157.3				
FLOAT SECTION #1	1	-	145	150
LENGTH: 412 FT	2	-	180	131
	3	135	148	132
	4	135	142	129
	5	153	149	165
	6	-	167	137
VELOCITY:		2.92	2.66	2.93
FLOAT SECTION #2	1	155	271	191
LENGTH: 500 FT	2	153	169	193
	3	125	138	155
	4	123	157	180
	5	133	147	164
	6	143	177	169
VELOCITY:		3.61	2.83	2.85

Table C.23. Relative humidity values measured by Zion National Park.

DATE	ZION REL HUM AVERAGE %	ZION REL HUM 1400 %
6-1-88	36	20
6-2-88	32	21
6-3-88	32	18
6-4-88	32	8
6-5-88	22	11
6-6-88	22	11
6-7-88	28	12
6-8-88	20	9
6-9-88	14	7
6-10-88	20	10
6-11-88	19	10
6-12-88	27	18
6-13-88	35	18
6-14-88	20	12
6-15-88	21	13
6-16-88	19	10
6-17-88	53	44
6-18-88	40	24
6-19-88	47	35
6-20-88	36	23
6-21-88	39	26
6-22-88	46	28
6-23-88	22	14
6-24-88	30	18
6-25-88	42	36
6-26-88	38	20
6-27-88	44	24
6-28-88	30	21
6-30-88	28	18
7-1-88	13	8
7-2-88	28	16
7-3-88	16	34
7-4-88	25	17
7-5-88	38	23
7-6-88	24	15
7-7-88	20	15
7-8-88	28	16
7-9-88	22	11
7-10-88	27	16
7-11-88	30	22
7-12-88	20	13
7-13-88	13	8
7-14-88	20	10
7-15-88	17	11
7-16-88	25	13
7-17-88	17	11
7-18-88	18	10
7-19-88	13	9
7-20-88	19	11
7-21-88	28	20
7-22-88	29	19
7-23-88	23	18
7-24-88	26	15
7-25-88	26	15
7-26-88	26	16
7-27-88	75	67
7-28-88	54	36
7-29-88	40	26
7-30-88	26	18
7-31-88	52	32

Table C.24. Official state of the weather, windspeed, and wind direction data collected at Zion National Park weather station.

DATE	STATE OF THE WTHR	WIND SPD mph	WIND DIRECTION
6-1-88	0	3	S
6-2-88	1	3	NE
6-3-88	0	3	SW
6-4-88	0	10	SW
6-5-88	1	8	S
6-6-88	0	10	S
6-7-88	0	3	SW
6-8-88	0	3	E
6-9-88	0	5	S
6-10-88	0	8	SW
6-11-88	1	5	S
6-12-88	2	3	N
6-13-88	1	3	SW
6-14-88	1	4	W
6-15-88	0	2	NW
6-16-88	2	3	NE
6-17-88	3	4	NE
6-18-88	1	0	0
6-19-88	1	5	NE
6-20-99	2	3	NE
6-21-88	2	5	NW
6-22-88	1	1	N
6-23-88	1	1	S
6-24-88	1	1	S
6-25-88	3	7	N
6-26-88	1	8	N
6-27-88	1	5	SW
6-28-88	2	2	S
6-29-88			
6-30-88	1	2	S

DATE	STATE OF THE WTHR	WIND SPD mph	WIND DIRECTION
7-1-88	1	2	S
7-2-88	1	2	SW
7-3-88	2	0	0
7-4-88	1	7	S
7-5-88	2	8	S
7-6-88	2	15	SW
7-8-88	0	4	S
7-9-88	1	2	SW
7-10-88	1	4	S
7-11-88	0	3	S
7-12-88	0	7	S
7-13-88	0	2	SW
7-14-88	0	3	S
7-15-88	0	5	S
7-16-88	0	3	S
7-17-88	0	5	SW
7-18-88	1	5	SW
7-19-88	0	4	SW
7-20-88	0	2	S
7-21-88	0	8	NW
7-22-88	0	3	E
7-23-88	1	4	SE
7-24-88	1	8	S
7-25-88	1	6	SE
7-26-88	1	2	SE
7-27-88	2	3	S
7-28-88	3	4	N
7-29-88	2	10	SW

STATE OF THE WEATHER CODE:

0 Clear (less than 1/10th of sky cloud covered)
1 Scattered clouds (1/10 to 5/10 cloud covered)
2 Broken clouds (6/10 to 9/10 could covered)
3 Overcast (more than 9/10 of sky cloud covered)
4 Foggy
5 Drizzling
6 Raining
7 Snowing or sleeting
8 Showering (showers in sight or occurring at station)
9 Thunderstorm in progress (lightening seen or thunder heard)

Table C.25. Channel profiles of cross sections #1 and #2.

A relative benchmark was established at 100 ft.

----- CROSS SECTION #1 ------
VRM 157.3 - VRM 158.4

BACKSIGHT: 10.89 ft
INSTRUMENT HEIGHT: 110.89 ft

STATION	FORE-SIGHT	ELEVATION (ft)	
-0.7	4.1	106.8	
0.0	4.5	106.4	
1.3	5.6	105.3	
5.1	6.3	104.6	
7.1	7.7	103.2	
12.2	8.4	102.5	
15.9	8.7	102.2	
16.7	8.9	102.0	
18.7	9.4	101.5	
20.9	10.4	100.5	
21.6	10.9	100.0	
21.9	11.1	99.8	LEW
22.2	11.6	99.3	
24.5	11.7	99.2	
27.3	11.6	99.3	
30.0	11.6	99.3	
32.0	11.8	99.1	
35.0	11.8	99.1	
37.6	11.8	99.1	
40.0	11.9	99.0	
42.3	11.9	99.0	
44.4	11.9	99.0	
46.1	11.7	99.2	
46.5	11.1	99.8	REW
47.8	10.6	100.3	
50.6	9.8	101.1	
51.6	9.0	101.9	
53.0	9.0	101.9	
55.0	8.3	102.6	
57.3	8.0	102.9	
59.5	6.3	104.6	
61.4	5.9	105.0	
65.3	5.7	105.2	
66.8	5.2	105.7	

----- CROSS SECTION #2 ------
VRM 158.4 - VRM 159.5

BACKSIGHT: 12.1 ft
INSTRUMENT HEIGHT: 112.1 ft

STATION	FORE-SIGHT	ELEVATION (ft)	
-0.7	8.1	104.0	
1.0	8.2	103.9	
2.4	9.1	103.0	
7.7	10.4	101.7	
9.2	10.6	101.5	
10.3	10.9	101.2	
10.9	11.2	100.9	
13.1	11.8	100.3	
15.5	11.9	100.2	
18.5	12.4	99.7	
19.3	12.3	99.8	
22.0	12.2	99.9	
26.9	12.8	99.3	LEW
28.8	13.1	99.0	
30.1	13.2	98.9	
31.3	13.4	98.7	
33.7	13.5	98.6	
34.8	13.5	98.6	
36.9	13.5	98.6	
39.0	13.7	98.4	
42.1	13.5	98.6	
45.0	13.6	98.5	
47.5	13.6	98.5	
48.4	13.3	98.8	
48.6	13.6	98.5	
50.7	13.6	98.5	
51.9	13.5	98.6	
52.3	12.8	99.3	REW
53.2	12.1	100.0	
54.9	11.6	100.5	
55.7	11.1	101.0	
58.2	10.2	101.9	
61.0	9.4	102.7	
63.9	7.8	104.3	

Table C.26. Channel profiles of cross sections #3 and #4.

A relative benchmark was established at 100 ft.

----- CROSS SECTION #3 ------
VRM 159.5 - VRM 160.0

BACKSIGHT: 12.17 ft
INSTRUMENT HEIGHT: 112.17 ft

STATION	FORE-SIGHT	ELEVATION (ft)	
0.0	4.9	107.3	
5.0	5.7	106.5	
7.0	6.4	105.8	
8.0	9.6	102.6	
11.0	10.8	101.4	
13.5	11.0	101.2	
15.5	10.6	101.6	
19.3	11.7	100.5	
21.2	11.7	100.5	
23.5	11.9	100.3	
23.7	13.9	98.3	
24.2	14.1	98.1	LEW
25.4	14.6	97.6	
27.0	15.1	97.1	
29.0	15.1	97.1	
31.0	15.3	96.9	
32.2	15.4	96.8	
34.5	15.4	96.8	
36.0	15.3	96.9	
37.0	15.3	96.9	
38.0	15.1	97.1	
39.0	15.2	97.0	
43.0	14.7	97.5	
45.5	14.5	97.7	
47.2	14.0	98.2	REW
50.5	13.1	99.1	
63.1	13.0	99.2	
64.5	12.4	99.8	
65.3	11.2	101.0	
66.4	11.5	100.7	
66.5	9.6	102.6	
69.0	9.0	103.2	
71.5	8.1	104.1	
72.3	6.7	105.5	
76.2	5.7	106.5	
77.6	5.0	107.2	

----- CROSS SECTION #4 ------
VRM 160.0 - VRM 160.7

BACKSIGHT: 10.19 ft
INSTRUMENT HEIGHT: 110.19 ft

STATION	FORE-SIGHT	ELEVATION (ft)	
80.3	3.8	106.4	
76.5	4.1	106.1	
72.7	5.7	104.5	
69.9	6.0	104.2	
68.9	6.5	103.7	
67.9	7.3	102.9	
66.0	7.7	102.5	
62.1	7.9	102.3	
61.0	8.2	102.0	
58.2	8.5	101.7	
52.0	9.2	101.0	
50.0	10.0	100.2	
48.5	11.1	99.1	LEW
48.0	12.1	98.1	
45.0	12.1	98.1	
41.0	11.9	98.3	
38.0	11.9	98.3	
35.0	12.0	98.2	
32.0	11.9	98.3	
29.0	11.8	98.4	
26.0	11.6	98.6	
23.2	11.2	99.0	REW
22.1	10.3	99.9	
21.3	9.6	100.6	
19.6	9.2	101.0	
12.7	5.7	104.5	
10.0	5.1	105.1	
6.8	4.5	105.7	
4.5	3.6	106.6	
0.0	3.0	107.2	

Table C.27. Channel Profile of cross section #5, #6, and #7.

A relative benchmark was established at 100 ft.

----- Cross Section #5 ------
VRM 160.7 - VRM 161.5

BACKSIGHT: 11.1 ft
INSTRUMENT HEIGHT: 111.1 ft

STATION	FORE-SIGHT	ELEVATION (ft)	
0	6.1	105.0	
1.7	6.5	104.6	
4.3	7.9	103.2	
5.5	8.9	102.2	
9.0	10.0	101.1	
10.0	10.7	100.4	
10.5	10.9	100.2	
12.3	11.3	99.8	
13.5	11.9	99.2	LEW
13.7	12.6	98.5	
14.5	12.7	98.4	
16.0	12.8	98.3	
18.0	12.8	98.3	
20.0	12.6	98.5	
22.0	12.6	98.5	
25.0	12.5	98.6	
28.0	12.5	98.6	
31.0	12.5	98.6	
34.0	12.4	98.7	
37.0	12.3	98.8	
40.0	12.4	98.7	
42.0	12.5	98.6	
43.1	12.4	98.7	
45.2	11.9	99.2	REW
46.2	11.4	99.7	
47.0	9.9	101.2	
48.9	8.5	102.6	
50.3	6.3	104.8	
52.5	4.9	106.2	

----- Cross Section #6 ------
VRM 161.5 - VRM 162.2

BACKSIGHT: 6.12 ft
INSTRUMENT HEIGHT: 106.12 ft

STATION	FORE-SIGHT	ELEVATION (ft)	
0	5.1	101.0	
4.0	5.6	100.5	
8.6	6.5	99.6	
11.0	7.6	98.5	
14.0	8.2	97.9	
16.6	9.2	96.9	
17.8	9.7	96.4	
18.2	10.2	95.9	
18.9	10.3	95.8	
22.0	11.2	94.9	LEW
22.8	11.3	94.8	
24.1	11.6	94.5	
24.8	11.5	94.6	
25.0	11.8	94.3	
26.8	12.0	94.1	
30.0	11.9	94.2	
34.0	11.9	94.2	
38.0	12.0	94.1	
41.0	11.9	94.2	
44.0	11.8	94.3	
47.0	11.5	94.6	
49.0	11.5	94.6	
50.3	11.1	95.0	REW
50.5	10.7	95.4	
53.8	10.0	96.1	
55.2	9.2	96.9	
56.8	8.8	97.3	
57.7	8.2	97.9	
59.0	7.9	98.2	
60.2	6.9	99.2	
63.4	6.5	99.6	
65.4	6.0	100.1	
68.0	5.2	100.9	

----- Cross Section #7 ------
VRM 162.2 - VRM 163.1

BACKSIGHT: 11.04 ft
INSTRUMENT HEIGHT: 111.04 ft

STATION	FORE-SIGHT	ELEVATION (ft)	
0			
0.5	0.3	110.74	
4.0	4.9	106.14	
5.4	5.6	105.44	
6.0	6.8	104.24	
7.7	7.2	103.84	
8.5	7.8	103.24	
10.0	8.7	102.34	
14.2	8.8	102.24	
14.9	9.6	101.44	
16.9	10.0	101.04	
18.0	10.5	100.54	
22.3	11.0	100.04	
24.2	11.4	99.64	
27.3	12.0	99.04	LEW
28.8	12.2	98.84	
34.5	13.2	97.84	
38.2	12.9	98.14	
39.0	13.0	98.04	
41.1	12.9	98.14	
44.0	12.9	98.14	
46.4	13.1	97.94	
49.0	12.8	98.24	
51.3	12.2	98.84	
53.7	11.8	99.24	REW
54.5	11.6	99.44	
56.7	11.1	99.94	
57.0	6.8	104.24	
58.0	6.6	104.44	
60.0	6.2	104.84	
63.0	3.6	107.44	
65.0	2.2	108.84	
66.5	1.4	109.64	

Table C.28 Survey of water surface elevations upstream and downstream of cross section #1 through #7 along the study reach.

TRANSECT	THALWEG FORE-SIGHT	LEW FORE-SIGHT	REW FORE-SIGHT	AVERAGE FORE-SIGHT	ELEVATION (ft)
CROSS SECTION #1: VRM 157.3 - VRM 158.4					
BACKSIGHT:		7.25 ft			
INSTRUMENT HEIGHT:		107.25 ft			
1.00	7.69*	7.69*	7.65	7.69	99.56
2.00	7.42	7.43	7.43	7.43	99.82
3.00	7.34	7.34	7.34	7.34	99.91
CROSS SECTION #2: VRM 158.4 - VRM 159.5					
BACKSIGHT:		5.49 ft			
INSTRUMENT HEIGHT:		105.49 ft			
1.00	6.27	6.27	6.27	6.27	99.22
2.00	6.23	6.20	6.23	6.22	99.27
3.00	5.70	5.70	5.71	5.70	99.79
CROSS SECTION #3: VRM 159.5 - VRM 160.0					
BACKSIGHT:		6.70 ft			
INSTRUMENT HEIGHT:		106.70 ft			
1.00	8.69	8.70*	8.71*	8.71	98.00
2.00	8.64	8.66	8.62	8.64	98.06
3.00	-	8.55	8.54	8.55	98.16
4.00	-	8.54	8.54	8.54	98.16
CROSS SECTION #4: VRM 160.0 - VRM 160.7					
BACKSIGHT:		5.81 ft			
INSTRUMENT HEIGHT:		105.81 ft			
1.00	6.97	7.00*	6.98*	6.99	98.82
2.00	6.72	6.75*	6.74*	6.75	99.07
3.00	6.50	6.49	6.50	6.50	99.31
CROSS SECTION #5: VRM 160.7 - VRM 161.5					
BACKSIGHT:		5.38 ft			
INSTRUMENT HEIGHT:		105.38 ft			
1.00	6.89*	6.87	6.90*	6.90	98.49
2.00	6.43	6.31*	6.34*	6.33	99.05
3.00	6.23	6.21	6.23	6.22	99.16
4.00	6.07	6.09	6.08	6.07	99.31

* Best readings and thus will be used to calculate the water surface elevation.

Table C.28 (cont'd). Survey of water surface elevations upstream and downstream of cross section #1 through #7 along the study reach.

TRANSECT	THALWEG FORE-SIGHT	LEW FORE-SIGHT	REW FORE-SIGHT	AVERAGE FORE-SIGHT	ELEVATION (ft)
CROSS SECTION #6: VRM 161.5 - VRM 162.2					
BACKSIGHT:		6.12 ft			
INSTRUMENT HEIGHT:		106.12 ft			
1.00	11.20	11.23*	11.23*	11.23	94.89
2.00	11.13	11.15	11.14	11.15	94.98
3.00	10.71*	-	10.74	10.71	95.42
CROSS SECTION #7: VRM 162.2 - VRM 163.1					
BACKSIGHT:		6.16 ft			
INSTRUMENT HEIGHT:		106.16 ft			
1	7.24*	7.25	7.27	7.24	98.92
2	7.18	-	-	7.18	98.98
3	7.07*	7.09	7.08	7.07	99.09
4	7.05	7.04	-	7.05	99.12

* Best readings and thus will be used to calculate the water surface elevation.

Table C.29. Rating table for flow greater than 100 cfs at cross section #1 and #2.

Cross Section #1 VRM 157.3 - VRM 158.4				Cross Section #2 VRM 158.4 - VRM 159.5			
STAGE FT	DISCH. CFS	VEL. FT/S	TOP WIDTH FT	STAGE FT	DISCH. CFS	VEL. FT/S	TOP WIDTH FT
0.20	1.6	0.81	15.1	0.20	0.7	0.57	10.9
0.65	24.2	1.95	24.4	0.58	14.3	1.57	23.0
1.10	67.9	2.87	25.8	0.96	42.5	2.31	25.9
1.55	127.7	3.58	27.9	1.34	81.8	2.83	30.0
2.00	202.7	4.15	30.4	1.71	131.9	3.14	37.6
2.45	297.2	4.72	32.2	2.09	204.0	3.56	42.5
2.90	404.6	5.19	34.5	2.47	300.7	4.07	44.5
3.35	507.9	5.35	40.2	2.85	414.3	4.55	46.3
3.80	631.3	5.52	46.5	3.23	537.2	4.93	49.2
4.25	799.3	5.86	50.7	3.61	677.5	5.28	52.1
4.70	1017.9	6.38	51.9	3.99	834.9	5.62	55.0
5.15	1258.2	6.87	53.2	4.36	1010.8	5.95	57.8
5.60	1519.7	7.33	54.4	4.74	1213.6	6.32	59.6
6.05	1736.5	7.46	59.7	5.12	1440.1	6.70	60.9
6.50	1989.6	7.61	65.1	5.50	1683.3	7.07	62.2

Table C.30. Rating table for flow less than 100 cfs at cross section #1 and #2.

Cross Section #1 VRM 157.3 - VRM 158.4				Cross Section #2 VRM 158.4 - VRM 159.5			
STAGE FT	DISCH. CFS	VEL. FT/S	TOP WIDTH FT	STAGE FT	DISCH. CFS	VEL. FT/S	TOP WIDTH FT
0.20	1.6	0.81	15.1	0.20	0.7	0.57	14.3
0.30	3.6	0.94	23.0	0.31	2.8	0.87	20.4
0.39	7.7	1.25	24.1	0.42	6.5	1.18	21.4
0.49	13.0	1.53	24.2	0.52	11.5	1.46	22.3
0.59	19.4	1.79	24.3	0.63	17.4	1.69	23.5
0.68	26.8	2.03	24.4	0.74	24.7	1.91	24.3
0.78	35.0	2.25	24.6	0.85	33.0	2.12	25.0
0.88	44.0	2.45	24.9	0.96	42.3	2.31	25.9
0.97	53.7	2.64	25.3	1.06	52.4	2.48	26.9
1.07	64.2	2.82	25.7	1.17	63.6	2.63	28.0
1.16	75.5	2.98	26.1	1.28	75.8	2.79	29.0
1.26	87.6	3.15	26.5	1.39	87.0	2.86	31.2
1.36	100.3	3.30	26.9	1.49	96.2	2.83	35.5
1.45	113.7	3.44	27.4	1.60	113.1	2.98	36.5
1.55	127.7	3.58	27.9	1.71	131.2	3.13	37.5

Table C.31. Rating table for flow greater than 100 cfs at cross section #3 and #4.

Cross Section #3 VRM 159.5 - VRM 160.0				Cross Section #4 VRM 160.0 - VRM 160.7			
STAGE FT	DISCH. CFS	VEL. FT/S	TOP WIDTH FT	STAGE FT	DISCH. CFS	VEL. FT/S	TOP WIDTH FT
0.20	0.5	0.47	7.5	0.20	0.6	0.48	16.1
0.90	14.1	1.20	20.3	0.76	22.4	1.70	24.2
1.60	51.4	1.88	23.8	1.31	71.1	2.60	26.2
2.30	108.1	2.41	26.5	1.87	141.2	3.33	27.7
3.00	179.1	2.48	40.7	2.43	228.8	3.93	29.4
3.70	288.8	2.86	45.7	2.99	325.4	4.31	33.3
4.40	436.4	3.25	49.5	3.54	433.7	4.53	39.4
5.10	602.6	3.49	56.7	4.10	577.1	4.83	44.5
5.80	831.7	3.91	58.5	4.66	739.3	5.06	51.1
6.50	1082.6	4.25	61.5	5.21	970.3	5.53	53.4
7.20	1372.2	4.59	63.7	5.77	1232.4	5.99	55.3
7.90	1705.1	4.96	64.5	6.33	1494.6	6.30	59.2
8.60	2067.0	5.31	65.1	6.89	1789.0	6.59	63.3
9.30	2411.2	5.54	68.5	7.44	2115.4	6.87	67.5
10.00	2759.8	5.69	73.7	8.00	2496.9	7.21	70.7

Table C.32. Rating table for flow less than 100 cfs at cross section #3 and #4.

Cross Section #3 VRM 159.5 - VRM 160.0				Cross Section #4 VRM 160.0 - VRM 160.7			
STAGE FT	DISCH. CFS	VEL. FT/S	TOP WIDTH FT	STAGE FT	DISCH. CFS	VEL. FT/S	TOP WIDTH FT
0.20	0.5	0.47	7.5	0.20	0.6	0.48	16.1
0.35	1.5	0.59	13.4	0.32	2.8	0.81	19.4
0.50	3.8	0.81	15.0	0.44	6.4	1.09	21.3
0.65	7.0	0.98	16.7	0.56	11.3	1.33	22.7
0.80	11.0	1.12	18.9	0.68	17.6	1.56	23.6
0.95	16.1	1.26	20.6	0.80	25.0	1.77	24.5
1.10	22.6	1.42	21.5	0.92	33.5	1.96	25.3
1.25	30.1	1.57	22.4	1.04	43.6	2.17	25.5
1.40	38.6	1.71	23.0	1.15	54.7	2.36	25.8
1.55	48.1	1.84	23.6	1.27	66.8	2.54	26.1
1.70	58.4	1.97	24.2	1.39	79.8	2.71	26.4
1.85	69.6	2.09	24.8	1.51	93.7	2.87	26.7
2.00	81.6	2.20	25.4	1.63	108.6	3.03	27.1
2.15	94.5	2.31	25.9	1.75	124.3	3.18	27.4
2.30	108.1	2.41	26.5	1.87	140.9	3.33	27.7

Table C.33. Rating table for flow greater than 100 cfs at cross section #5 and #6.

Cross Section #5 VRM 160.7 - VRM 161.5				Cross Section #6 VRM 161.5 - VRM 162.2			
STAGE FT	DISCH. CFS	VEL. FT/S	TOP WIDTH FT	STAGE FT	DISCH. CFS	VEL. FT/S	TOP WIDTH FT
0.50	7.0	1.07	29.9	0.20	1.6	0.68	19.0
0.93	42.2	2.13	31.8	0.65	21.0	1.70	26.5
1.36	99.0	2.93	33.5	1.10	63.2	2.52	29.4
1.79	173.7	3.58	35.4	1.55	122.8	3.16	32.3
2.21	267.4	4.18	36.8	2.00	199.5	3.68	35.8
2.64	379.3	4.74	37.6	2.45	300.5	4.26	37.1
3.07	502.7	5.22	39.1	2.90	415.3	4.73	39.3
3.50	638.6	5.63	41.0	3.35	545.0	5.14	41.9
3.93	790.9	6.01	42.9	3.80	697.6	5.57	43.7
4.36	967.0	6.44	44.0	4.25	851.2	5.83	47.4
4.79	1160.3	6.86	44.8	4.70	1043.4	6.22	49.4
5.21	1364.8	7.24	45.8	5.15	1253.7	6.59	51.2
5.64	1582.5	7.59	46.8	5.60	1447.5	6.75	55.7
6.07	1814.1	7.93	47.9	6.05	1672.8	6.96	59.8
6.50	2049.0	8.21	49.4	6.50	1922.4	7.17	63.8

Table C.34. Rating table for flow less than 100 cfs at cross section #5 and #6.

Cross Section #5 VRM 160.7 - VRM 161.5				Cross Section #6 VRM 161.5 - VRM 162.2			
STAGE FT	DISCH. CFS	VEL. FT/S	TOP WIDTH FT	STAGE FT	DISCH. CFS	VEL. FT/S	TOP WIDTH FT
0.50	7.0	1.07	29.9	0.20	1.6	0.68	19.0
0.59	12.5	1.34	30.3	0.30	4.1	0.99	20.0
0.68	19.2	1.58	30.7	0.39	7.6	1.24	21.1
0.78	27.0	1.80	31.1	0.49	11.7	1.42	23.1
0.87	35.8	2.01	31.6	0.59	16.7	1.56	26.0
0.96	45.7	2.20	31.9	0.68	23.3	1.76	26.7
1.05	56.6	2.38	32.3	0.78	30.7	1.94	27.7
1.15	68.4	2.56	32.7	0.88	39.3	2.11	28.5
1.24	81.1	2.72	33.0	0.97	48.9	2.29	28.9
1.33	94.7	2.88	33.4	1.07	59.5	2.46	29.3
1.42	109.2	3.04	33.7	1.16	70.9	2.63	29.7
1.51	124.7	3.19	34.0	1.26	83.1	2.78	30.1
1.61	140.5	3.33	34.5	1.36	95.7	2.92	30.7
1.70	157.1	3.46	34.9	1.45	108.9	3.04	31.5
1.79	174.5	3.59	35.4	1.55	122.8	3.16	32.3

Table C.35. Rating table for flow greater than 100 cfs at cross section #7.

--------- Cross Section #7 ---------
VRM 162.2 - VRM 163.1

STAGE FT	DISCH. CFS	VEL. FT/S	TOP WIDTH FT
0.50	3.2	0.68	17.7
1.18	26.1	1.38	24.9
1.86	71.5	1.87	31.7
2.54	141.1	2.29	37.3
3.21	241.7	2.74	39.9
3.89	365.6	3.14	42.2
4.57	491.0	3.37	47.0
5.25	667.9	3.75	48.2
5.93	866.8	4.11	49.2
6.61	1066.7	4.35	52.1
7.29	1296.7	4.60	54.8
7.96	1560.9	4.89	56.4
8.64	1847.9	5.16	58.1
9.32	2162.1	5.43	59.4
10.00	2495.2	5.68	60.9

Table C.36. Rating table for flow less than 100 cfs at cross section #7.

--------- Cross Section #7 ---------
VRM 162.2 - VRM 163.1

STAGE FT	DISCH. CFS	VEL. FT/S	TOP WIDTH FT
0.50	3.2	0.68	17.7
0.65	6.5	0.88	19.1
0.79	10.7	1.04	20.5
0.94	15.9	1.19	21.9
1.08	21.8	1.31	23.6
1.23	28.6	1.41	25.5
1.37	36.7	1.52	27.1
1.52	46.0	1.63	28.5
1.67	56.3	1.74	29.9
1.81	67.7	1.84	31.3
1.96	80.3	1.93	32.6
2.10	94.0	2.03	33.9
2.25	109.3	2.13	34.8
2.39	124.9	2.21	36.1
2.54	141.6	2.29	37.4

Table D.1 . Velocity comparison on 7-10-88 between float test measurements and random point samples.

RANDOM POINT SAMPLES BY
VERTICAL AXIS CURRENT METER:

	CROSS SECTION				
VERTICAL	1 ft/s	2 ft/s	3 ft/s	4 ft/s	5 ft/s
1	2.47	1.67	1.44	2.07	0.87
2	1.29	0.9	2.62	1.64	1.64
3	2.08	1.64	2.13	2.62	2.62
4	1.74	1.59	2.23	3.15	2.32
5	1.84	2.71	1.01	1.93	1.79
6	2.08	0.83	EDDY	1.35	2.03

AVERAGE VELOCITY: 1.87 ft/s

FLOATING CHIP MEASUREMENTS:

VRM 159.5 - VRM 157.3
FLOAT SECTION #2
LENGTH: 500 ft

FLOAT #	TIME seconds
1	138
2	153
3	152
4	152
5	143
6	179

AVERAGE TIME: 153 seconds
AVERAGE VELOCITY: 3.27 ft/s * (.85) = 2.78 ft/s

Table D.2 . Modeled and measured hourly stream temperature values at VRM 157.3 for existing conditions on 6-30-88, 7-08-88, 7-15-88, and 7-21-88.

	---- 6-30-88 -----		---- 7-08-88 -----		---- 7-15-88 -----		---- 7-21-88 ----	
TIME	MODELED STREAM TEMP C	MEAS. STREAM TEMP C	MODELED STREAM TEMP C	MEAS. STREAM TEMP C	MODELED STREAM TEMP C	MEAS. STREAM TEMP C	MODELED STREAM TEMP C	MEAS. STREAM TEMP C
210	18.2	19.9	17.9	19.8	17.2	19.7	18.3	20.4
310	17.7	19.6	17.4	19.3	16.7	18.9	18.0	19.8
410	17.4	19.1	16.9	18.6	16.3	18.3	17.7	19.2
510	17.0	18.6	16.5	18.1	16.0	17.6	17.4	18.9
610	16.6	18.2	16.1	17.6	15.7	17.2	17.1	18.4
710	16.2	17.9	15.8	17.2	15.3	16.6	16.7	17.9
810	16.0	17.8	15.6	16.8	14.9	16.3	16.4	17.5
910	16.7	18.3	16.4	16.8	15.6	16.2	17.0	17.5
1010	18.0	19.2	17.8	17.4	17.0	16.8	18.2	18.2
1110	19.8	21.2	19.7	18.7	18.9	18.0	20.0	19.6
1210	21.8	23.1	21.8	20.7	20.9	20.2	21.9	21.5
1310	24.3	24.6	24.1	22.9	23.2	22.5	24.2	23.1
1410	26.2	26.0	26.0	24.2	25.2	24.1	25.9	25.0
1510	27.9	26.7	27.5	25.7	26.8	25.5	27.3	26.5
1610	28.9	27.2	28.4	26.4	27.7	26.5	28.1	27.4
1710	29.2	27.2	28.4	27.0	27.7	26.9	28.1	27.8
1810	28.8	26.2	27.9	26.9	27.1	26.8	27.5	27.8
1910	27.7	25.3	26.7	26.5	25.8	26.3	26.3	27.6
2010	26.0	24.3	24.9	25.0	24.2	25.0	24.8	26.5
2110	24.2	23.2	23.1	23.8	22.8	23.8	23.1	25.5
2210	22.7	22.1	21.9	22.9	21.6	22.7	21.9	24.2
2310	21.1	21.5	20.4	22.0	20.0	22.0	20.6	23.4
10	19.8	20.7	19.4	21.4	18.8	21.4	19.5	22.5
110	18.8	20.0	18.5	20.6	17.8	20.6	18.8	21.7
MEAN	21.7	22.0	21.2	21.5	20.5	21.2	21.4	22.4

Table D.3 . Modeled and measured maximum, minimum, and mean stream temperatures at VRM 157.3 for 6-30-88, 7-08-88, 7-15-88, and 7-21-88.

DATE	MAXIMUM TEMP. MODEL C	MAXIMUM TEMP. MEAS. C	MINIMUM TEMP. MODEL C	MINIMUM TEMP. MEAS. C	MEAN TEMP. MODEL C	MEAN TEMP. MEAS. C
6-30-88	29.2	27.2	16.0	17.8	21.7	22.0
7-08-88	28.4	27.0	15.6	16.7	21.2	21.5
7-15-88	27.7	26.9	14.9	16.2	20.5	21.2
7-21-88	28.1	27.8	16.4	17.5	21.4	22.4

Table D.4 . Modeled energy transfer rate in Langley/minute at hourly intervals on 6-30-88.

TIME	NET SOLAR FLUX Ly/min	NET LONGWAVE FLUX Ly/min	EVAP FLUX Ly/min	CONV FLUX Ly/min	NET BEDROCK FLUX Ly/min	NET ENERGY FLUX Ly/min
132	0.000	-0.036	-0.143	0.042	0.004	-0.132
232	0.000	-0.039	-0.136	0.039	0.000	-0.138
332	0.000	-0.043	-0.131	0.036	0.000	-0.138
432	0.000	-0.048	-0.125	0.031	0.000	-0.144
532	0.000	-0.053	-0.120	0.026	0.000	-0.144
632	0.006	-0.055	-0.114	0.025	0.000	-0.138
732	0.046	-0.052	-0.109	0.027	0.000	-0.090
832	0.410	-0.043	-0.109	0.035	-0.001	0.294
932	0.773	-0.030	-0.121	0.046	-0.001	0.666
1032	1.073	-0.018	-0.143	0.057	-0.003	0.972
1132	1.314	-0.014	-0.171	0.061	-0.004	1.188
1232	1.474	-0.024	-0.216	0.053	-0.005	1.290
1332	1.540	-0.031	-0.257	0.048	-0.005	1.302
1432	1.509	-0.036	-0.300	0.045	-0.005	1.218
1532	1.381	-0.038	-0.332	0.044	-0.004	1.056
1632	1.167	-0.036	-0.347	0.046	-0.003	0.828
1732	0.883	-0.029	-0.346	0.051	-0.002	0.558
1832	0.508	-0.029	-0.332	0.051	0.004	0.204
1932	0.112	-0.038	-0.301	0.043	0.004	-0.180
2032	0.014	-0.050	-0.262	0.033	0.005	-0.258
2132	0.000	-0.064	-0.229	0.021	0.005	-0.264
2232	0.000	-0.068	-0.197	0.017	0.005	-0.246
2332	0.000	-0.056	-0.172	0.026	0.005	-0.198
2432	0.000	-0.039	-0.153	0.040	0.005	-0.144

Table D.5 . Modeled energy transfer rate between the air/water interface in Langley/day.

DATE	NET SOLAR Ly/day	NET LONGWAVE Ly/day	EVAP Ly/day	CONV Ly/day	H Ly/day
6-30-88	733	-58	-292	57	442
7-08-88	724	-51	-364	80	390
7-15-88	713	-42	-442	113	345
7-21-88	705	-24	-480	149	351

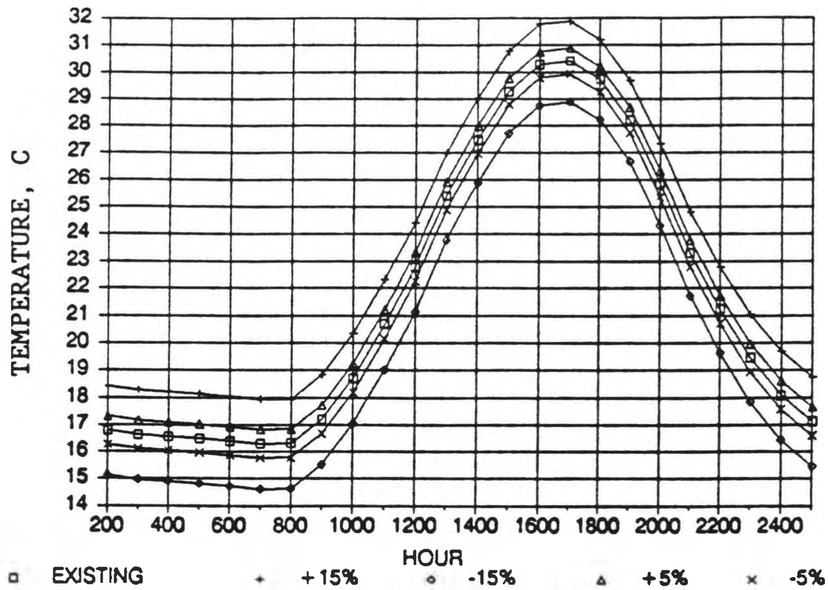

Fig. D.1. Change in modeled stream temperature at VRM 157.3 with ±5% and ±15% change in the inflow stream temperature input

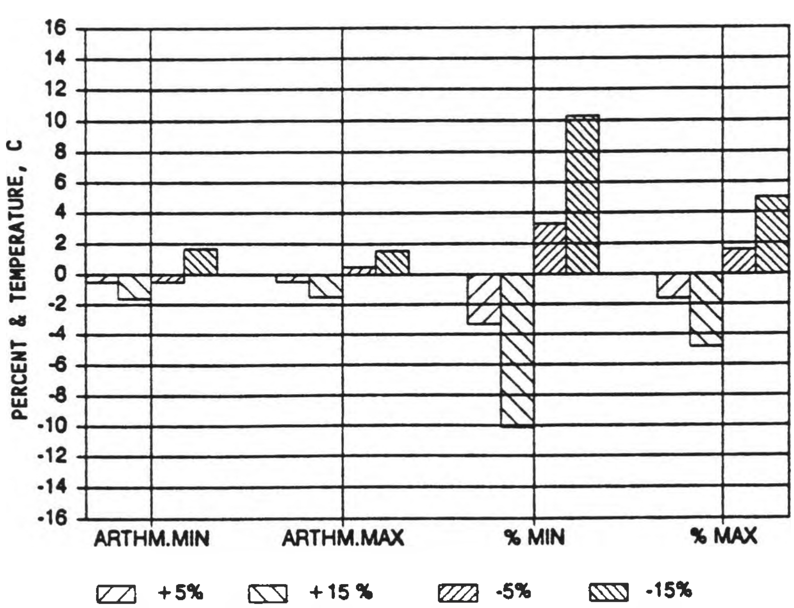

Fig. D.2. Sensitivity of TEMP-84 modeled maximum and minimum temperature to changes in inflow stream temperature in terms arithmetic and percent difference from existing condition

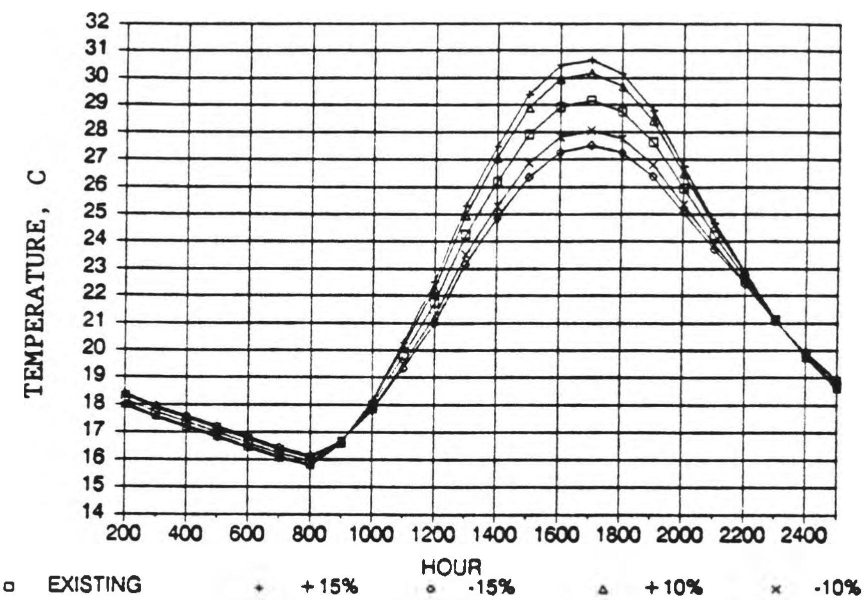

Fig. D.3. Change in modeled stream temperature at VRM 157.3 with ±10% and ±15% change in the width input.

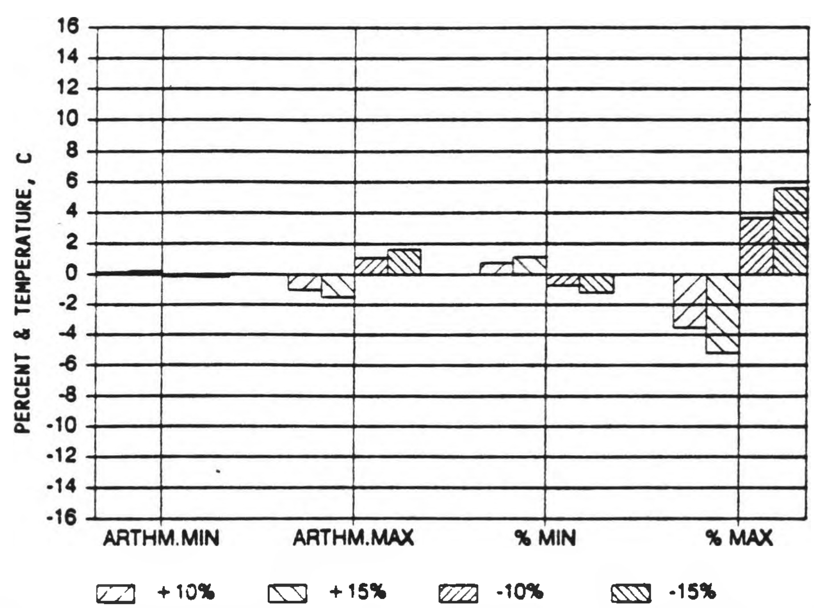

Fig. D.4. Sensitivity of TEMP-84 modeled maximum and minimum temperature to changes in width in terms of arithmetic and percent difference from existing conditions.

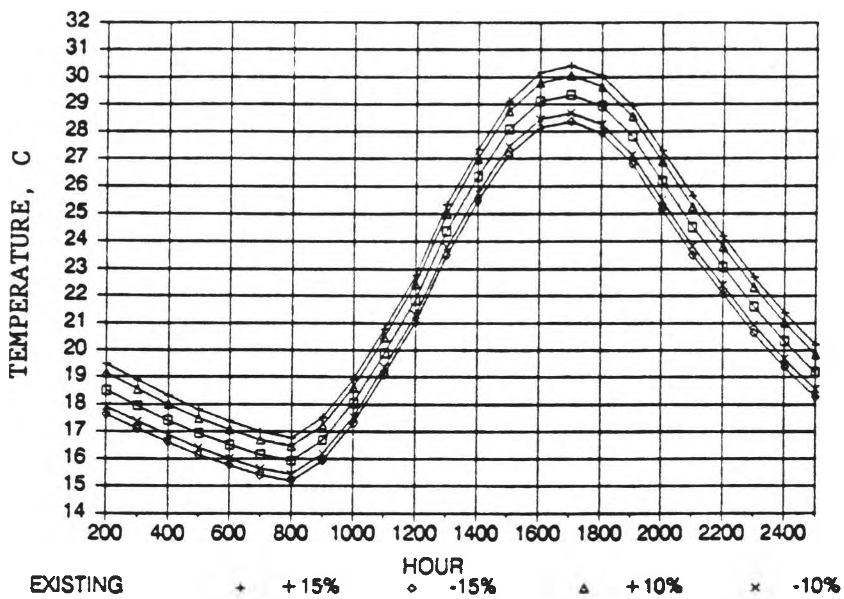

Fig. D.5. Change in TEMP-84 modeled stream temperature at VRM 157.3 with ±10% and ±15% change in the air temperature input.

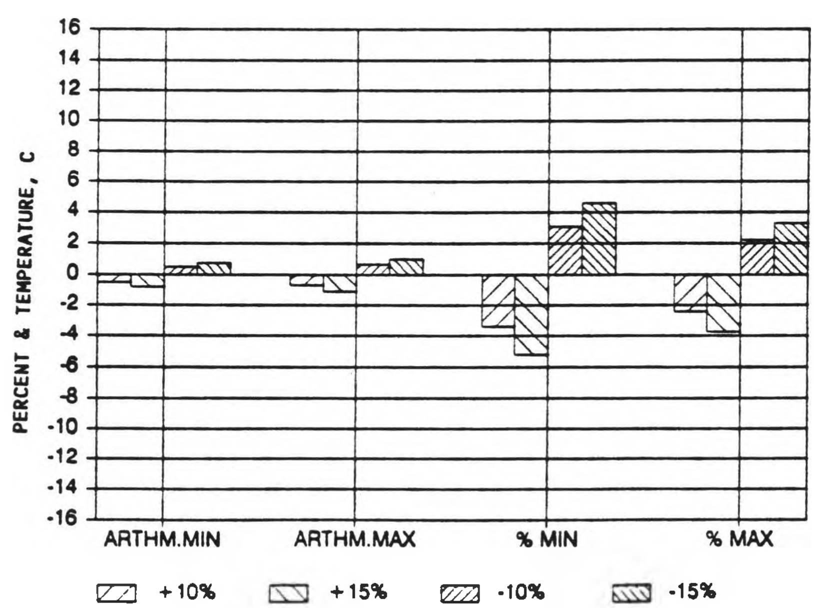

Fig. D.6. Sensitivity of TEMP-84 modeled maximum and minimum temperature to changes in air temperature in terms of arithmetic and percent difference from existing conditions.

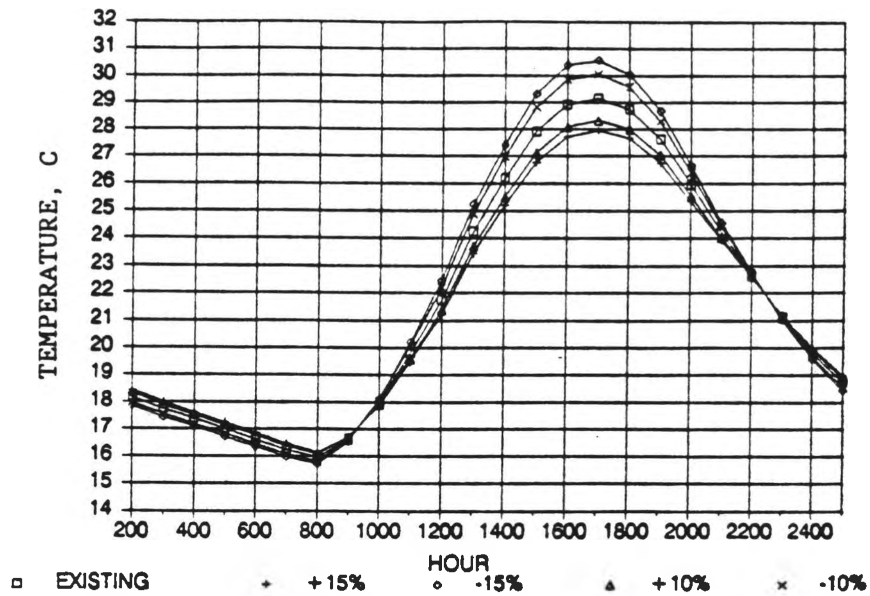

Fig. D.7. Change in TEMP-84 modeled stream temperature at VRM 157.3 with ±10% and ±15% change in the discharge input.

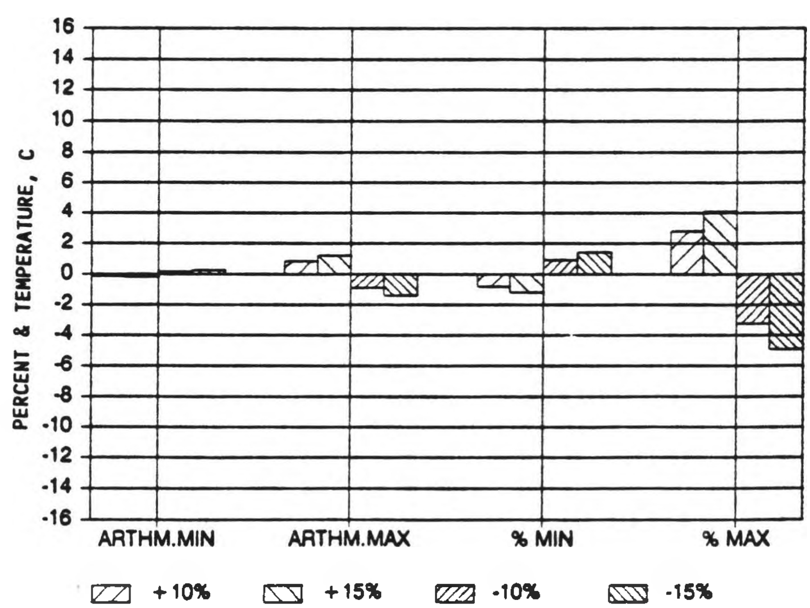

Fig. D.8. Sensitivity of TEMP-84 modeled maximum and minimum temperature to changes in discharge in terms of arithmetic and percent difference from existing conditions.

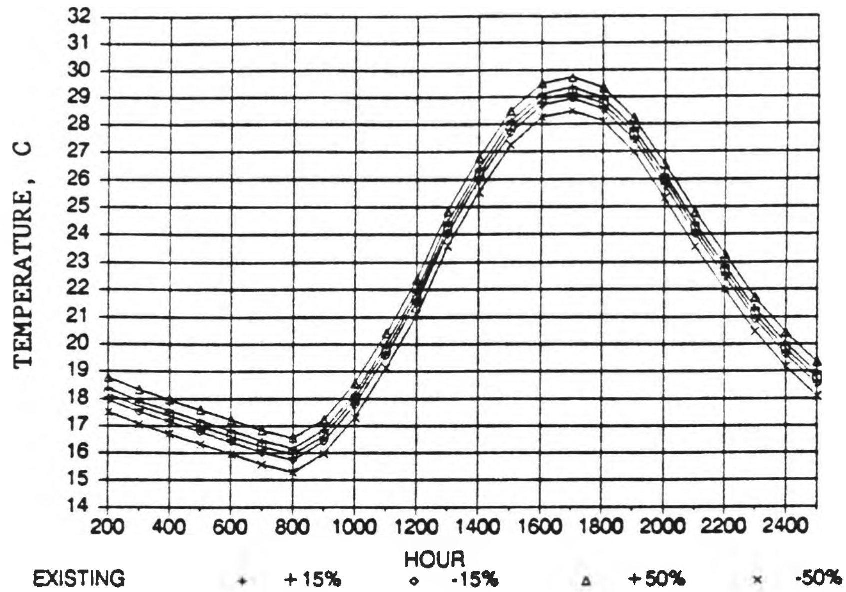

Fig. D.9. Change in TEMP-84 modeled stream temperature at VRM 157.3 with ±15% and ±50% change in the relative humidity input.

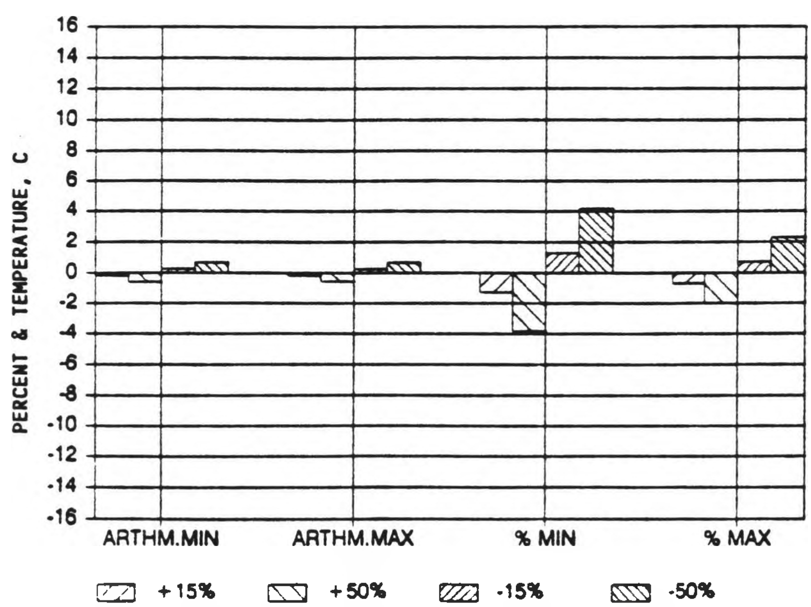

Fig. D.10. Sensitivity of TEMP-84 modeled maximum and minimum temperature to changes in relative humidity in terms of arithmetic and percent difference from existing conditions.

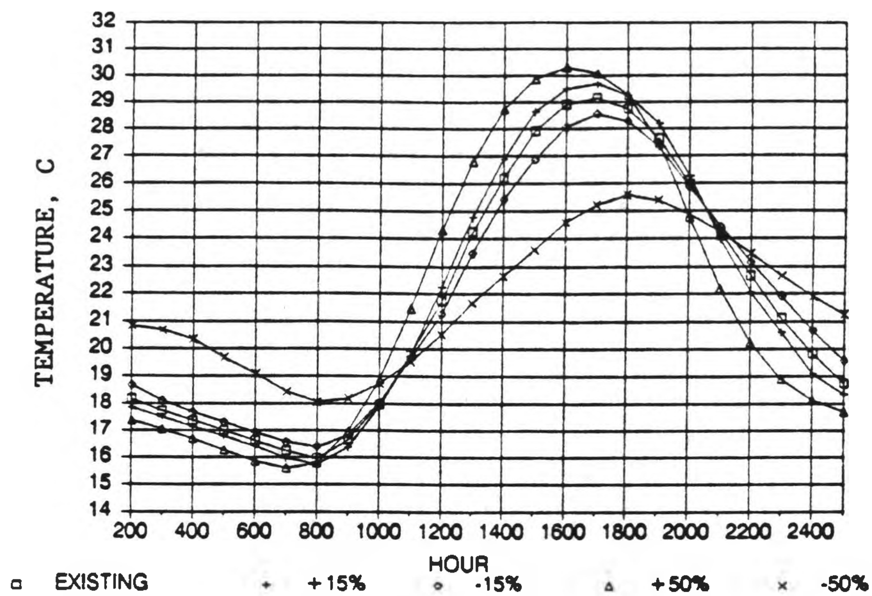

Fig. D.11. Change in TEMP-84 modeled stream temperature at VRM 157.3 with ±15% and ±50% change in the velocity input.

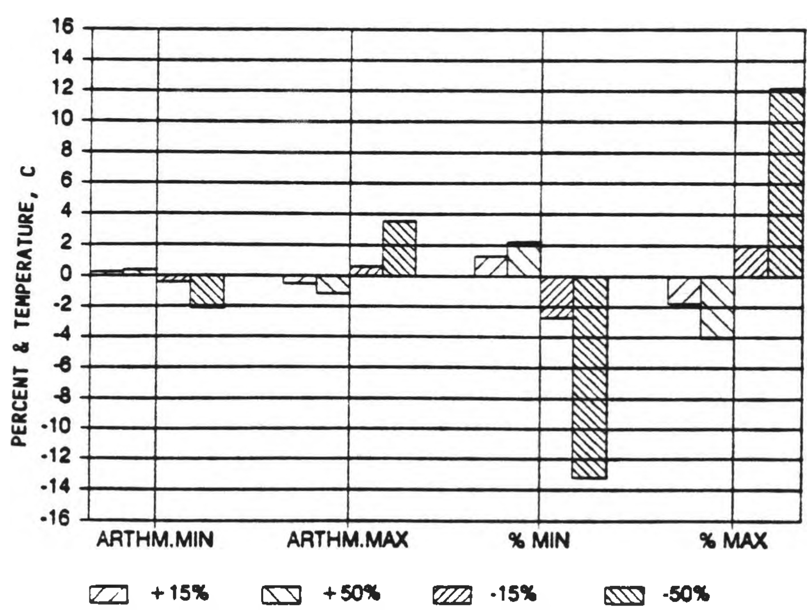

Fig. D.12. Sensitivity of TEMP-84 modeled maximum and minimum temperature to changes in velocity in terms of arithmetic and percent difference from existing conditions.

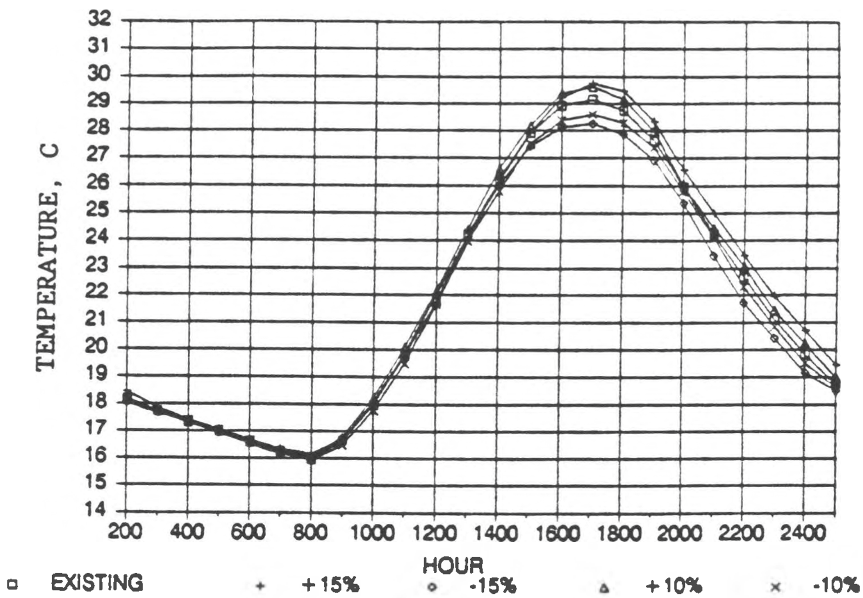

Fig. D.13. Change in TEMP-84 modeled stream temperature at VRM 157.3 with ±10% and ±15% change in the length input.

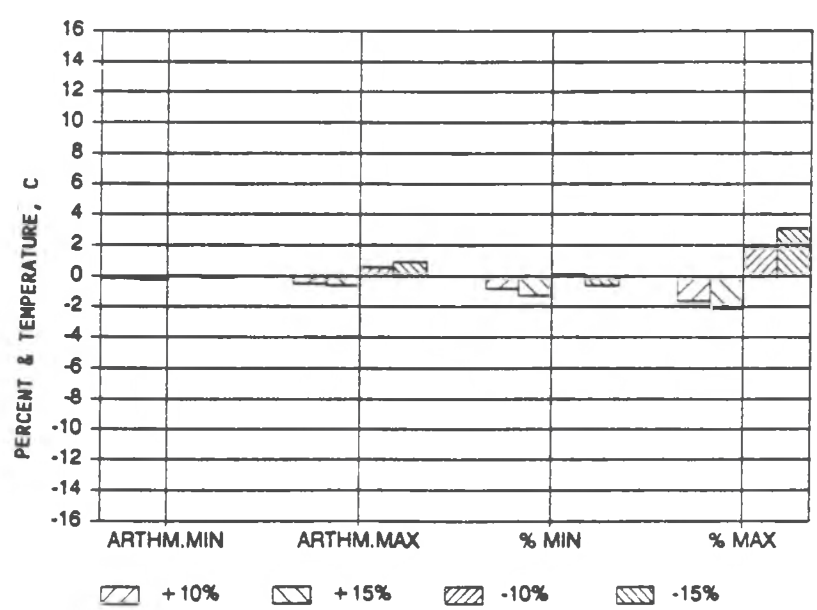

Fig. D.14. Sensitivity of TEMP-84 modeled maximum and minimum temperature to changes in length in terms of arithmetic and percent difference from existing conditions.

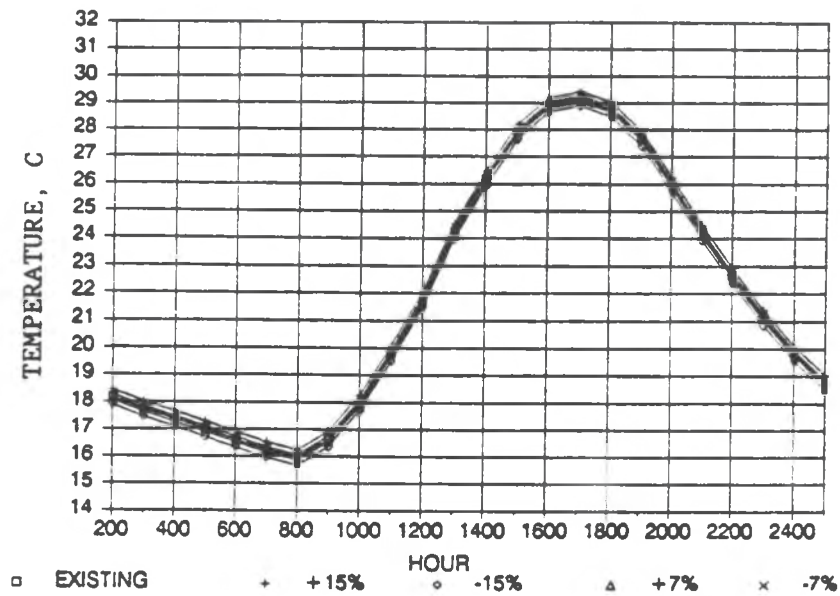

Fig. D.15. Change in TEMP-84 modeled stream temperature at VRM 157.3 with ±7% and ±15% change in the groundwater temperature input.

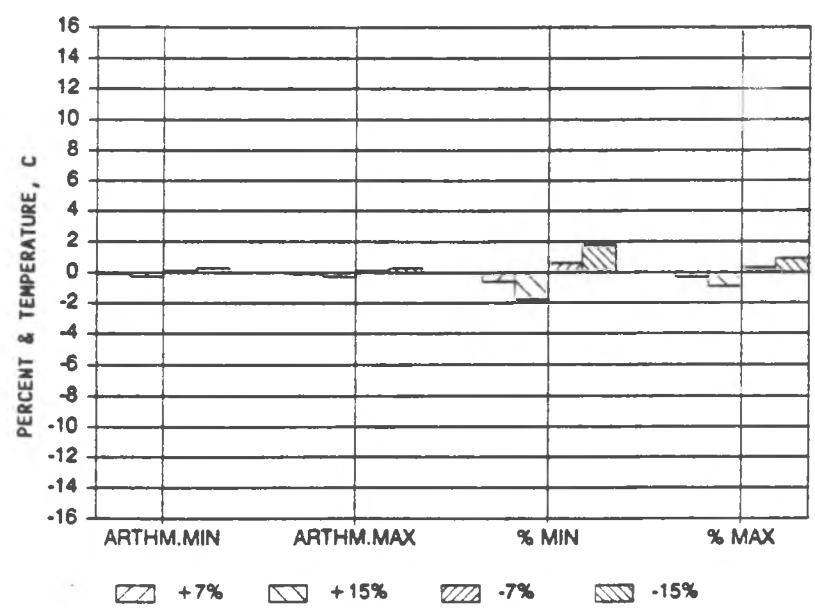

Fig. D.16. Sensitivity of TEMP-84 modeled maximum and minimum temperature to changes in groundwater temperature in terms of arithmetic and percent difference from existing conditions.

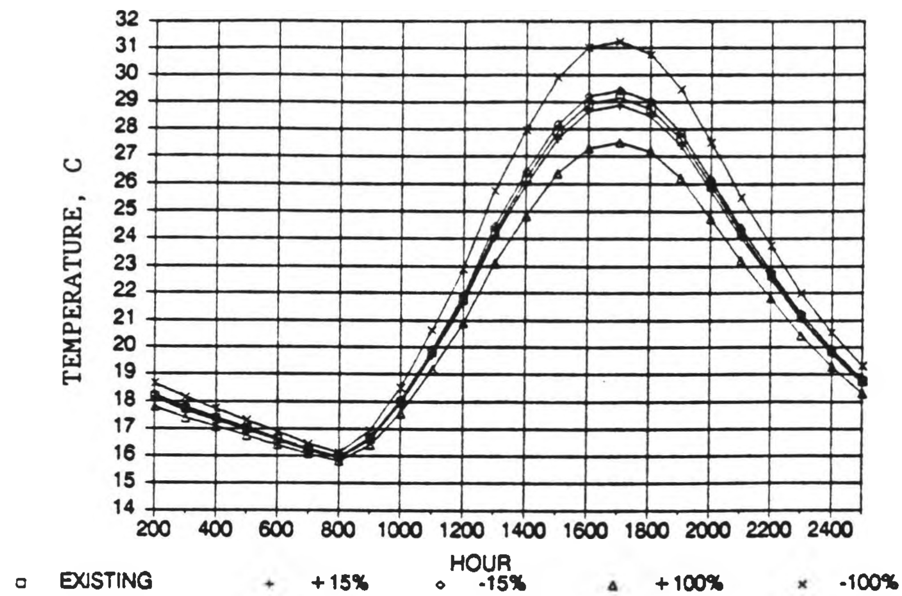

Fig. D.17. Change in TEMP-84 modeled stream temperature at VRM 157.3 with±15% and ±100% change in the groundwater inflow rate input.

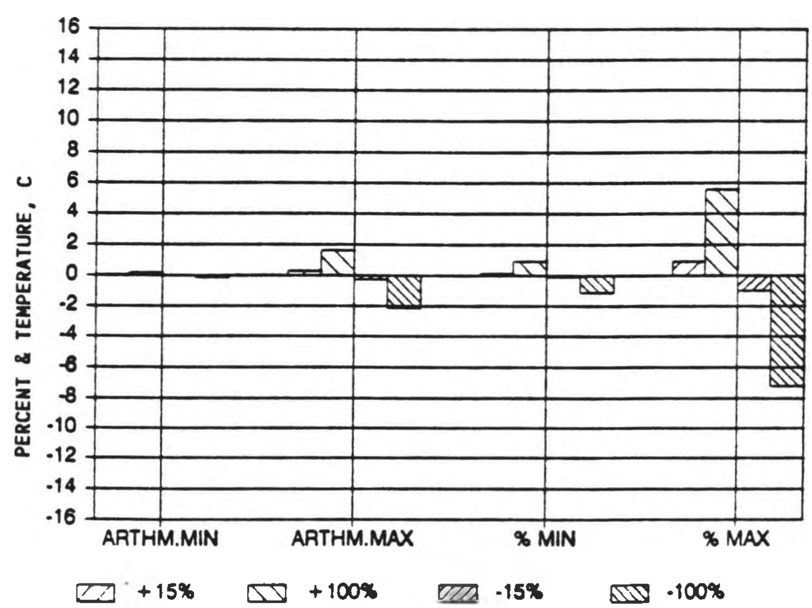

Fig. D.18. Sensitivity of TEMP-84 modeled maximum and minimum temperature to changes in groundwater inflow rate in terms of arithmetic and percent difference from existing conditions.

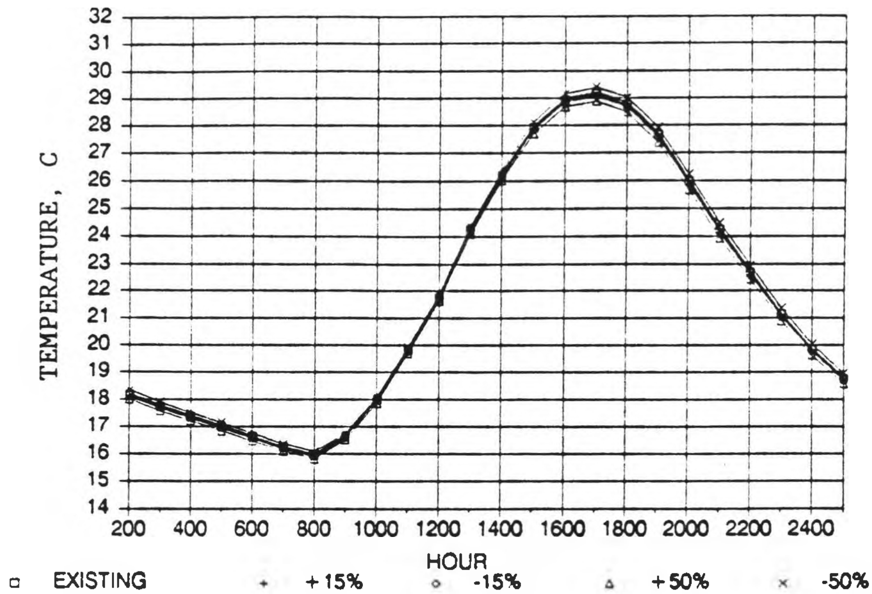

Fig. D.19. Change in TEMP-84 modeled stream temperature at VRM157.3 with ±15% and ±50% change in the wind input.

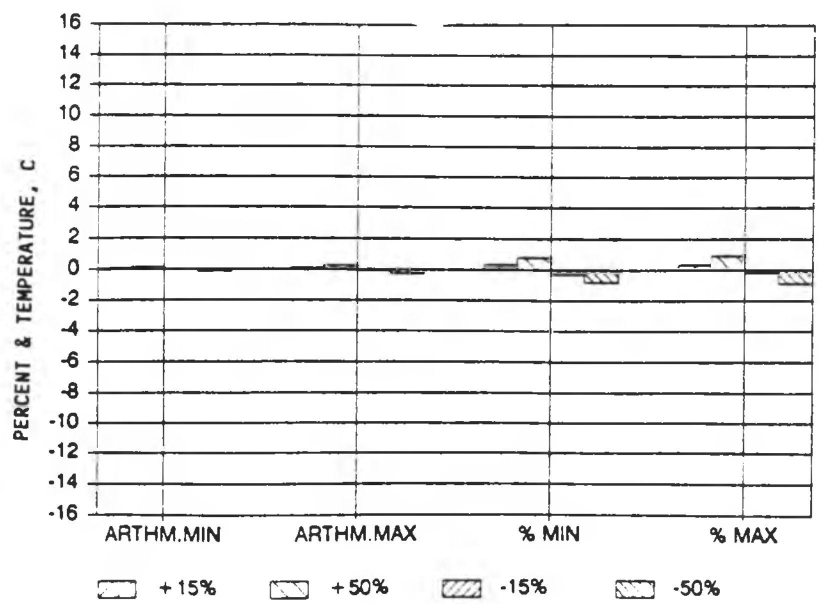

Fig. D.20. Sensitivity of TEMP-84 modeled maximum and minimum temperature to changes in wind speed in terms of arithmetic and percent difference from existing conditions.

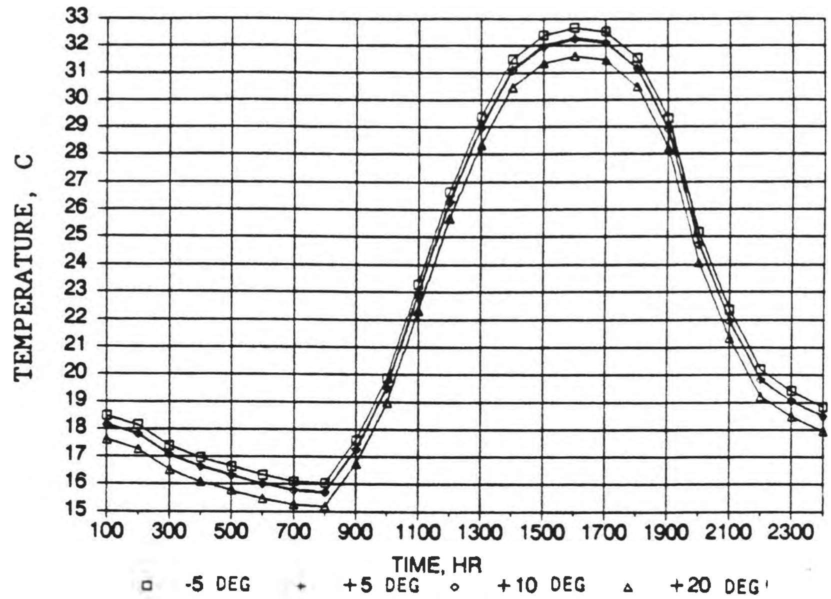

Fig. D.21. Change in TEMP-84 modeled stream temperature at VRM 157.3 with ±5, +10, and +20 degree change in the hillslope angle input.

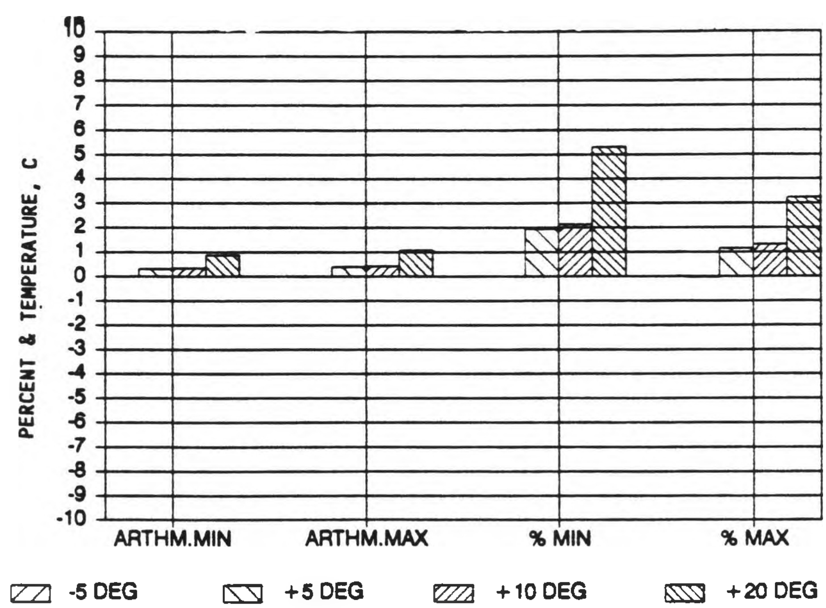

Fig. D.22. Sensitivity of TEMP-84 modeled maximum and minimum temperature to changes in hillslope angle in terms of arithmetic and percent difference from existing conditions.

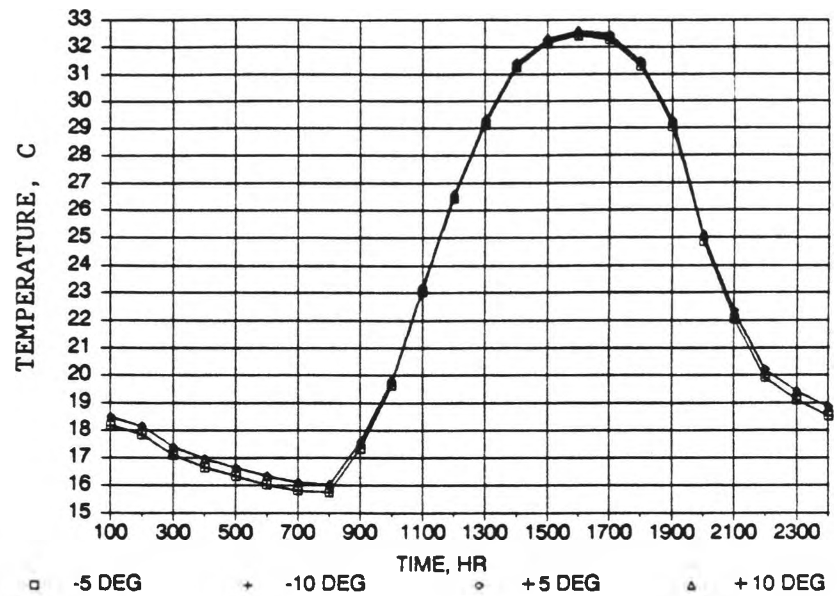

Fig. D.23. Change in TEMP-84 modeled stream temperature at VRM 157.3 with ±5 and ±10 degree change in the forest angle input.

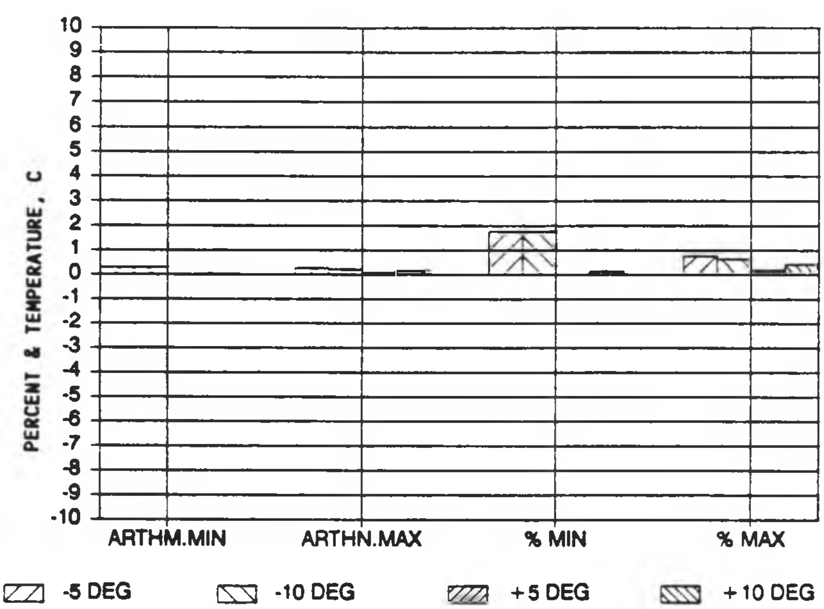

Fig. D.24. Sensitivity of TEMP-84 modeled maximum and minimum temperature to changes in forest angles in terms of arithmetic and percent difference from existing conditions.

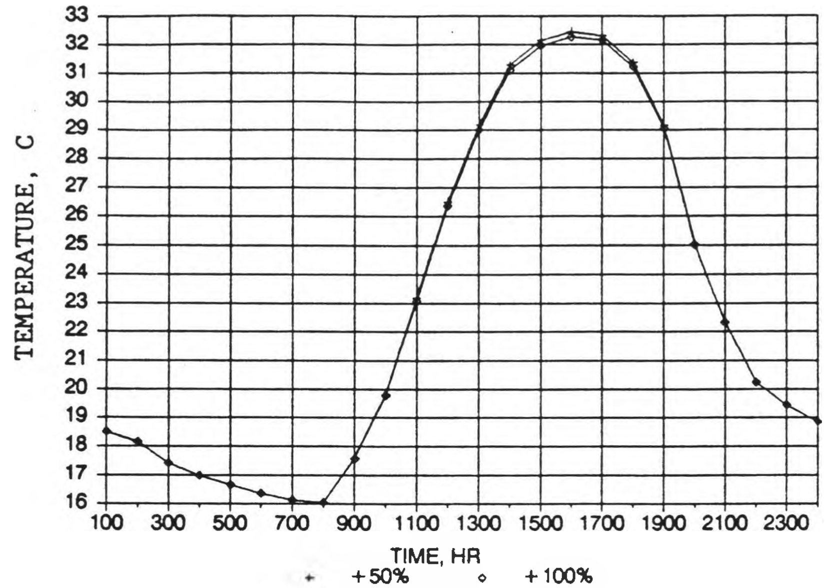

Fig. D.25. Change in TEMP-84 modeled stream temperature at VRM 157.3 with ±50% and ±100% change in the percent directly shaded

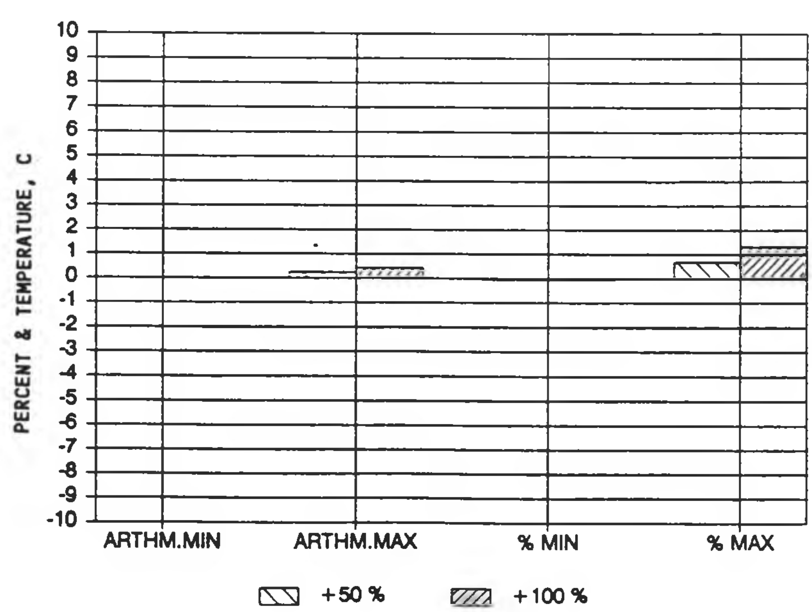

Fig. D.26. Sensitivity of TEMP-84 modeled maximum and minimum temperature to changes in the percent directly shaded in terms of arithmetic and percent difference from existing conditions.

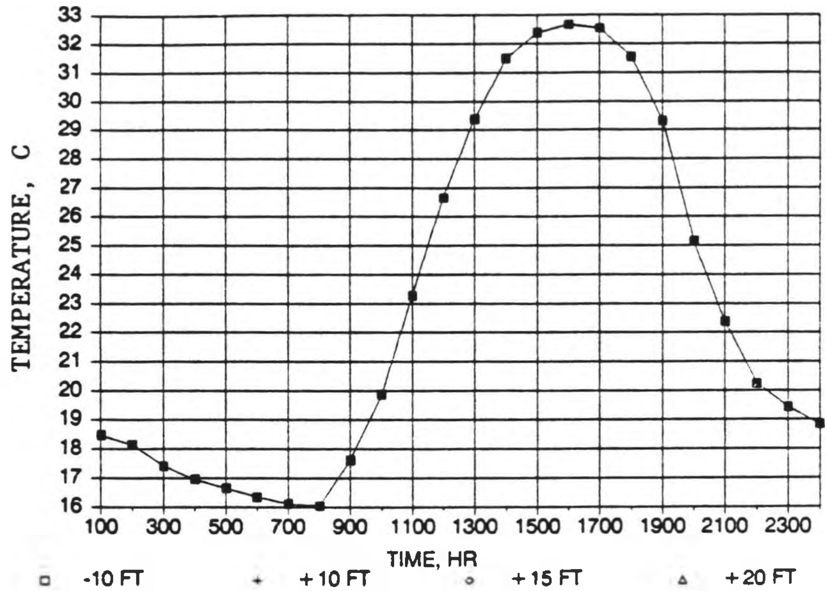

Fig. D.27. Change in TEMP-84 modeled stream temperature at VRM 157.3 with ±10, +15, and +20 feet change in the tree height input.

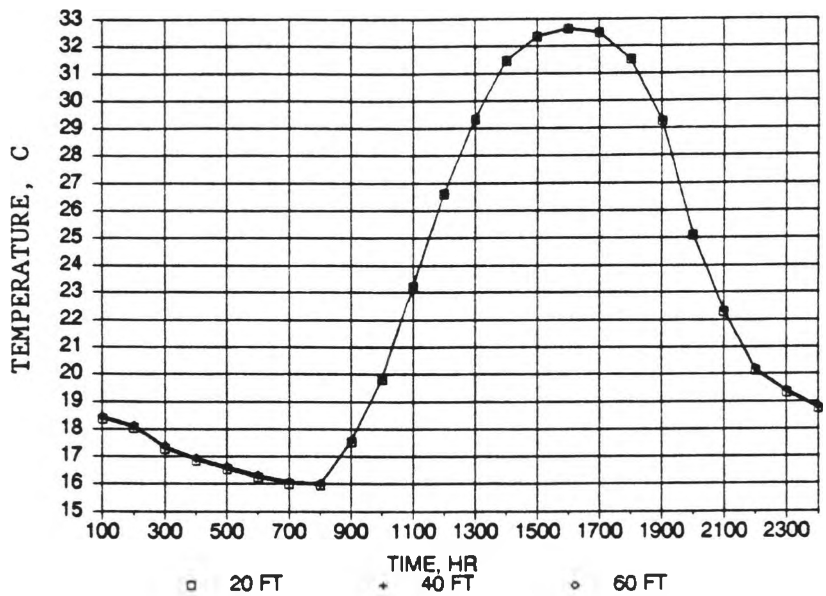

Fig. D.28. Change in TEMP-84 modeled stream temperature at VRM 157.3 with buffer width values set at 20, 40, and 60 feet.

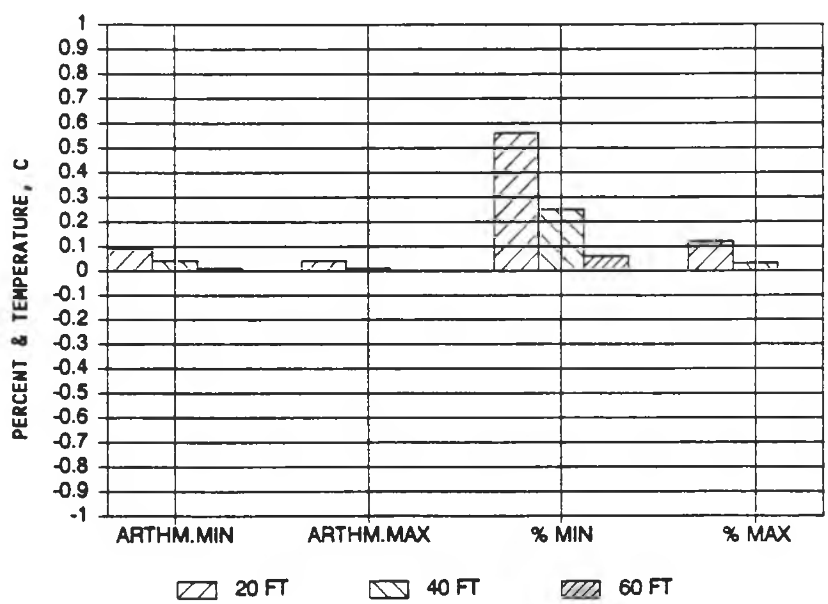

Fig. D.29. Sensitivity of TEMP-84 modeled maximum and minimum temperature to changes in the buffer width in terms of arithmetic and percent difference from existing conditions.

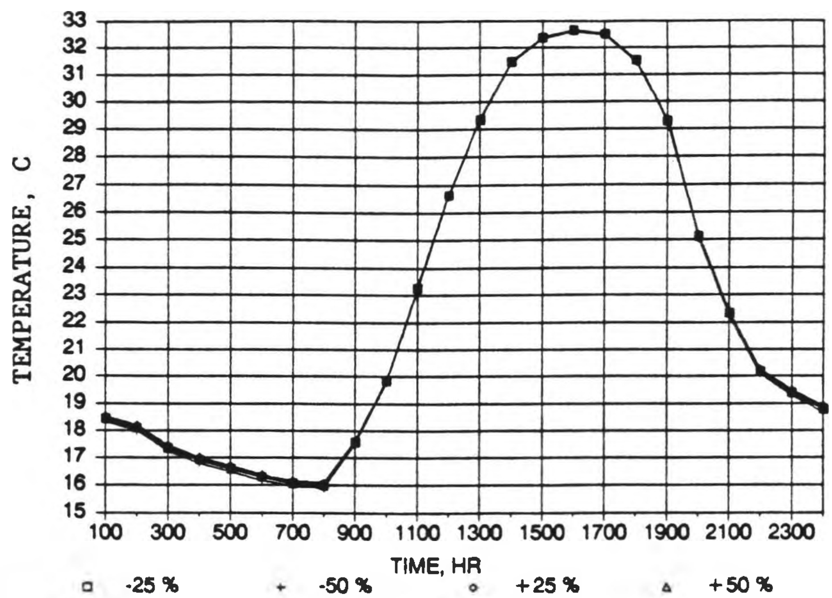

Fig. D.30. Change in TEMP-84 modeled stream temperature at VRM 157.3 with ±25% and ±50% change in canopy cover input.

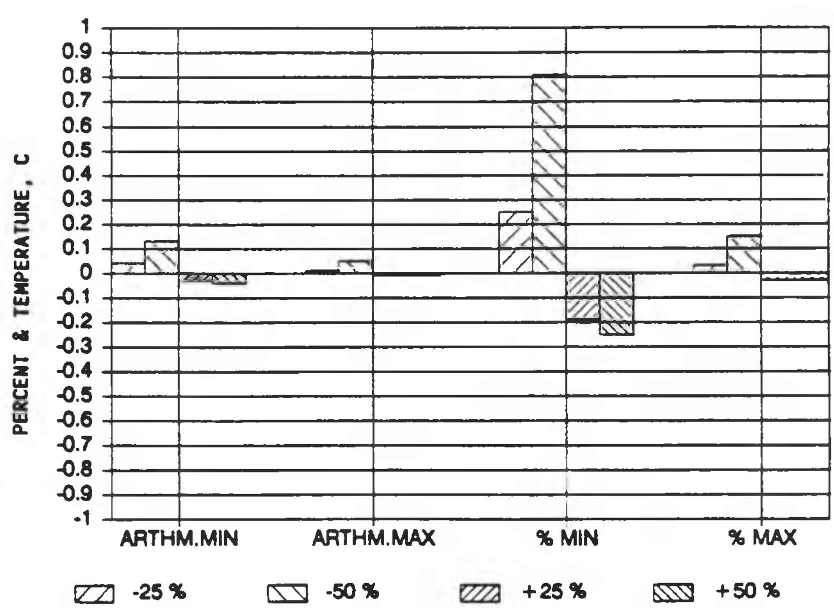

Fig. D.31. Sensitivity of TEMP-84 modeled maximum and minimum temperature to changes in the canopy cover in terms of arithmetic and percent difference from existing conditions.

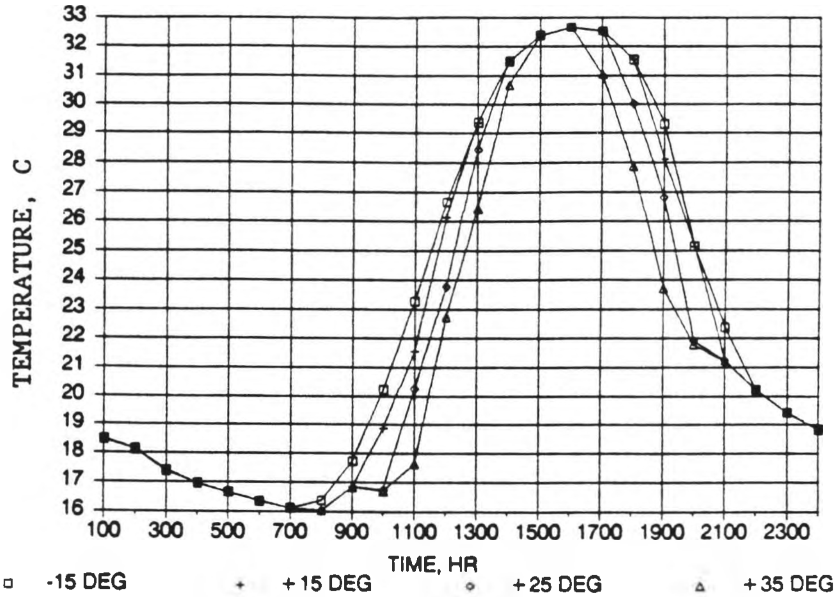

Fig. D.32. Change in TEMP-84 modeled stream temperature at VRM 157.3 with ±15, +25, and +35 degree change in vegetation shading angle input.

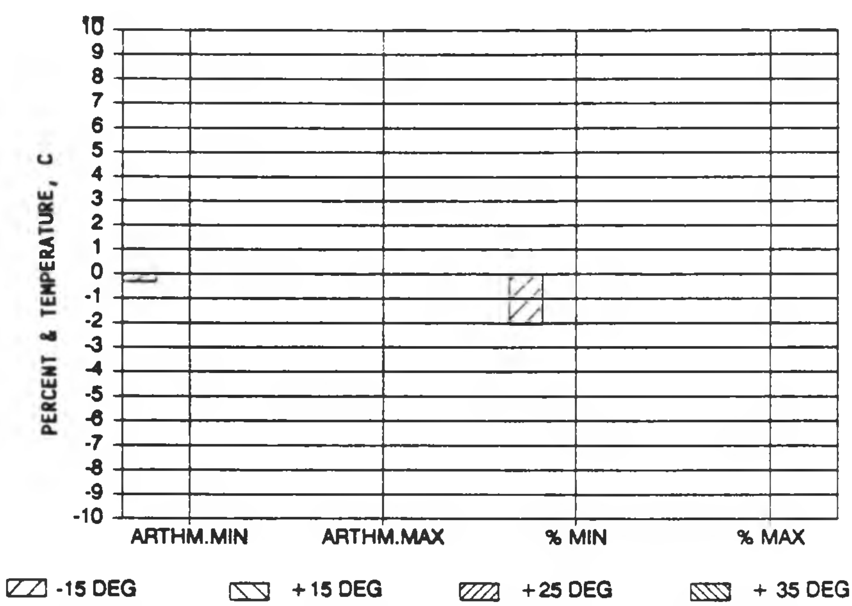

Fig. D.33. Sensitivity of TEMP-84 modeled maximum and minimum temperature to changes in the vegetation shading angles in terms of arithmetic and percent difference from existing conditions.

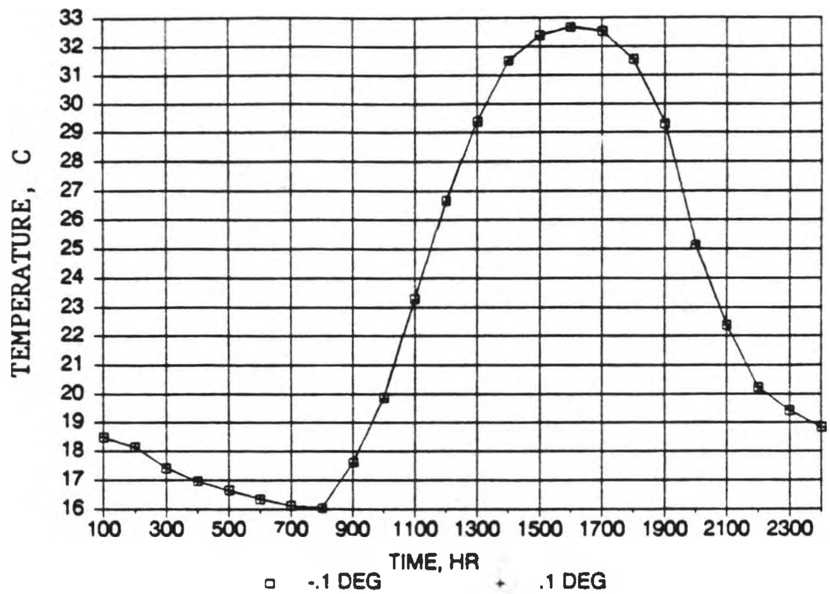

Fig. D.34. Change in TEMP-84 modeled stream temperature at VRM 157.3 with ±0.1 degree change in longitude input.

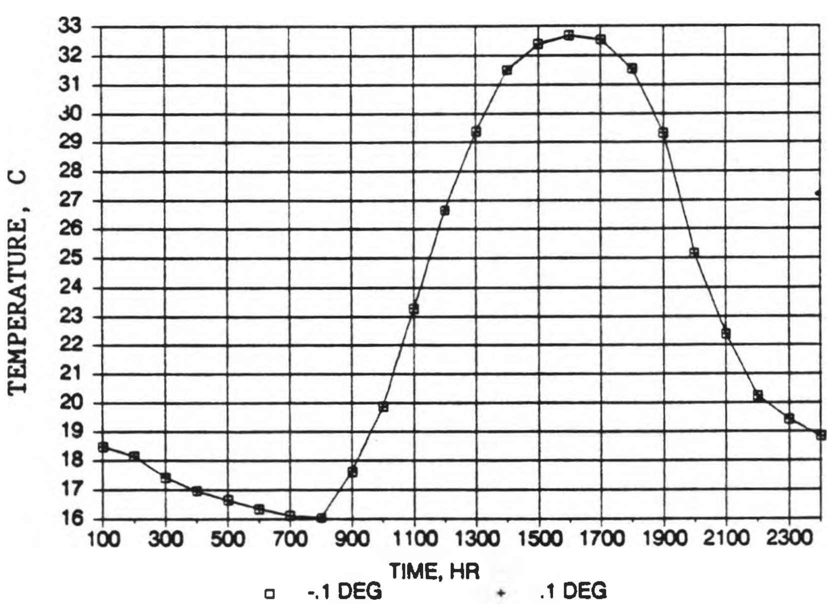

Fig. D.35. Change in TEMP-84 modeled stream temperature at VRM 157.3 with ±0.1 degree change in the latitude input.

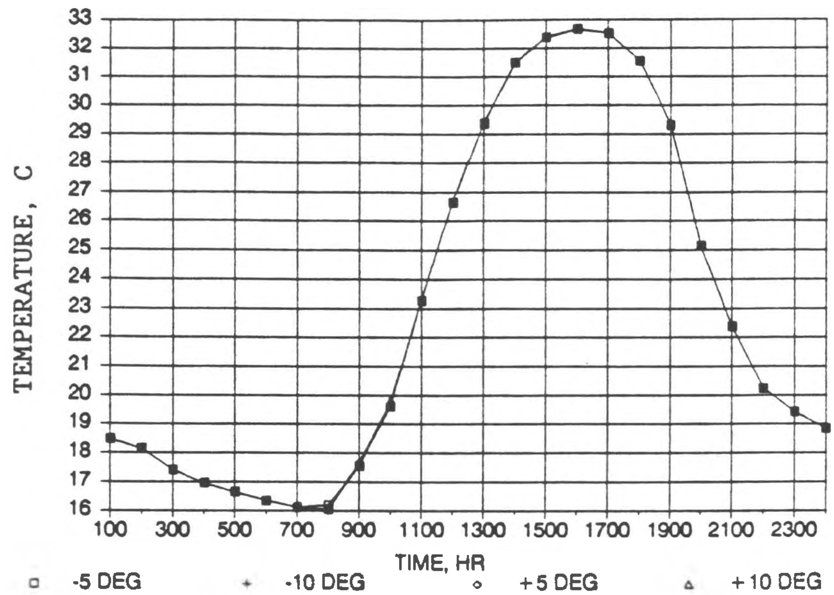

Fig.D.36. Change in TEMP-84 modeled stream temperature at VRM 157.3 with ±5 and ±10 degree change in the stream aspect input.

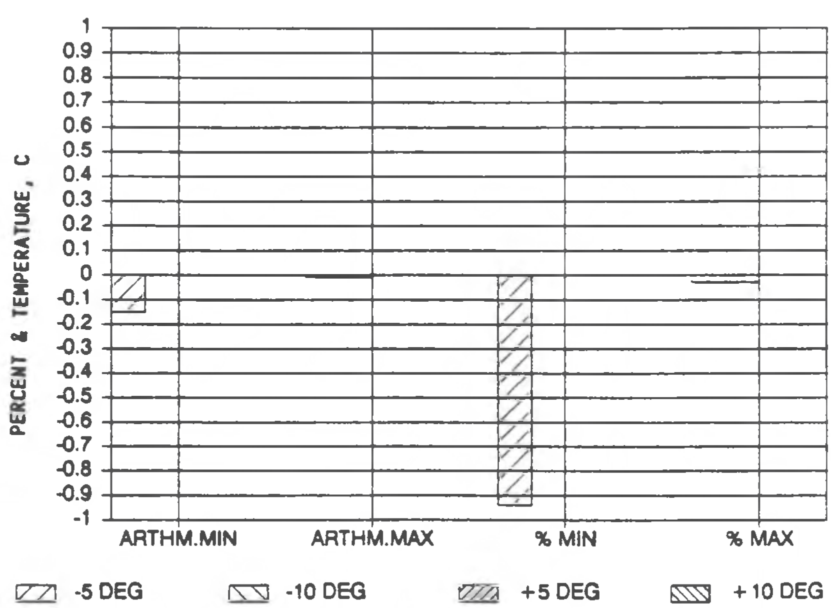

Fig. D.37. Sensitivity of TEMP-84 modeled maximum and minimum temperature to changes in the stream aspect in terms of arithmetic and percent difference from existing conditions.

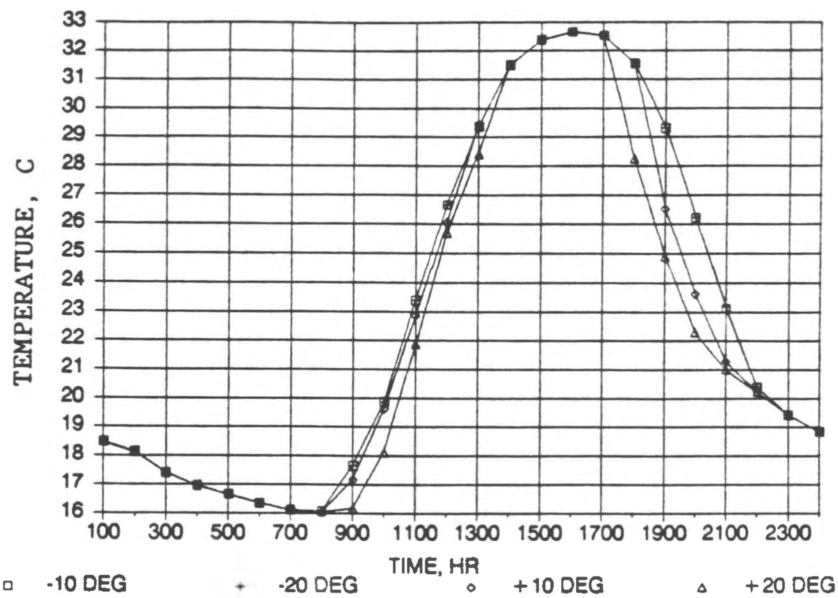

Fig. D.38. Change in TEMP-84 modeled stream temperature at VRM 157.3 with ±10 and ±20 degree change in the topographic shading input.

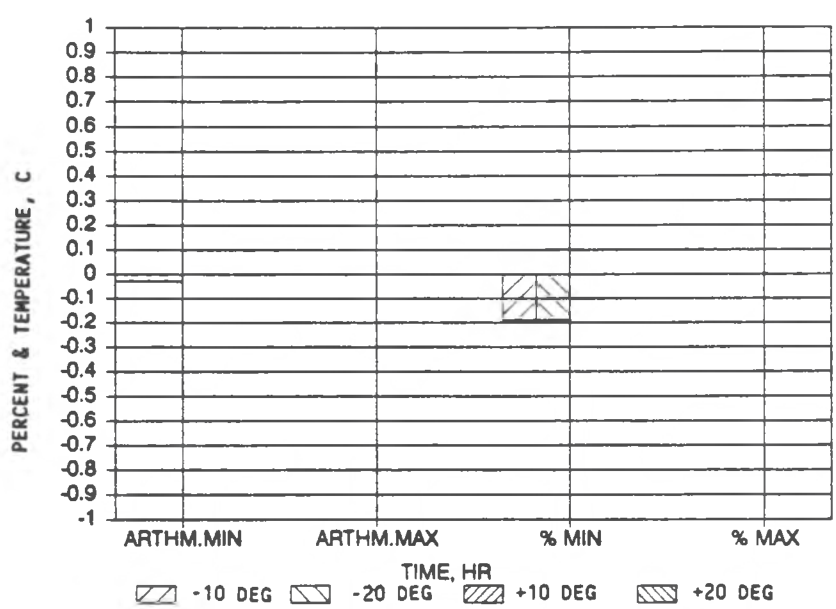

Fig. D.39. Sensitivity of TEMP-84 modeled maximum and minimum temperature to changes in the topographic shading angle in terms of arithmetic and percent difference from existing conditions.

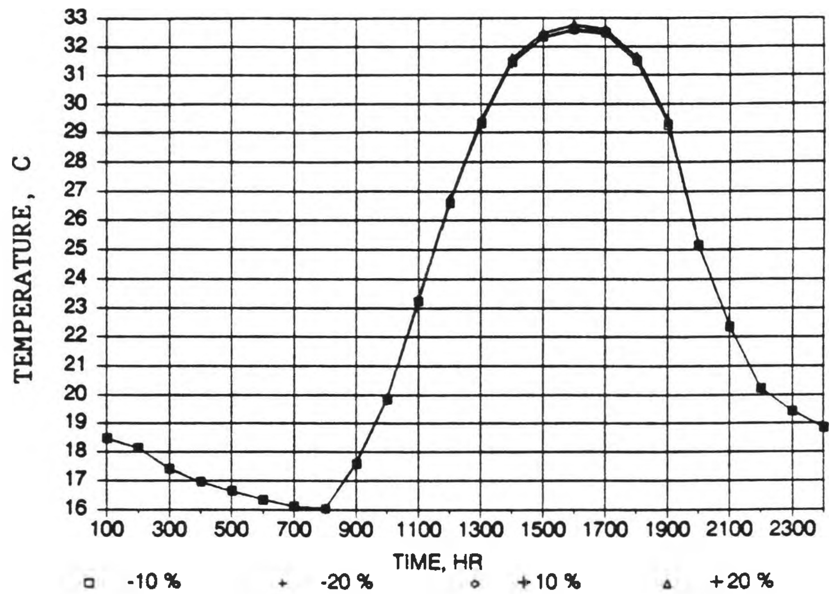

Fig. D.40. Change in TEMP-84 modeled stream temperature at VRM 157.3 with ±10% and ±20% change in the mean elevation.

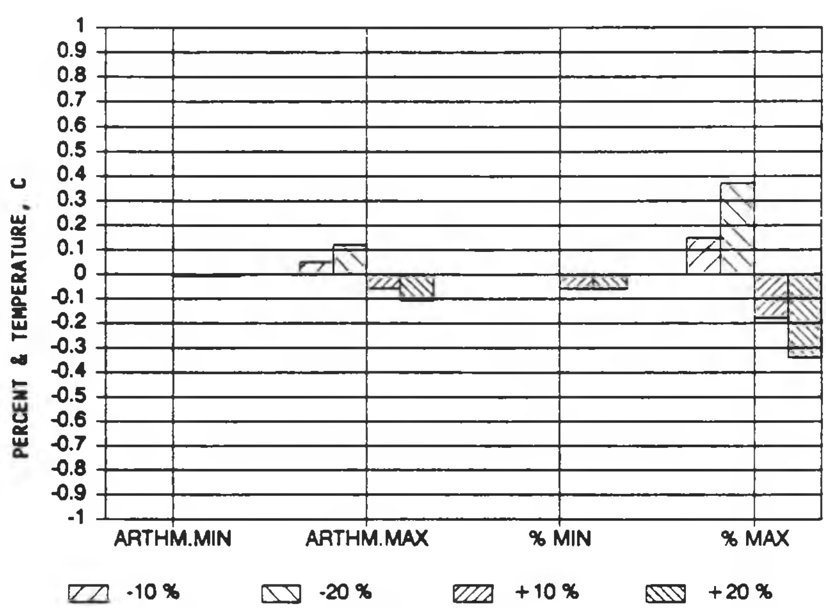

Fig. D.41. Sensitivity of TEMP-84 modeled maximum and minimum temperature to changes in the mean elevation in terms of arithmetic and percent difference from existing conditions.

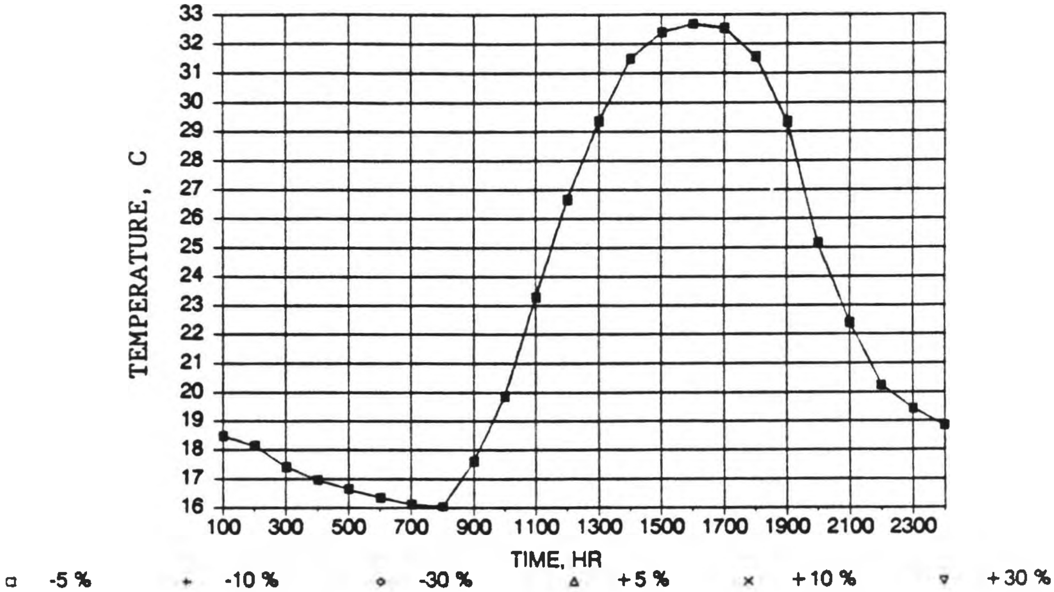

Fig. D.42. Change in TEMP-84 modeled stream temperature at VRM157.3 with ±5%, ±10%, and ±30% change in the stream gradient input.

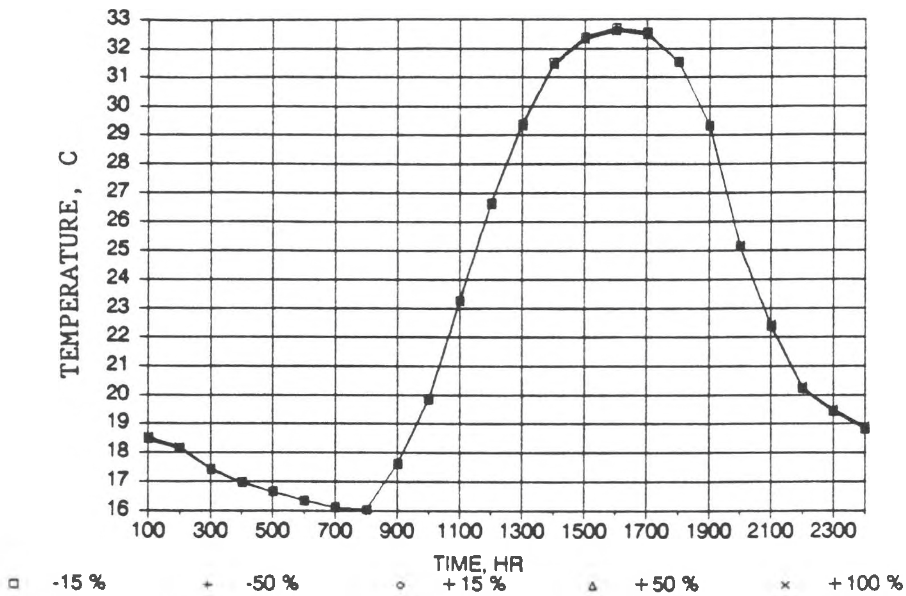

Fig. D.43. Change in TEMP-84 modeled stream temperature at VRM 157.3 with ±15%, ±50%, and +100% change in the percent of stream bed comprised of bedrock.

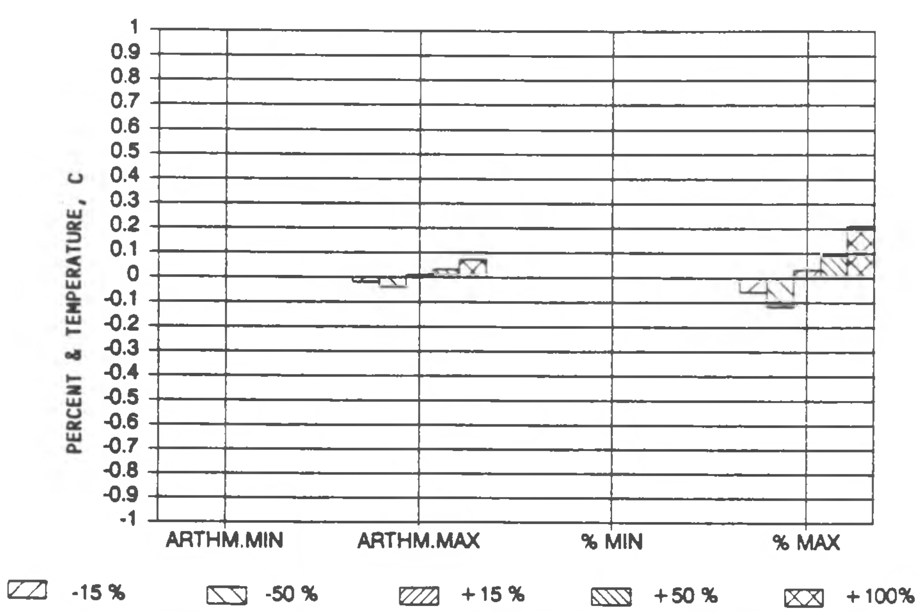

Fig. D.44. Sensitivity of TEMP-84 modeled maximum and minimum temperature to changes in the percent of stream bed comprised of bedrock in terms of arithmetic and percent difference from existing conditions.

Table E.1 . Modeled and measured maximum, minimum, and mean stream temperatures at VRM 157.3 for 6-30-88, 7-08-88, 7-15-88, and 7-21-88.

	MAXIMUM			MINIMUM			MEAN		
DATE	MODEL EMPIRICAL DATA C	MODEL FIELD DATA C	MEAS. C	MODEL EMPIRICAL DATA C	MODEL FIELD DATA C	MEAS. C	MODEL EMPIRICAL DATA C	MODEL FIELD DATA C	MEAS. C
6-30-88	30.2	29.2	27.2	15.6	16.0	17.8	21.6	21.7	22.0
7-08-88	29.4	28.4	27.0	15.2	15.6	16.7	21.2	21.2	21.5
7-15-88	28.6	27.7	26.9	14.6	14.9	16.2	20.5	20.5	21.2
7-21-88	28.9	28.1	27.8	16.1	16.4	17.5	21.4	21.4	22.4

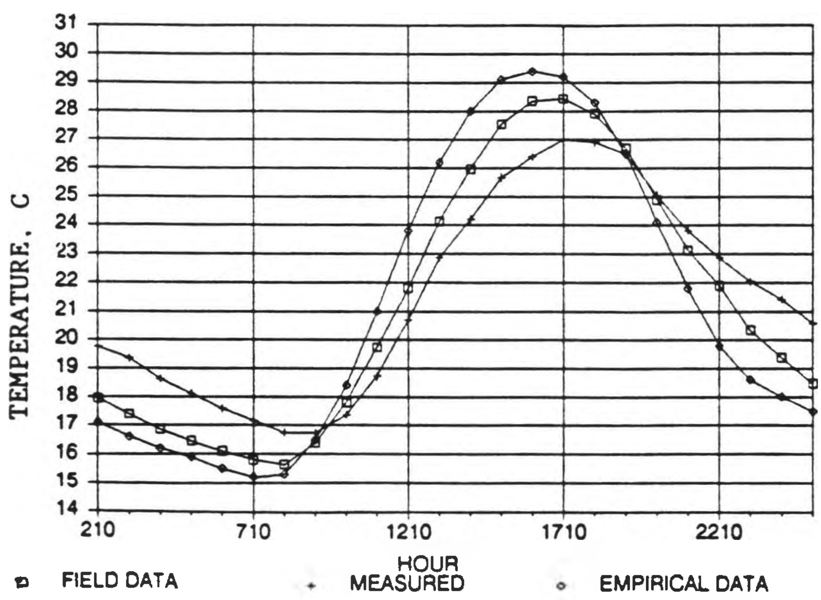

Fig. E.1 Diurnal fluctuation in stream temperature on 7-08-88 as measured and as modeled with field data and empirically derived data.

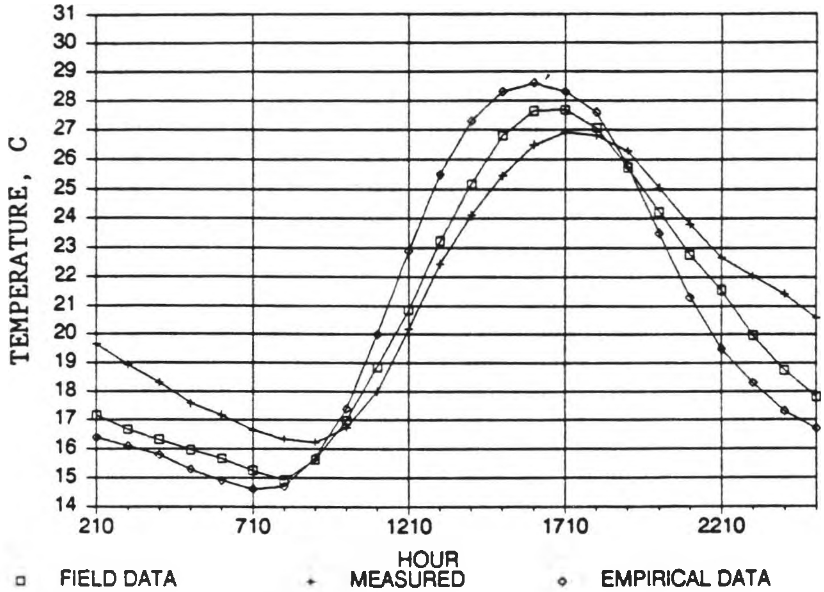

Fig. E.2. Diurnal fluctuation in stream temperature on 7-15-88 as measured and as modeled with field data and empirically derived data.

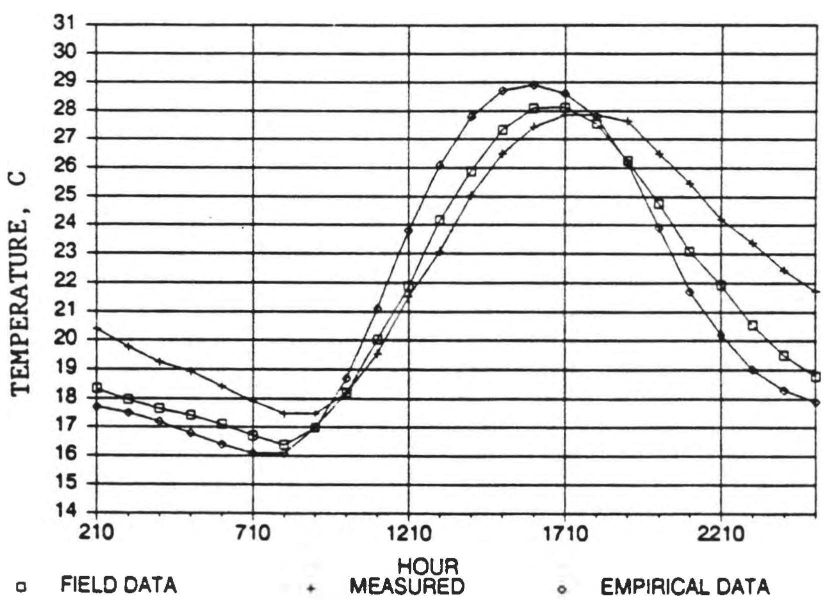

Fig. E.3. Diurnal fluctuation in stream temperature on 7-21-88 as measured and as modeled with field data and empirically derived data.

Table E.2 . Modeled stream temperature at VRM 157.3 for 6-30-88 under hypothetical flow conditions.

	FLOW						
	1000 CFS	500 CFS	100 CFS	75 CFS	32 CFS	20 CFS	10 CFS
TIME	STREAM TEMP C	STREAM TEMP C	STREAM TEMP C	STREAM TEMP C	STREAM TEMP C	STREAM TEMP C	STREAM TEMP C
210	18.1	18.2	18.2	18.1	17.4	16.8	16.1
310	17.7	17.7	17.8	17.7	17.1	16.5	15.7
410	17.3	17.3	17.3	17.2	16.7	16.2	15.4
510	17.0	17.0	16.9	16.8	16.3	15.8	15.1
610	16.8	16.8	16.6	16.5	15.9	15.4	14.8
710	16.5	16.5	16.4	16.2	15.6	15.2	14.5
810	16.4	16.4	16.3	16.2	15.7	15.5	14.4
910	16.4	16.5	16.7	16.7	16.7	17.2	16.0
1010	16.6	16.9	17.8	17.9	18.5	19.6	19.1
1110	16.9	17.4	19.0	19.4	21.1	22.7	22.6
1210	17.3	17.9	20.4	21.1	24.0	26.2	26.7
1310	18.0	18.6	21.6	22.5	26.5	29.2	31.0
1410	18.9	19.5	22.5	23.7	28.5	31.6	34.0
1510	20.3	20.7	23.4	24.6	29.7	32.9	36.4
1610	21.6	22.0	24.1	25.2	30.2	33.2	37.4
1710	22.1	22.5	24.8	25.7	30.0	32.7	37.1
1810	22.1	22.5	24.9	25.7	29.3	31.3	35.6
1910	21.7	21.8	24.0	24.7	27.7	28.9	33.1
2010	21.1	21.2	22.5	23.0	25.0	25.6	28.8
2110	20.6	20.6	21.1	21.3	22.4	22.7	25.3
2210	20.0	20.0	20.2	20.2	20.4	20.3	22.3
2310	19.5	19.5	19.5	19.4	18.9	18.6	19.7
10	19.1	19.1	19.0	18.8	18.1	17.6	17.9
110	18.7	18.6	18.6	18.4	17.7	17.1	16.6
MEAN	18.9	18.9	20.0	20.3	21.6	22.4	23.6

Table E.3 . Modeled stream temperature at VRM 157.3 for 7-08-88 under hypothetical flow conditions.

	FLOW					
	500 CFS	100 CFS	75 CFS	32 CFS	20 CFS	10 CFS
TIME	STREAM TEMP C	STREAM TEMP C	STREAM TEMP C	STREAM TEMP C	STREAM TEMP C	STREAM TEMP C
210	18.2	18.0	17.8	17.1	16.4	15.8
310	17.8	17.6	17.4	16.6	15.9	15.3
410	17.4	17.2	17.1	16.2	15.6	14.8
510	17.0	16.8	16.7	15.9	15.2	14.4
610	16.7	16.4	16.3	15.5	14.9	14.0
710	16.4	16.2	16.0	15.2	14.7	13.8
810	16.2	16.1	16.0	15.3	15.1	13.9
910	16.3	16.5	16.5	16.5	16.9	15.7
1010	16.6	17.6	17.7	18.4	19.4	18.9
1110	17.0	18.9	19.3	21.0	22.6	22.6
1210	17.5	20.1	20.8	23.8	26.0	26.5
1310	18.1	21.2	22.2	26.2	28.8	30.6
1410	19.0	22.1	23.3	28.0	31.0	33.3
1510	20.1	22.9	24.1	29.1	32.0	35.3
1610	21.3	23.6	24.7	29.4	32.2	35.9
1710	22.0	24.1	25.0	29.2	31.5	35.3
1810	22.2	24.1	24.9	28.3	30.1	33.7
1910	21.7	23.3	23.9	26.5	27.4	30.9
2010	21.1	22.0	22.3	24.1	24.5	27.1
2110	20.5	20.8	20.9	21.8	21.7	23.5
2210	19.9	20.0	19.9	19.8	19.5	21.1
2310	19.3	19.3	19.2	18.6	18.2	18.8
10	18.9	18.8	18.7	18.0	17.4	17.3
110	18.6	18.4	18.2	17.5	16.9	16.3
MEAN	18.7	19.7	19.9	21.2	21.8	22.7

Table E.4 . Modeled stream temperature at VRM 157.3 for 7-15-88 under hypothetical flow conditions.

	FLOW					
	500 CFS	100 CFS	75 CFS	32 CFS	20 CFS	10 CFS
TIME	STREAM TEMP C	STREAM TEMP C	STREAM TEMP C	STREAM TEMP C	STREAM TEMP C	STREAM TEMP C
210	17.8	17.6	17.4	16.4	15.7	14.9
310	17.3	17.2	17.0	16.1	15.4	14.5
410	16.9	16.7	16.6	15.8	15.1	14.2
510	16.6	16.3	16.1	15.3	14.7	13.9
610	16.3	16.0	15.8	14.9	14.2	13.5
710	15.9	15.7	15.5	14.6	14.0	13.2
810	15.6	15.5	15.4	14.7	14.3	13.1
910	15.8	15.8	15.8	15.7	15.9	14.7
1010	16.2	16.9	17.0	17.4	18.3	17.7
1110	16.7	18.2	18.6	20.0	21.5	21.3
1210	17.1	19.6	20.3	22.9	25.0	25.2
1310	17.6	20.8	21.7	25.5	27.9	29.3
1410	18.6	21.6	22.7	27.3	30.1	32.1
1510	19.9	22.4	23.5	28.3	31.1	34.0
1610	21.2	23.1	24.1	28.6	31.2	34.6
1710	21.8	23.7	24.6	28.3	30.5	33.9
1810	21.8	23.8	24.5	27.6	29.1	32.3
1910	21.2	22.9	23.5	25.8	26.7	29.5
2010	20.6	21.5	21.8	23.5	23.8	25.9
2110	20.0	20.4	20.4	21.3	21.3	22.8
2210	19.5	19.5	19.5	19.5	19.2	20.5
2310	19.1	18.9	18.7	18.3	17.7	18.4
10	18.6	18.3	18.1	17.3	16.6	16.7
110	18.3	17.9	17.7	16.7	16.1	15.6
MEAN	18.3	19.2	19.4	20.5	21.0	21.7

Table E.5 . Modeled stream temperature at VRM 157.3 for 7-21-88 under hypothetical flow conditions.

	FLOW					
	500 CFS	100 CFS	75 CFS	32 CFS	20 CFS	10 CFS
TIME	STREAM TEMP C	STREAM TEMP C	STREAM TEMP C	STREAM TEMP C	STREAM TEMP C	STREAM TEMP C
210	18.8	18.7	18.5	17.7	17.1	16.5
310	18.3	18.3	18.2	17.5	16.9	16.3
410	17.8	17.9	17.8	17.2	16.7	16.1
510	17.5	17.4	17.3	16.8	16.4	15.9
610	17.2	17.1	16.9	16.4	16.0	15.6
710	16.9	16.8	16.6	16.1	15.6	15.2
810	16.7	16.6	16.5	16.1	16.0	15.0
910	16.7	17.0	17.0	17.0	17.5	16.6
1010	17.2	18.0	18.1	18.7	19.7	19.2
1110	17.7	19.3	19.6	21.1	22.6	22.7
1210	18.2	20.6	21.2	23.8	25.7	26.2
1310	18.7	21.7	22.7	26.1	28.3	29.6
1410	19.6	22.6	23.6	27.8	30.2	31.9
1510	20.7	23.3	24.3	28.7	31.0	33.3
1610	21.9	23.9	24.9	28.9	31.1	33.7
1710	22.5	24.4	25.2	28.6	30.3	33.0
1810	22.6	24.4	25.1	27.8	28.8	31.5
1910	22.1	23.6	24.1	26.2	26.5	28.6
2010	21.4	22.3	22.5	23.9	23.9	25.5
2110	21.0	21.2	21.2	21.7	21.6	22.7
2210	20.5	20.4	20.4	20.2	19.8	20.6
2310	19.9	19.8	19.6	19.0	18.5	18.8
10	19.5	19.2	19.1	18.3	17.7	17.6
110	19.2	18.9	18.7	17.9	17.4	16.9
MEAN	19.3	20.1	20.4	21.4	21.9	22.4

Table E.6. Percent difference of modeled hypothetical flow maximum stream temperature from modeled existing maximum stream temperature.

DATE	500 CFS MAX STR TEMP % DIFF	100 CFS MAX STR TEMP % DIFF	75 CFS MAX STR TEMP % DIFF	20 CFS MAX STR TEMP % DIFF	10 CFS MAX STR TEMP % DIFF
6-30-88	25.5	17.6	14.9	-9.9	-23.8
7-08-88	24.5	18.0	15.0	-9.5	-22.1
7-15-88	23.8	16.8	14.0	-9.1	-21.0
7-21-88	21.8	15.6	12.8	-7.6	-16.6
MEAN	23.9	17.0	14.2	-9.0	-20.9
VARIANCE	2.45	1.12	1.04	1.01	9.45
STD DEV	1.56	1.06	1.02	1.01	3.07

Table E.7. Percent difference of modeled hypothetical flow mean stream temperature from modeled existing mean stream temperature.

DATE	500 CFS MEAN STR TEMP % DIFF	100 CFS MEAN STR TEMP % DIFF	75 CFS MEAN STR TEMP % DIFF	20 CFS MEAN STR TEMP % DIFF	10 CFS MEAN STR TEMP % DIFF
6-30-88	12.5	7.4	6.0	-3.7	-9.3
7-08-88	11.8	7.1	6.1	-2.8	-7.1
7-15-88	10.7	6.3	5.4	-2.4	-5.9
7-21-88	9.8	6.1	4.7	-2.3	-4.7
MEAN	11.2	6.7	5.6	-2.8	-6.8
VARIANCE	1.42	0.39	0.42	0.41	3.85
STD DEV	1.19	0.62	0.65	0.64	1.96

Table E.8. Percent difference of modeled hypothetical flow minimum stream temperature from modeled existing minimum stream temperature.

DATE	500 CFS MIN STR TEMP % DIFF	100 CFS MIN STR TEMP % DIFF	75 CFS MIN STR TEMP % DIFF	20 CFS MIN STR TEMP % DIFF	10 CFS MIN STR TEMP % DIFF
6-30-88	-5.1	-4.5	-3.8	2.6	7.7
7-08-88	-6.6	-5.9	-5.3	3.3	9.2
7-15-88	-6.8	-6.2	-5.5	4.1	10.3
7-21-88	-3.7	-3.1	-2.5	3.1	6.8
MEAN	-5.6	-4.9	-4.3	3.3	8.5
VARIANCE	2.10	2.03	1.98	0.39	2.42
STD DEV	1.45	1.43	1.41	0.62	1.56

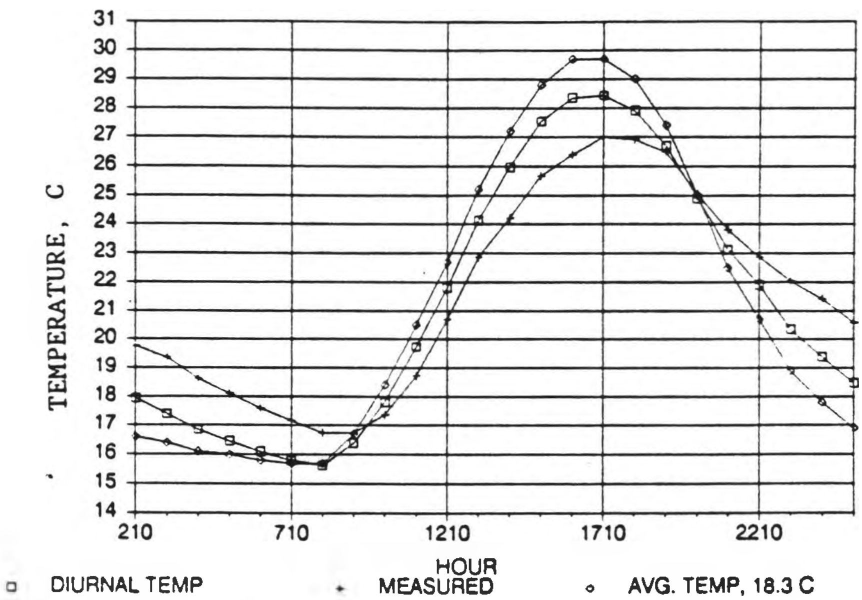

Fig. E.4. Diurnal fluctuation in stream temperature on 7-08-88 as measured and as modeled with diurnal inflow stream temperature and average inflow stream temperature.

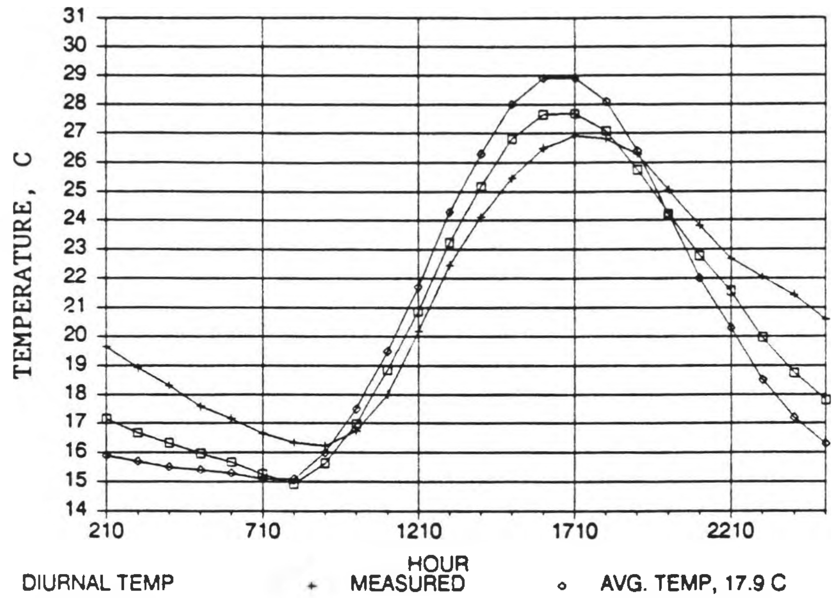

Fig. E.5. Diurnal fluctuation in stream temperature on 7-15-88 as measured and as modeled with diurnal inflow stream temperature and average inflow stream temperature.

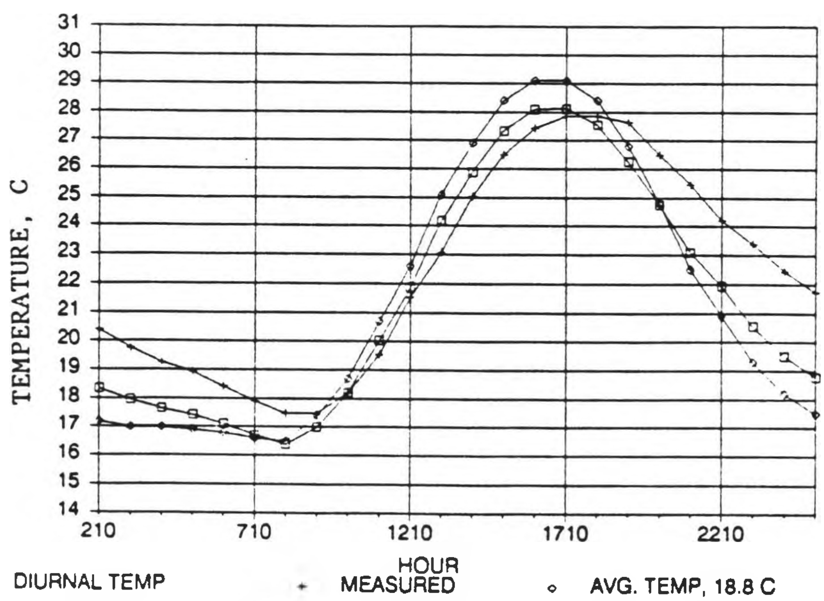

Fig. E.6. Diurnal fluctuation in stream temperature on 7-21-88 as measured and as modeled with diurnal inflow stream temperature and average inflow stream temperature.

Table E.9 , Modeled and measured maximum, minimum, and mean stream temperatures at VRM 157.3 for 6-30-88, 7-08-88, 7-15-88, and 7-21-88.

DATE	MAXIMUM			MINIMUM			MEAN		
	MODEL AVG. INFLOW TEMP. C	MODEL DIURNAL INFLOW TEMP. C	MEAS. C	MODEL AVG. INFLOW TEMP. C	MODEL DIURNAL INFLOW TEMP. C	MEAS. C	MODEL AVG. INFLOW TEMP. C	MODEL DIURNAL INFLOW TEMP. C	MEAS. C
6-30-88	30.4	29.2	27.2	16.3	16.0	17.8	21.7	21.7	22.0
7-08-88	29.7	28.4	27.0	15.7	15.6	16.7	21.2	21.2	21.5
7-15-88	28.9	27.7	26.9	15.1	14.9	16.2	20.5	20.5	21.2
7-21-88	29.1	28.1	27.8	16.5	16.4	17.5	21.4	21.4	22.4

Table E.10. Modeled stream temperature at VRM 157.5 for 6-30-88 an 7-08-88 under hypothetical inflow temperature conditions.

	6-30-88			7-8-88		
	INFLOW TEMPERATURE			INFLOW TEMPERATURE		
	GW TEMP 14.7 C	AVG. AMBIENT 26.5 C	AVG. EXISTING 18.5 C	GW TEMP 14.7 C	AVG. AMBIENT 27.4 C	AVG. EXISTING 18.3 C
TIME	STREAM TEMP C	STREAM TEMP C	STREAM TEMP C	STREAM TEMP C	STREAM TEMP C	STREAM INFLOW C
210	14.5	21.4	16.8	14.6	21.3	16.6
310	14.4	21.2	16.6	14.3	21.1	16.4
410	14.3	21.1	16.6	14.1	20.9	16.1
510	14.2	21.1	16.5	13.9	20.7	16.0
610	14.1	21.0	16.4	13.8	20.6	15.8
710	14.0	20.9	16.3	13.7	20.5	15.7
810	14.0	20.9	16.3	13.7	20.5	15.7
910	14.9	21.8	17.2	14.7	21.5	16.7
1010	16.4	23.3	18.7	16.3	23.1	18.4
1110	18.4	25.2	20.7	18.5	25.2	20.5
1210	20.6	27.3	22.8	20.7	27.3	22.7
1310	23.2	29.8	25.4	23.3	29.7	25.2
1410	25.3	31.8	27.5	25.3	31.6	27.2
1510	27.2	33.5	29.3	27.0	33.1	28.8
1610	28.2	34.4	30.3	27.9	33.9	29.7
1710	28.4	34.5	30.4	27.9	33.9	29.7
1810	27.7	33.8	29.8	27.0	33.1	29.0
1910	26.1	32.3	28.2	25.6	31.5	27.4
2010	23.8	30.0	25.9	23.2	29.2	25.0
2110	21.2	27.5	23.3	20.6	26.8	22.5
2210	19.1	25.5	21.2	18.8	25.1	20.7
2310	17.3	23.9	19.5	16.9	23.4	18.9
10	15.9	22.6	18.1	15.8	22.4	17.8
110	14.9	21.7	17.1	14.9	21.6	16.9
MEAN	19.5	26.1	21.7	19.3	25.7	21.2

Table E.11 Modeled stream temperature at VRM 157.5 for 7-15-88 an 7-21-88 under hypothetical inflow temperature conditions.

	7-15-88			7-21-88		
	INFLOW TEMPERATURE			INFLOW TEMPERATURE		
	GW TEMP 14.7 C	AVG. AMBIENT 28.1 C	AVG. EXISTING 17.9 C	GW TEMP 14.7 C	AVG. AMBIENT 29.2 C	AVG. EXISTING 18.8 C
TIME	STREAM TEMP C	STREAM TEMP C	STREAM INFLOW C	STREAM TEMP C	STREAM TEMP C	STREAM TEMP C
210	14.2	21.0	15.9	15.3	21.7	17.2
310	13.9	20.8	15.7	15.1	21.5	17.0
410	13.8	20.6	15.5	15.0	21.4	17.0
510	13.7	20.5	15.4	14.9	21.4	16.9
610	13.5	20.4	15.3	14.8	21.3	16.8
710	13.4	20.3	15.1	14.6	21.1	16.6
810	13.4	20.2	15.1	14.6	21.0	16.5
910	14.2	21.1	16.0	15.4	21.8	17.4
1010	15.8	22.6	17.5	16.7	23.2	18.7
1110	17.8	24.6	19.5	18.7	25.1	20.7
1210	20.0	26.7	21.7	20.7	27.0	22.6
1310	22.6	29.2	24.3	23.2	29.3	25.1
1410	24.7	31.1	26.3	25.1	31.0	26.9
1510	26.5	32.6	28.0	26.6	32.3	28.4
1610	27.4	33.4	28.9	27.4	32.9	29.1
1710	27.4	33.3	28.9	27.4	32.8	29.1
1810	26.6	32.5	28.1	26.7	32.0	28.4
1910	24.9	30.8	26.4	25.1	30.5	26.8
2010	22.6	28.7	24.2	23.1	28.6	24.8
2110	20.4	26.6	22.0	20.8	26.4	22.5
2210	18.7	25.0	20.3	19.1	25.0	20.9
2310	16.8	23.3	18.5	17.4	23.5	19.3
10	15.5	22.1	17.2	16.3	22.5	18.2
110	14.6	21.4	16.3	15.6	21.9	17.5
MEAN	18.8	25.4	20.5	19.6	25.6	21.4

Table E.12. Percent change in modeled maximum, mean, and minimum stream temperature of hypothetical inflow temperature simulations from modeled existing stream temperatures.

	INFLOW TEMPERATURE					
	GW TEMP			AVG. AMBIENT		
DATE	MAX STR TEMP % CHG	MEAN STR TEMP % CHG	MIN STR TEMP % CHG	MAX STR TEMP % CHG	MEAN STR TEMP % CHG	MIN STR TEMP % CHG
6-30-88	6.6	10.1	14.1	-13.5	-20.3	-28.2
7-08-88	6.1	9.0	12.7	-14.1	-21.2	-30.6
7-15-88	5.2	8.3	11.3	-15.6	-23.9	-33.8
7-21-88	5.8	8.4	11.5	-13.1	-19.6	-27.3
MEAN	5.9	9.0	12.4	-14.1	-21.3	-30.0
VARIANCE	0.34	0.68	1.67	1.20	3.55	8.44
STD DEV	0.58	0.83	1.29	1.10	1.88	2.91